

Small but numerous – The spatial distribution of microplastics in the North Sea

by

Claudia Lorenz

a Thesis submitted in partial fulfillment
of the requirements for the degree of

**Doctor of Philosophy
in Biology**

Approved Dissertation Committee

Prof. Dr. Matthias Ullrich
Jacobs University Bremen

Prof. Dr. Laurenz Thomsen
Jacobs University Bremen

Dr. Gunnar Gerdtz
Alfred Wegener Institute

Date of Defense: 31 August 2020

Department of Life Sciences and Chemistry

Statutory Declaration

Family Name, Given/First Name	Lorenz, Claudia
Matriculationnumber	20331577
What kind of thesis are you submitting: Bachelor-, Master- or PhD-Thesis	PhD-Thesis

English: Declaration of Authorship

I hereby declare that the thesis submitted was created and written solely by myself without any external support. Any sources, direct or indirect, are marked as such. I am aware of the fact that the contents of the thesis in digital form may be revised with regard to usage of unauthorized aid as well as whether the whole or parts of it may be identified as plagiarism. I do agree my work to be entered into a database for it to be compared with existing sources, where it will remain in order to enable further comparisons with future theses. This does not grant any rights of reproduction and usage, however.

The Thesis has been written independently and has not been submitted at any other university for the conferral of a PhD degree; neither has the thesis been previously published in full.

German: Erklärung der Autorenschaft (Urheberschaft)

Ich erkläre hiermit, dass die vorliegende Arbeit ohne fremde Hilfe ausschließlich von mir erstellt und geschrieben worden ist. Jedwede verwendeten Quellen, direkter oder indirekter Art, sind als solche kenntlich gemacht worden. Mir ist die Tatsache bewusst, dass der Inhalt der Thesis in digitaler Form geprüft werden kann im Hinblick darauf, ob es sich ganz oder in Teilen um ein Plagiat handelt. Ich bin damit einverstanden, dass meine Arbeit in einer Datenbank eingegeben werden kann, um mit bereits bestehenden Quellen verglichen zu werden und dort auch verbleibt, um mit zukünftigen Arbeiten verglichen werden zu können. Dies berechtigt jedoch nicht zur Verwendung oder Vervielfältigung.

Diese Arbeit wurde in der vorliegenden Form weder einer anderen Prüfungsbehörde vorgelegt noch wurde das Gesamtdokument bisher veröffentlicht.

21.12.2020, 
Date, Signature

"I was taught that the way of progress is neither swift nor easy."

Marie Curie

Table of contents

Summary	ix
Introduction	1
Thesis Aims	17
Thesis Outline	19
Chapter I	22
Spatial distribution of microplastics in sediments and surface waters of the southern North Sea	
Chapter II	44
Assessing the weathering status of marine microplastics in the southern North Sea – A multivariate approach	
Chapter III	64
Paraffin waxes in the southern North Sea	
Chapter IV	80
Different stories told by small and large microplastics in sediment – first report of microplastic concentrations in an urban recipient in Norway	
General Discussion	108
Conclusion	130
Outlook	132
Supplement	134
Supplement Chapter I	136
Supplement Chapter II	170
Supplement Chapter III	188
Supplement Chapter IV	194

Table of contents

Supplement General Discussion	206
References	210
List of publications	235
Acknowledgments	237

Summary

Along with the steadily growing global plastics production, the awareness of the ubiquity of marine plastics pollution in the marine environments has increased over the past decades. Consequently, the research activity in this field increased as well, recently focusing on microplastics (MP, <5 mm), which are recognized as an emerging global threat but including also other petroleum-based pollutants such as paraffin waxes (PWs). Thus, much effort has been spent on developing methods to analyze MP in environmental samples, resulting in a plethora of approaches for sampling, sample processing and analyzing MP. So far, no standard operating procedures (SOP) exist, but more and more attempts on harmonization are made.

Meanwhile, legal frameworks such as the European Marine Strategy Framework Directive (MSFD) have been initiated to target marine plastic pollution, including MP. The MSFD, focusing on European waters, provides thus the legal framework for MP research in the North Sea. To date, studies addressing marine plastic pollution in the North Sea have mainly concentrated on meso- and macroplastics (>5 mm). The few studies that approached MP focused on specific regions in the North Sea or only one compartment (i.e. sediment or surface water) and depended on visual identification of MP with chemical identification of a subset of putative MP at most.

Hence, this thesis aimed to provide a spatial distribution of MP in sediments and surface waters of the southern North Sea. The results (Chapter I, published in *Environmental Pollution*) present the first comprehensive analysis of MP concentrations and polymer types in a size range from 11 to 5000 μm for this region. Sediment and surface water samples from 24 stations along the coastline and in the more central part of the southern North Sea were analyzed applying state-of-the-art methods for sample processing and MP identification. All large MP (500–5000 μm) were identified by attenuated total reflection (ATR) Fourier transform infrared (FTIR) spectroscopy, a commonly applied technique in the field of MP research. For the identification of small MP (11–500 μm), independently from any visual pre-selection, state-of-the-art focal plane array (FPA) based FTIR imaging combined with automated identification and quantification was utilized. Based on this approach, providing a detailed dataset on MP concentrations, polymer types and size distribution, significant differences were found between the two sampled compartments regarding their polymer composition. In surface waters, low-density polymers like polyethylene (PE) and polypropylene (PP) represented more than one-third of the polymer composition. In sediments, PP was omnipresent as well, but less abundant, and accompanied by acrylates/polyurethanes/varnish and rubbers such as polychloroprene and ethylene-propylene-diene monomer (EPDM). In sediments, MP were also significantly

smaller than in surface waters. In sediments on average 98% of the MP were <100 μm , while in surface waters it was 86%.

Differences in the polymer composition and the overall MP concentration could also be recorded concerning the spatial distribution of MP in the southern North Sea. In surface waters, the highest MP concentration (245 particles m^{-3}) was detected close to the English Channel and the Rhine-Meuse-delta. This area is influenced by oceanic as well as riverine input. In turn, the highest MP concentration in the sediment (1189 particles kg^{-1}) was found in a more central part of the southern North Sea. Potentially MP accumulating there were received through a northeasterly-directed horizontal transport from areas with high land-based input.

This comprehensive dataset served as the basis for an *in silico* study (Chapter II, to be submitted to *Chemosphere*) assessing the weathering status of polyethylene (PE) and polypropylene (PP) particles detected in the two sampled compartments by analyzing their carbonyl indices. The carbonyl indices were calculated based on the ratio of the integrated area of the absorption band of carbonyl groups (1800–1700 cm^{-1}) and methylene vibrations (1480–1400 cm^{-1}). The results showed a significant difference between the two sampled compartments for both polymer types. Average carbonyl indices for small MP in sediments were 0.14 for PE and 0.00 for PP, while in surface water lower for PE (0.07) and higher for PP (0.06). Furthermore, significant differences could also be found among the different size classes of both polymer types in both compartments. When comparing the average carbonyl indices of small MP to the ones of large MP in surface water, the latter were considerably lower for PE (0.03) and PP (0.02). These results indicate a connection between size and weathering status, which might be related to weathering dependent fragmentation modes. Apart from the wavenumber range, restricted to the carbonyl groups, the full-recorded spectral range was analyzed for PE, PP, polystyrene (PS) and polyvinyl chloride (PVC). Significant differences were found for all four polymer types when comparing the spectra of the naturally weathered MP to reference spectra of pristine MP. However, they were less prominent when comparing the spectra between the two sampled compartments. Furthermore, the wavenumber region characteristic for hydroxyl groups (3500–3200 cm^{-1}) was confirmed as another potential indicator for weathering.

Furthermore, putative PWs, floating in southern North Sea surface waters were sampled along with the MP with a 100- μm net and analyzed in a separate study (Chapter III, submitted to *Marine Pollution Bulletin*). Putative PWs were detected at most of the sampled stations and most frequently at two stations that were influenced by oceanic as well as riverine input. The softer texture of PWs distinguished them from the more rigid MP. Utilizing ATR-FTIR the synthetic origin of PWs (500–5000 μm) could be confirmed, and the additional application of

gas chromatography-mass spectrometry (GC-MS) provided a more detailed insight into the chemical composition, allowing for unambiguous identification. Thus, an analysis of selected individual PWs with ATR-FTIR complemented with a bulk-analysis with GC-MS of these PWs of similar appearance provides the fastest and most reliable approach, which would be compatible with MP monitoring efforts.

Finally, since sublittoral sediments are considered to accumulate MP, the results from the North Sea sediments were compared to sublittoral sediments from an urban fjord in Norway, connected to the northern North Sea via the Norwegian Coastal Current. The methods for sample processing and MP analysis used for this study (Chapter IV, published in *Marine Pollution Bulletin*) were harmonized between the studies, thus facilitating a comparison of results. The MP concentrations in the fjord sediments ranged between 12×10^3 and 205×10^3 particles kg^{-1} dry weight sediment and exceeded the highest concentrations in the southern North Sea by factor 10 and 100, respectively. This discrepancy might be attributed to the discharge of partially untreated wastewater in the sampling area and the sediment trapping efficiency of a fjord system.

The differences between the two studies on sublittoral sediments confirm that regional input processes influence the MP concentrations in the respective areas greatly. However, the similarities in the polymer composition as well as the size distribution point towards polymer type and size being driving factors in vertical transport processes. One of the main findings of both published studies was that small MP exhibited much higher concentrations and more diverse polymer compositions than large MP. This result emphasizes that future studies and monitoring efforts should include small MP, preferably $<100 \mu\text{m}$, to give a realistic appraisal of the actual MP pollution in the marine environment and provide robust data for environmental risk assessment. Additionally, this thesis highlighted that harmonized methods that provide comprehensive data in terms of MP concentrations, polymer composition and size class distribution are indispensable for inter-study comparisons and monitoring efforts.

Introduction

It is a truth universally acknowledged, that plastics are an indispensable part of our everyday life. During the past 70 years, there has been a steep increase in plastics production starting with a global annual production of only 1.7 million metric tons (Mt) in 1950, which then in 2018 amounted to 359 Mt (PlasticsEurope, 2012, 2019). This increase, combined with poor waste disposal strategies, has led to an estimated annual plastic waste input to the oceans of 50 to 120 Mt for 2018, extrapolated from a calculation of 4 to 12 Mt in 2010 (Jambeck et al., 2015). Consequently, we are facing now considerable plastic pollution of the marine but also several other aquatic environments. The same properties of plastics, like being versatile and durable, which led to their success and vast production, become an issue when they enter the marine environment, where they steadily accumulate.

The interest of society concerning plastic pollution, in general, can be associated with the discovery of the Great Pacific garbage patch by Charles Moore in the late 1990s (Moore et al., 2001). Since then, there has been rising awareness of plastics accumulating in the marine environment and the presence of several of these garbage patches have been modelled and confirmed (Maximenko et al., 2012; van Sebille et al., 2012; Eriksen et al., 2014; Lebreton et al., 2018). However, the first records of small-sized plastics in the form of polystyrene (PS) spheres in the marine environment, in surface waters and washed ashore, date back to the early 1970s (Carpenter et al., 1972; Carpenter & Smith, 1972). A few years later, the occurrence of these PS spheres together with cylindrical polyethylene (PE) pre-production pellets, packaging films and fragments of larger plastics have been recorded along the US east coast by Colton et al. (1974). Despite the early discoveries of these “microplastics” in the marine environment, it was not until 30 years later that Richard Thompson and colleagues coined this term (Thompson et al., 2004). Since then, the attention microplastics (MP) have been receiving in the scientific community, as well as in politics and society, has been increasing continuously (Connors et al., 2017). Nowadays, the issue of marine (micro)plastic pollution is well-known and even integrated into the concept of planetary boundaries as chemical pollution or novel entities (Rockström et al., 2009; Steffen et al., 2015; Villarrubia-Gómez et al., 2018).

In politics, plastic pollution in general was considered from early on. One of the first measures was the MARPOL Convention for the Prevention of Pollution from Ships initiated by the International Maritime Organisation (IMO) in 1973. More recently, the United Nations Environment Programme (UNEP) established the Sustainable Development Goals with No. 14 concerning “Life below water” and consequently marine plastic pollution. Individual bans, mainly targeting single-use plastics or microbeads, have been issued in several states in the USA (i.e. Illinois, New Jersey, New York, Ohio and California), several European countries (i.e.

the Netherlands, Austria, Luxembourg, Belgium, Sweden, Ireland and Italy) as well as other countries (i.e. Canada, UK, New Zealand, Australia, Taiwan, South Korea and India) (Crawford & Quinn, 2017b; Frias & Nash, 2019).

The European Marine Strategy Framework Directive (MSFD) issued by the European Union in 2008 (Directive 2008/56/EC) covers MP within Descriptor 10 while other petroleum-based pollutants, like oil, are covered in Descriptor 8 (European Parliament Council, 2008). This directive also provides the legal framework for MP research in European waters (OSPAR, 2010; Crawford & Quinn, 2017b).

In the scientific community, the issue of (micro)plastics pollution has been occasionally featured but has picked up its pace in publications, especially regarding MP, tremendously during the past 15 years since the milestone/keystone publication by Thompson et al. (2004). This steep increase is illustrated in Figure 1, depicting the annual output of publications from 2004 until now, using the term “microplastic(s)” or the terms “microplastic(s)” and “marine” in the title, abstract or the keywords.

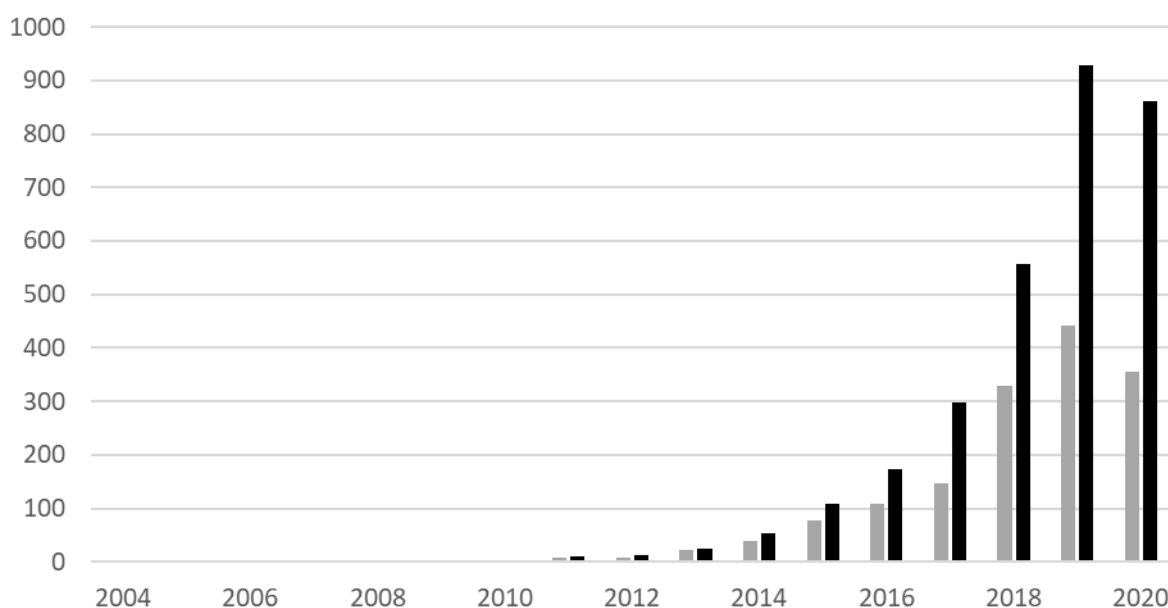


Figure 1: Number of publications on “microplastic(s)” (black bars) and “microplastic(s)” + “marine” (grey bars) sorted by year from 2004 to 2020, based on a literature search having these search words in the title, abstract or keywords in Scopus (on June 13th 2020).

Five years ago, the yearly number of publications surpassed 100 and undoubtedly will this year reach beyond 1000. The number of publications on MP in the marine environment has been growing as well, but it appears that recently the focus has been shifted to include other fields, too. This increasing number of studies on MP through different fields of research makes it essential to agree on some common definitions (Hartmann et al., 2019).

Microplastics & Co. - Characteristics of MP and other semi-solid, petroleum-based pollutants

Plastics are a diverse group of materials having in common that they are all synthetically produced polymers usually based on petroleum but increasingly also from renewable, biobased sources, such as starch (Hartmann et al., 2019; PlasticsEurope, 2019). Thus, to define (micro)plastics, Hartmann et al. (2019) formulated seven classification criteria, considering several characteristics and properties, which are worth looking at more in detail.

The first criterion is the **chemical composition** of the material, in which regard, plastics can be divided into two main categories based on their re-shaping capabilities (see Figure 2). One being thermoplastics, which can be melted and shaped when heated and remain solid under ambient conditions. The other group are thermosets, which change in their chemical structure when heated and can therefore not be re-melted and re-shaped once cooled. However, this would exclude some elastomers such as rubbers (i.e. tire wear particles), and some paints/surface coatings, which both are or contain synthetic polymers, though, and were thus suggested to be included in the definition (Hartmann et al., 2019). Another way to group plastics is regarding their molecular structure into plastics with C-C backbone and the ones containing heteroatoms (e.g. oxygen) in their backbone. This aspect can be helpful regarding the degradation behavior, since polymers with heteroatoms in their backbone show higher thermal stability (Gewert et al., 2015).

Introduction

	Thermoplastics	Elastomers/Rubbers	Thermosets
C-C backbone	polyethylene (PE) polystyrene (PS) polypropylene (PP) polyvinyl chloride (PVC) acrylonitrile butadiene styrene (ABS) poly(methyl methacrylate) (PMMA) polytetrafluoroethylene (PTFE) ethylene vinyl acetate (EVA)	polychloroprene (CR) polybutadiene (PBD) polyisoprene (IR) chlorinated ethylene propylene diene monomer rubber (EPDM) nitrile rubber (NBR)	acrylic resins
Heteroatoms	polyethylene terephthalate (PET) polysulfone (PSU) polycarbonate (PC) polyamide (PA) cellulose acetate (CA) polylactic acid (PLA) polycaprolactone (PCL) polyoxymethylene (POM) polyetherketone (PEEK)	silicone (Q)	unsaturated polyester (PES) epoxy resin polyimide (PI) polyurethanes (PUR)

Figure 2: Some common synthetic polymer types sorted into categories regarding their structure (C-C backbone vs heteroatoms in the backbone) and re-shaping capabilities (thermoplastics vs thermosets and elastomers/rubber). Sources: (Peters, 2015; Crawford & Quinn, 2017a; CROW, 2019; PlasticsEurope, 2019).

The second criterion is the **solid state** of the particles under ambient conditions, which, for example, discerns them from waxes (e.g. petroleum wax, i.e. paraffin). However, Hartmann et al. (2019) pointed out that also conventional plastics like PE can be wax-like or semi-solid. Thus, in the framework of this thesis, semi-solid petroleum-based pollutants like paraffin waxes (PWs) will be considered as MP as well.

The third criterion considers the **solubility** of the synthetic polymer, which should be insoluble or poorly soluble in water, meaning a solubility $<1 \text{ mg L}^{-1}$ at 20°C , (Hartmann et al., 2019). However, this does exclude persistent, widely used polymers that are soluble in water like polyacrylamides and polycarboxylates (Arp & Knutsen, 2020).

The fourth criterion is **size**, which drives the distinction between nano-, micro-, meso-, and macroplastics. There exists a multitude of size definitions with the lower size limit of MP ranging between 100 nm (EFSA, 2016) and 335 μm (Koelmans et al., 2017). However, typically, the lower size limit is set at 1 μm (e.g. (GESAMP, 2015; Crawford & Quinn, 2017b; Hartmann et al., 2019). Consequently, it would be intuitive to set the upper size limit for MP to 1 mm. However, more commonly an upper limit of 5 mm is used since this has been set up at an

international workshop hosted by the National Oceanic and Atmospheric Administration (NOAA) in 2008 (Arthur et al., 2009). Since then, this has been the most frequently used and well-accepted value (e.g. Hidalgo-Ruz et al., 2012; Frias & Nash, 2019; Primpke et al., 2020a). Furthermore, the methodology used for sampling, sample processing as well as identification and quantification of MP in environmental matrixes occasionally requires the fractionation of samples into constrained size categories, which do not always cover the full range of the defined size range of MP. For example, when sampling the water body with nets, its mesh size influences the lower size limit. The same applies to further processing of the sample when filtration steps are involved. Finally, the analytical method used can have a detection limit which consequently sets the lower size limit of detectable MP. Thus, it is recommended to state the investigated size range in every MP study to allow for harmonization and comparison of results.

The fifth criterion is the **shape and structure** where the main distinction is into regular shaped spheres/beads and pellets, fibers and usually irregular shaped fragments and films. Spheres/beads are characterized by a high circularity. The elongation and length to width ratio are commonly considered to be at minimum 3:1 for fibers, to differentiate between elongated fragments and fibers (e.g. Cole, 2016; Primpke et al., 2019; Vianello et al., 2019). The shape of MP, apart from polymer density and size, is another factor that will influence the sinking behavior of the particles.

The sixth criterion is **color**. MP come in many colors from transparent over muted to bright colors and in black or white. Furthermore, the initial coloration, usually achieved by adding additives like pigments, will most likely change during ageing of the plastic polymer by yellowing or discoloration (Andrady, 2017). Thus, it is considered as an additional characteristic since it could indicate potential sources and more importantly, coincide with preferences in prey for some organisms (Hartmann et al., 2019). Due to the subjectivity of color, Hartmann et al. (2019) recommended the use of a standardized color palette.

The seventh criterion is the **origin**. Cole et al. (2011) differentiated in this regard between primary (produced in micrometer dimensions) and secondary (resulting from the fragmentation of larger plastic items) MP. The most well-known example of primary MP are microbeads contained in skin care products (Möhlenkamp et al., 2018). To some extent, the shape and origin of MP can be linked. The regular shaped pellets and microbeads are considered as primary MP, while irregular shaped fragments and films are usually the results of the fragmentation of larger plastic pieces. These fragmentation processes also continue on smaller size scales resulting in MP covering a broad size range.

Mostly in agreement with the criteria described by Hartmann et al. (2019), Frias and Nash (2019) define MP as “any synthetic solid particle or polymeric matrix, with regular or irregular

shape and with size ranging from 1 μm to 5 mm, of either primary or secondary manufacturing origin, which are insoluble in water.”

In this thesis MP will be defined in accordance with these criteria and definitions, including rubbers and paints/varnish, but will look at PWs separately. Due to the analytical detection limit the size range will include MP from 11 to 5000 μm with considering 11–500 μm as small MP and 500–5000 μm as large MP.

How to assess MP characteristics in environmental samples and why

Although MPs research is blooming, there have been no standard operating procedures (SOP) agreed upon, so far. This deficiency has been pointed out already in an intensive review on methods for MP analysis by Hidalgo-Ruz et al. (2012). Since then, this lack of SOP, and along with it the difficulty to compare data between studies, has been addressed by many researchers (e.g. Filella, 2015; Löder & Gerdt, 2015; Costa & Duarte, 2017; Potthoff et al., 2017; Hamm et al., 2018). Nevertheless, during the past decade, much progress has been made in terms of method development concerning sampling, sample processing as well as identification and quantification of MP in environmental matrixes. Up to date, some attempts on harmonization have been made as well (e.g. Hanke et al., 2013; Masura et al., 2015; Cowger et al., 2020b; Primpke et al., 2020a). Harmonization of methods has recently been also a declared goal of the BASEMAN project, funded by the EU Joint Programming Initiative Healthy and Productive Seas and Oceans (JPI-Oceans), where several advances in that direction were made (Gerdt, 2019).

Sampling

Taking the samples from the environment is the first step. The most appropriate sampling technique is defined by the targeted compartment (e.g. beaches, sublittoral sediments, sea surface, water column) as well as the subsequent processing and analysis capabilities. Beaches are relatively easy to sample, due to being a readily accessible compartment. In the MSFD monitoring guidelines for marine litter, Hanke et al. (2013) focused on recommendations on how to sample MP, e.g. on transects along the strandline of sandy shores and suggested sampling the surface down to 5 cm. What is, however, less trivial is the decision on the number of replicates taken along a transect as well as the final sample volume that can be deemed representative, due to the high spatial heterogeneity of beaches (Löder & Gerdt, 2015; Frias et al., 2018). Sampling sublittoral sediments is even more complex since a vessel and grabs or corers are necessary to retrieve the samples. Generally, corers, such as Multiple or box corers, leave the sediment surface relatively undisturbed but usually provide smaller sample volumes when compared to grabs, such as Van Veen or Ekman grabs, (Löder & Gerdt, 2015; Frias et al., 2018). Sediment samples are considered as bulk-samples unless sieving them on-

site to reduce their volume. Contrary to this, taking bulk-samples of sea surface water (e.g. with a rotating drum sampler, Ng and Obbard, 2006) or the water column (e.g. with Niskin bottles attached to a rosette sampler, Bagaev et al., 2017; Courtene-Jones et al., 2017; Kanhai et al., 2018) is the exception. Typically, the sea surface is sampled by trawling a net alongside the vessel for a certain amount of time. The two most common versions are manta trawl and neuston nets with a mesh size of 333 μm (e.g. Frias et al., 2014; de Lucia et al., 2018; Vianello et al., 2018), which are also recommended following the MSFD guidelines (Hanke et al., 2013; Gago et al., 2018). Other devices are the AVANI trawl (Eriksen et al., 2018), plankton (WP2) nets (Frias et al., 2014; de Lucia et al., 2018) or a neuston catamaran (Löder & Gerdt, 2015; Kirstein et al., 2016). For a volume-reduced sampling of the water column, either sub-surface trawls with bongo nets (Doyle et al., 2011) or special “multi-level-trawls” can be performed (Reisser et al., 2015; Kooi et al., 2016). Alternatively, the Continuous Plankton Recorder (Thompson et al., 2004) or pumping systems coupled to filtering units with varying mesh size can be used (e.g. Enders et al., 2015; Zobkov et al., 2019; Tekman et al., 2020). The advantage over bulk-sampling methods is that a larger water volume can be sampled. Another aspect to consider when using volume-reduced sampling, especially with nets, is that the size of the smallest MP to quantify is theoretically already influenced during sampling by the mesh or filter size used.

Other compartments to be sampled in the marine environment include biota, which are normally sampled selectively (e.g. Besseling et al., 2013; Rummel et al., 2016; Piarulli et al., 2019), snow and ice, which are sampled similar to beaches and sublittoral sediments (e.g. Peeken et al., 2018; Bergmann et al., 2019) and air, which can be sampled actively with a filtration device (Dris et al., 2017; Vianello et al., 2019; Allen et al., 2020) or passively by atmospheric fallout (Dris et al., 2015; Wright et al., 2020).

With all types of sampling comes a risk of contamination mostly from sampling equipment, clothes of the operators and airborne pollutants. Thus, contamination prevention measures like avoiding the use of plastic items, taking air-blanks during sampling, and paint scrapes from the vessel, should be taken (Gago et al., 2018).

Sample processing

Upon successfully securing the samples, these contain, apart from the MP, mainly the environmental matrix. Regarding sediment samples, the matrix is mostly inorganic, consisting of minerals (e.g. clay and silicates) with a higher density than most plastics (Crawford & Quinn, 2017d). Therefore, density separation is applied most commonly to extract the MP from the inorganic matrix (Harvey et al., 2017). The selected salt solution and its corresponding density is the decisive factor for its efficiency. Salt solutions available and used include: sodium

chloride (NaCl, $\rho=1.2 \text{ g cm}^{-3}$, e.g. Thompson et al. 2004), calcium chloride (CaCl_2 , $\rho=1.30\text{--}1.46 \text{ g cm}^{-3}$, Stolte et al., 2015; Crichton et al., 2017), sodium iodide (NaI, $\rho=1.2 \text{ g cm}^{-3}$, e.g. Nuelle et al., 2014; Crichton et al., 2017; Fischer & Scholz-Böttcher, 2017), zinc chloride (ZnCl_2 , $\rho=1.5\text{--}1.7 \text{ g cm}^{-3}$, e.g. Imhof et al., 2012; Bergmann et al., 2017; Liu, F. et al., 2019b; Mani et al., 2019c), and sodium tungstate (Na_2WO_4 , $\rho=1.4\text{--}1.8 \text{ g cm}^{-3}$, Corcoran et al., 2015; K  ppler et al., 2016; Frias et al., 2018; Pagter et al., 2018). Recently, some studies proposed a density-independent approach utilizing the hydrophobicity of plastics, by using canola oil (Crichton et al., 2017), receiving recovery rates of 96% for MP between 1 and 5 mm, and castor oil (Mani et al., 2019b), with 95% recovery of MP down to 300 μm in size, for polymer types with densities up to 1.3 g cm^{-3} . These fluids present cost-effective and non-toxic alternatives but their efficiency needs to be tested for MP smaller 300 μm still. Another consideration to take into account is about the device used for the density separation. The most simple, and thus inexpensive version, is the utilization of Erlenmeyer flasks (Mani et al., 2019c) or separatory funnels (Liu, F. et al., 2019b). Other devices like the SMI (Coppock et al., 2017) provide a still portable option as well. However, these devices are limited to relatively small volumes of sediment (<250 g dry weight (dw) sediment). A large scale device completely made out of stainless steel is the “Microplastic Sediment Separator” (MPSS) first described by Imhof et al. (2012), now commercially available from HydroBios, and since used by a growing number of studies (Imhof et al., 2016; K  ppler et al., 2016; Bergmann et al., 2017; Bord  s et al., 2019; Tekman et al., 2020). It allows for the efficient extraction (95.5% recovery) of MP down to 40 μm in size from 1–6 L of sediments (Imhof et al., 2012). Other, less frequently applied, forms of extracting the MP from the inorganic matrix include elutriation (e.g. Claessens et al., 2013; Nuelle et al., 2014; Zhu, 2015; Kedzierski et al., 2016; Pagter et al., 2018) froth flotation (Imhof et al., 2012), and electrostatic separation (Felsing et al., 2018).

Recently, Li, Q. et al. (2019) and Liu, F. et al. (2019b) have shown that sediment samples containing a high content of biogenic organic matter (e.g. soil, sludge or stormwater pond sediments), should be pre-oxidized to facilitate the subsequent density separation. The content of biogenic organic matter in sediments after the density separation is usually relatively low when compared to biota or water samples, after removing the water through filtration. Several maceration agents can be used to remove this organic matrix of biological origin (e.g. phyto- or zooplankton, detritus). Quite effective, but also destructive to the synthetic polymers, are acids like sulphuric acid (H_2SO_4), nitric acid (HNO_3), and hydrochloric acid (HCl), which have been used in varying concentrations in a couple of studies (e.g. Claessens et al., 2013; De Witte et al., 2014; Klein et al., 2015). Another widely applied approach for biota samples, is the utilization of alkaline solutions like potassium hydroxide (KOH) and sodium hydroxide (NaOH) (e.g. Foekema et al., 2013; Dehaut et al., 2016; Karami et al., 2017). The most common

treatment is oxidation with hydrogen peroxide (H_2O_2) or occasionally also sodium hypochlorite (NaClO) (e.g. Nuelle et al., 2014; Avio et al., 2015; Collard et al., 2015). The adverse side effects of oxidation with H_2O_2 at 35% concentration on the synthetic polymers, including discoloration and partial degradation, occur only after a long incubation time (>7 days) according to Nuelle et al. (2014). To increase the efficiency of the oxidation and reduce the time demand, the addition of a catalyst, namely iron sulfate (FeSO_4), has been recommended by Masura et al. (2015). This so called Fenton reaction is exothermic, pH- as well as temperature-sensitive but efficient and non-destructive (Hurley et al., 2018a). Hence it is applied by a growing number of studies (e.g. Bergmann et al., 2017; Tagg et al., 2017; Simon et al., 2018; Mani et al., 2019c). Another, even more gentle, approach is the maceration with enzymes, which target macromolecules like polysaccharides, proteins, and lipids, specifically (Hamm et al., 2018). In a simple approach only one, most often proteolytic enzyme, such as proteinase-K, trypsin or Corolase, (Cole et al., 2014; Catarino et al., 2016; Courtene-Jones et al., 2017; Karlsson et al., 2017) or an enzyme blend (von Friesen et al., 2019) is utilized. (Löder et al., 2017) recently presented a more sophisticated approach, applying several enzymes (protease, amylase, lipase, cellulase, and chitinase) consecutively after treatment with the surfactant sodium sulfate (SDS). This treatment is most effective when combined with an oxidation step using H_2O_2 or Fenton's reagent. The protocol can be adjusted to the prerequisites of the environmental target matrix and has been used, in some modifications, in a couple of studies (e.g. Fischer & Scholz-Böttcher, 2017; Mintenig et al., 2017; Cabernard et al., 2018; Simon et al., 2018; Liu, F. et al., 2019b; Mintenig et al., 2020).

Identification and quantification

Regarding the final aspect, the identification and quantification of MP, the available methods can roughly be divided into two groups: visual techniques and chemical techniques.

Among the visual techniques are the visual inspection with the naked eye only, which is limited to MP larger 1 mm (Primpke et al., 2020a), and optical microscopy, usually using a stereomicroscope (Shim et al., 2017; Cowger et al., 2020b; Primpke et al., 2020a). Putative MP are sorted out as such based on specific criteria like the absence of cellular structures and equal thickness for fibers (Norén, 2007; Crawford & Quinn, 2017e). Slightly more information, specifically on the surface structure, can be received by scanning electron microscopy (SEM) (Zarfl, 2019; Primpke et al., 2020a). Another method is fluorescence microscopy, which comes in useful when dye-staining methods are applied. The most established dye in MP research is the hydrophobic fluorescent Nile red (e.g. Erni-Cassola et al., 2017; Maes et al., 2017a; Primpke et al., 2020a). However, this dye does not stain all polymer types equally reliable and additionally does stain other natural organic materials, e.g. cotton and lipids (Shim et al., 2016;

Primpke et al., 2020a). Nonetheless, this method, especially after thorough removal of the biogenic organic matter, can facilitate the distinction of targeted MP from the non-targeted matrix.

Although these optical methods are widely used, the solely visual identification is prone to human bias (e.g. favoring of brightly colored particles and overlooking of transparent ones) even by experienced operators (e.g. Hidalgo-Ruz et al., 2012; Lenz et al., 2015; Löder & Gerdt, 2015; Primpke et al., 2020a). Furthermore, they do not provide reliable identification of the polymer type and other chemical characteristics. Thus, the chemical techniques are focusing on the chemical identification of the MP and can usually be combined with microscopy.

One of the first methods applied to identify the chemical composition of single MP particles was Fourier transform infrared (FTIR) spectroscopy (Thompson et al., 2004). It is a widely utilized method to analyze MP concentrations in terms of numbers and individual polymer types. According to a recent review conducted by Cowger et al. (2020b), taking into account 127 peer-review articles published between 1995 and 2019, FTIR spectroscopy was utilized in 57% of the 90 studies applying chemical techniques for MP identification. The basic principle is that IR light excites molecular bonds in the irradiated material resulting in vibrations that can be detected and transferred into substance specific absorbance or transmittance spectra. Several modes of FTIR spectroscopy exist. The most widely used is attenuated total reflection (ATR) FTIR spectroscopy (Primpke et al., 2020a). It is a surface technique where the particle of interest is pressed on a crystal (e.g. diamond, germanium, zinc selenide) with a clamp. The IR beam is then reflected but also partly penetrates the sample just below the surface and interacts with the target substance. Less common is the use of reflectance without the ATR accessory, where the IR beam is reflected after hitting the surface. Thus, the thickness of the particle does not matter, but its morphology (Harrison et al., 2012). In contrast to this, the transmission mode is thickness dependent and provides high-quality spectra for thin samples, but with thick samples, the IR beam might get fully absorbed when it passes through (Löder et al., 2015). All these modes can be applied to handpicked particles but, when coupled to a microscope, also to particles down to 10 μm enriched on a suitable surface (e.g. Anodisc filters, silicone membranes, zinc selenide windows) (e.g. K  ppler et al., 2015; L  der et al., 2015; Simon et al., 2018). Single point measurements of large surface areas can take up a lot of time and the use of line or focal plane array (FPA) detectors, allowing FTIR imaging, is recommended to overcome this problem by simultaneously omitting visual preselection of particles of interest (e.g. Harrison et al., 2012; Vianello et al., 2013; L  der et al., 2015; Primpke et al., 2020a). The recorded IR spectra can then be compared to known reference spectra and thus the particle identified. Recently, advances have been made to (semi)automatize the identification of the recorded spectra. Combined with image analysis these can provide information on the particle

properties like number, size, shape and polymer type (Primpke et al., 2017b; Renner et al., 2017; Primpke et al., 2018; Primpke et al., 2020b; Renner et al., 2020).

The second most popular chemical technique, with 19% utilization according to Cowger et al. (2020b), is Raman spectroscopy, which is considered to be complementary to FTIR spectroscopy (Käppler et al., 2016). Here, a monochromatic laser with visible or NIR light emission induces vibrations of the molecules, resulting in scattering of the light, which is visualized in a Raman spectrum characteristic for the substance. Raman spectroscopy can also be coupled to microscopy and has successfully been used to analyze MP in different environmental matrices (e.g. Enders et al., 2015; Frère et al., 2016; Anger et al., 2018; Cabernard et al., 2018). Similar to FPA-based FTIR imaging, also μ Raman spectroscopy can be applied for imaging and thus automated particle analysis (e.g. Anger et al., 2018; Anger et al., 2019).

In contrast to the spectroscopic techniques that provide particle related data, thermal degradation techniques, such as Pyrolysis-gas chromatography-mass spectrometry (Pyr-GC-MS), provide mass related data. Here, a sample is pyrolyzed, and the resulting decomposition products are separated in a chromatographic column and analyzed based on their masses. It also allows for the simultaneous detection of a vast range of compounds in the sample, thus, GC-MS methods can analyze PWs (Kienhuis et al., 2018). Initially, Pyr-GC-MS was applied to analyze preselected particles (e.g. Fries et al., 2013). Recent developments of methods even provide mass concentrations of eight to ten common plastic polymer types in processed environmental bulk-samples (Fischer & Scholz-Böttcher, 2017, 2019; Gomiero et al., 2019). Furthermore, suitable Pyr-GC-MS procedures have been identified to analyze and quantify car tire treads in environmental matrixes (Lachowicz et al., 2012; Unice et al., 2013).

A point many researchers agree on is that, also in the light of environmental risk management, it is essential to record, apart from MP concentrations in terms of numbers and masses, certain properties of theirs like polymer type, shape, surface properties and size (Potthoff et al., 2017).

Identifying the polymer type might help to understand the behavior of MP in the marine environment. The density of MP is related to the polymer type, which is a key factor concerning especially vertical transport mechanisms because it determines which MP are more likely to sink in seawater and which are more likely to float (Crawford & Quinn, 2017b). However, the density does not only depend on the pristine polymer type but also on additives that give the plastics certain desirable properties like color by adding pigments or heat-resistance through flame retardants etc. (Hahladakis et al., 2018; Hermabessiere et al., 2018). Concerning this, some polymer types can be considered more problematic than others, e.g. polyvinyl chloride (PVC), PS, polyurethane (PUR), and polycarbonate (PC), since they partially consist of

potentially harmful materials, like plasticizers, and on top, are also more difficult to recycle (Lithner et al., 2011; Rochman et al., 2013). These added chemicals have the potential to be taken up by marine organisms and transferred to their tissue (Hermabessiere et al., 2017). In this regard, it is an advantage of GC-MS-based analytical techniques that, unlike by FTIR and Raman spectroscopy, not only the polymer backbone is identified but also additives contained in the plastic. This advantage extends to adsorbed pollutants, which also can evoke adverse effects in organisms. Regarding the absorption of these pollutants like persistent organic pollutants (POPs), the size, shape and surface properties play important roles (Crawford & Quinn, 2017c). This is because the adsorption capacity is directly related to the surface area available. The surface area of irregularly shaped MP is relatively large compared to their respective size and volume. Furthermore, the surface area can also increase due to weathering (i.e. small cracks form on the surface of the particle) or biofouling. With respect to size, the smaller a particle, the larger is its surface-area-to-volume ratio and consequently its capacity to adsorb POPs.

Additionally, size becomes especially important when transport mechanisms within the marine environment, uptake through various organisms and translocation into tissues within the organism are concerned. The size of a particle defines whether it falls into the prey range of certain organisms. The smaller the particles are, the more likely they are available for a larger number of small-sized animals. The latter are at the basis of the marine food web or play critical ecological roles within it (Wright et al., 2013; Lusher, 2015; Galloway et al., 2017). Moreover, Lehtiniemi et al. (2018) showed in their feeding experiments that, next to the concentration, the size of the MP particles used in ecotoxicology studies has a more significant impact than the shape.

Since all of these characteristics will influence the fate and behavior of MP in the marine environment to a certain degree, it is of high importance to assess as many of these when analyzing MP in environmental matrices (Potthoff et al., 2017; Hartmann et al., 2019; Kögel et al., 2020).

The fate of MP in the marine environment

Concordantly, MP are considered ubiquitous in the marine environment. The occurrence of MP have been recorded all over the globe in surface waters (e.g. Lusher et al., 2015b; Cabernard et al., 2018; Vianello et al., 2018; Tekman et al., 2020), the water column (e.g. Bagaev et al., 2017; Choy et al., 2019; Tekman et al., 2020), sublittoral sediments (e.g. Claessens et al., 2013; Vianello et al., 2013; Bergmann et al., 2017; Gomiero et al., 2019), beaches (e.g. Dekiff et al., 2014; Stolte et al., 2015), various biota (e.g. van Franeker et al., 2011; Lusher et al., 2015a; Rummel et al., 2016; Duncan et al., 2019; Piarulli et al., 2019),

arctic sea ice (Obbard et al., 2014; Peeken et al., 2018) and recently also in the sea spray (Allen et al., 2020). It is widely assumed that most of the marine plastic litter, about 80%, reach the ocean from land-based sources while the other 20% originate from sea-based sources (e.g. Andrady, 2011; Li, W. C., 2018). Sea-based sources include mainly derelict fishing gear (e.g. Wilcox et al., 2014), aquaculture related litter (e.g. (Hinojosa & Thiel, 2009) and paraffin (e.g. Suaria et al., 2018). Regarding land-based sources, mismanaged waste is considered as most significant source (Jambeck et al., 2015), but also sewage and stormwater from highly industrialized urban environments contribute substantially. Furthermore, rivers are considered to present the major pathway of (micro)plastics into the marine environment (e.g. Schmidt et al., 2017). Recently, atmospheric transport and deposition have been shown to contribute as well (e.g. Bergmann et al., 2019; Liu, K. et al., 2019a; Brahney et al., 2020).

As pointed out before, MP can either be introduced as such (primary MP) or form in the marine environment through fragmentation of larger plastic litter (secondary MP). Regardless of their origin, MP are subject to environmental degradation, which is defined as “a chemical change in the polymer brought about by environmental factors” (Andrady, 1994). There exists a number of degradation mechanisms. One of these is biodegradation, which is caused by organisms such as fungi and bacteria (Andrady, 1994). Several microorganisms have demonstrated the potential to degrade certain polymer types (Crawford & Quinn, 2017a). Among these were also several marine bacteria isolated from water samples that had a degrading effect on polyethylene (Harshvardhan & Jha, 2013). However, under marine conditions, the effects of biodegradation are much slower and less pronounced compared to the other abiotic degradation mechanisms (Andrady, 2011). The effect of abiotic factors on synthetic polymers is commonly referred to as **weathering** (Searle, 2005). One mechanism induced by high temperatures is thermal degradation, which can be neglected in the marine environment as well as hydrolysis (Andrady, 2011). The other two more essential mechanisms, which are frequently interlocked, are photo- and thermooxidative degradation (Andrady, 2011; Crawford & Quinn, 2017a). The starting point is usually provided by photo-oxidative degradation, which creates an increase in oxygenated moieties, like carboxylic acids, ketones and esters that contribute to the carbonyl signal in the wavenumber region $1850\text{--}1650\text{ cm}^{-1}$ and can be assessed using FTIR spectroscopy (Ter Halle et al., 2017b). Based on this carbonyl signal, compared to the absorbance of a reference band of the spectrum, the carbonyl index, also considered as an ageing index, is used to assess the progress of oxidation (Guadagno et al., 2001). Photo- and thermooxidative degradation will form cracks in the surface of the MP (Ter Halle et al., 2016; Andrady, 2017). Breakdown of the brittle plastics will be facilitated by mechanical stress exhibited by waves and abrasion with sand (Crawford & Quinn, 2017a). However, fragmentation does not always occur in the form that a particle is split into several

pieces. Since the embrittlement is usually strongest at the particle surface, Andrady (2017) hypothesized a surface-ablation mode of MP resulting in the parent particle shedding smaller sized, most probably relatively flat, MP. Laboratory experiments have shown that the number of particles produced from fragmentation increases exponentially with decreasing particle size (e.g. Song et al. 2017).

Weathering can change the coloration of MP (i.e. yellowing, discoloration) and will alter their surface structure and properties eventually providing a larger area for biofilm formation (Guo & Wang, 2019). In the marine environment, any surface is readily covered by a biofilm and this “biofouling” will affect the sinking behavior of MP since it will influence their apparent densities (Dobretsov, 2010; Rummel et al., 2017). Generally, the main factor driving the **vertical transport** is the density of the particles. The density, however, depends on the polymer type and additives but is also influenced by biofouling (Lobelle & Cunliffe, 2011). Other factors affecting the sinking behavior of particles are size and shape (e.g. Kowalski et al., 2016; Chubarenko et al., 2018a).

Regarding particle size, Stolte et al. (2015) highlighted that for particles smaller 1 mm the density is of less importance because the particle might be held afloat by surface tension. However, most MP will rarely persist in the marine environment as freely floating particles but will be trapped with transparent exopolymer particles (TEP) as marine aggregates (Andrady, 2017).

To a certain degree, horizontal transport is also influenced by the density since MP floating at the sea surface are more readily transported over longer distances driven by wind ocean currents and the proximity to the coast (Li, W. C., 2018). Both transport mechanisms influence the spatial distribution of MP in the marine environment.

The North Sea and its history with (micro)plastics

The North Sea is a shallow shelf sea connected to the North Atlantic Ocean via the English Channel in the south-west and the Norwegian Sea in the north. Especially south of the Dogger Bank, beneath 54 °north latitude, water depth is usually below 40 m (Howarth, 2001). The catchment area of all the European rivers that discharge into the Southern North Sea amounts to 652800 km² (OSPAR, 2000). The main rivers included in this are the Elbe, Weser, Rhine, Scheldt, Meuse, Thames and Humber, which are all passing through industrialized regions (Howarth, 2001). The yearly freshwater run-off from these streams is considered to be 164–198 km³ and amounts to 296–354 km³ when taking the whole North Sea area into account (OSPAR, 2000). This is augmented by the freshwater coming from the Baltic Sea and then mixed with the annual input of 55000 km³ of oceanic water (Otto et al., 1990). For the Southern North Sea, the substantial input of oceanic water with high salinities is coming from the English

Channel through the Strait of Dover in the south-west and is according to (Howarth, 2001) of an average input flow of about 0.1 Sv. While the inflow of Atlantic water from the North Atlantic Channel is considerably more significant than the input from the south, its strong influence is limited to the north and central parts of the North Sea (Emeis et al., 2015).

The North Sea is a very dynamic system, dominated by wind-driven circulation and tides. The dominant state is a strong cyclonic (counterclockwise, CCW) circulation driven by prevailing westerly winds (Sündermann & Pohlmann, 2011). As stated by Howarth (2001), the inflow through the English Channel is also heavily influenced by the wind and can, when the westerly winds abate, even be reversed. The longterm circulation is additionally affected by the salinity and, thereby, density distribution (Howarth, 2001). Being a coastal system, the North Sea shows a gradient from more brackish conditions close to the estuaries, river mouths at the land interface (mostly in the south and the east) to oceanic conditions in the more open and deeper northern part of the basin (Emeis et al., 2015). Due to this density gradient combined with the tidal influence and the dominant wind-driven circulation, a frontal system along the continental coast is set up. Alongside these fronts, the prevalent coastal flow is from the Strait of Dover into the German Bight and then northward across Denmark and entering the Norwegian Coastal Current (Howarth, 2001). This current also coincides with the major shipping routes through the North Sea making especially the southern part a marine environment with a strong anthropogenic input.

Moreover, the North Sea also contains particular ecological regions like the Wadden Sea and the Dogger Bank. To manage, monitor and assess activities in this marine environment on a regional level is the role of the Convention for the Protection of the Marine Environment of the North-East Atlantic, commonly known as OSPAR convention (OSPAR, 1992, 2010). The Greater North Sea is considered as Region II of the OSPAR maritime area (OSPAR, 2000). The work done by OSPAR is further complemented by the aforementioned MSFD, which since 2008 introduced new rules to achieve “good environmental status” of European waters by 2020. The MSFD takes into account several stressors, among others marine litter (Descriptor 10), and consequently, also macroplastic debris and MP (Galgani et al., 2010; Galgani et al., 2013; Hanke et al., 2013).

It was back in the 1970s and 1980s that (micro)plastics were first recorded in the North Sea and the adjacent European Shelf Seas. Morris and Hamilton (1974) detected PS spheres in the Bristol Channel, a part of the Celtic Sea connected to the North Sea via the English Channel. Holmström (1975) recorded the presence of LDPE films on the bottom of the Skagerrak, which connects the North Sea with the Baltic Sea. Dixon and Dixon (1983) provided the first survey of plastics, as part of marine litter, floating in North Sea surface waters. Another

survey of this kind was conducted three decades later by Thiel et al. (2011) in the German Bight. The seafloor was investigated for marine litter by trawling in an intensive survey of European Coastal waters by Galgani et al. (2000). More recently, Gutow et al. (2018) investigated marine litter floating at the sea surface as well as covering the seafloor of the south-eastern North Sea. Concerning MP, there has been a couple of studies focusing on specific regions. Along the German coast, MP were detected in the Wadden Sea floating in the Jade bay, which is connected to the Weser estuary (Dubaish & Liebezeit, 2013), as well as on beaches of the East Frisian Island Norderney (Fries et al., 2013; Dekiff et al., 2014). Furthermore, Leslie et al. (2011) documented the presence of MP in the Dutch marine environment. A first baseline study on MP in the broader area of the North Sea has been conducted by Maes et al. (2017b). Apart from surface water samples from net trawls, also sediment samples were taken. However, this specific survey was not conducted at the same stations.

Thesis Aims

Marine pollution in the form of petroleum-based pollutants like MP and PWs has been recognized as an emerging threat globally. The ubiquity of these pollutants has been recorded in an increasing number of studies during the past decades. Due to their widespread prevalence and potential impacts on the marine environment, legal frameworks have been initiated to hamper their further increase and monitor their occurrence in the environment. In particular, the European Marine Strategy Framework Directive (MSFD) specifically targets European waters, among which falls the North Sea. As a coastal system subjected to important riverine inputs, the North Sea is susceptible to a wide range of land-based sources of marine pollution and in being a densely navigated sea, ship-based sources alike. This anthropogenically highly impacted shelf sea has thus been investigated for marine pollutants over a couple of years.

However, most studies investigating plastics in the North Sea have only focused on plastic particles larger 5 mm (meso- and macroplastics), or, when focusing on MP, these studies were either restricted to a small region or have riveted on one compartment only (i.e. surface water or sediment). Moreover, all previous studies relied on a visual pre-selection of putative MP and confirmed at most a sub-sample of these via chemical identification techniques.

Thus, the aim of my PhD thesis was to analyze the spatial distribution of MP (11–5000 μm) in surface waters and sediments of the southern North Sea. This was achieved by applying state-of-the-art methods allowing for the unambiguous identification of visually pre-selected large MP (500–5000 μm) and of small MP (11–500 μm) via FPA-based FTIR imaging, independent from visual pre-selection. Furthermore, through this approach, MP properties that influence the behavior of the particle in the marine environment, namely polymer type, size distribution and weathering status, were assessed in detail. Another aim was to investigate other petroleum-based semi-solids than MP, i.e. PWs, and to determine whether a common monitoring strategy for floating petroleum-based pollutants is feasible. Lastly, considering the potential of sublittoral sediments to accumulate MP, sediment samples of an urban Norwegian fjord, adjacent to the North Sea, were analyzed for MP and compared to the results of southern North Sea sediments. Harmonized methods were applied to facilitate a comparison between the two study areas.

Hence, in the framework of this thesis, the following research questions are addressed in individual chapters:

Chapter I – “Spatial distribution of microplastics in sediments and surface waters of the southern North Sea”

- (1) Do parameters such as polymer type and size class differ significantly between MP sampled from surface waters and sediments?
- (2) If so, which of the polymer types and size classes contribute most to these differences?
- (3) Do spatial patterns driven by polymer composition or size distribution exist within each of the two sampled compartments?

Chapter II – “Assessing the weathering status of marine microplastics in the southern North Sea – A multivariate approach”

- (1) Do carbonyl indices of MP differ considering the sampled compartment (surface water and sediment)?
- (2) Do carbonyl indices of MP differ between size classes?
- (3) Are there significant differences in the full range FTIR spectra ($3600\text{--}1250\text{ cm}^{-1}$) of MP sampled from the two compartments and when compared to reference spectra?
- (4) Which wave number regions in the spectra, apart from carbonyl groups ($1750\text{--}1650\text{ cm}^{-1}$), might be alternative indicators for weathering?

Chapter III – “Paraffin waxes in the southern North Sea”

- (1) Can PWs floating in surface waters be collected with nets utilized for MP sampling?
- (2) Are methods that are applied for MP analysis, such as ATR-FTIR or gas chromatography-based methods, suitable to analyze PWs, and which is the more suitable?

Chapter IV – “Different stories told by small and large microplastics in sediment – first report of microplastic concentrations in an urban recipient in Norway”

- (1) How are MP concentration ranges compared to other studies using unbiased state-of-the-art analysis methods?
- (2) How does the spatial distribution pattern coincide with the current system and organic matter contents at the sampling sites?

Outline of the thesis

The present thesis consists of a general Introduction, four Chapters, and a general Discussion and Outlook. The chapters represent one manuscript each which has been either published (Manuscript I, IV), submitted (Manuscript III) or is about to be submitted (Manuscript II).

Manuscript I (published in *Environmental Pollution*, September 2019)

Lorenz, C., Roscher, L., Meyer, M.S., Hildebrandt, L., Prume, J., Löder, M.G.J., Primpke, S. & Gerdt, G.

Spatial distribution of microplastics in sediments and surface waters of the southern North Sea

Environmental Pollution 252(B): 1719-1729. doi: <https://doi.org/10.1016/j.envpol.2019.06.093>

This manuscript investigated the spatial distribution patterns of microplastics (MP) in sublittoral sediment and surface water samples at 24 stations in the southern North Sea. Samples were processed using an approach with enzymatic maceration and oxidation in newly developed MP reactors as well as density separation. MP in a size range of 11–5000 μm were analyzed using Fourier transform infrared spectroscopy (FTIR). All analyzed samples contained MP in concentrations ranging between 2.8–1188.8 particles kg^{-1} in sublittoral sediments and 0.1–245.4 particles m^{-3} in surface waters. Furthermore, it was revealed that the great majority of MP in sediments (98%) and surface waters (86%) were smaller 100 μm and that the diversity of the polymer composition increased with decreasing MP particle size. This important finding highlights the importance of analyzing MP in environmental samples down to small sizes (<500 μm) to get a realistic view on MP contamination and consequently risk assessment in the marine environment.

Sampling was planned and conducted by Dr Martin G.J. Löder and Dr Gunnar Gerdt in 2014. Claudia Lorenz together with the master students Lisa Roscher, Melanie S. Meyer, Lars Hildebrandt, and Julia Prume carried out the sample processing and FTIR analysis under the guidance of Dr Sebastian Primpke and Dr Gunnar Gerdt. Claudia Lorenz conducted the data analysis and writing of the manuscript under the guidance of Dr Sebastian Primpke und Dr Gunnar Gerdt. All authors commented on the manuscript and approved of the final version.

Manuscript II (to be submitted to *Chemosphere*)

Lorenz, C., Primpke, S. & Gerdts, G.

Assessing the weathering status of marine microplastics in the southern North Sea – A multivariate approach

This manuscript presents an in silico study utilizing a comprehensive dataset of spectral data to analyze the weathering status of microplastics (MP) in the southern North Sea. Fourier-transform Infrared (FTIR) spectra of MP in a size range of 11–5000 µm, extracted from several surface water as well as sediment samples, were analyzed. The respective carbonyl indices for MP identified as polyethylene (PE) and polypropylene (PP) were determined and significant differences for MP extracted from the two different compartments were found. When analyzing the fully recorded spectral range of the PP and PE particles, as well as MP identified as polystyrene (PS) and polyvinyl chloride (PVC), significant differences were found between the naturally weathered MP compared to pristine plastics. The differences when comparing spectra associated with the two different compartments were less prominent and present mainly in the spectral range of carbonyl and hydroxyl groups. The main outcome is that the carbonyl index provides a good insight on the weathering status but taking other wavenumber regions of the spectra into account might provide further information.

Data evaluation and manuscript writing were carried out by Claudia Lorenz under the guidance of Dr Sebastian Primpke and Dr Gunnar Gerdts.

Manuscript III (submitted to *Marine Pollution Bulletin*, July 2020)

Lorenz, C., Schafberg, M., Roscher, L., Meyer, M.S., Primpke, S., Kraus, U.R. & Gerdts, G.

Paraffin waxes in the southern North Sea

This manuscript describes the occurrence of paraffin waxes (PWs), petroleum-based semi-solid pollutants, floating in southern North Sea surface waters. The study highlights the advantageous use of two complementary techniques, Attenuated total reflectance Fourier-transform infrared spectroscopy (ATR-FTIR) and gas chromatography coupled with a flame ionization detector (GC-FID) as well as GC coupled with mass spectrometry (GC-MS). The study revealed that PWs were present at several stations throughout the southern North Sea and the particles consisted not solely of paraffin but contained also other compounds like fatty acids and lubricants.

Claudia Lorenz together with the master students Lisa Roscher and Melanie S. Meyer performed the sample processing and ATR-FTIR analysis. Michaela Schafberg carried out the

GC-FID and GC-MS analysis under the guidance of Dr Uta R. Kraus. The manuscript was written by Claudia Lorenz under the guidance of Dr Sebastian Primpke and Dr Gunnar Gerds. All authors commented on the manuscript and approved of the final version.

Manuscript IV (published in Marine Pollution Bulletin, April 2019)

Haave, M., Lorenz, C., Primpke, S. & Gerds, G.

Different stories told by small and large microplastics in sediment – first report of microplastic concentrations in an urban recipient in Norway

Marine Pollution Bulletin 141: 501-513. doi: <https://doi.org/10.1016/j.marpolbul.2019.02.015>

The manuscript presents the first report of MP concentrations in a size range of 11–5000 µm in sediments of an urban Norwegian fjord. The concentrations were quite high and ranged from 12×10^3 to 2×10^5 particles per kg dry weight sediment. MP smaller 100 µm were most frequent (95%). Concentrations as well as polymer composition differed significantly between small MP (11–500 µm) and large MP (500–5000 µm) highlighting that future monitoring attempts should strive for reporting data on small MP.

Dr Marte Haave conducted the sampling and sample preparation. Claudia Lorenz carried out the stereomicroscopic imaging, ATR-FTIR analysis and µFTIR imaging under the guidance of Dr Sebastian Primpke and Dr Gunnar Gerds. Data analysis was performed by Dr Marte Haave and Dr Sebastian Primpke together with Claudia Lorenz. The manuscript was written by Dr Marte Haave with the input from Claudia Lorenz, Dr Sebastian Primpke under the guidance of Dr Gunnar Gerds.

Chapter I

Spatial distribution of microplastics in sediments and surface waters of the southern North Sea

Claudia Lorenz^{*,a}, Lisa Roscher[†], Melanie S. Meyer^a, Lars Hildebrandt^{a,b}, Julia Prume^{a,c}, Martin G. J. Löder^d, Sebastian Pimpke^a and Gunnar Gerds^{*,a}

^a Department of Microbial Ecology, Biologische Anstalt Helgoland, Alfred Wegener Institute, Helmholtz Centre for Polar and Marine Research, Kurpromenade 201, 27498 Helgoland, Germany

^b Department for Marine Bioanalytical Chemistry, Helmholtz Centre Geesthacht, Centre for Materials and Coastal Research, Max-Planck Str. 1, 21502 Geesthacht, Germany (present addresse)

^c Department of Physics, Philipps University of Marburg, Hans-Meerwein-Straße 6, 35043 Marburg, Germany (present addresse)

^d Department of Animal Ecology I and BayCEER, University of Bayreuth, Universitätsstraße 30, 95440 Bayreuth, Germany

*Corresponding authors:

Claudia Lorenz: claudia.lorenz@awi.de

Gunnar Gerds: gunnar.gerds@awi.de

Published in *Environmental Pollution* 252(B): 1719-1729.

doi: <https://doi.org/10.1016/j.envpol.2019.06.093>

Abstract

Microplastic pollution within the marine environment is of pressing concern globally. Accordingly, spatial monitoring of microplastic concentrations, composition and size distribution may help to identify sources and entry pathways, and hence allow initiating focused mitigation. Spatial distribution patterns of microplastics were investigated in two compartments of the southern North Sea by collecting sublittoral sediment and surface water samples from 24 stations. Large microplastics (500–5000 μm) were detected visually and identified using attenuated total reflection (ATR) Fourier transform infrared (FTIR) spectroscopy. The remaining sample was digested enzymatically, concentrated onto filters and analyzed for small microplastics (11–500 μm) using Focal Plane Array (FPA) FTIR imaging. Microplastics were detected in all samples with concentrations ranging between 2.8–1188.8 particles kg^{-1} for sediments and 0.1–245.4 particles m^{-3} for surface waters. On average 98% of microplastics were <100 μm in sediments and 86% in surface waters. The most prevalent polymer types in both compartments were polypropylene, acrylates/polyurethane/varnish, and polyamide. However, polymer composition differed significantly between sediment and surface water samples as well as between the Frisian Islands and the English Channel sites. These results show that microplastics are not evenly distributed, in neither location nor size, which is illuminating regarding the development of monitoring protocols.

Keywords: FTIR imaging; microplastic; enzymatic sample treatment; polymer diversity; spatial distribution patterns

Capsule

Microplastic concentrations and compositions differ significantly between environmental compartments. Geographic distribution patterns are revealed by a statistical approach. Microplastics <500 μm are more abundant and diverse than >500 μm ones, rendering the exclusive analysis of later ones insufficient for environmental risk assessment.

Introduction

Increasing plastics production and improper disposal have consequently led to an input of plastics into the marine environment which has been quantified to up to 12 million tons worldwide in 2010 (Jambeck et al., 2015). Once plastics reach the oceans, they are almost impossible to remove and merely disintegrate by chemical, physical and biological processes over time into smaller and more numerous microplastics (MP, <5 mm (Arthur et al., 2009)). Due to its ubiquity and longevity, plastic pollution in the marine environment has been recognized as a threat globally and is one of the “novel entities” referred to in the planetary boundaries concept (Rockström et al., 2009; Steffen et al., 2015; Villarrubia-Gómez et al., 2018). Moreover, marine pollution has been included in descriptor 10 (marine litter) in the European Marine Strategy Framework Directive (MSFD) 2008/56/EC (European Parliament Council, 2008; Galgani et al., 2010). More recently the issue of MP and the monitoring criteria of MP have been established by the EU Commission decision 2017/848 of 17 May 2017 (European Commission, 2017).

With decreasing particle size, the unambiguous identification of polymer type becomes more challenging. As of yet, no universally accepted standard operating procedure (SOP) exists, the harmonization of methods is urgently needed to allow for a comparison of data (Hidalgo-Ruz et al., 2012; Löder & Gerdt, 2015; Rochman et al., 2017).

According to Kroon et al. (2018) a merely visual identification of the potential MP particles is not sufficient. More than 60% of the particles might be misassigned (Hidalgo-Ruz et al., 2012; Kroon et al., 2018), if results are not validated by chemical identification. According to Rivers et al. (2019), a meaningful inter-study comparison requires not only data on particle number but also on particle size. As stated by Potthoff et al. (2017) it is very important to gain as much information as possible from MP particles, including number, polymer type, shape, size distribution and weathering status, to do a qualified risk assessment. This stresses the need to use spectroscopic methods, which can provide this information.

In this study, we aimed to gain a valuable insight into the spatial distribution of MP in the southern North Sea, in terms of the MP concentrations, polymer types and size classes. To achieve this, we sampled two marine compartments, sediments and surface waters, at 24 stations. We employed state-of-the-art techniques to extract MP and analyze samples based on attenuated total reflection (ATR) Fourier transform infrared (FTIR) spectroscopy and focal plane array (FPA) based FTIR imaging. In the present study we also applied a novel approach based on uni- and multivariate statistics to investigate the questions: (1) Do MP metric parameters differ significantly between the two sampled compartments?; (2) Which polymer

types and size classes contribute most to these differences?; (3) Do spatial patterns driven by polymer composition or size distribution exist within each compartment?

In this study we applied innovative analytical techniques to expand the field of environmental MP research and to generate assured and comparable data for the ongoing development of MP monitoring strategies.

Materials and Methods

Sampling

Sampling was conducted during a survey aboard the RV Heincke (He430) in the southern North Sea between the 30th of July and the 11th of August 2014. Sediment and water samples were taken at 24 stations (Figure 3, Supporting Information (SI) Table S1). Surface water was sampled using a Neuston Catamaran (HydroBios Apparatebau GmbH) towed alongside the vessel for up to 20 min. The attached net had an opening of 0.15 m × 0.30 m and a mesh size of 100 µm, capturing particles >100 µm but also smaller particles trapped in aggregates and due to clogging of the mesh during sampling. The sampled water volume and surface area were determined by a mechanical flowmeter (HydroBios Apparatebau GmbH) mounted at the opening of the net (SI Table S1). All materials collected in the cod end were rinsed into a 1-L Kautex-bottle (polyvinyl chloride with polyethylene containing lit, Kautex Textron GmbH & Co KG). Sediment samples were taken with a Van-Veen grab deployed at each station, with the upper 5 cm of the sediment transferred into 1-L Kautex-bottles with a metal spoon. All samples were immediately stored at -20 °C until further processing in the lab.

MP extraction from sediment and surface water samples

Multiple steps were taken to remove natural organic and inorganic matter to facilitate effective MP analysis. Measures for contamination prevention during sample processing are described in the SI Paragraph S1. Sediment samples of around 2 kg wet weight each were defrosted, transferred into glass jars, and then homogenized. Triplicates of approximately 5 cm³ each were taken to determine the dry weight of each sediment sample. Extraction of MP from the remaining sediments was performed using the MicroPlastics Sediment Separator (MPSS, HydroBios Apparatebau GmbH) with a high density zinc chloride solution (ZnCl₂, $\rho=1.7 \text{ g cm}^{-3}$) (Imhof et al., 2012). The general procedure of density separation followed the methodology of Bergmann et al. (2017) and Haave et al. (2019) and is shortly described in the SI Paragraph S2.

A size fractionation of each sample was conducted, as sample processing and analytical approaches varied for different MP size categories. The extracted sediment samples and the defrosted surface water samples were screened over a 500-µm stainless steel mesh (Haver & Boecker OHG). The material retained on the mesh was thoroughly rinsed with filtered water (Milli-Q, 0.2 µm), and Ethanol (30%) also to remove any residual ZnCl₂ in the case of the extracted sediment samples. This step divided the sample into two size fractions potentially containing particles of either >500 µm and <500 µm respectively.

All steps taken in the laboratory are displayed in a flow scheme (SI Figure S1), and are explained in the subsequent sections.

MP >500 μm

The >500 μm fraction was rinsed into a beaker and manually sorted in a Bogorov chamber under a stereo microscope (Olympus SZX16, Olympus) at a 100–320x magnification. All putative MP particles were transferred into glass petri dishes, photographed under the microscope (Olympus DP26 Digital Camera, Olympus) and measured (length at their longest dimension) using image analysis software (cellSens, Olympus).

MP <500 μm

The general approach to purify and extract MP from the <500 μm fraction followed the enzymatic-oxidative treatment published by Löder et al. (2017) which had proven effective for the degradation of a broad range of environmental matrices. This protocol was performed in newly developed Microplastic Reactors (Gerdt, 2017) (SI Figure S2). These semi-enclosed filtration units contain 20- μm stainless steel filters (Haver & Boecker OHG) and allow to add and remove solutions via vacuum and pressure filtration. Samples could be kept in the reactors and be exposed to the different chemical and enzyme treatment steps without requiring further sample transfers, by that reducing the risk of particle loss and sample contamination. The <500 μm sample fraction was transferred into the reactors before sodium dodecyl sulfate solution (SDS, 10%, Carl Roth) was added and the reactors were sealed and incubated at 50 °C for 24 hours. Following this, the technical enzyme purification steps with protease, cellulase and chitinase (ASA Spezialenzyme GmbH) as well as hydrogen peroxide (H_2O_2 , 35%, Carl Roth) were performed sequentially. The samples were incubated at optimal pH and temperature conditions for each step. Between treatments the samples were flushed and rinsed several times using Milli-Q. A more detailed description of the full multi-step procedure can be found in the SI Paragraph S3.

About two-thirds of the surface water samples ($n=16$), containing large amounts of biomass, were additionally treated with a Proteinase-K step after the second H_2O_2 treatment. The procedure was adapted from the protocol of Cole et al. (2014), using H_2O_2 instead of sodium perchlorate (NaClO_4).

Inorganic material (e.g. sand, calcium carbonate) was removed by a density separation performed in separation funnels containing ZnCl_2 ($\rho=1.7 \text{ g cm}^{-3}$). Over a period of usually one to three days ($n=30$), but in some cases extended to seven days ($n=16$), the denser materials settled to the bottom and were removed.

The upper phase of the density separation treatment, containing the lighter material, was passed through 20- μm stainless steel filters to remove the ZnCl_2 . The retained material was

transferred into 100-mL glass bottles by rinsing the filter with Milli-Q and stored for analysis. For FTIR measurement the processed sample needed to be transferred onto aluminum oxide filters (Anodisc, 0.2 μm , Whatman GmbH) (Löder et al., 2015). Each sample was concentrated onto a 13 mm diameter filter area, using in-house fabricated glass filter funnels and a vacuum filtration unit. Prior to this a FlowCam (Fluid Imaging Technologies) was used to determine a suitable subsample volume that could be applied onto the filter area without overloading it (SI Paragraph S4) (Bergmann et al., 2017). Based on the FlowCam assessments, aliquots ranging from 1.2–73.2% (surface water samples) and 10.8–75.4% (sediment samples) of the total sample volumes were taken by mixing the sample thoroughly and pipetting the determined volume on an aluminum oxide filter each (SI Table S2). The loaded filters were transferred into covered glass petri dishes and dried for 48 hours at 30 °C.

Identification and quantification of MP >500 μm using ATR-FTIR

All putative plastic particles were identified individually using an ATR-FTIR unit (Bruker Optik GmbH) with the exception of 30 particles which were analyzed within an accompanying study by Cabernard et al. (2018) using Raman spectroscopy. The IR spectra were collected in the spectral range of 400–4000 cm^{-1} and compared against our reference library (Primpke et al., 2018). Particles with a match of at least 700 (out of 1000) were counted as safely identified. If the match ranged between 600 and 700 the spectra were manually compared to database spectra and evaluated based on expert knowledge, as suggested by other studies (Hanke et al., 2013; Lusher et al., 2013; Kroon et al., 2018).

Spectral analysis of MP <500 μm using FTIR imaging

Particles of the smaller size fraction were analyzed using a FTIR-microscope (Hyperion 3000 coupled to a Tensor 27 spectrometer, Bruker Optik GmbH) equipped with a 15x objective and a focal plane array (FPA) detector. Settings for the measurements were similar to previous studies (Löder et al., 2015; Bergmann et al., 2017; Mintenig et al., 2017; Primpke et al., 2017b; Peeken et al., 2018; Primpke et al., 2018; Mintenig et al., 2019) defining the lower detection limit of 11 μm . Technically, during processing of the samples the lower size limit is defined by the mesh size of the filters. However, also smaller particles will have been captured allowing a semi-quantitative analysis of particles between 11 μm and 20 μm .

By measuring a grid of 77×77 (surface waters) or 78×78 (sediments) FPA fields, corresponding to a filter area of 184 mm^2 and 188 mm^2 , respectively, every particle was analyzed.

The FTIR imaging data were automatically analyzed following Primpke et al. (2017b) with the adaptable database design (Primpke et al., 2018). Based on the identified spectra a subsequent image analysis provided particle numbers, polymer types and size classes of all

identified particles. The threshold for this image analysis was set based on a manual spectra evaluation of a data-subset (SI Paragraph S5 and Table S3).

Data handling and statistical analysis

The MP counts of each analyzed filter were extrapolated to the respective sample based on the analyzed proportion (SI Table S2) and corrected for contamination recorded in procedural blank samples (n=6). The total amount of MP in both size fractions was combined and presented as MP per kg dry weight sediment (particles kg⁻¹ (DW)) or water volume sampled (particles m⁻³).

Percentages of polymer types and size classes were arcsine square root (univariate statistics) or square root transformed (multivariate statistics) (Sokal & Rohlf, 1995). The multivariate analyses were carried out based on Hellinger distance transformation, a recommended measure for ordination and clustering of (polymer) species abundance data, which does not put high weights on rare (polymer) species (Rao, 1995; Legendre & Gallagher, 2001). To assess the polymer diversity, species richness and Shannon-Wiener-index H' (log base e) was calculated. To test if samples from the two compartments (sediment, surface water) differed significantly in their polymer composition or size class distribution, permutational multivariate analysis (PERMANOVA) (Anderson & Walsh, 2013) with 999 permutations at a significance level of p<0.001 was applied. To visualize these differences cluster analysis and canonical analysis on the principal coordinates (CAP) (Anderson & Willis, 2003) were performed with PRIMER plus the add-on PERMANOVA+ (PRIMER-E version 7.013) (Clarke & Gorley, 2015).

Analyses of variances (ANOVA) was performed with Statistica 13 (Statsoft) to show which polymer types or size classes had the greatest influence on observed differences. To identify which stations of both compartments individually group in terms of polymer composition and size distribution a non-hierarchical clustering based on k-means and coupled to similarity profile test (SIMPROF, henceforth referred to as kR-clustering) was performed using PRIMER-7 on the basis of the Hellinger distance matrix with square root transformed data. The significance level for SIMPROF was set to 5% and performed with 999 permutations to define the optimal number of k-groups (between 2 and 10) to describe the clustering of the samples, which is based on maximizing R (Clarke & Gorley, 2015). An ANOVA followed by a Tukey HSD test was used to test the influence of each polymer type on the respective group.

Maps showing the geographical position of the samples along with the MP concentration, polymer composition and diversity as well as assigned groups were prepared using QGIS (version 3.2 'Bonn'). The displayed shoreline data was taken from the Global Self-consistent, Hierarchical, High-resolution Geography Database (GSHHS)

Chapter I

<https://www.ngdc.noaa.gov/mgg/shorelines/gshhs.html>, hosted by the National Oceanic And Atmospheric Administration (NOAA) by Wessel and Smith (1996).

RESULTS

Comparison of two size fractions of MP in sediment and surface water samples

Microplastics from 23 sediment and 23 surface water samples, out of 24 sampled stations, could successfully be extracted and analyzed. For each sample two size fractions (MP >500 μm and MP <500 μm) were analyzed separately and their results later combined for statistical analyses. The two size fractions differed considerably concerning polymer composition and size distribution. Overall, for MP > 500 μm , only one polymer type (polyester) was identified in sediment samples and eight different polymer types were found in surface water samples. Concerning MP <500 μm , 21 different polymer types were found in the sediment samples and 19 different polymer types in surface water samples.

In sediment samples only 0.04% of all detected particles were >500 μm while 99.96% were MP <500 μm . For surface water samples 6.02% of all the detected particles were >500 μm while 93.98% accounted for MP <500 μm . A selection of MP >500 μm detected in five surface water samples can be found in the SI Figure S3. Two examples of filters with MP <500 μm and their respective false color plot of one station for sediments and surface waters each are shown in the SI Figure S4.

Comparison of MP occurrence in sediments and surface waters of the southern North Sea

Combining both size fractions, MP concentrations in sediments ranged from 2.8 (station 11) to 1188.8 particles kg^{-1} (DW) (station 23) and for surface waters from 0.1 (station 22) to 245.4 particles m^{-3} (station 20) (SI Table S4, Figure 3).

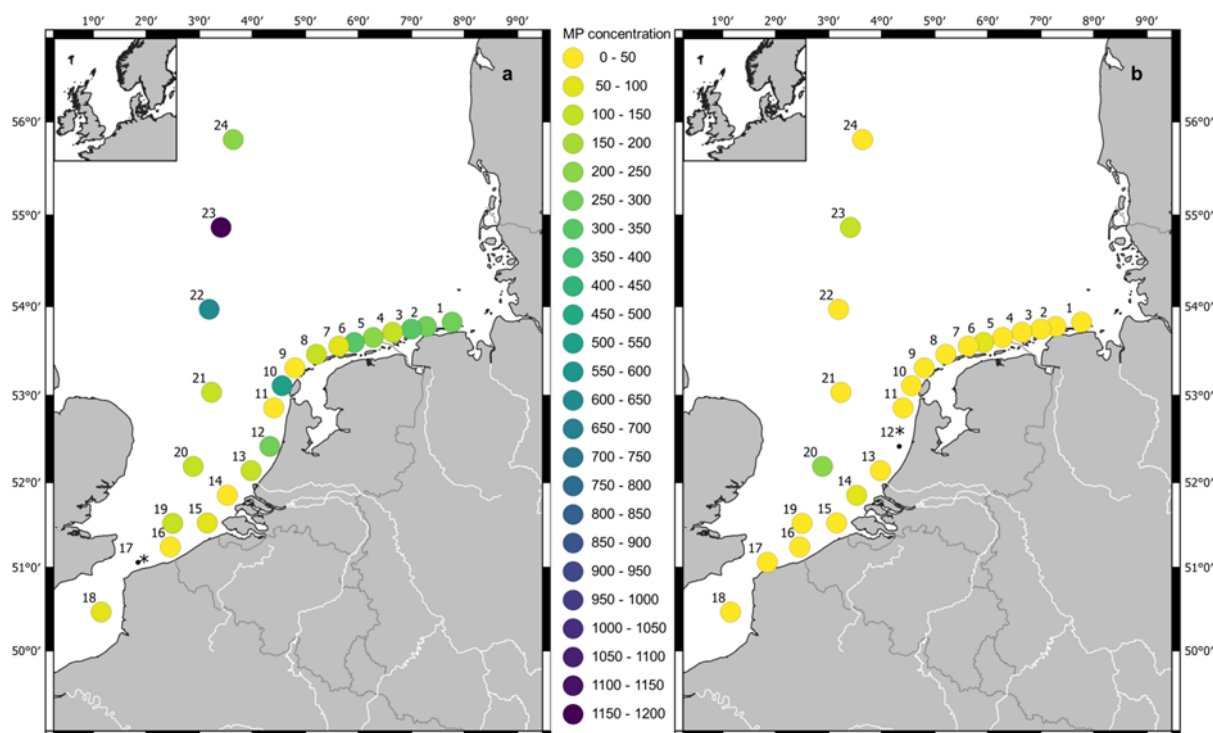


Figure 3: Geographic distribution of microplastic concentration in the southern North Sea. Microplastic concentration for sediment samples (a) reported in particles per kg and surface water samples (b) reported in particles per m³. Stations where no sample was analyzed are marked with *.

The two investigated compartments, sediments and surface waters, differed greatly regarding MP-concentration (Figure 3) and polymer composition (PERMANOVA, p -value=0.001, SI Table S5). This was also confirmed in the cluster analysis where samples from the same environmental compartment were grouped together (SI Figure S5). The separation of most of the samples into the two a priori defined groups, sediments and surface waters, was also supported by CAP, depicted in SI Figure S6, with a reasonably high correlation value of 0.89 and revealed six samples to be mismatched with a mis-classification error of 13.04%. Sediment samples from three stations (11, 18, and 21) were falsely allocated to surface waters and three surface water samples (stations 6, 22, and 23) were allocated to sediments. ANOVA was significant when comparing polymer richness and Shannon-Wiener index H' based on polymer types for both compartments (p -value=0.001) (SI Table S6). The spatial distribution of this polymer diversity is depicted in SI Figure S7. Figure 4 shows the relative polymer composition for sediments (Figure 4a) and surface waters (Figure 4b). The number of different polymer types in sediment samples was on average 11 and ranged between 3 (station 11) and 15 (station 1) with Shannon-Wiener index H' ranging between 0.89 (station 11) and 2.29 (station 5). For surface water samples on average 7 different polymer types were detected ranging from 1 (station 15) to 14 (stations 2, 6 and 17) with Shannon-Wiener index H' ranging from 0 (station 15) to 2.07 (station 17).

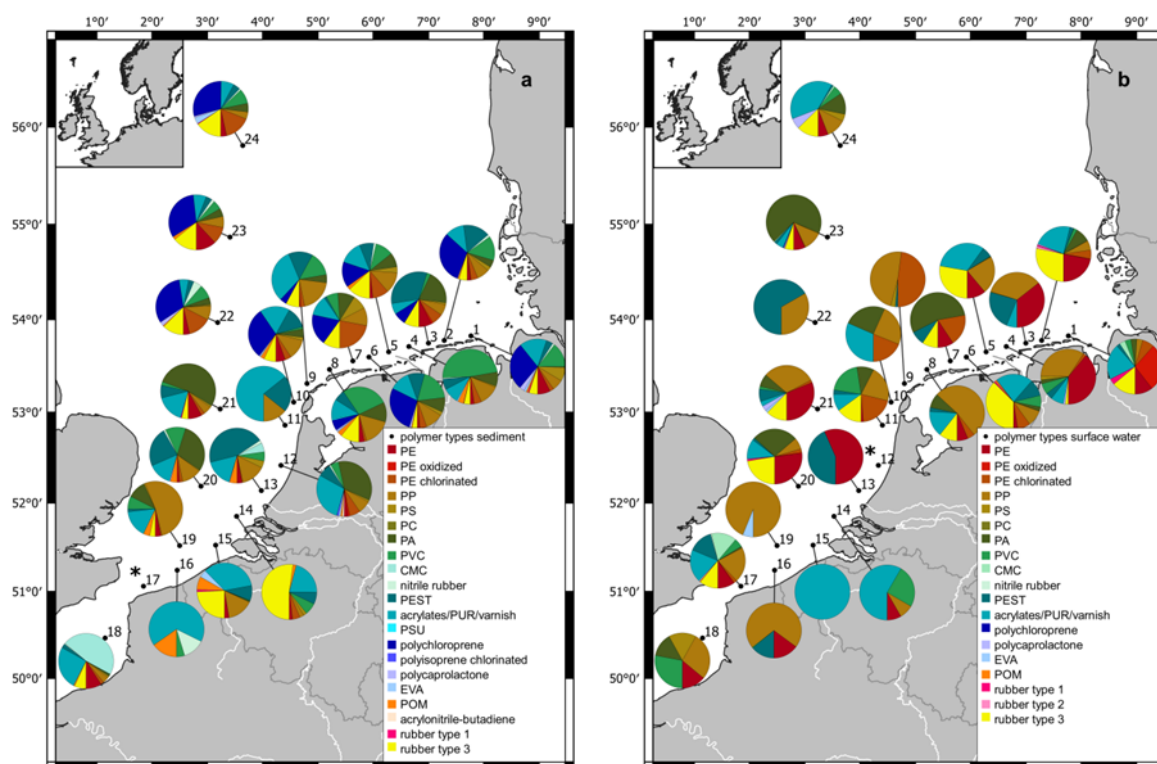


Figure 4: Spatial distribution of the relative polymer composition for sediment (a) and surface water samples (b). PE: polyethylene, PP: polypropylene, PS: polystyrene, PC: polycarbonate, PA: polyamide, PVC: polyvinyl chloride, CMC: chemically modified cellulose, PEST: polyester/polyethylene terephthalate, PUR: polyurethane, PSU: polysulfone, EVA: ethylene vinyl acetate, POM: polyoxymethylene. Stations where no sample was analyzed are marked with *.

Polyethylene (PE), polypropylene (PP), and polyester/polyethylene terephthalate (PEST) were present in more than 75% of all samples from both compartments. In sediment samples acrylates/polyurethane/varnish (acrylates/PUR/varnish) were omnipresent. Additionally to the aforementioned polymers, PE chlorinated, polystyrene (PS), polyamide (PA), polyvinyl chloride (PVC), and rubber type 3 were frequent. Figure 5 shows that, in sediment samples, 13 different polymer types contributed on average between 1.3% (nitrile rubber) and 21.0% (acrylates/PUR/varnish) to the polymer composition while eight polymer types contributed less than 1% (in descending order): ethylene vinyl acetate (EVA), polycaprolactone, rubber type 1, PE oxidized, polyisoprene chlorinated, acrylonitrile butadiene, polycarbonate (PC), and polysulfone (PSU). In surface water samples nine different polymer types contributed on average between 1.3% (PS) and 26.7% (PP) to the polymer composition while ten polymer types contributed less than 1% (in descending order): chemically modified cellulose (CMC), polycaprolactone, EVA, rubber type 1, polyoxymethylene (POM), PE oxidized, PC, nitrile rubber, rubber type 2, and polychloroprene (Figure 5). Furthermore, an ANOVA revealed the polymer types contributing most to the dissimilarity of surface water and sediment samples: PE (ANOVA, p -value=0.010), PP (ANOVA, p -value=0.042), PVC (ANOVA, p -value=0.007),

nitrile rubber (ANOVA, p -value=0.001), polychloroprene (ANOVA, p -value=0.000), and POM (ANOVA, p -value=0.000) (SI Table S7).

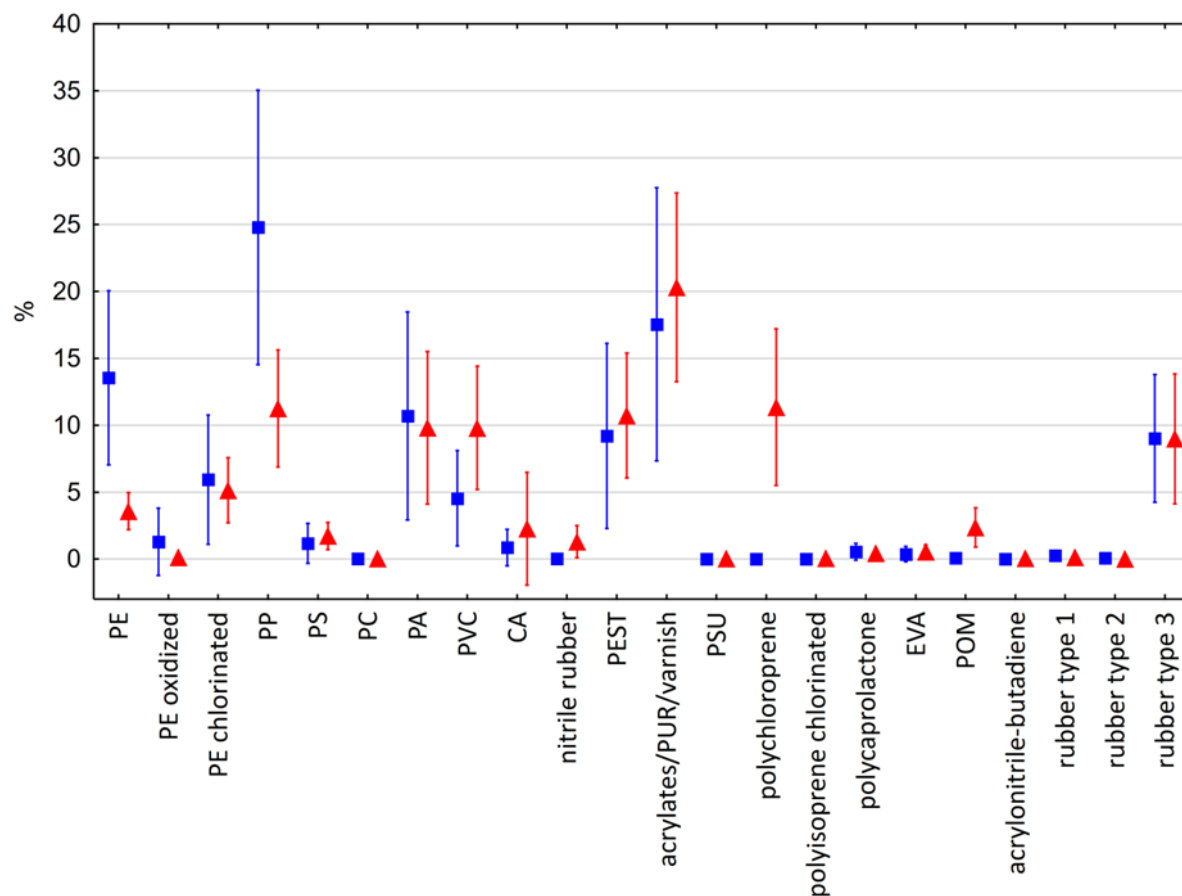


Figure 5: Mean percentage of each polymer type for sediment (red triangle) and surface water samples (blue square). PE: polyethylene, PP: polypropylene, PS: polystyrene, PC: polycarbonate, PA: polyamide, PVC: polyvinyl chloride, CMC: chemically modified cellulose, PEST: polyester/polyethylene terephthalate, PUR: polyurethane, PSU: polysulfone, EVA: ethylene vinyl acetate, POM: polyoxymethylene. Whiskers show the 95% confidence interval.

When comparing the size distribution (11–5000 μm) of polymers in sediment and surface water samples, they differed significantly (PERMANOVA, p -value=0.001) (SI Table S8). Cluster analysis revealed a higher variance in surface water than in sediment samples (SI Figure S8). This was highlighted by CAP which had a moderately large correlation value of 0.61 and revealed only surface water samples ($n=8$) to be mis-classified with a relatively low mis-classification error of 17.39% (SI Figure S9). Furthermore, in both compartments the size distribution of MP is clearly skewed towards the smallest size classes (Figure 6). The ANOVA for the individual size classes revealed that the average abundance of polymers in the size classes 25–50 μm (p -value=0.008) and 50–75 μm (p -value=0.007) was significantly higher for sediment than surface water samples. This was the opposite for size classes 500–1000 μm

(p -value=0.031), 2000–2500 μm (p -value=0.038), and 2500–3000 μm (p -value=0.004) (SI Table S9).

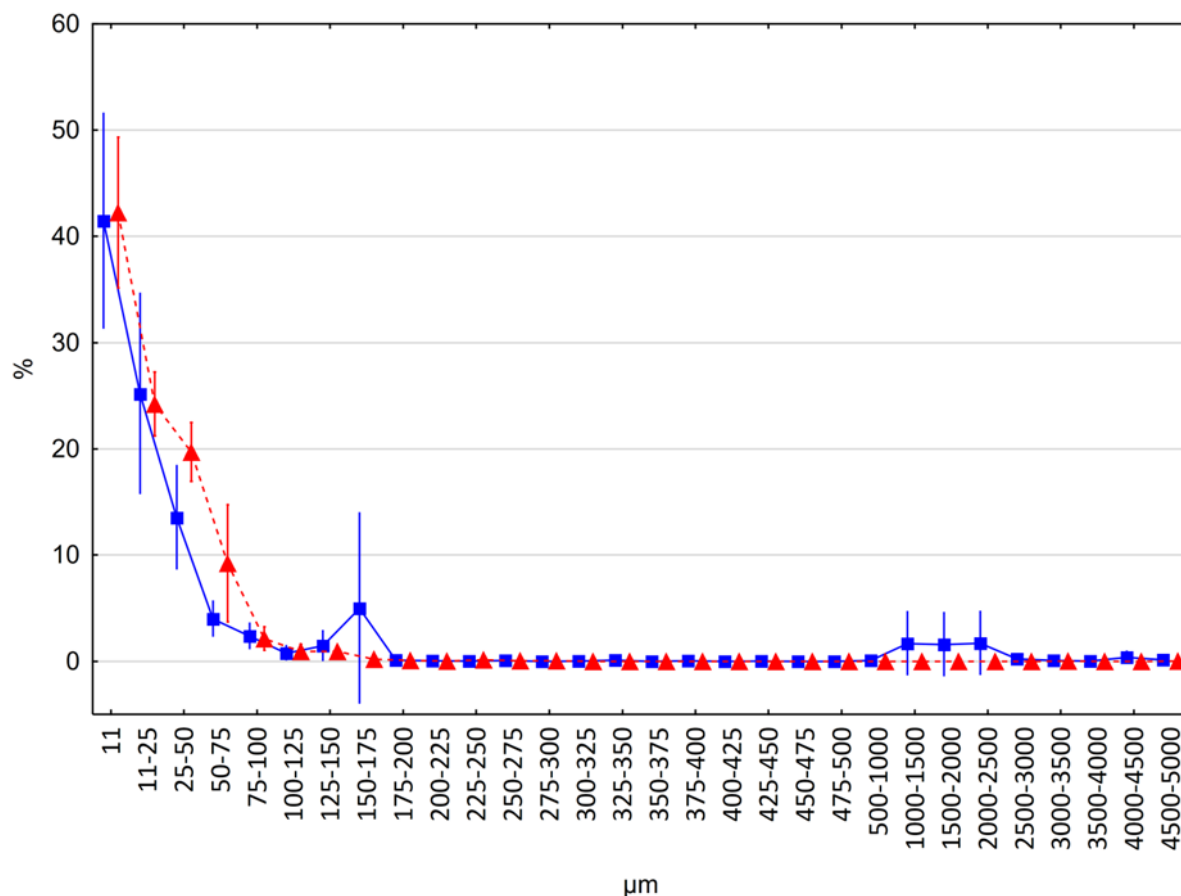


Figure 6: Mean percentage of each size class in μm for sediment (red triangle) and surface water samples (blue square). Whiskers show the 95% confidence interval.

Spatial distribution of MP occurrence in the southern North Sea

After confirming significant differences between the sediment and surface water compartments, intra-compartmental variations between sampling stations were investigated. A kR-clustering with SIMPROF was applied to highlight stations that were more similar concerning their polymer composition. Figure 7 shows the spatial distribution of these identified kR groups. Five groups (A–E) were found to best represent the clustering of sediment samples ($R=0.921$) (SI Figure S10) with most samples belonging to group D ($n=12$) (Figure 7a). Furthermore, the result of CAP reinforces the significant differences between the samples of the five groups with high correlation values (0.931–0.996) with only two samples being mis-classified (SI Figure S11). One sample from group C was mis-classified as belonging to group B (station 11) and one sample from group B was mis-classified as being part of group E (station 15) with a low mis-classification error of 8.70%. To discover which polymer types drive this clustering in sediment samples an ANOVA with a subsequent Tukey HSD was performed. This analysis revealed six polymer types that contributed significantly to the dissimilarity between the

grouped stations (SI Table S10), which are PE chlorinated, PA, CMC, acrylates/PUR/varnish, polychloroprene and rubber type 3. Polychloroprene dominated samples belonging to group D (n=12, stations 1–3, 5–10, and 22–24). Polyamide was preeminent for group E (n=5, stations 4, 12, and 19–21). Sediment samples from the Rhine-Meuse-delta (station 14, 15) belonged to group B (n=2) and were dominated by rubber type 3. Group C (n=2) was characterized by a low polymer diversity (station 11, 16) and the prevalence of acrylates/PUR/varnish and CMC was distinct for group A (n=2, station 13, 18).

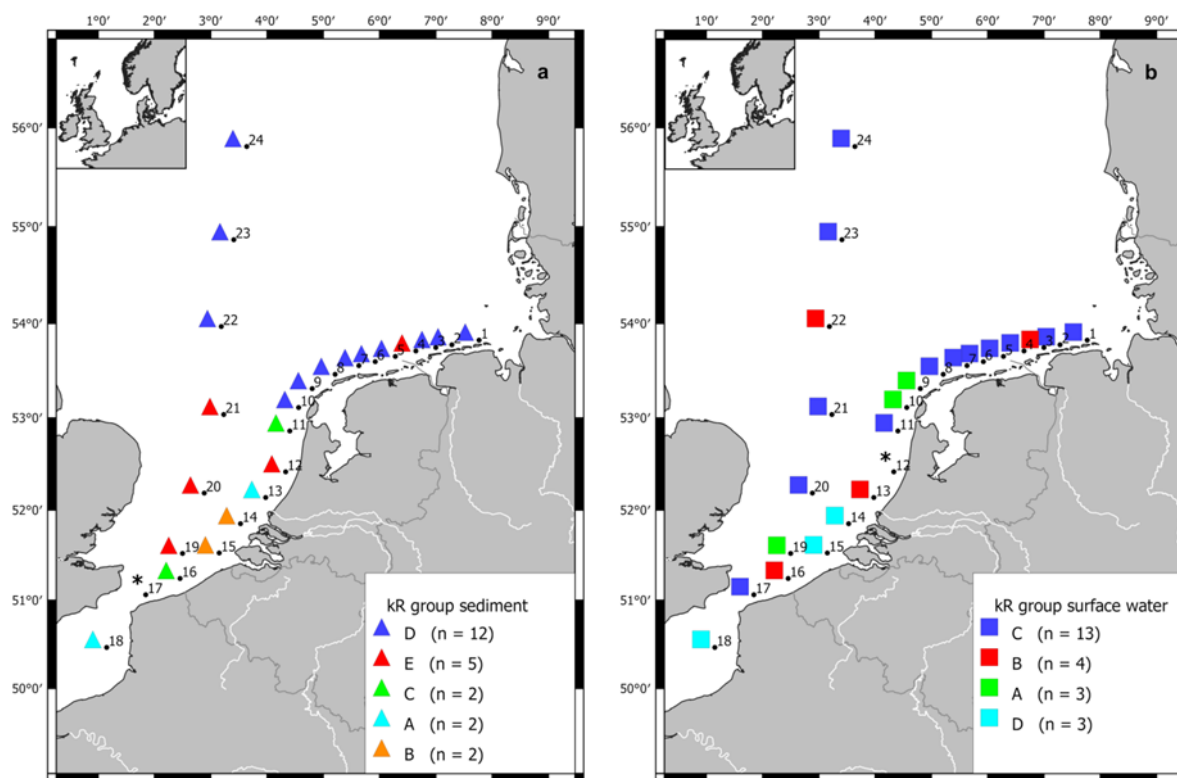


Figure 7: Map of the southern North Sea with the 24 stations of sediment (a) and surface water sampling (b) and their assigned groups (different colors) respectively based on kR-clustering. Stations where no sample was analyzed are marked with *.

For surface water samples kR-clustering revealed four groups (A–D) that represented the best possible clustering ($R=0.868$), where most samples are clustering closely and belong to group C (n=13) (Figure 7b, SI Figure S12). The clustering was confirmed by CAP with relatively high correlation values (0.811–0.970) (Figure S13). Only two samples (stations 15 and 18) were mis-classified to group C instead of group D resulting in an overall low mis-classification error of 8.7%. Six polymers, (PE, PE chlorinated, PVC, PEST, acrylates/PUR/varnish and rubber type 3), were revealed by ANOVA, with a subsequent Tukey HSD, to show significant differences between the four identified groups (SI Table S11). The presence of rubber type 3 characterized group C (n=13, station 1–2, 4–8, 11, 17, 20–21, and 23–24). Group B had significantly relatively more abundant (p -value=0.000) PEST (station 4, 13, 16, and 22). The

absence of PE, PVC, and rubber type 3, as well as the relatively high presence of PE chlorinated, characterized group A (n=3, station 9, 10, and 19). Group D (n=3) was defined by an absence of PE chlorinated, PEST, and rubber type 3, as well as a relatively high presence of PVC and acrylates/PUR/varnish (station 14, 15, and 18).

Discussion

Through the integration of effective sample preparation together with state-of-the-art FTIR imaging and an automated analysis technique, MP could be detected in all analyzed sediment and surface water samples in the southern North Sea. The investigated compartments differed significantly in their polymer composition and particle size distribution. Average MP concentrations were considerably higher in sediments (234.5 ± 254.3 particles kg^{-1} (DW)) than in surface waters (27.2 ± 52.5 particles m^{-3}). However, a direct comparison is difficult because of different units of reference. When comparing the abundance of MP in a certain surface area the difference is even more striking with numbers ranging from 9.5 to 4041.9 particles m^{-2} in sediments and 0.01 to 24.5 particles m^{-2} in surface waters (SI Table S4). Furthermore, both compartments were clearly dominated by MP $< 500 \mu\text{m}$. Although the numbers of MP $> 500 \mu\text{m}$ in surface water samples were noticeable, they had hardly any influence on the sample comparison between stations.

Along the West and East Frisian Islands (station 1–9) MP concentrations were of average extent in surface waters (3.5 – 58.6 particles m^{-3}) as well as sediments (38.7 – 318.4 particles kg^{-1} (DW)). Furthermore, sediment samples from this region were grouped together by cluster analysis since they showed similar polymer compositions with overall high polymer diversities. Both compartments in this region showed the lowest MP concentration at station 9, situated north of Texel, the most western Frisian Island, and the highest concentration at station 6, north of Ameland. It is very striking that samples from the mouth of the Scheldt and Rhine-Meuse-delta (station 14 and 15) differed greatly from all the others concerning their polymer composition, with surface water samples being dominated by acrylates/PUR/varnish and sediments additionally by rubber type 3, both indicating the influence of high marine traffic. In the English Channel region (station 16–19) polymer diversity and composition showed high variability, which was also true for the west coast of the Netherlands (station 10–13).

There is no clear gradient visible for surface waters, but those in the proximity to the English Channel, particularly station 20, which are influenced by riverine input from the Thames and the Rhine as well as channel water, exhibited the highest MP concentration (245.4 particles m^{-3}) with a decrease in the northern direction. These results agree with results from two studies where frequency of MP in fish and fulmars were highest in the Channel area (van Franeker et al., 2011; Foekema et al., 2013). For sediments MP concentration was highest at station 23 (1188.8 particles kg^{-1} (DW)), situated at the Dogger Bank and characterized by fine sediments. Further spatial patterns could be revealed by applying multivariate statistics, which has been attempted in previous studies as well (Suaria et al., 2016; Hajbane & Pattiaratchi, 2017). Hajbane and Pattiaratchi (2017) used multi-dimensional scaling (nMDS) to describe the

differences in MP concentration and size classes between three distinct stations over time. Suaria et al. (2016) used principal component analysis (PCA) to compare a large number of surface water samples ($n=74$) regarding the relative frequencies of the seven most common polymer types. We used kR-clustering to reveal a spatial pattern regarding polymer composition followed by ANOVA to uncover the polymer types which drive this structure. The differences in polymer composition show a clear pattern with an imaginary line that can be drawn along 53° N. Stations below 53° N are more diverse in their polymer composition, which might be related to the influence coming from the English Channel as well as the high riverine input by the Thames, the Scheldt, the Rhine and the Meuse. On the contrary, stations located above 53° N exhibit a more similar polymer composition. ANOVA revealed that the sediment samples of these stations were characterized by the presence of polychloroprene and surface water samples by rubber type 3, represented by ethylene-propylene-diene monomer rubber (EPDM).

Interstudy comparison

In sediments sampled along the Belgian coast, Claessens et al. (2011) detected MP concentrations of up to $269 \text{ particles kg}^{-1}$ (DW) on the shelf sea samples and $390 \text{ particles kg}^{-1}$ (DW) in harbor areas, both in the size range of $38\text{--}1000 \mu\text{m}$. They extracted MP by applying a density separation approach with sodium chloride (NaCl) and MP were visually preselected and identified using FTIR spectroscopy. In sediments of the Dutch North Sea coast Leslie et al. (2017) detected between $100\text{--}3600 \text{ particles kg}^{-1}$ (DW). In their extensive study, they analyzed several compartments, among others sublittoral sediments close to the stations of this study. They analyzed only small aliquots of 20 g each which infers a large degree of extrapolation when referring to particles per kg and used NaCl for density separation which might have resulted in an underestimation of some denser polymer types. Furthermore, they mostly detected fibers of which only a small proportion (6%) was analyzed spectroscopically. Regardless of these potential limitations, concentrations were of the same order of magnitude as found in this study. Another study by Maes et al. (2017b) reported similar numbers for MP in sediments in the same area ($0\text{--}3146 \text{ particles kg}^{-1}$ (DW)). It is noteworthy to highlight that no MP fragments were counted in this study but mostly spheres and fibers contrary to our study. Maes et al. (2017b) also used small aliquots of 25 g for density separation with NaCl and identified plastics based on visual criteria only. When comparing results for surface water samples from the same study, MP concentrations were considerably higher in our study ($0\text{--}1.5$ vs. $0.1\text{--}245.4 \text{ particles m}^{-3}$). The most considerable differences between the two studies were in the mesh size of the sample net ($333 \mu\text{m}$ vs. $100 \mu\text{m}$) and the method for identification of MP (visual vs. ATR-FTIR and FTIR imaging). Relatively small aliquots of the samples were processed in these studies, especially regarding sediment samples. Our protocol enabled us

to process the whole sample consisting of 1309–1770 g dry sediment and 15500–51300 L surface water concentrated by the net, respectively. It was however inevitable that we would only be able to analyze aliquots of the processed samples on the measuring filters, for practical reasons, i.e. to improve spectra quality and reduce time demand for analysis. However, for sediments the aliquots comprised on average 48.8% of the samples, being equivalent to a range of 141 to 1253 g sediment (DW), and for surface water samples the aliquots comprised on average 15.6% of the sample resulting in an equivalent volume of sea water ranging from 190 to 18236 L. To overcome the need for any extrapolation, multiple filters per sample could have been analyzed, but this would have increased the time demand by at least two days per filter. With new advances in reducing the analysis time, more filters could be analyzed more rapidly than has been possible until now. These developments in methodology are discussed further in the SI Paragraph S6.

We acknowledge that the lower limit of the filtration during sample processing was theoretically 20 μm . However, this limit can be considered lower when filters become clogged. For this reason, the number of particles between 11–20 μm should be considered as semi-quantitative, and therefore the total detected number is most likely an underestimation. Same applies to some extent also to the fraction 10–100 μm of the surface water samples due to the mesh size of the net. However, this emphasizes even more that very small MP are numerous and should be included in further research.

As in agreement with other studies (Hidalgo-Ruz et al., 2012; Filella, 2015; Ivleva et al., 2016), difficulties in interstudy comparisons due to variable sampling, sample preparation and analytical methods are well illustrated. Concerning possible analytical methods, the range includes simple visual identification only (Maes et al., 2017b), fluorescent tagging of synthetic polymers (Maes et al., 2017a), visual presorting followed by chemical identification of (a subset of) putative plastics (Enders et al., 2015; Leslie et al., 2017; Martin et al., 2017), spectroscopic imaging of whole sample filters using FTIR imaging (Vianello et al., 2013; Tagg et al., 2015; Bergmann et al., 2017; Mintenig et al., 2017; Peeken et al., 2018; Haave et al., 2019; Mintenig et al., 2019), μRaman spectroscopy (Cabernard et al., 2018), and thermoanalytical methods like Pyrolysis gas chromatography coupled to mass spectrometry (Py-GC-MS) (Fischer & Scholz-Böttcher, 2017) or thermal extraction-desorption (TED) GC-MS (Dümichen et al., 2017; Dümichen et al., 2019).

It has been shown that visual identification alone is insufficient (Song et al., 2015; Kroon et al., 2018) and the same can be said for methods relying on a visual preselection stage from which only a subset are verified by spectroscopic or thermoanalytical methods. When aiming for particle related data, the complementary spectroscopic methods of Raman microscopy and

FTIR imaging are the most commonly used (Hanke et al., 2013; K  ppler et al., 2016; Silva et al., 2018). Generally, there is a requirement within the research field to establish the usage of polymer characterization methods that omit the need for pre-sorting. If a pre-selection is unavoidable, it should follow certain criteria (Nor  n, 2007; Hidalgo-Ruz et al., 2012; Kroon et al., 2018) or be aided by dying with Nile red (Erni-Cassola et al., 2017; Maes et al., 2017a).

Implications

Beyond the harmonization of methods for reliable comparisons of MP data, another important issue in the field of marine environmental MP research is the need for clear identification of pathways, especially entry pathways. Previous research has shown that rivers are to be considered as one of the major sources (Lebreton et al., 2017; Schmidt et al., 2017). Studies focusing on rivers entering into the North Sea report relatively high numbers of MP (Mani et al., 2015; Leslie et al., 2017; Mani et al., 2019a). Noteworthy, it has been shown in a recent study by Hurley et al. (2018b) that MP from the river beds (approx. 70%) can be resuspended, flushed by flooding events and hence be introduced into the oceans. This implies that MP from riverine surface waters alongside those locked in bed sediments should both be considered as having the potential of entering the North Sea. In this regard, it is even more notable, considering that most of the polymer types reported in these riverine studies would be buoyant in seawater ($\rho \leq 1.025 \text{ g cm}^{-3}$), that the concentrations detected in North Sea surface waters are surprisingly low. One explanation might be the very conservative approach of our study. The other, more significant, factor might be that the hydrodynamics of the North Sea have a generally anti-clockwise circulation in the center and a northeasterly export along the coast (Howarth, 2001; Thiel et al., 2011). This makes it less likely for MP to accumulate in North Sea surface waters. However, this horizontal transport facilitates the distribution of MP in the North Sea along with their chemical load and attached biofilm communities. In this regard it is noteworthy that Kirstein et al. (2016) confirmed the presence of potentially pathogenic bacteria in biofilms from MP collected in North Sea surface waters. Another aspect to acknowledge when considering distribution pathways is the vertical transport of MP. M  hlenkamp et al. (2018) showed that buoyant MP that become incorporated into aggregates can sink and eventually settle into the benthic boundary layer, providing an explanation to the presence of positively buoyant plastics in sublittoral sediments. This evidence was backed by another study by Porter et al. (2018) in which they showed the incorporation of different plastic types (PE, PP, PA, PS, and PVC), of different shapes (fibers, spheres, and fragments), and sizes (7–3000 μm) into marine snow. The incorporation of normally buoyant polymers in organic-rich aggregates increased the sinking velocity of all tested polymer types (Porter et al., 2018). The authors of both studies recorded that in case of a polymer buoyant in seawater, such as PE, as well as with a mixture of plastic microbeads (extracted from facial cleansers), sinking

velocities increased to up to 818 and 831 m d⁻¹ respectively (Möhlenkamp et al., 2018; Porter et al., 2018). This exceeds general sinking velocities of phytoplankton aggregates (53±22 m d⁻¹) (Möhlenkamp et al., 2018) and fecal pellets, which range, depending on the composition of the phytoplankton bloom, between 70–100 m d⁻¹ (Frangoulis et al., 2001).

A final consideration on the topic of vertical transport would be that the bioavailability of MP to filter and suspension feeders has been shown to be increased by their incorporation in aggregates (Ward & Kach, 2009; Porter et al., 2018). Recently, Katija et al. (2017) showed that MP are captured by larvaceans and that these can be contained in their fecal pellets or discarded houses, and may thus sink to the seafloor as part of these structures where they are available for benthic organisms.

Robust monitoring protocols are needed which should not only focus on large MP (>500 µm). In this study we demonstrated that it is not possible to extrapolate conclusions from analyzing MP >500 µm to ascertain data on MP <500 µm. For the development of risk management and assessment protocols, and to monitor trends in changes of polymer concentrations and composition, it is of importance that the focus should shift to be on the small or even very small size fraction (<100 µm). In agreement with previous studies (Leslie et al., 2017; Maes et al., 2017b) we found North Sea sediments to be considerably more contaminated than surface waters and that these may act as potential sinks. This clearly supports the statement of Leslie et al. (2017) to track changes in MP pollution in sediments in future monitoring approaches.

Acknowledgments

We like to thank the crew of the research vessel *Heincke* for technical support and sampling. Further thanks go to the Deutsche Bundesstiftung Umwelt (DBU) for funding C. Lorenz with a Ph.D. scholarship. This work was also supported by the German Federal Ministry of Education and Research (Project BASEMAN - Defining the baselines and standards for microplastics analyses in European waters; BMBF grant 03F0734A).

Furthermore, we thank N. Mackay-Roberts for proof reading. We also would like to thank the anonymous reviewers for their helpful comments and suggestions which improved the original manuscript.

Chapter II

Assessing the weathering status of marine microplastics in the southern North Sea – A multivariate approach

Claudia Lorenz^{*,a,b}, Sebastian Pimpke^a, Gunnar Gerds^{*,a}

^a Department of Microbial Ecology, Biologische Anstalt Helgoland, Alfred Wegener Institute, Helmholtz Centre for Polar and Marine Research, Kurpromenade 201, 27498 Helgoland, Germany

^b Department of the Built Environment, Aalborg University, Thomas Manns Vej 23, 9220 Aalborg, Denmark (present address)

*Corresponding authors:

Claudia Lorenz: claudia.lorenz@awi.de

Gunnar Gerds: gunnar.gerds@awi.de

In preparation to be submitted to *Chemosphere*

Abstract

Annual worldwide plastics production has kept increasing during the past decade. Plastic debris, which enter the marine environment, will persist for a considerable time but break down into small and smaller items called microplastics (MP). Knowledge of the fate and behavior of MP in marine ecosystems is still scarce. One factor associated with this is environmental degradation. One indicator commonly used to assess the weathering status of different polymers is the carbonyl index. Thus, in this *in silico* study we analyzed carbonyl indices of thousands of FTIR spectra derived from polyethylene (PE) and polypropylene (PP) particles (11–5000 μm) identified in southern North Sea waters and sediments. We found significant differences in the carbonyl indices of both polymer types between the two sampled compartments as well as different size classes. For large MP (500–5000 μm) detected in surface water samples, the average carbonyl index for PE was 0.03 and for PP it was 0.02. The mean carbonyl index for small MP (11–500 μm) in surface waters was considerably higher with 0.07 for PE and 0.06 for PP. Small MP in sediments showed a higher average carbonyl index for PE (0.14) and a low one for PP (0.00).

Furthermore, also the full spectral range (3600–1250 cm^{-1}) of these PE and PP particles and additionally spectra from polystyrene (PS) and polyvinyl chloride (PVC) particles was analyzed. The spectra were compared to pristine reference spectra as well as between the compartments they were extracted from (surface water and sediment) and between size classes. The differences to the pristine reference spectra were significant for all four investigated polymer types (PE, PP, PS, and PVC), however, less prominent when comparing the spectra between the sampled compartments, surface water and sediment. Apart from the carbonyl bands, the wave number region 3500–3200 cm^{-1} , characteristic for hydroxyl groups, displayed differences comparing the spectra of pristine and naturally weathered MP in in both compartments for all four polymer types and might be considered as an additional indicator for weathering.

Keywords: μFTIR imaging, microplastics, weathering, carbonyl index, full range spectral data, *in silico* study

Introduction

Plastics are versatile materials firmly linked with our modern society. Global plastics production has risen from 257 to 348 million tons in the last decade (2007–2017) with European plastics production recently making up 18.5% of it (PlasticsEurope, 2015, 2018). Due to their high demand, high and low density polyethylene (HDPE/LDPE), polypropylene (PP), polyvinyl chloride (PVC), polyurethane (PUR), polyethylene terephthalate (PET) and polystyrene (PS) are deemed the “big six” (Paul-Pont et al., 2018). They make up around 81% of the European plastics demand (PlasticsEurope, 2018). These are also the most commonly encountered polymer types, in terms of numbers, in the marine environment (Erni-Cassola et al., 2019). Once plastic litter items have entered the ocean, they will persist for a long time in the marine environment. During this residence time, they are affected by several chemical, physiochemical and biological factors, which alter their physical and chemical state leading to fragmentation and the generation of microplastics (MP).

One of the most important physicochemical processes is photo-degradation (induced by ultraviolet (UV) irradiation) which is considered to be substantial at beaches and the sea surface (Ter Halle et al., 2016; Pimpke et al., 2017a; Song et al., 2017). Several studies reported the loss in tensile strength and even fragmentation of plastic litter items already after a few weeks of exposure, (O’Brine & Thompson, 2010; Weinstein et al., 2016; Karlsson et al., 2018). Finally, a complete breakdown of the plastics can be observed and the formation of smaller and more numerous MP (<5 mm, Arthur et al. (2009)). However, the full mineralization of plastics in the marine environment is suspected to be a very slow process (Andrady, 2009). Hence, when trying to understand the fate and pathways of plastic litter items in the oceans, environmental degradation, defined as “a chemical change in the polymer brought about by environmental factors” (Andrady, 1994), is an important process to consider. According to Searle (2005), “the environmental effect on the polymeric materials” is referred to as “weathering” and its status can be assessed using a variety of partly complimentary techniques (e.g. differential scanning calorimetry, scanning electron microscopy, tensile strain test). One other is Fourier transform infrared (FTIR) spectroscopy. It can detect changes in the molecular structure, like the increase in oxygenated moieties, namely aldehydes, ketones, carboxylic acids, hydroperoxides and alcohols (Andrady, 2017). According to Brandon et al. (2016) alterations in the hydroxyl, carbon-oxygen and carbonyl bonds can be readily assessed for artificially as well as naturally weathered PP, LDPE and HDPE. Krehula et al. (2014) stated that the degradation of polyethylene (PE) is dominated by the formation of carbonyl groups and vinyl species. For PS the formation of carbonyl as well as hydroxyl groups has been documented (Shi et al., 2019).

A well-known indicator for weathering is the carbonyl index, defined as the ratio between the absorbance of a carbonyl peak and a C-H-reference peak, which is considered to increase with an increasing degree of degradation (Karlsson et al., 2018). The carbonyl index, measuring the presence of carbonyl moieties, is considered as an indicator for weathering of polyolefin polymers and therefore also termed “aging index” (Guadagno et al., 2001; Ter Halle et al., 2017b). Several authors stated recently that it is of importance to assess as many characteristics as possible of MP sampled in the environment to get a more thorough picture of the status of MP pollution especially in the light of environmental risk assessment (Filella, 2015; Potthoff et al., 2017; Kögel et al., 2020). One of these proposed parameters is the weathering status. Many studies have been carried out assessing aging behavior of different polymer types, however, most of them focused on artificial weathering rather than on natural weathering (Brandon et al., 2016). Just recently, Hebner and Maurer-Jones (2020) stressed that there is a lack of data on degradation of small sized MP collected from environmental compartments. Furthermore, Kedzierski et al. (2019) stated that the history of degradation of polymers might result in small variations in their spectral data that should be studied by means of large datasets. Thus, in this study we aimed to assess the weathering status for MP collected from southern North Sea surface waters and sediments on a cruise in 2014 (Lorenz et al., 2019) using an *in silico* approach. In this meta-analysis of several thousand FTIR spectra, we focused on five different polymer types, HDPE, LDPE, PP, PS and PVC, with C-C backbone, which are part of the “big six” (Gewert et al., 2015). Due to the similarity of LDPE and HDPE FTIR-spectra, in the observed wave number range, these two polymer types were combined and considered as polyethylene (PE). PE, PP, PS and PVC represented on average 46% and 26% of MP detected in a recent study of North Sea surface waters and sediments (Lorenz et al., 2019). To assess the weathering status, the carbonyl indices of MP identified as PE and PP covering sizes of 11 to 5000 μm were considered in our study. Furthermore, full range attenuated total reflection (ATR) FTIR (4000–400 cm^{-1}) and focal plane array (FPA) based FTIR imaging (3600–1250 cm^{-1}) spectra were considered for PE, PP, and additionally also PS and PVC, to identify whether changes in certain wave numbers or ranges might indicate the weathering status.

According to this, four main research questions were addressed: (i) How do carbonyl indices differ between MP of the sampled compartments (surface water and sediment)? (ii) Do carbonyl indices derived from MP of different size classes show any difference? (iii) Do full range FTIR spectra derived from samples of the two different sampled compartments differ among each other and when compared to reference spectra? (iv) Are there wave number regions in the spectra, apart from carbonyl groups, which might indicate the weathering status?

Materials and Methods

Data Selection

All spectral data used in this study was collected from surface water and sediment samples taken, prepared and analyzed for MP within the framework of a previous study by Lorenz et al. (2019). For MP in the size range of 11 to 500 μm , concentrated on Anodisc filters, spectra had been recorded in the wave number range of 3600–1250 cm^{-1} using μFTIR imaging in transmission mode. For details on spectral data collection see Supporting Information (SI) Paragraph S7. At all stations at least one of the targeted polymer types was detected in this size range. Samples considered for statistical analysis in this study were chosen by the highest number of spectra available. Their geographic locations are marked in Figure 8. We selected five surface water (marked in blue) and five sediment samples (marked in red) based on the number of identified PE, PP, PS and PVC spectra (1). At twelve stations (marked with a black circle) 91 particles identified as PE, 30 as PP and 10 as PS, respectively, were selected in the size range between 500 to 5000 μm . Only one PVC particle was identified in this size range and therefore not considered for the statistical analysis. Spectra of these larger MP had been collected in triplicate by means of ATR-FTIR spectroscopy in the wave number range 4000–400 cm^{-1} (SI Paragraph S7).

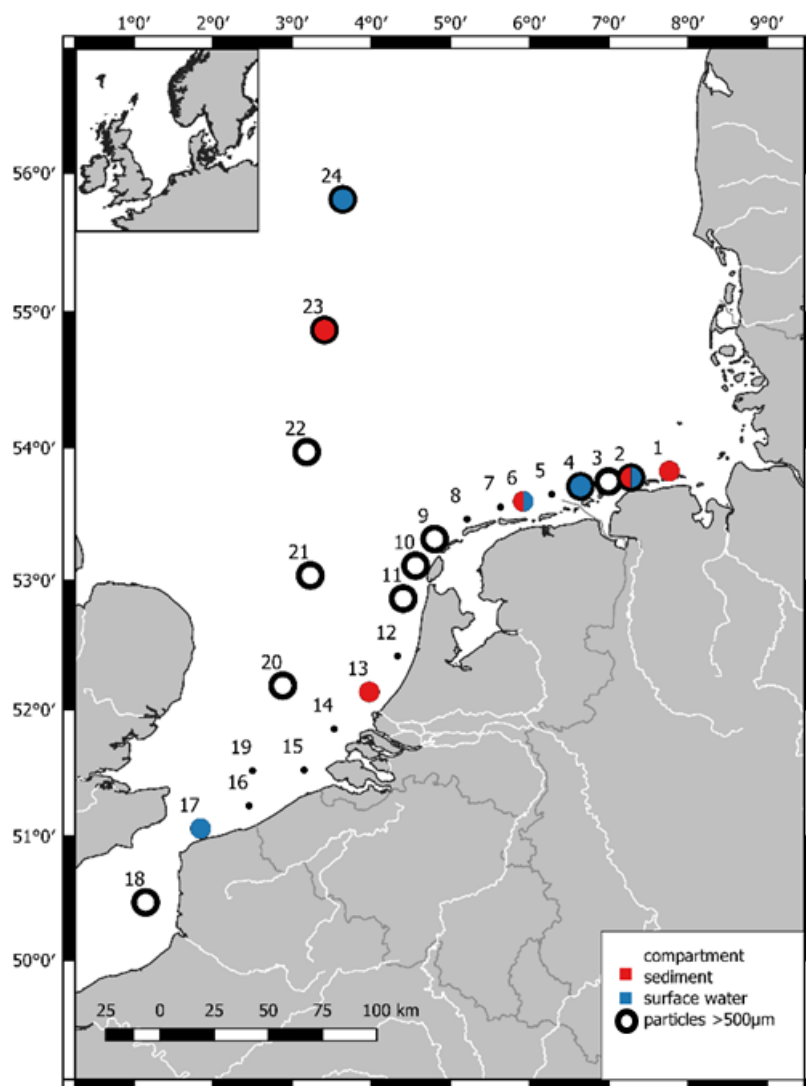


Figure 8: Map of the surface water (blue) and sediment sample (red) taken on RV Heincke cruise (He430) in 2014 (Lorenz et al., 2019), which were analyzed further on their weathering status.

Data analysis

Due to the difference in recorded spectral range, all the analyses were performed separately on the two size fractions. The number of spectra considered (“n”) is larger than the number of particles, since all particles >11 µm consist of several spectra.

To assess the extent of weathering of the selected particles the carbonyl index was determined. This was done for MP identified as PE and PP, since literature on the carbonyl index exists mainly for these two polymer types. Therefore, spectra of 305 identified PE (n=5123) and 293 identified PP (n=6568) particles in the size range 11 to 500 µm and 91 identified PE (n=271) and 30 PP (n=92) particles in the size range 500 to 5000 µm were considered. All these spectra were loaded into OPUS 7.5 and integrated in the wavenumber range between 1800 and

1700 cm^{-1} (Rajakumar et al., 2009; Lv et al., 2015; Lv et al., 2017) using integration OPUS Method B. As reference wave number range the absorption band for methylene between 1480 and 1400 cm^{-1} was chosen and integrated using OPUS Method B. Via an OPUS Macro (available upon request) the carbonyl indices for each spectrum were calculated as ratio of the integrated area within these wave number ranges. Furthermore, these calculated carbonyl indices were linked to the corresponding particle identities and their respective size class using a specialized Python (Python 3.7) script (available upon request). All carbonyl indices, independent of their particle identity, were then plotted and a Kruskal-Wallis test was performed, using SigmaPlot (version 11), to see whether a difference existed in the extent of weathering regarding the sampled compartments and the size classes.

Further, analyses of the complete spectral range were performed, to assess whether the FTIR spectra of these polymer types exhibited some general variations with regard to sampled compartment and size class of the particles. For this analysis also spectra for PS and PVC were included in addition to the spectral data for PE and PP. Thus, spectra of 39 identified PS ($n=1439$) and 200 identified PVC ($n=1488$) particles were included in the further analyses of the 11–500 μm size fraction and of 10 PS ($n=30$) particles for the analysis of the 500–5000 μm size fraction.

For the size fraction 11 to 500 μm , all spectra were made compatible (offset removed due to usage of two different FTIR microscopes) and the wave number range 2420–2200 cm^{-1} exhibiting CO_2 signal removed by creating a straight line using OPUS 7.5. All spectra, categorized per polymer type and sample, were compiled and baseline corrected (baseline offset removed to avoid negative absorbance values) using The Unscrambler X (version 10.4.1). One spectrum each were collected from pristine particles of these four polymer types (PE: $n=24$, PP: $n=12$, PS: $n=7$ and PVC: $n=7$) from the database published by Primpke et al. (2018). Finally, these datasets consisted of 5147 spectra for PE, 6580 spectra for PP, 1446 spectra for PS, and 1495 spectra for PVC. These datasets were analyzed using PRIMER 6 (PRIMER-E, UK). Data was standardized by the maximum of each sample and a distance matrix based on Euclidean distance was generated. For ordination of the data, principal coordinates analysis (PCoA) was performed with five axes to visualize patterns in spectra comparison. Analysis of similarities (ANOSIM) was performed to show the degree of separation between the sampled compartments and size classes. An analysis of similarity percentages (SIMPER) was applied to the standardized data to identify wave numbers, contributing most to the similarities and dissimilarities in the spectra between the different sampled compartments (Clarke, 1993).

Results

Carbonyl indices for small MP (11–500 μm)

Carbonyl indices, considering the wave number range 1800–1700 cm^{-1} , were obtained for all selected spectra of the PE or PP particles from the five surface water and sediment samples, respectively. The carbonyl indices for both environmental compartments are displayed in Figure 9. The mean carbonyl index for PE was 0.07 in surface water and 0.14 in sediment samples and for PP 0.06 and 0.00, respectively. Kruskal-Wallis test reveals significant differences of the groups ($p < 0.001$) with $H=197.705$ and 3 degrees of freedom (dF). All pairwise multiple comparisons were significant as well ($p < 0.05$) with differences between surface water and sediment being higher for PE than for PP (see Supporting Information Table S12).

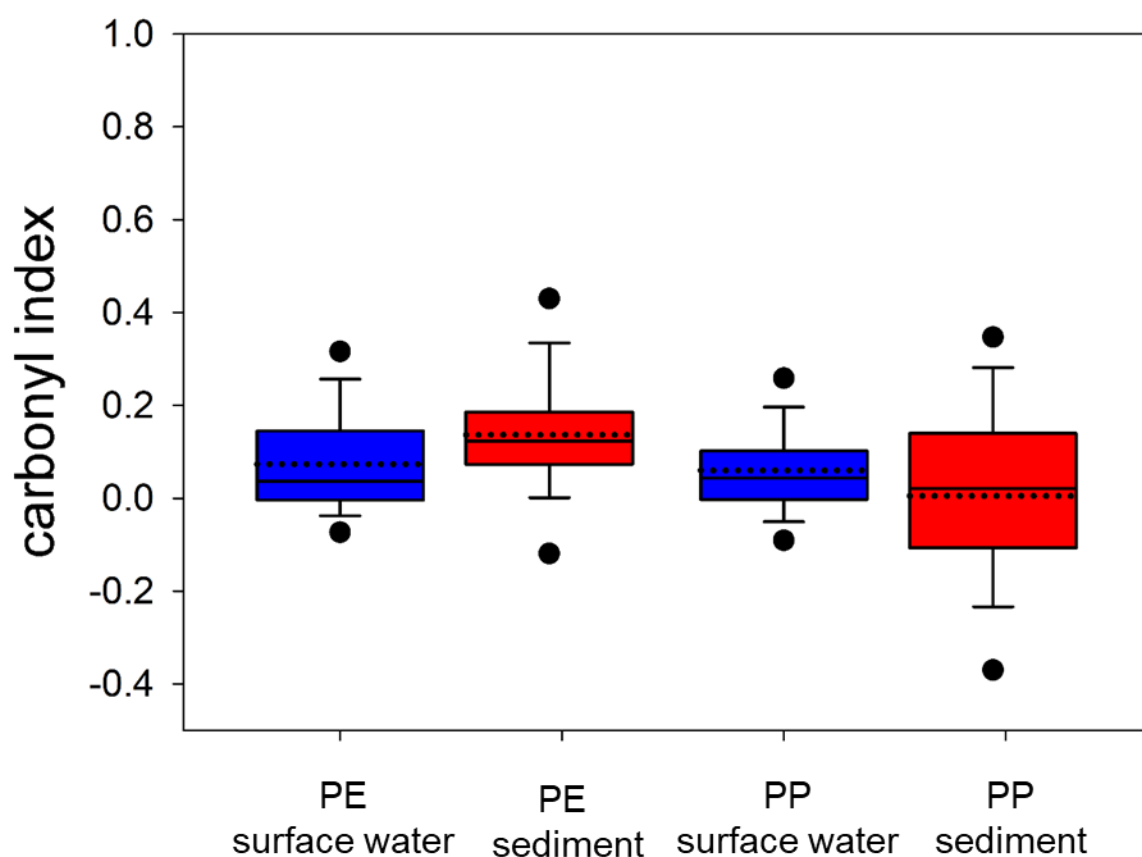


Figure 9: Box plots for carbonyl indices of small MP (11–500 μm) identified as polyethylene (PE) in surface water ($n=4822$ spectra) and sediments ($n=301$ spectra) and polypropylene (PP) in surface water ($n=5684$ spectra) and sediment ($n=884$ spectra). The colors refer to the sampled compartment, surface water (blue) and sediment (red). All outliers, plotted as black dots, represent the 5th and 95th percentiles. Mean values are represented by the dotted line.

The carbonyl indices for MP of different size classes are displayed in Figure 10. There is a significant difference between the median among the size classes according to Kruskal-Wallis test ($p < 0.001$, see SI Table S13) for PE detected in surface water samples. Dunn's test for multiple pairwise comparison (MPC) showed that the median of carbonyl indices of almost all groups were significantly different to each other ($p < 0.05$, see SI Table S14). For PE identified in sediments the sample size was much smaller, resulting in a lower H-value, but still showing significant ($p=0.001$) differences in the median (see Table S13). Dunn's test for MPC only confirmed that the size class 25–50 μm was significantly different to size class 11 μm and 50–75 μm ($p < 0.05$, see SI Table S14). For PP in surface water the median of the carbonyl indices between size classes differed significantly (see SI Table S13). The MPC showed that mainly the median of carbonyl indices in the size class 125–150 μm was significantly different to the others as well as the two largest size classes, 325–350 μm and 375–400 μm ($p < 0.05$, see SI Table S14). Finally, also for PP particles in sediment samples there were significant differences in the median carbonyl indices ($p < 0.001$, see SI Table S13) with size class 125–150 μm being significantly different to the others according to Dunn's test ($p < 0.05$, see SI Table S14). Nevertheless, for all of these four datasets it can be seen in Figure that the smaller the particles the more variance appeared in the carbonyl indices within the size class with maximum values of the 95th percentile decreasing with increasing particle size.

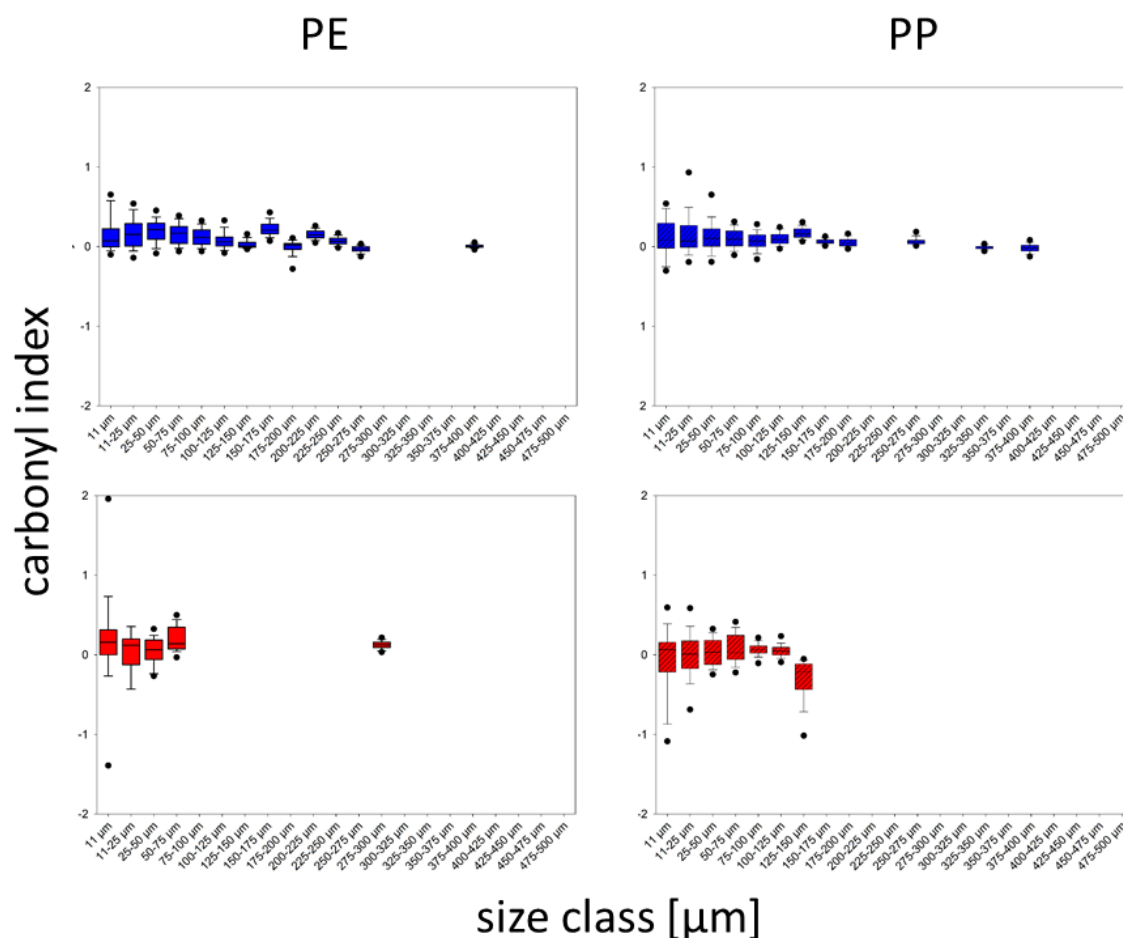


Figure 10: Box plots for the carbonyl indices of small MP (11–500 μm) for polyethylene (PE, left) and polypropylene (PP, right) identified in the two sampled compartments, surface water (blue) and sediment (red). All outliers, plotted as black dots, represent the 5th and 95th percentiles.

Carbonyl indices for large MP (500–5000 μm)

MP in the size range of 500 to 5000 μm were only found in surface water samples but not in sediment samples. The average carbonyl index for PE was 0.03 and for PP 0.02. When looking at carbonyl indices with regard to particle size class distribution there is no clear trend visible for neither PE nor PP in this size range (SI Figure S14). However, Kruskal-Wallis test revealed that there is a significant difference in the median of the carbonyl indices among size classes for PE ($p < 0.001$, $H=28.753$, $dF=8$). Only one of the pairwise multiple comparisons, between the size classes 1500–2000 μm and 2500–3000 μm , was significant ($p < 0.05$) (SI Table S15). For the size classes of PP no significant difference could be detected ($p=0.920$, $H=2.591$, $dF=7$).

Full spectral analysis (3600–1250 cm⁻¹) for small MP (11–500 µm)

Apart from the integral of the carbonyl groups (1800–1700 cm⁻¹/1480–1400 cm⁻¹) also the full spectral range recorded using µFTIR imaging (3600–1250 cm⁻¹) was analyzed for PE, PP and additionally for PS and PVC (spectra are available upon request) and compared to reference spectra. Results from the PCoAs showed a clear separation between the reference group and the two compartments, surface water and sediment, for all four polymer types (SI Figure S15) but a less clear separation between the compartments themselves. When looking at the different size classes to which the analyzed spectra belonged no clear separation or grouping could be observed in the results of the respective PCoA (SI Figure S16). The ANOSIM results indicated only low ($R < 0.3$, $p = 0.001$) or moderate ($0.3 < R < 0.5$, $p = 0.001$) differences among the polymer types regarding compartments and size class (Table 1). When comparing the results for the classifiers, compartment was for each polymer type the one indicating the biggest difference with the one for PE being the highest ($R = 0.357$, $p = 0.001$) as can be seen in Table 1.

Table 1: Summary of analysis of similarities (ANOSIM) results regarding compartment and size class with 999 permutations. PE=polyethylene (n=5123 spectra), PP=polypropylene (n=6568 spectra), PS=polystyrene (n=1439 spectra), PVC=polyvinyl chloride (n=1488 spectra). All spectra were recorded using µFTIR imaging in the wave number range 3600–1250 cm⁻¹.

Classifier	PE		PP		PS		PVC	
	Global R	%p	Global R	%p	Global R	%p	Global R	%p
Compartment	0.357	0.1	0.137	0.1	0.251	0.1	0.184	0.1
Size class	0.139	0.1	0.013	0.4	0.133	0.1	0.067	0.1

Therefore, ANOSIM results for pairwise comparison are only provided for compartments in Table 2. These results confirmed that the difference between reference spectra and the spectra of the respective compartment were significantly different ($R > 0.5$, $p = 0.001$) except for PVC for the comparison of sediments to the reference ($R = 0.254$, $p = 0.004$). The significance level was $p = 0.001$ for all other pairwise comparisons also between the two compartments but the R Statistic was lower 0.5. For the comparison between the two compartments, it was highest for PE with 0.315 followed by PS with 0.242. The index of multivariate dispersion (IMD) was around 1 for the pairwise comparison of each compartment to the reference for PE, PP and PS and around 0.8 for PVC.

Chapter II

Table 2: Analysis of similarities (ANOSIM) and multivariate dispersion (MVDISP) results regarding compartment. The statistic R, significance level % p and index of multivariate dispersion (IMD) were calculated for each of the selected polymer types polyethylene (PE, n=5123 spectra), polypropylene (PP, n=6568 spectra), polystyrene (PS, n=1439 spectra), and polyvinyl chloride (PVC, n=1488 spectra), based on pairwise comparison of similarities matrix with Euclidean distance with 999 permutations. All spectra were recorded using μ FTIR imaging in the wave number range 3600–1250 cm^{-1} .

Pairwise comparison	PE			PP			PS			PVC		
	R	%p	IMD	R	%p	IMD	R	%p	IMD	R	%p	IMD
Surface water, sediment	0.315	0.1	0.054	0.128	0.1	-0.1	0.242	0.1	-0.33	0.179	0.1	-0.31
Surface water, reference	0.848	0.1	1	0.71	0.1	0.997	0.789	0.1	1	0.682	0.1	0.805
Sediment, reference	0.914	0.1	1	0.579	0.1	0.999	0.785	0.1	1	0.254	0.4	0.855

The SIMPER analyses assessed the similarities and dissimilarities of the spectra, based on Euclidean distance matrix, within and between the groups. Furthermore, it provides the percentage of contribution for the individual wave numbers to these similarities and dissimilarities. The average squared distance indicates how similar the spectra belonging to each group are as well as how different the two compared groups are. The higher the value, the greater is the difference between the groups.

Results from the SIMPER analyses, presented in the SI Table S16–S19, show that there were more similarities within the group of reference spectra than within the group of spectra from surface water or sediment samples, respectively, except for PVC where the average squared distances were in a similar order of magnitude for all compartments. Furthermore, the pairwise comparison of the different compartments showed which wave number (regions) contributed most to the differences between the compartments and when comparing them to the reference (SI Table S16). The highest contribution for PE comparing surface water spectra to the reference was 1.5% around 2941 cm^{-1} and 1.1% at the same wave number for sediment compared to the reference spectra (SI Table S16). For PP a maximum contribution of 0.9% or 0.7% (2972 cm^{-1}) and for PS of 1.0% (2941 cm^{-1}) or 0.8% (2949 cm^{-1}) was found when comparing surface water or sediment, respectively, to the reference (SI Table S17, SI Table S18). For PVC spectra, the overall highest contribution was 1.0% (2926 cm^{-1}) when comparing surface water to reference spectra. When comparing sediments to reference spectra the highest contribution was 0.6% at the same wave number range (SI Table S19).

When comparing the average spectrum of MP from the surface water samples to the averaged reference spectrum some wave number regions display a noteworthy contribution to the dissimilarities between the groups but did not surpass the 0.5% threshold (Figure 11). In the average surface water spectrum the presence of a broad band in the wave number range 3500–3200 cm^{-1} , characteristic for –OH bonds, is signaling for hydroxyl groups for all four

polymer types. The other notable difference lies in the presence of bands in the wave number range 1750–1650 cm^{-1} , signaling for carbonyl and carboxyl groups, in the surface water spectra, which is most distinct for PE (Figure 11).

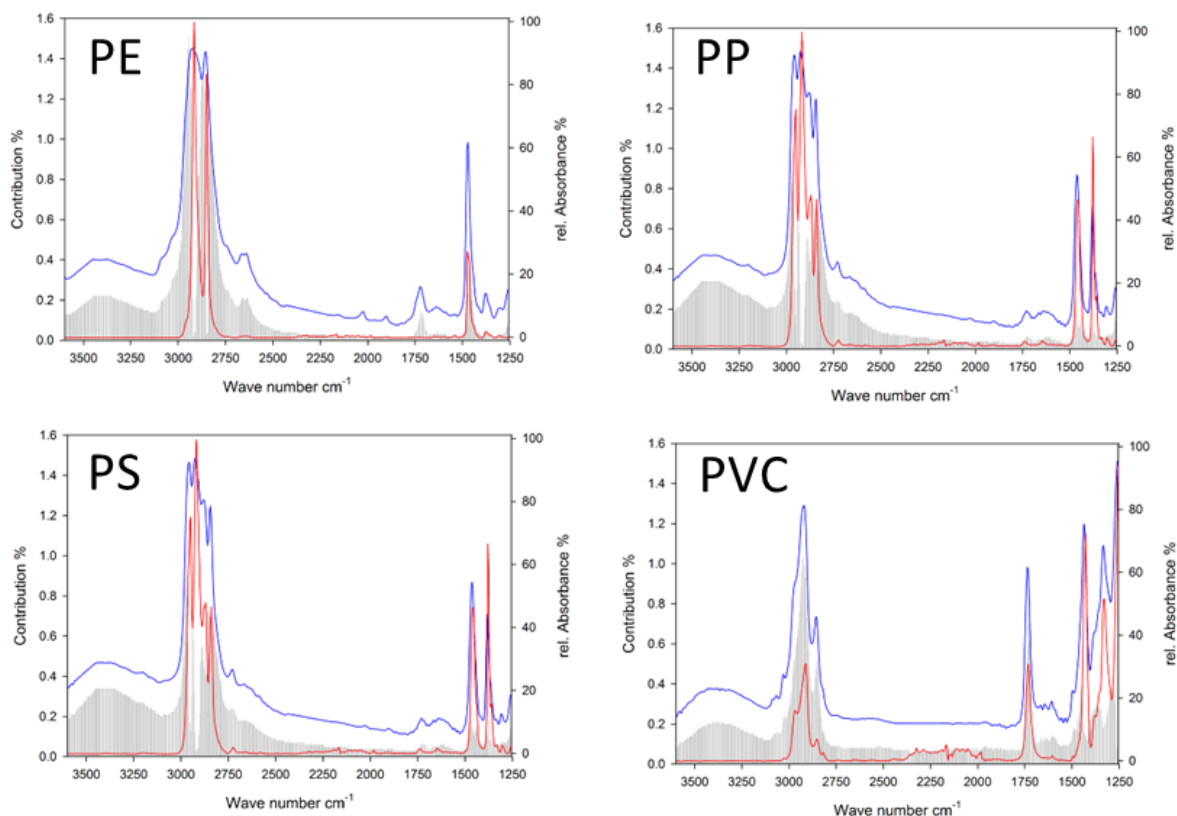


Figure 11: Results of the contribution to the dissimilarities based on SIMPER analysis when comparing the average relative absorbance of surface water samples (blue) to reference spectra (red) for four polymer types. PE=polyethylene, PP=polypropylene, PS=polystyrene, PVC=polyvinyl chloride.

In addition, when comparing the average spectrum from sediment samples to the averaged reference spectrum the broad band signaling for hydroxyl groups in the sediment spectra is clearly visible for all four investigated polymer types (Figure 12). The bands characteristic for carbonyl and carboxyl groups are also present in the sediment spectra, least prominent for PS (Figure 12). Instead, for PS the higher absorbance in the wave number range 1300–1250 cm^{-1} of the average sediment spectrum compared to the reference is salient.

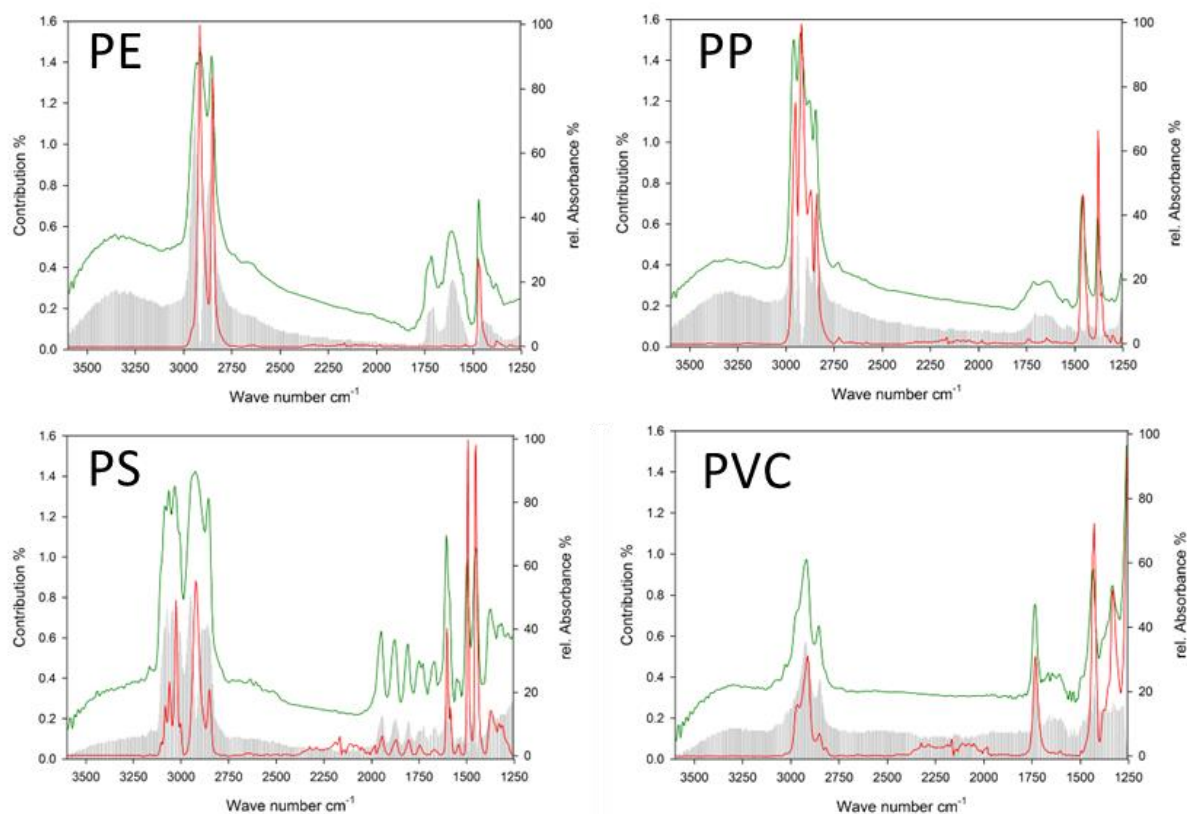


Figure 12: Results of the contribution to the dissimilarities based on SIMPER analysis when comparing the average relative absorbance of sediment samples (green) to reference spectra (red) for four polymer types. PE=polyethylene, PP=polypropylene, PS=polystyrene, PVC=polyvinyl chloride.

When comparing the average relative absorbance of the spectra from surface water and sediment samples, which were not significantly different according to ANOSIM, there were, however, some wave number ranges, which were noticeable different between the two spectra (SI Figure S17). For PE this was in the wave number range 1579–1625 cm^{-1} , characteristic for carboxyl groups, where the average relative absorbance for the sediment samples was considerably higher than for surface water samples (SI Figure S17). The contribution of this difference was larger than 0.5% in the SIMPER results, with the highest contribution of 0.7% at 1602 cm^{-1} (SI Table S16). For PP the relative absorbance in the same wave number range was slightly higher for sediment than for surface water as well (SI Figure S17) but with a lower contribution not surpassing the 0.5% threshold (SI Table S17). For PS there was also no wave numbers contributing more than 0.5% when comparing the two compartments. Nevertheless, there was a higher relative absorbance in the spectra from MP in sediments in the wave number range 1300–1250 cm^{-1} , potentially related to some background signals from silicates, which had elevated contribution in the SIMPER results (SI Figure S17). For PVC the highest contribution was 0.8% (2915 cm^{-1}) when comparing the two compartments, with weaker absorbance at this wave number for the average sediment spectrum. Simultaneously, the

absorbance in the wave number range around 1600 cm^{-1} was higher in the average sediment spectrum than in the surface water spectrum (SI Figure S17).

Full spectral analysis (4000–400 cm^{-1}) for large MP (500–5000 μm)

The spectra of large MP identified as PE, PP and PS were likewise analyzed considering the full spectral range which had been recorded with ATR-FTIR (4000–400 cm^{-1}) and compared among each other and to the reference spectra. When looking at the PCoAs for each polymer type regarding size classes no clear pattern could be seen except for PS (SI Figure S18). The grouping for PS can be explained by the scarcity of data since the dataset only included 30 spectra measured, in triplicate, from ten particles. The grouping can therefore be related mostly to the same particle. Accordingly, the ANOSIM results indicate for PE only low ($R < 0.3$, $p < 0.003$) and for PP at most moderate ($0.3 < R < 0.5$, $p < 0.004$) differences regarding size class and even compartment, representing the direct comparison of surface water to reference (Table 3). The ANOSIM results for PS were all highly significant ($R > 0.5$, $p = 0.001$) but also this might be due to the size of the dataset.

Table 3: Summary of analysis of similarities (ANOSIM) of spectral data (n) regarding compartment and size class with 999 permutations for large MP (500–5000 μm). PE=polyethylene (n=271 spectra), PP=polypropylene (n=92 spectra), PS=polystyrene (n=30 spectra). All spectra were recorded with ATR-FTIR in the wavenumber range 4000–400 cm^{-1} .

Classifier	PE		PP		PS	
	Global R	%p	Global R	%p	Global R	%p
Compartment	0.209	0.3	0.324	0.4	0.641	0.1
Size class	0.237	0.1	0.157	0.2	0.578	0.1

Discussion

When plastics enter the marine environment, they are subjected to various environmental influences that alter their physicochemical properties. One of these processes is UV-radiation induced weathering. Here can be distinguished between artificial weathering of plastics under laboratory conditions which is often times accelerated and natural weathering occurring in the environment. Understanding this weathering of plastics in the marine environment is paramount for understanding the fate of MP. The weathering status might influence the sinking behavior of the plastics (Kowalski et al., 2016), facilitate fragmentation and thus formation of smaller MP and influences also the sorption behavior of pollutants since weathered MP have a higher capacity to sorb pollutants in comparison to virgin MP (Guo & Wang, 2019). Till date little is known about the weathering status of MP in the marine environment, especially for sizes smaller than 300 μm (Hebner & Maurer-Jones, 2020). A study by Ter Halle et al. (2017b) investigated the extent of weathering of PE mesoplastics and MP extracted from North Atlantic surface waters by determining the carbonyl index amongst a number of other parameters. They analyzed the carbonyl index of 11 PE mesoplastics and 46 PE MP and reported mean indices of 0.7 and no statistical difference between these two plastic categories (Ter Halle et al., 2017b). They also assumed that no higher carbonyl index was recorded since the oxidation takes place mostly in the upper layer of the polymer, which becomes brittle and erodes, leaving behind an unoxidized layer (Guo & Wang, 2019). This theory is in accordance to the surface ablation fragmentation proposed by Andrady (2017). This theory would thus suggest that when the oxidized surface layer of a plastic particle becomes brittle and fragments into smaller particles, showing a high degree of oxidation, hypothetically it would leave behind a less oxidized surface on the larger particle they originated from. An indication to this hypothesis in our study could be that the average carbonyl indices for PE and PP in surface water samples were higher for small MP (11–500 μm) compared to larger MP (500–5000 μm).

Another study, which investigated PE as well as PP weathered naturally in the marine environment and compared it also to artificially weathered PE and PP, was conducted by Brandon et al. (2016). The authors found that the carbonyl indices of HDPE particles, collected from the North Pacific, were between 0 and 0.2, thus in the same range as of HDPE weathered experimentally in seawater and sunlight for 0 to 9 or 18 to 36 month (Brandon et al., 2016). However, for PP no significant overlap in the values between the naturally and artificially weathered particles could be observed and values of the collected PP particles were usually higher than the ones exposed to seawater and sunlight for up to 36 month.

Next to studies exploring the extent of naturally weathered plastics based on the carbonyl index, other studies focused mainly on artificial weathering. Since natural weathering of MP is a long

process, these experiments are performed under accelerated weathering conditions. Additionally, the control conditions allow for a more detailed look on the changes in the polymer properties. In one of these studies, Song et al. (2017) reported a linear increase of the carbonyl index with UV exposure duration for PE. However, for PP no linear change but a rapid increase was detected which reached a plateau after two months followed by another rise after six months. In artificial weathering experiments also the environmental conditions can be mimicked and their impact detected. Julienne et al. (2019) showed that the environment in which the weathering took place clearly had an impact. Films made of LDPE, which were weathered in Milli-Q-water for 25 weeks under a xenon lamp with an irradiation intensity of 60 W/m^2 , showed a higher tendency for fragmentation than films weathered in air. For oxidation the picture was reversed and the carbonyl index was significantly higher in films weathered in air than in water (Julienne et al., 2019). Hebner and Maurer-Jones (2020) irradiated PP films with UV light of different wave lengths and found differences, although not significant, in the carbonyl index. However, the irradiated PP films exhibited a significantly higher carbonyl index than the non-irradiated ones (Hebner & Maurer-Jones, 2020).

According to Brandon et al. (2016) the carbonyl index seems to be more befitting for PE than for PP since the indices for experimentally weathered PP and ocean-collected PP did overlap less than for LDPE and HDPE. Also in our study we found that the differences in carbonyl indices for PP extracted from surface waters and sediments differed less than for PE and also the contribution to the spectral differences when compared to PP reference spectra were lower than 0.5% in the wave number range of carbonyl moieties. Table 4 compares the carbonyl indices assessed in different studies focusing on experimental and natural weathering. It shows how difficult a comparison of carbonyl indices between studies is because different wave number ranges are considered for the carbonyl area as well as for the reference band. Generally, it seems like the carbonyl index is a good indicator for the weathering status of PE. In our study the wave number region from $1800\text{--}1500 \text{ cm}^{-1}$ showed for PE relatively high contributions to the differences between the reference spectra and spectra derived from particles extracted from the surface water or sediment. This finding is in accordance with Karlsson et al. (2018) who stated that more information is gained by including the large area of carbonyls and carboxylates ($1523\text{--}1835 \text{ cm}^{-1}$) than just considering the carbonyl index.

Chapter II

Table 4: Carbonyl indices for polyethylene (PE) and polypropylene (PP) and how they were obtained in different studies focussing on experimental and natural weathering.

Polymer	Wavenumber (region) for carbonyl index	Wavenumber (region) for reference band	Carbonyl index range (mean)	Weathering conditions	Reference
PE	1714 cm ⁻¹	1470 cm ⁻¹	0–1.2	experimental	Gulmine et al. (2003)
PE	1720 cm ⁻¹	2020 cm ⁻¹	1.2–3.0	experimental	Krehula et al. (2014)
PE	1810–1550 cm ⁻¹	2920–2908 cm ⁻¹	0–0.2	experimental & natural	Brandon et al. (2016)
PE	1780–1600 cm ⁻¹	1490–1420 cm ⁻¹	0–1.6 (0.7)	natural	Ter Halle et al. (2017b)
PE	1712 cm ⁻¹	1375 cm ⁻¹	0–38	experimental	Song et al. (2017)
PE	1714 cm ⁻¹	1462 cm ⁻¹	0.1	experimental & natural	Karlsson et al. (2018)
PE	1835–1644 cm ⁻¹	1462 cm ⁻¹	132–134	experimental & natural	Karlsson et al. (2018)
PE	1970–1560 cm ⁻¹	1450–1540 cm ⁻¹	5.7	experimental	Julienne et al. (2019)
PP	1715 cm ⁻¹	974 cm ⁻¹	0–0.4	natural	Rajakumar et al. (2009)
PP	1810–1550 cm ⁻¹	2940–2885 cm ⁻¹	0–0.2	experimental & natural	Brandon et al. (2016)
PP	1712 cm ⁻¹	1375 cm ⁻¹	0.2–1.1	experimental	Song et al. (2017)
PP	1800–1680 cm ⁻¹	2722 cm ⁻¹	0–105	experimental & natural	Lv et al. (2015) & Lv et al. (2017)
PP	1715 cm ⁻¹	974 cm ⁻¹	0–4.6	experimental	Hebner and Maurer-Jones (2020)
PE / PP	1800–1700 cm ⁻¹	1480–1400 cm ⁻¹	-0.2–0.5	natural	This study

Thus, in our study we looked, next to the carbonyl index, also at a broader wave number range to see whether differences in the spectra related to weathering existed. We found that the wave number region 3500–3200 cm⁻¹, characteristic for hydroxyl groups, showed some distinction between reference spectra and spectra from marine surface water and sediment samples. Brandon et al. (2016) considered the area in the wavenumber range 3400–3300 cm⁻¹ for PE and PP for the hydroxyl index. They found an increase for this index in experimentally weathered LDPE, HDPE and PP after five months being most distinct after 36 months. Thus, the hydroxyl band seems to be readily showing when MP are weathered but is also susceptible to moisture and has to be considered with care. Furthermore Karlsson et al. (2018) noticed for PE films, which previously underwent a thermooxidative pretreatment at 90 °C for up to 30 days, a formation of hydroxyl groups (3000–3700 cm⁻¹) after field exposure. The pretreated PE films were exposed to natural weathering condition in floating cages in a fjord and retrieved after 4, 8 and 12 weeks, respectively. However, the authors stated that no clear relation to the levels of pretreatment could be made (Karlsson et al., 2018). A quantification of the weathering

status through the hydroxyl index does not seem feasible. However, also the carbonyl index, used as quantitative method, has its limitations and is only applicable for an early stage of weathering because further degradation affiliated with the loss of CO₂ occur subsequently (Fernando et al., 2007; Andrady, 2017). Since MP extracted from environmental matrices are naturally all in different stages of weathering a quantification of the weathering status of MP in the marine environment cannot be so easily attempted. However, a qualitative assessment can be made as has been shown by Brandon et al. (2016) and Ter Halle et al. (2017b). A first attempt on estimating the age of weathered plastics in the marine environment has been made by Ioakeimidis et al. (2016). They compared ATR-FTIR spectra of polyethylene terephthalate (PET) bottles of different indicated age and noted different intensities of certain bands as well as the appearance of new bands (Ioakeimidis et al., 2016). For MP collected from the (marine) environment without an indicated age an estimation like this approach is of course not possible. Furthermore, for spectra collected with FPA-based FTIR imaging of samples on Anodisc filters, as has been performed in this study, only a limited wave number range is available including only two of the indicator bands (1715 cm⁻¹ and 1435 cm⁻¹). Brandon et al. (2016) also tried to relate experimental weathering to natural weathering by using next to the carbonyl index also a hydroxyl index and one for carbon-oxygen groups considering LDPE, HDPE and PP. However, in the environment the weathering behaviour is more complex because it is influenced by many factors. As stated by Ter Halle et al. (2017b) it has to be kept in mind that even for the same polymer type the physicochemical properties might differ a lot because of the different fabrication and manufacturing processes. Many plastics contain antioxidants and UV stabilizers in different amounts to slow down the degradation through photooxidation (Rani et al., 2015). Additionally, the presence of a biofilm would retard photooxidation. Furthermore, Andrady (2011) stated that seawater slows down photodegradation by a factor of ten when comparing floating plastics to beached ones. Thus, the nature of the initial polymer, before environmentally degraded, remains unknown and references of virgin and artificially weathered polymers of the same type can only provide slight indications.

Conclusion

With regard to our research questions, we found with this *in silico* analysis of a comprehensive dataset of FTIR spectra significant differences in carbonyl indices for PE and PP in terms of sampled compartment (i) and size class (ii), except for larger PP particles (500–5000 μm). When looking at the full spectral range (3600–1250 cm^{-1}) of the naturally weathered MP, the differences to the pristine reference spectra were significant for all four investigated polymer types (PE, PP, PS, and PVC), however, less prominent when comparing the spectra between the sampled compartments, surface water and sediment (iii). Apart from the wave number region characteristic for carbonyl groups (1750–1650 cm^{-1}), we found differences in the spectra of pristine and naturally weathered MP in the wave number region 3500–3200 cm^{-1} , characteristic for hydroxyl groups, in both compartments for all four polymer types (iv). This underlines that the carbonyl index is but one parameter to consider when assessing the weathering status of MP and a look into the full range of FTIR spectra can give additional indication on the environmental degradation of naturally weathered MP.

Acknowledgments

We would like to thank the Deutsche Bundesstiftung Umwelt (DBU) for funding C. Lorenz with a Ph.D. scholarship. Furthermore, this work was also supported by the German Federal Ministry of Education and Research (Project BASEMAN - Defining the baselines and standards for microplastics analyses in European waters; BMBF grant 03F0734A).

Chapter III

Paraffin waxes in the southern North Sea

Claudia Lorenz^{a,c,*}, Michaela Schafberg^b, Lisa Roscher^a, Melanie S. Meyer^a, Sebastian Primpke^a, Uta R. Kraus^b, Gunnar Gerds^{a,*}

^a Shelf Seas Systems Ecology, Biologische Anstalt Helgoland, Alfred Wegener Institute, Helmholtz Centre for Polar and Marine Research, Kurpromenade 201, 27498 Helgoland, Germany

^b Federal Maritime and Hydrographic Agency (BSH), Bernhard-Nocht-Str. 78, 20359 Hamburg, Germany

^c Department of The Built Environment, Aalborg University, Thomas Manns Vej 23, 9220 Aalborg Øst, Denmark

* Corresponding authors:

Claudia Lorenz: claudia.lorenz@awi.de

Gunnar Gerds: gunnar.gerds@awi.de

Submitted to *Marine Pollution Bulletin* in July 2020

Abstract

Paraffin waxes (PWs) are recognized as ubiquitously emerging marine pollutants. However, knowledge on their occurrence, particularly as persistent floaters of small size (<5 mm) in marine surface water, is scarce.

For this study, 24 samples were collected in the North Sea by net-sampling (100µm-mesh). Particles of wax-like appearance were detected at 14 stations. Similar appearing PWs from six stations with highest abundances were pooled per station and analyzed by ATR-FTIR (Attenuated total reflectance Fourier-transform infrared spectroscopy) and gas chromatography. Samples contained PW particles, being partly accompanied by substances like fatty acids and fatty alcohols. Using both analytical techniques provided a reliable detection of PWs and more details on their chemical composition. Furthermore, exemplarily the presence of PWs of 20–500 µm size was proven by µFTIR imaging. This study gives valuable insights into PW pollution in the North Sea, emphasizing the need for harmonized detection methods, ideally accompanying microplastics monitoring.

Keywords: Petroleum waxes; marine pollution; sea-based sources; ATR-FTIR; GC-FID; GC-MS

Highlights

- Paraffin waxes have been detected in several samples of North Sea surface waters
- ATR-FTIR, as well as GC-FID and GC-MS, used for identification of paraffin waxes
- Apart from paraffin also fatty acids and alcohols were detected
- First record of paraffin waxes in small size (20–500 µm) in the southern North Sea

Introduction

Marine pollution is an environmental issue of global concern. Thus, it is one of the targets of the Sustainable Development Goals, Goal 14: Life Below Water, adopted by the United Nations Development Programme (UNEP) (Desa, 2016). One of its aims is to prevent and reduce marine pollution by 2025. One way for pollutants to enter the marine environment is by land when pollutants enter rivers that discharge into the oceans. Another way of entry is through ocean-based sources, mainly being ship-based. The latter issue has been addressed as early as the 1970s with the International Convention for the Prevention of Pollution from Ships (MARPOL) issued by the International Maritime Organization (IMO). Annex I of this convention aims at the prevention of pollution by oil, Annex II regulates the discharge of noxious liquid pollutants at sea and Annex V prevents the discarding of garbage from ships. Still, several petroleum-based pollutants enter the marine environment this way. The most well-known form of marine pollution is oil spills. It is estimated that 150,000 tons of crude oil enter the marine environment annually from ship-based transport (Transportation Research Board National Research Council, 2003). In the European Union legislation, this form of pollution from ships has been addressed in Descriptor 8, contaminants, of the European Marine Strategy Framework Directive 2008/56/EC (MSFD). Solid types of pollutants are in turn covered by Descriptor 10, marine litter, which is defined as “any persistent, manufactured or processed solid material discarded, disposed of or abandoned in the marine and coastal environment” by the Technical Subgroup on Marine Litter (Galgani et al., 2013). Since plastics make up the vast majority of marine litter, up to 95%, they have been the main focus of marine litter monitoring and research (Galgani et al., 2015). The assessment of the “composition, amount and spatial distribution” (Commission Decision 2017/848/EU) of large litter items has been defined as one criterion while the focus on micro-litter has been another (European Commission, 2017). Thus, more recently, the focus in research has also been on microplastics, defined by Frias and Nash (2019) as “any synthetic solid particle or polymeric matrix, with regular or irregular shape and with size ranging from 1 μm to 5 mm, of either primary or secondary manufacturing origin, which are insoluble in water”. Petroleum waxes, mainly paraffin waxes (PWs), are another solid form of petroleum-based pollutants, which fall under Descriptor 10 and are included in the monitoring guidelines for the MSFD (MSFD GES TSG Marine Litter, 2011; Hanke et al., 2013). They are considered as “high-viscosity or solidifying substances” in the latest version of MARPOL Annex II, entered into force in 2007 (IMO, 2004). They fall within the intermediate pollution category Y: “Noxious Liquid Substances which, if discharged into the sea from tank cleaning or deballasting operations, are deemed to present a hazard to either marine resources or human health or cause harm to amenities or other legitimate uses of the sea and therefore justify a limitation on the quality and quantity of the discharge into the marine

environment” (IMO, 2004). Petroleum waxes are transported over the sea with commercial tank vessels that load or unload (‘stripping’) the waxes in liquid form which is considered to be the main source for PWs at sea (Fitz et al., 2017). The regulation provides that the tanks have to be unloaded as much as possible before performing a prewashing of tanks to remove any residues (IMO, 2004). The water containing residues from the prewash should then be brought to special reception facilities. However, Suaria et al. (2018) mentioned that there are some exceptions which entail that the discharge of certain amounts within the “stripping limits” ($75\text{--}300\text{ L} \pm 50\text{ L}$) are legal under some conditions.

PWs are derivatives of crude oil consisting mainly of saturated long-chain hydrocarbons, mainly alkanes in the range C18–C65 (Dwivedi et al., 2017; Suaria et al., 2018). These waxes are thermoplastics that are however not considered as plastics due to their relatively low molecular weight. They have a low melting point ($35\text{--}50\text{ }^{\circ}\text{C}$) but are usually solid at ambient temperatures (Kienhuis et al., 2018). The texture can be rather soft but also brittle and hard (Suaria et al., 2018). Their appearances vary from white over yellow to brown, and their surface texture can be smooth and shiny or rough and dull (Supporting Information SI, Figure S19). They have a wide range of application from cosmetic products, over candles to skiing wax and coating of cheese (Kienhuis et al., 2018).

The occurrence of PWs in the marine environment is mostly noticed when large amounts are stranded on beaches like recently on Sylt and Rügen (Germany) in spring 2014, at the Côte d’Opale (France) in November 2016 and July 2017 and the Ligurian Sea (Italy) in June 2017 (UEG, 2014; Sea-Mer Asso, 2017; Suaria et al., 2018). To date, most studies focus on PWs washed ashore, but little is known about the amount of PWs, especially in a small size range not visible in aerial or nautical surveys, floating on the ocean surface. Thus this study aimed to evaluate whether PWs in the size range of $500\text{--}5000\text{ }\mu\text{m}$ can be successfully sampled in surface water by utilizing nets used for microplastics sampling and identified by ATR-FTIR (Attenuated total reflectance Fourier-transform infrared spectroscopy) and gas chromatography analysis as well as to gain an insight into the spatial distribution of PWs floating in southern North Sea surface waters.

Materials and Methods

Sampling, sample preparation and FTIR analysis

Surface seawater was sampled with a microplastics net (100 µm mesh size, HydroBios, Kiel, Germany) at 24 stations during a cruise with the RV Heincke in summer 2014 (SI, Figure S20). All samples were filtered through a 500 µm stainless steel mesh. The filtrate was concentrated on 20 µm stainless steel meshes and processed and analyzed for microplastics in the framework of an accompanying study (Lorenz et al., 2019). As proof-of-concept that PWs are also present in this small size fraction (20–500 µm), one sample (station 20) was selected for further analysis with µFTIR imaging (SI Paragraph S8).

The particles remaining on the 500 µm mesh were inspected and sorted under a stereomicroscope (Olympus SZX16, Olympus). Particles that appeared synthetic, wax-like and displayed a soft texture were sorted out as putative PW particles. Potential microplastic particles were analyzed separately in the context of the accompanying study by Lorenz et al. (2019) as well. All the putative PW particles were sorted into eight different categories based on their appearance (Table 5, Figure S19).

Some putative PW particles of each of these eight categories and per station were measured using ATR-FTIR in the wavenumber range of 4000–400 cm⁻¹ with a resolution of 4 cm⁻¹ and 32 scans (Tensor 27 spectrometer with a diamond-crystal ATR module and the software OPUS 7.5, Bruker Optics). Spectra were compared to a freely available database (Pimpke et al., 2018).

Table 5: Descriptions of the appearance of the putative paraffin wax particles according to categories and the stations of their occurrence. Only samples with sufficient abundance were analyzed using gas chromatography techniques, and the station number per category is highlighted in bold.

Category	Description	Station present
1	White to yellow, spherical to ellipsoid, rough surface	21
2	White to yellow, amorph, chunks, rough but shiny	2, 3, 4, 5, 8, 14, 19, 20
3	White to yellow, amorph, aggregated spheres, rough but shiny	1, 2, 5, 8, 9, 14 , 16, 20, 22, 24
4	Transparent to white, spherical, soft, smooth and shiny	2, 3, 20, 21
5	Pale yellow, spherical, soft, smooth, mostly dull	2, 3, 20
6	Transparent to white, amorph, very soft, smooth and shiny	20
7	White, amorph, foam-like	2, 20
8	Dark yellow to brown, spherical, dry and brittle	3

Sample preparation and analysis with GC-FID and GC-MS

The remaining putative PW particles were pooled per sampling station and category, as presented in Table 5, resulting in 30 composite samples of which 16 were further analyzed with gas chromatography coupled with a flame ionization detector (GC-FID) and gas chromatography coupled with a mass spectrometer (GC-MS). The other 14 pooled samples only consisted of single particles with an insufficient mass for further analysis.

The eligible 16 composite samples were, in duplicates of 0.1–3.0 mg each, solved in 1 mL *n*-hexane and incubated in an ultrasonic bath for 10 min. Some of the particles in the duplicates did not solve completely, marked by streaks or a deposit, but to a sufficient extent. Details on the solubility of each sample can be found in the Supporting Information (SI, Table S20). The sufficiently solved samples were analyzed using GC-FID and GC-MS. The applied method was following the workflow for oil spills given in CEN (2012) and modified from Fitz et al. (2017) (see SI Table S21 for details).

In short, GC-FID analyses were performed on a DB-5 capillary column (10 m x 0.1 mm x 0.1 µm) installed in an Agilent 6890N gas chromatograph (Agilent Technologies Inc., Santa Clara, USA). The final temperature was held for 13.6 min.

The GC-MS analyses were performed on an HP-5ms Ultra inert column (30m x 0.25 mm x 0.25 µm) installed in an Agilent 7890 gas chromatograph coupled to a triple quadrupole mass spectrometer (Agilent 7000C, Agilent Technologies). The initial temperature was 42 °C, held for 0.8 min, increased to 325 °C at a rate of 5.5 °C min⁻¹, and held for 20 min. The constant flow was 1.1 mL/min. The MS was used in scan mode from 50 to 450 m/z (scan time 500 ms). The system was connected to a Gerstel injection system (Gerstel GmbH & CO.KG, Mülheim an der Ruhr, Germany) including a Multipurpose sampler, CIS 4 injector and a controller C506.

All GC analyses were evaluated with OpenChrom Enterprise Version: 1.2.0 and 1.3.0. by Lablicate GmbH (Hamburg, Germany).

Results

FTIR

The ATR-FTIR spectra of the analyzed particles showed all prominent bands around 2916 cm^{-1} and 2848 cm^{-1} , characteristic for the asymmetric and symmetric stretching of C-H bonds. Furthermore, they all had a less intense band in between $2980\text{--}2950\text{ cm}^{-1}$ (shoulder) in common, which corresponds to the stretching of CH_3 groups. Particles assigned to category 1, 2 and 4 had a band around 719 cm^{-1} in common, characteristic for CH_2 rocking and signaling for alkanes. Generally, bands in the wavenumber region $1000\text{--}700\text{ cm}^{-1}$ are characteristic for alkenes. Particles from category 2 and 4 showed only one more band at 1463 cm^{-1} characteristic for CH_2 bending. These bands were also detectable in particles from category 1 and 5 additionally to three and four other bands respectively. One appeared at 1740 cm^{-1} , characteristic for C-C double bonds, one at 1539 cm^{-1} and one at 1173 cm^{-1} . Category 5 particles had one more additional band at 1576 cm^{-1} . Exemplarily, ATR-FTIR spectra of four particles representative for four different categories (1, 2, 4, and 5) are shown in Figure 13.

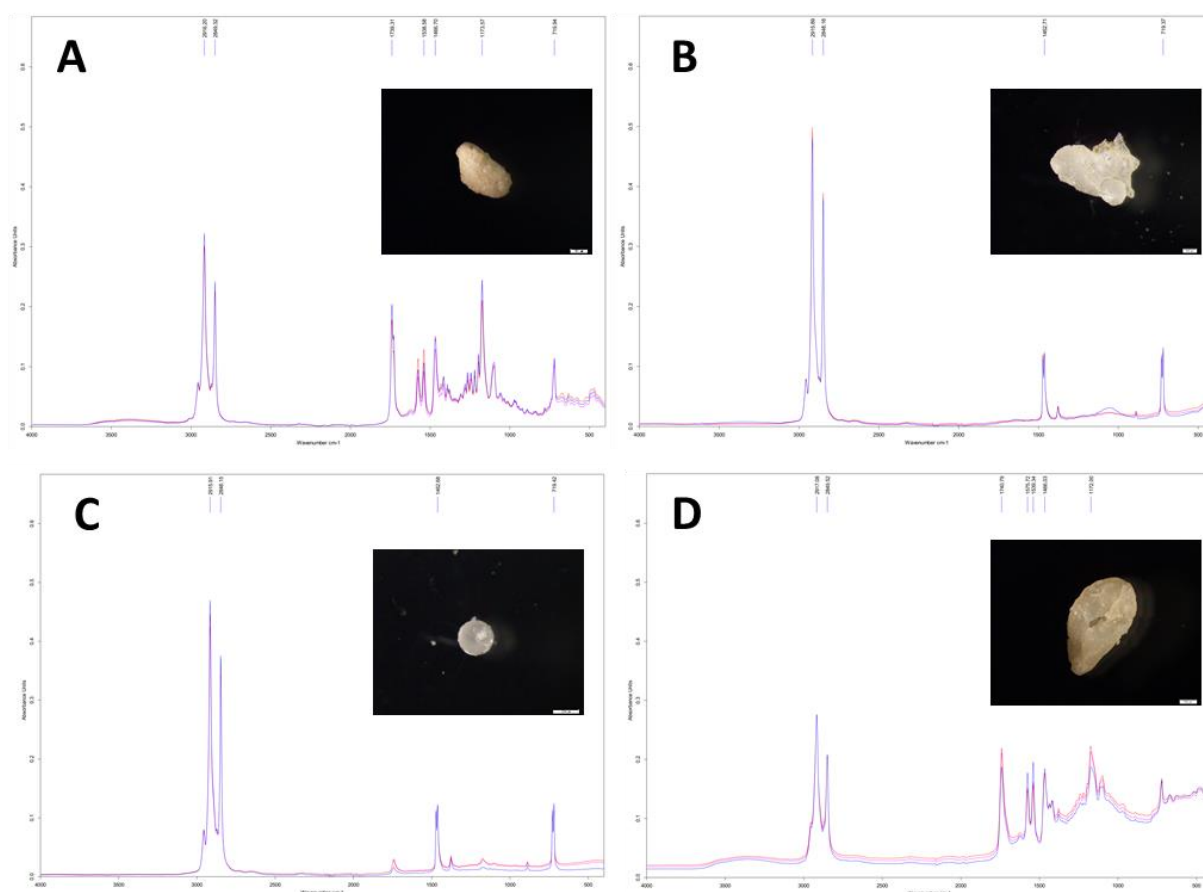


Figure 13: ATR-FTIR spectra of four putative paraffin wax particles of four different categories. Each particle was measured three times in the wavenumber range $4000\text{--}400\text{ cm}^{-1}$. A: category 1 station 21, B: category 2 station 2, C: category 4 station 2, D: category 5 station 2.

Furthermore, also within the size fraction 20–500 μm of one sample (station 20) putative PWs were detected. The visual image from the FTIR microscope showed that some of these particles exhibited a characteristic corona, most likely stemming from melting processes due to drying of the sample on the filter at 30 °C (Figure 14 A). This was confirmed by the spectroscopic analysis since most of these particles and the corona around them exhibited spectra which were matched with polyethylene (PE) wax (Figure 14 B). Additionally, in Figure 14 also three selected areas of interest, squares of 1 mm^2 , are highlighted, where ten spectra each were extracted and averaged which show a similarity to the spectra of category 2 and 4 PWs (Figure 14 C).

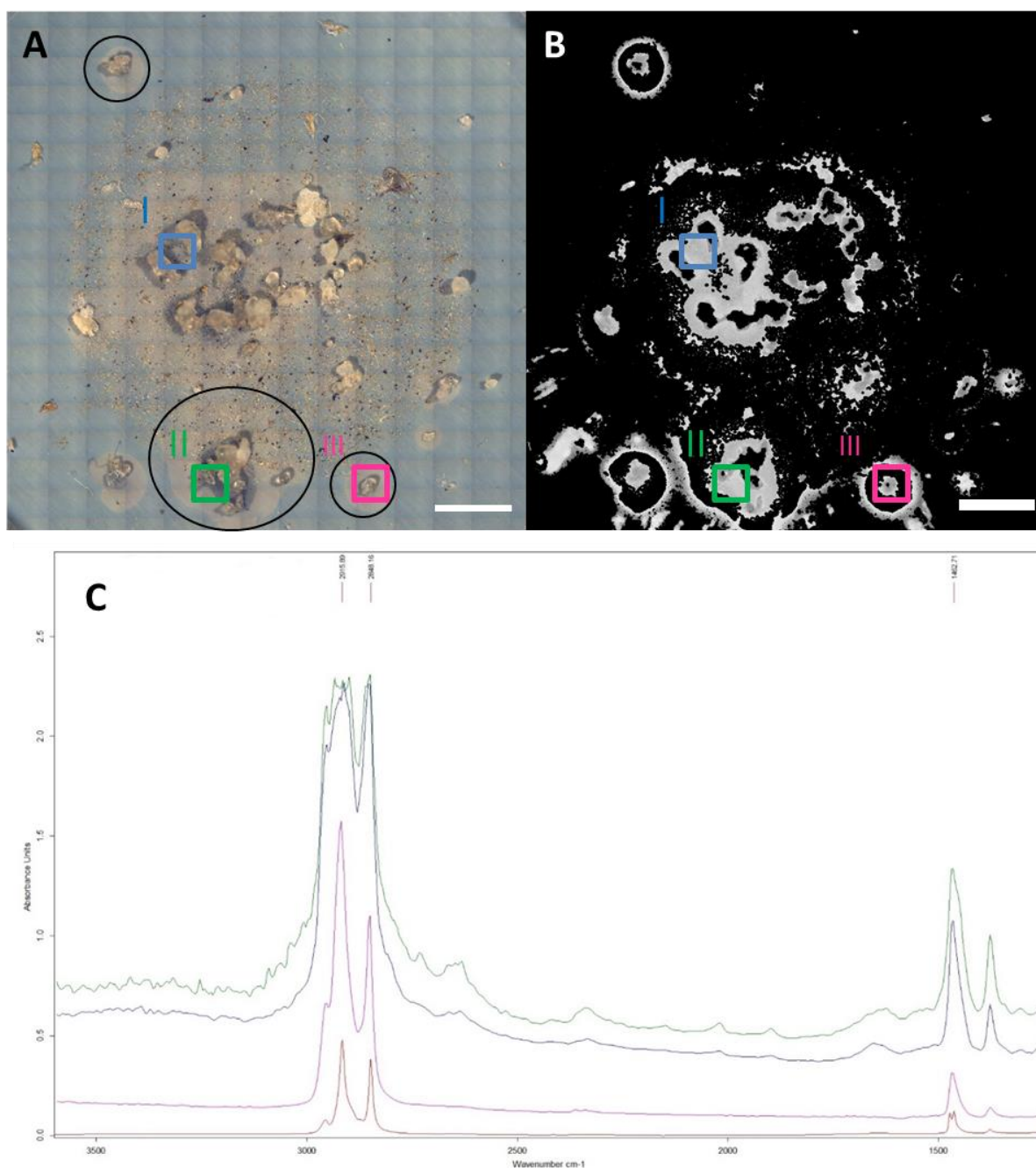


Figure 14: Visual image (a) and chemical image (b) of an Anodisc filter containing a subsample (3.5%) of the size fraction 20–500 μm from station 20 and spectra corresponding to paraffin (c). The visual image (a) shows in some areas (encircled) the partial melting of several putative paraffin wax particles. The chemical image (b) highlights areas with spectra that have been identified as polyethylene (wax), whereby the brighter the coloration, the stronger is the correlation with the reference spectra (30–100%). Within three areas of interest (I=blue, II=green, III=magenta), ten spectra each were averaged and compared to a reference spectrum characteristic for polyethylene or polyethylene wax (red) identified in the >500 μm size fraction of station 2 (c). Scale bar: 2 mm.

GC-FID and GC-MS

Ten of the 16 composite samples, analyzed by GC-FID and GC-MS, exhibited a clear signal for paraffin being the main component (Table 6). This was characterized by the presence of *n*-alkanes in the range of C21 to C47 in a bell-shaped pattern with PWs in the range of C26 to C47 being described as high boilers (Figure 15 A, B). One of the samples assigned to category 2 (station 20) and two assigned to category 4 (station 2 and 20) showed mainly *n*-alkanes and almost no *iso*-alkanes. On the contrary, samples assigned to category 3 (station 14), category 6 (station 20) and category 2 (station 2) showed considerably more *iso*-alkanes than the other samples. Two more samples assigned to category 2 (station 3 and 5) and two more from category 4 (station 3 and 21) showed the pattern characteristic for high boiling PWs. Some samples showed additionally also signals for fatty alcohols, namely the samples assigned to category 2 (station 3), category 3 (station 14) and category 4 (station 21). Only one sample, category 2 (station 14) showed fatty alcohols (C18–C28) as the main component (Figure 15 D). However, it also exhibited a weak paraffin pattern. The other samples from the remaining four categories (1, 5, 7, and 8) deviated strongly from the ones with the paraffin pattern and were characterized by the presence of fatty acids. The samples assigned to category 1 (station 21), category 7 (station 2) and category 8 (station 3) showed the presence of hexadecanoic acid (palmitic acid), Bis(2-ethylhexyl) decanedioate and oxiran-2-ylmethyl hexadecanoate (glycidyl palmitate). The sample from category 5 (station 2) showed the presence of dodecanoic acid (lauric acid) and tetradecanoic acid (myristic acid) next to a paraffin pattern. The remaining sample assigned to category 7 (station 20) showed no peaks in the chromatogram because the available sample mass was too small for analysis.

Table 6: Overview of the main components identified in the analyzed samples (n=16). Identified paraffin waxes are highlighted in green (high boilers=dark green). Fatty acids and Bis(2-ethylhexyl) decanedioate / glycidyl palmitate as main components are highlighted in blue. Fatty alcohols as main components are highlighted in orange. If other components were identified as well, they have been added as text: PAR=paraffin, FA= fatty acids, FOH=fatty alcohols. Samples marked with * showed no identifiable peaks in the chromatogram because of the low sample mass.

Station	Category 1	Category 2	Category 3	Category 4	Category 5	Category 6	Category 7	Category 8
He430_2		FA			PAR			
He430_3		FAO						
He430_5								
He430_14		PAR	FOH					
He430_20								*
He430_21				FOH				

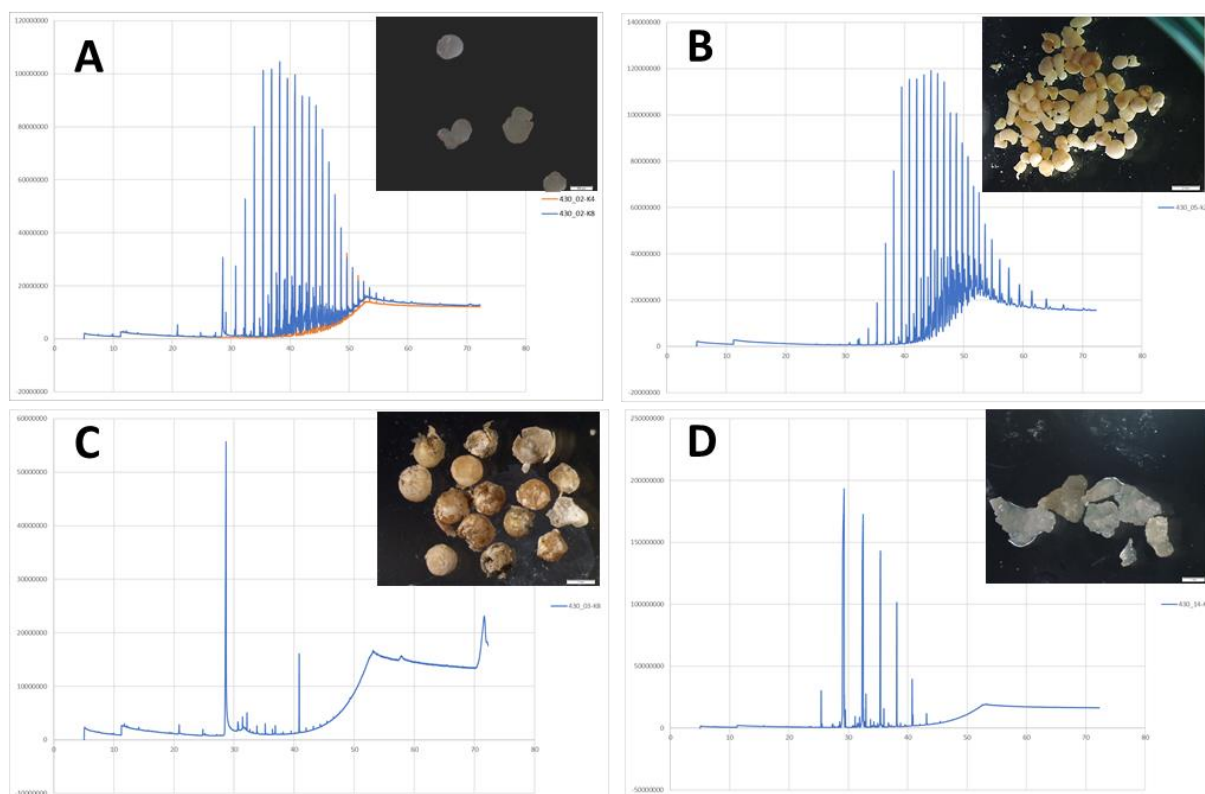


Figure 15: Total ion chromatograms of the main components acquired from samples consisting of putative paraffin wax particles retrieved from different sampling stations in the southern North Sea and assigned to different categories based on their appearance. A: paraffin (station 2, category 3 and 4), B: high boiling aliphates (station 5, category 2), C: fatty components - fatty acids / glycerides (station 3, category 8), D: fatty alcohols (station 14, category 2).

The spatial distribution of PWs floating in the southern North Sea based on the results for all 24 stations sampled is shown in Figure 16. At eight, marked with a red dot, putative PWs have been sorted out but could not be confirmed by GC methods due to their low abundance. The pie charts at the other six stations show the shares of the different main components, being paraffin (green), fatty alcohols (orange) and fatty acids and Bis(2-ethylhexyl) decanedioate /glycidyl palmitate (blue), identified as wax particles. At all these six stations wax particles with the main component being paraffin were detected and had higher relative shares compared to the other components. At station 5, paraffin was also the only component. At station 14, the relative share for paraffin and fatty alcohols was approximately equal. At station 2, the relative percentage of particles with fatty acids and Bis(2-ethylhexyl) decanedioate /Glycidylpalmitate being the main component dominated over the ones containing mainly paraffin. The size of the pie charts relates to the total number of identified PW particles per analyzed sample. Most PW particles were detected at station 20 followed by station 21 and station 2 with 132, 123 and 91 particles respectively. At station 3, 5 and 14 the particle numbers were lower with 38, 18 and 13 particles respectively.

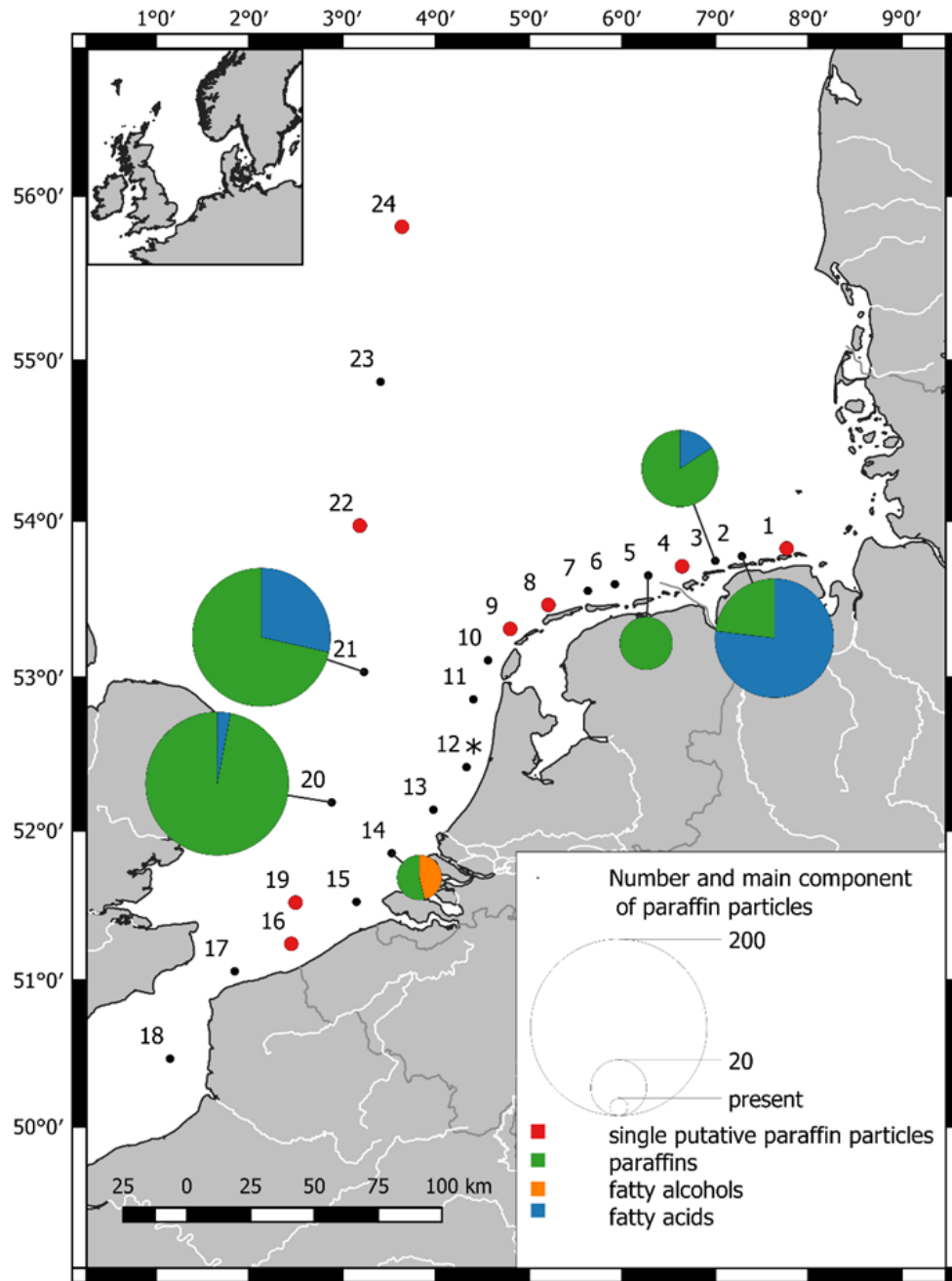


Figure 16: Spatial distribution of paraffin wax (PW) particles (500–5000 μm) in the southern North Sea. The pie charts at the stations where PWs were detected are showing the relative shares of the particles based on the main component identified via gas chromatographic techniques. The size of the pie chart relates to the number of PW particles detected. Stations, where putative PW particles were detected but not further analyzed, are marked with a red dot. Stations, where no sample was analyzed, are marked with *.

Discussion

PWs have been successfully identified in several surface water samples from the southern North Sea. The particles had been sorted into eight different categories based on their appearance. However, the analysis of the chemical composition with spectroscopic and GC methods, revealed that some of these visually distinct categories were chemically more similar to others. The ATR-FTIR spectra of particles assigned to category 2 and 4 were highly similar. Same can be said about spectra from particles of category 1 and 5. Bands in the wavenumber range around 1462 cm^{-1} (deformation of C-H bonds) and around 727 cm^{-1} (rocking of CH_2 groups,) are characteristic for a linear saturated aliphatic structure, and thus petroleum waxes like PWs (Dwivedi et al., 2017). These bands, as well as the shoulder around 2950 cm^{-1} , occur in all the recorded spectra of the putative PW particles of this study. The ATR-FTIR spectra of particles sorted here into category 2 and 4 are also very similar to the ones recorded of stranded material assigned to microcrystalline wax, a petroleum wax, by Suaria et al. (2018). On the other hand, ATR spectra of particles sorted into category 1 (station 21), and category 5 (station 2) showed a more complex pattern of bands indicating that they might be a composite of paraffin and other substances. Svečnjak et al. (2015) pointed out the presence of bands around $1739\text{--}1745\text{ cm}^{-1}$ and 1173 cm^{-1} or 1158 cm^{-1} as being indicative for free fatty acids and esters in beeswax and beef tallow. These bands correspond to the ones present in some of our putative PWs (Figure 19 A, D). Furthermore, they showed that mixtures of beeswax with paraffin exhibit additional bands of varying intensity in the wavenumber range $1765\text{--}1700\text{ cm}^{-1}$, which are characteristic for free fatty acids and esters (Svečnjak et al., 2015). This might indicate that not all of the putative PWs comprised of pure paraffin but might contain fatty acids, either intentionally added in the form of, e.g. tallow or beeswax, or associated with biota.

The exemplary analysis using μFTIR imaging for the size fraction $20\text{--}500\text{ }\mu\text{m}$ of one of the samples (station 20), which contained a large number of PWs $>500\text{ }\mu\text{m}$, yielded spectra matching with PE (wax) in the database. This is, however, not surprising since most of the bands detected in the PWs are also characteristic for PE (Gulmine et al., 2002). Furthermore, PE is often added to the wax to improve its softness and to influence its color, texture and oil content (Kienhuis et al., 2018). However, the observation that these particles in the sample started to melt at $30\text{ }^\circ\text{C}$, which matches the low melting point of soft PW while PE has melting points above $118\text{--}146\text{ }^\circ\text{C}$ (Mark, 2009), indicates that these particles were PWs also containing other hydrocarbons with lower melting points, rather than PE. Most notably, however, this observation emphasizes that gentle sample preparation is of the utmost importance when PWs are to be identified with spectroscopic techniques. To the best of our

knowledge, this is the first study verifying the presence of PWs in the size range of 20–500 μm in marine samples using μFTIR imaging. The analysis for PW particles can be performed simultaneously with analysis for microplastics. Although the detection of PWs is possible, a reliable quantification could not yet be achieved. This is due to the complexity to distinguish the spectra of PE and PWs, even more, when being limited to a restricted wavenumber range (3600–1250 cm^{-1}) for analysis. A more reliable discrimination could possibly be achieved when the spectral databases were to be extended with more PWs or different filter material, allowing for a broader wavenumber range, is used. However, GC-FID and GC-MS proved to be a powerful tool for a subsequent validation of putative PWs in bulk.

GC analyses showed that all samples from category 2, 3 and 4 had paraffin as the main component (partly high boilers) with some (one of each category) also containing fatty alcohols. The only exception is the sample from station 14, sorted into category 2, which is mainly composed of fatty alcohols and to a lower level of paraffin. Fatty alcohols like 1-Icosanol (C20) to 1-Octasanol (C28) have various applications like emulsifier, surfactants or lubricants (Behr & Seidenstricker, 2017). Category 1 and 5 appear similar, however, particles assigned to category 1 seem to be more brittle and the surface less smooth. Both categories are characterized by having fatty alcohols as the main component. Still, category 5 particles exhibited also the paraffin pattern while category 1 particles also contained bis(2-ethylhexyl) decanedioate, a substance which can be used as plasticizer and lubricant (European Chemicals Agency (ECHA)). Oxiran-2-ylmethyl hexadecanoate, commonly known as glycidyl palmitate, a glycidyl ester of palmitic acid, can origin during the refining of fat and oil (Bundesinstitut für Risikobewertung (BfR), 2009). Thus, the results show that most of the putative PW particles were indeed comprised of paraffin but that other substances like fats and lubricants also accompany them. This finding is in line with the results of the spectroscopic analyses. It also highlights the fact that PWs can be blends of petroleum-based waxes, e.g. PWs or microcrystalline wax, with natural waxes, e.g. beeswax or tallow, (Maia et al., 2013; Svečnjak et al., 2015).

The results from the two different techniques are not directly comparable since the ATR-FTIR spectra were measured for individual particles and also only for a subset of particles while results from the GC-FID and GC-MS were received for composite samples consisting of a mixture of particles that were pooled together based on subjective visual resemblance. Generally, these two techniques should be considered as complementary. An analysis of putative PWs first with ATR-FTIR and later with GC-based techniques would be ideal but proved difficult because most of the particles could not be retrieved intact or at all after the spectroscopic analysis because of the destructive nature of the ATR mode (i.e. particles have to be tightly fixated with a pressure clamp on the crystal, sometimes being crushed in the

process). However, unambiguous identification of PWs solely relying on ATR-FTIR is not recommendable at the present stage due to the occurrence of PWs.

Putative PWs were detected floating in the North Sea at several stations. In samples of six of these stations, the identity of these PWs could be confirmed by spectroscopic and gas chromatographic methods. These stations are located close to the English Channel (station 20 and 21), the Rhine-Meuse-delta (station 14) and the Frisian Islands (stations 2, 3 and 5). Of these six stations the highest numbers of PWs, based on the visual counts of putative PW particles which were confirmed as bulk samples by GC-FID and GC-MS analyses, could be found at the stations influenced by inflow from the English Channel (station 20 and 21). This is no surprise since the southern North Sea, especially the route from the English Channel along the central European coast is one of the busiest in the North Sea, even more so in summer months according to NorthSEE (2016).

Usually, PWs are encountered in the marine environment at beaches rather than floating, and their identification is done visually, thus being restricted to sizes still visible to the naked eye. Most records of PWs found at beaches are related either to mass strandings (UEG, 2014; Sea-Mer Asso, 2017) or beach monitoring for marine litter (Dagevos et al., 2013). Since PWs are commonly not considered as plastics, they are usually not referred to in studies assessing the distribution of microplastics in the marine environment. However, their presence has been recognized in some studies. Esiukova (2017) reported the occurrence of PWs at all of the 13 sampling locations which she sampled for microplastics at Baltic Sea beaches in the Kaliningrad region. The presence of PWs at beaches in this region was later affirmed in another study by Chubarenko et al. (2018b). In another study in the Baltic Sea region, PWs were also encountered among the micro and macro litter and on Lithuanian beaches PWs of <1 cm in size were, with 55%, even the most abundant group (Haseler et al., 2018). For the North Sea, the presence of PWs at beaches all along the Dutch coastline in a survey period from 2002–2012 has been recorded in three size categories (0–1 cm, 1–10 cm, and >10 cm) according to OSPAR recommendations, with the smallest size class being the most abundant one (Dagevos et al., 2013). In a more recent report by Wenneker and Oosterbaan (2018) the analysis of 63 samples, collected during a beach cleanup in 2017, revealed that 54 of these could be clearly identified as PWs.

Because of their ubiquity and the repeating occurrence of mass strandings, some European countries and also NGOs like KIMO urged to tighten the regulations for the discharge of PWs at sea. Beginning of 2019 the IMO agreed on amendments to Annex II resulting in changes to regulation 13 providing that the tanks have to be unloaded as much as possible before performing a prewashing of the tanks to remove any residues and the water containing the

residues from the prewash should be brought to special reception facilities (IMO, 2019). This new regulation deems the discharge of paraffin at sea illegal. To see whether these amendments make an impact, methods for the unambiguous identification of PWs, also in the size range of microplastics, have to be improved and harmonized. The here presented approach using ATR-FTIR as well as gas chromatographic methods as two complementary techniques proved to be suitable to identify PWs of different chemical composition down to 500 μm . Furthermore, a first record of these PWs in a size range of 20–500 μm floating in North Sea surface waters has been made by utilizing μFTIR imaging. However, this approach needs to be further improved to allow for a validated quantification of these petroleum waxes. Finally, the assessment of PWs should be connected to the monitoring of microplastics.

Acknowledgements

C.L. would like to thank the “Deutsche Bundesstiftung Umwelt (DBU)” for financing her with a PhD scholarship. Furthermore, this work was supported by the German Federal Ministry of Education and Research (Project BASEMAN – Defining the baseline and standards for microplastics analyses in European waters; BMBF grant 03F0734A).

The Federal Maritime and Hydrographic Agency (BSH) in Hamburg is acknowledged for facilitating the GC-FID and GC-MS analysis and data evaluation.

Chapter IV

Different stories told by small and large microplastics in sediments - First report of microplastic concentrations in an urban recipient in Norway

Marte Haave^{a,*}, Claudia Lorenz ^b, Sebastian Primpke^b, and Gunnar Gerdt^b

^a NORCE Norwegian Research Centre, P.O.B 7810, 5020 Bergen - Norway;

^b Alfred Wegener Institute, Helmholtz Centre for Polar and Marine Research, 27483
Helgoland - Germany

Corresponding author:

Marte Haave: marte.haave@norce-research.no

Published in *Marine Pollution Bulletin* 141: 501-513.

doi: <https://doi.org/10.1016/j.marpolbul.2019.02.015>

Abstract

Microplastics (MP) in sediments from discharge sites for wastewater and deposition sites in deep regions in an urban fjord in Norway were extracted by density separation in a Microplastic Sediment Separator with ZnCl_2 . Particles ($>11\ \mu\text{m}$) were identified using FTIR. Twenty different polymer types were identified, at concentrations from 12000 to 200000 particles kg^{-1} dw. Over 95% of the MP were smaller than $100\ \mu\text{m}$. High deposition of small MP agreed with known areas for organic deposition. Polyurethane acrylate resins dominated the small MP while polyamide fibers dominated the larger MP. Particles $>500\ \mu\text{m}$ showed different maximum concentrations and spatial distribution from the smaller particles. This study is the first to report concentration ranges of identified plastic particles from a Norwegian fjord, down to sizes below the limit of visual identification. The results provides a baseline for future comparison, and point at relevant sizes for environmental risk assessments.

Keywords: Microplastic, Sediments, Extraction, Quantification, FTIR imaging

Introduction

Plastic is used in every part of modern society, and the production volume of 348 million tons per year in 2017 is increasing every year (PlasticsEurope, 2018) . At the same time, global concerns are rising, as plastic materials accumulate in remote areas of the world, far from human activities, in Arctic Sea ice and at the bottom of deep- seas (Woodall et al., 2014; Bergmann et al., 2017; Peeken et al., 2018). The number of species harmed and killed by plastic litter on land and in the oceans supports the definition of plastic as a harmful substance (Rochman et al., 2013). Although not yet defined as a persistent, bioaccumulative or toxic pollutant as such, the observed and predicted negative effects of plastic materials is of growing global concern, and plastic littering is addressed by the international and scientific community (da Costa, 2018). The EU commission addresses plastic as one of the challenges for the environment with a European Plastic Strategy (EU Commission, 2018), and address how to stop the continued uncontrolled release of plastic waste. Globally increasing production volumes, continued and uncontrolled release and plastic degradation urges the understanding of ecosystem tolerance and effects of plastic and microplastics (MP, here defined as <5 mm).

The EU Water Framework Directive (WFD) places a responsibility on local and national authorities to ensure Good Ecologic and Chemical Status in aquatic recipients. Good Environmental Status for Descriptor 10 of Annex I in the Marine Strategy Framework Directive (MSFD) has been defined as when “Properties and quantities of marine litter do not cause harm to the coastal and marine environment”. Fulfilment of this aim requires an understanding of the current and future concentrations with respect to ecosystem tolerance, and a definition of the described end-point “no harm”. These requirements are currently not in place.

Standardized monitoring of marine recipients is routinely undertaken, according to the EU-WFD. Such repeated monitoring programs provide in depth knowledge about biological and chemical status in coastal recipients, as well as abiotic factors. This can provide supporting information to understand MP distribution in areas impacted by human activities. Moreover, the understanding of the biodiversity at such monitoring sites may prove useful for relevant impact assessments and gaining knowledge about ecosystem effects or sensitive species. Previous studies show that MP deposit in the sediments at sites with low current in a similar way as organic debris (Lattin et al., 2004; Woodall et al., 2014; Bergmann et al., 2017; Maes et al., 2017b), and it is generally accepted that the ocean floor is a major sink for MP (Lattin et al., 2004; Van Cauwenberghe et al., 2013; Woodall et al., 2014; Bergmann et al., 2017). The MP distribution concentration ranges and extremes are however unknown in large parts of the world.

This study is the first Norwegian study targeting quantification and understanding of concentration ranges of small MP in sediments in an urban harbor. The study has two aims: to use unbiased methods and quantitative analyses to establish concentration ranges for future inter-study comparisons. To understand MP distribution patterns using quantification of MP in combination with in depth knowledge about the current systems and organic contents of the sampling sites.



Figure 17: Map over the coastal recipient Byfjorden outside the city of Bergen, in relation to the west coast of Norway, the outer archipelago and the sampling stations selected for microplastic quantification April 2015. Red stars: Wastewater treatment plants where samples were collected (35 meters depth), blue stars: deep deposition sites (315–330 meters depth), grey star: Wastewater treatment plant, not sampled.

Materials and Methods

Selected sites

The study area is in western Norway, outside the city of Bergen (Figure 17). The fjord (Byfjorden) is sheltered from strong coastal currents by the archipelagos known as Sotra and Askøy. Five sites were selected for an initial investigation of MP concentrations: Two discharge sites for combined sewage and surface runoff at wastewater treatment plants (WWTP), and three suspected deposition sites in the deep parts of Byfjorden near the Bergen city center (Figure 17). Characteristics of the selected sites are given in Table 7. Bergen has ~275,000 inhabitants, and the central urban area releases wastewater from about 200,000 person equivalents through three main WWTP along the eastern shoreline (Figure 17). Wastewater is known to contain MP particles (Magnusson, 2014; Mason et al., 2016; Mintenig et al., 2017), and the two largest WWTP discharge sites, namely Kvernavika (Kvr1) and Lyrneset (Lyr2) were selected for MP analyses. Grit separation, and mechanical filtration through 5 and 1 mm filters was applied to sewage in Bergen from the late nineties, and secondary treatment was not in general use at the time of sampling. At Kvernavika the 1 mm filters were disabled from June 2012 until October 2013, and for a period in August 2013 during renovation and upgrading to secondary treatment, thus untreated wastewater from approximately 40,000 persons was released at the time of sampling. At Lyrneset, wastewater from another 100,000 person equivalents were released without any other treatment than skimming of fat and grit separation at the time of sampling in 2015, which allows floating particles of all sizes to be released. The samples were taken as close to the outlet pipes as possible, approximately 20 meters from the outlets at 35 meters depth. The third and smaller WWTP at Fagerneset was not sampled for this study (Figure 17). Fagerneset had installed secondary treatment at the time of sampling, and released treated sewage from approximately 44,000 person equivalents. The sites selected to represent the deep deposition areas for MP were situated along the midline of the fjord: stations St4, St5 and St11 at 315–330 m depth (Figure 17). Here, the biotic and abiotic benthic conditions were well known after decades of benthic monitoring. Knowledge about historic values of organic content and sediment grain size at the sites leads to the prediction that the sites will receive varying input of urban surface run-off and varying degrees of particulates from sewage discharge from the city as well as discharge from small, private sewage outlets, thus likely showing a variation in MP concentrations. Investigation of this well-known system may help understand MP distribution in an urban system, and help identify likely hotspots for deposition.

Chapter IV

Table 7: Sites, sediment characteristics and calculated total number of identified synthetic polymer particles (11–500 µm) from Byfjorden (Bergen, Norway), April 2015.

Site		Depth (m)	TOM (%)	Grain size (%)		Dry matter (%)	Sample mass (g)		Subsample for FTIR (HP/WP)	MP concentration (kg ⁻¹ dw)	
(n=1)	Coordinates			Pelite	Sand		ww	dw	% of sample	<500 µm	>500 µm
Kvr1	E 295167 N 6708986	34	9.1	7.3	92.6	49±4.0 **	1013	496	1.5/13.76	(205±20) x10 ³	85
St4	E 294498 N 6705128	333	14.7	89.7	10	35±2.4 *	745	261	6.39/8.72	(71±17) x10 ³	107
St5	E 291909 N 6701608	322	7.1	45.3	54.6	56±1.9 *	797	446	8.17/40.58/ 6.73 [#]	(28±10) x10 ³	211
St11	E 293364 N 6710889	315	10.8	82.8	17	40±1.9 *	1261	504	11.17/36.4 0	(12±7) x10 ³	48

Coordinates as EUREF89 UTM 32V; TOM: Total Organic Matter (550°C); pelite: < 63µm, sand: 63µm-1mm, * from 2015 (n=6). **From 2013 (n=3), ww: wet weight, dw: dry weight, HP: *n*-hexane phase, WP: water phase [#]The water phase was split in two.

Sampling

Sediment samples were collected by Van Veen grab during an ongoing monitoring program in April 2015, following standardized methods for soft bottom sampling for chemical analyses (ISO NS 5667:19). Approximately one kilo of wet sediments from the top sediment layer (0–1 cm) of three grabs per site was collected, using a metal sampling spoon, pooled and stored at -20°C in chemically clean Rilsan-bags (Tub-ex). Sediment characteristics (water content, organic matter and grain size) were derived from previous analyses from the ongoing monitoring program, the latest from 2015 from the time of sampling (Kvalø et al., 2016).

Extraction and purification of microplastics from sediments

Isolation of MP by density separation was done using the Microplastic Sediment Separator (MPSS -Hydro-Bios) with Zinc-chloride solution (ZnCl₂) of density ~1.65–1.78 kg dm⁻³. The extraction efficiency for all size classes in one single extraction step has previously been validated (Imhof et al., 2012), and was not repeated for this study. The purification and isolation protocol was performed similar to (Bergmann et al., 2017). The sediment samples were weighed into 2L glass beakers, covered with aluminum foil and transferred to the MPSS filled with ZnCl₂. The rotor of the MPSS ran for ~30 minutes, and the system was visually inspected before mounting the top chamber. Large pieces of debris or plastic rising up into the MPSS standpipe were removed before closing the top chamber. The MPSS top chamber was then filled with ZnCl₂ within 2 cm from the top, and the rotor left running for 2–3 hours before standing overnight to separate.

Occasional samples produced gas during extraction (possibly caused by a reaction between CaCO₃ in seashells and the acidic ZnCl₂ releasing CO₂), resulting in bubble formation and foam that lifted material such as silt and sand into the top chamber of the MPSS. To remove

silt and other debris, we applied a second overnight density separation in a separation funnel, followed by slow centrifugation at 1000 rpm for 20–30 minutes in 300 mL ZnCl₂ in polycarbonate centrifugation flasks. The centrifugation was repeated once after pellet resuspension in another 300 mL ZnCl₂. The supernatants were collected in a glass flask, filtered through 30 µm stainless steel filters (Spectra/Mesh® woven filter, art. no. 145827). The pellets were inspected under a binocular microscope for fallout of suspected plastic particles.

After these extraction steps, samples were treated simultaneously to limit differences in potential contamination. Enzymatic purification was performed, following (Löder et al., 2017), with some modifications described below. Adjustments were: treatment in 10% SDS overnight (50 °C), followed by enzymatic treatment. Enzymes from ASA Spezialenzyme GmbH were filtered over sequentially finer glass fiber filters, down to 0.7 µm (Whatman™ GF/F™) before storage in sterile containers. The volume of buffered enzyme solution was 75–100 mL, enough to cover the sample in the glass beaker, and the samples placed under tin foil cover in a heater with gentle rocking (Hybaid Shake'n stack). Treatments were as follows: Protease in 0.1 M TRISBase (ratio 1:5) at pH 9.0 and 50 °C for 12 h then three days of Cellulase TXL in 0.1 M Na-Acetate buffer (ratio 1:5) at pH 5.0 and 50 °C changing the enzyme solution every day, followed by Chitinase in 0.1 M Na-Acetate buffer (ratio 1:25) at pH 5.0 and 37 °C. Care was taken to include all particles when changing the enzymes, rinsing down the sides of containers repeatedly with MilliQ® water (filtered at 0.22 µm). Filters were ultrasonicated in MilliQ® for 5–10 minutes and the washing water added to the final sample.

Pre-selection by phase separation

After the enzyme digestion steps, the samples still contained visible debris from coal, silt and plant material, which would interfere with further FTIR imaging (Shim & Thompson, 2015). Since coal will not sink out of ZnCl₂, attempts were made to make the coal absorb water to sink out of solution. Several different mixtures of organic solvents were tested for separation efficiency: a) cyclohexane and ethanol, b) *n*-Hexane with SDS, c) *n*-hexane with ethanol (99%), d) *n*-hexane only, all added to a water-phase of saturated sodium chloride (NaCl) solution. The separation efficiency was visually assessed by adding coal particles from a discarded sample and plastic particles made by cryo-milling known polymer types. The best separation, determined visually as separation of coal and polymer particles was achieved by using *n*-hexane and saturated NaCl solution, which was thus selected for further testing. The extracted and enzymatically purified MP samples from each site were added to a 250 mL glass separation funnel with saturated NaCl and *n*-hexane (1:1), shaken vigorously for 20 seconds and allowed to settle for 10 minutes (Figure 18). The settled debris was released into a dish, inspected visually in a stereomicroscope, and discarded. The *n*-hexane and the saltwater

layers were released into separate flasks, rinsed in MilliQ® and analyzed by focal plane array – Fourier Transform Infrared Spectroscopy (FPA FTIR) to quantify the total MP in each separation phase to check the efficiency of the phase separation method. The total MP counts per site represent combined results from both phases.

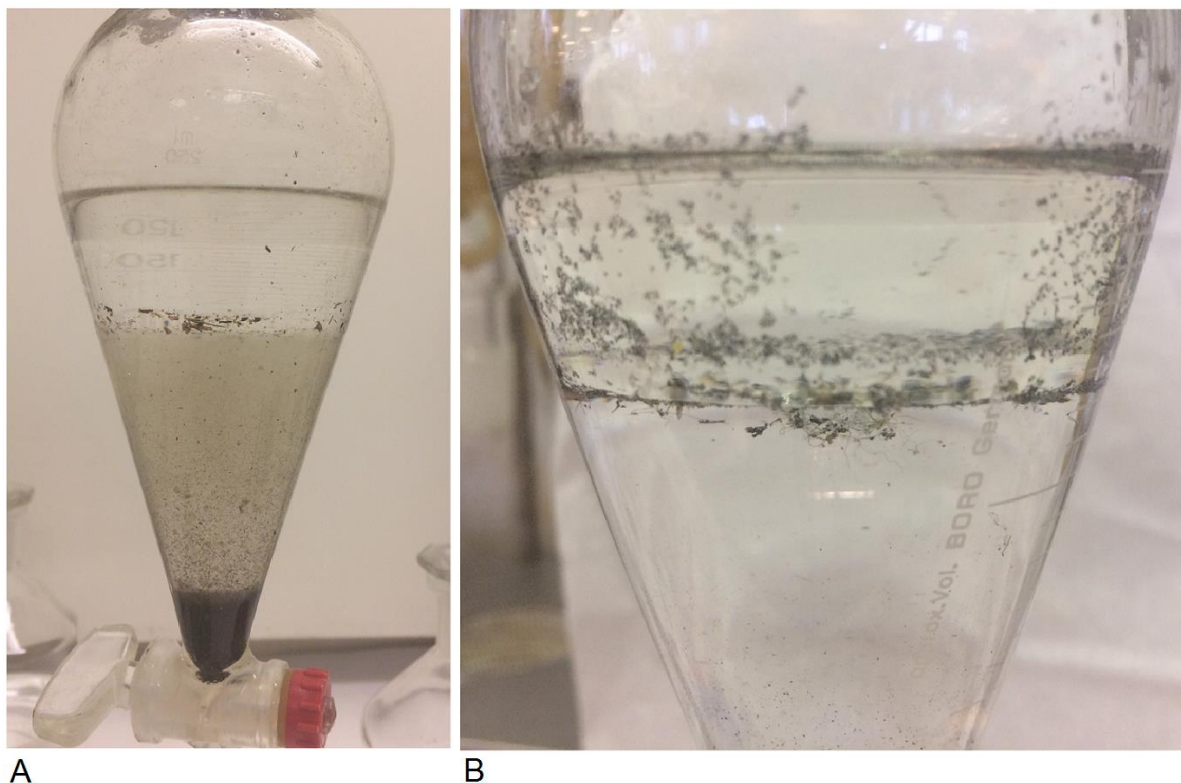


Figure 18: Set-up of pre-selection by phase separation using saturated NaCl solution /*n*-hexane (1:1) to allow separation of indigestible particles that would otherwise interfere with identification by FPA-FTIR (A). Fibers as well as some debris remaining at the interphase (B).

Prevention of contamination

Surfaces and equipment were rinsed and wiped with laboratory tissue paper, MilliQ® water, or prefiltered ethanol (Whatman GF/C: 0.7 µm) just prior to use. Lab personnel wore clothing and coats of natural fibers, avoiding synthetic polymers in the lab as far as possible. Synthetic polymers used were PTFE (Teflon) in the top chamber valve of the MPSS, in squeeze-bottles and in separation funnel valves, silicon tubes for the transfer of ZnCl₂, nitrile gloves and plastic goggles for protection, screwcap bottle tops (Schott bottles) of polypropylene (PP) for storage of reagents and transportation of samples. To limit contamination as far as practically possible, most work was done in ventilated closed cabinets wiped clean with MilliQ® and lab-tissue paper before use. Due to the lack of a plastic free, clean-lab, glassware was always rinsed with MilliQ® just before use, and samples were covered with clean, rinsed glass-lids or aluminum foil and exposed as little as possible to the open air during isolation and purification. Inspection of blank filters and open beakers of water for control of potential air-contamination

from dust did not reveal suspicious contamination with colored fibers or large particles visible in a stereo microscope. Smaller synthetic particles may however have escaped this control.

FTIR analyses

Before FTIR, particles >500 μm were separated using a 500 μm stainless steel mesh (Haver Multironden, Art. No 00600168 Haver and Boecker). The material retained on the 500 μm mesh was dried overnight at room temperature. All the particles were imaged and measured using the camera coupled to the microscope and the cellsens software (Olympus) and spectroscopically analyzed using an ATR unit with a Tensor 27 (Bruker). All acquired spectra were immediately compared to the reference library published in Primpke et al. (2018). In accordance with Hanke et al. (2013) (page 104), a Hit Quality Index (HQI) of 700/1000 was set as threshold for safe identification of polymers. If particles had scores lower than 700, three attempts for a positive ID were made. If scores were under 600, expert manual comparisons of spectra with known synthetic polymers were done before including or rejecting particles as synthetic polymers.

The fraction smaller than 500 μm was filtered on 20 μm stainless steel filter and rinsed with MilliQ® into pre-weighed 100 mL glass bottles. Three parallel subsamples of 1 mL were analyzed with FlowCam (Fluid Imaging) to calculate the adequate volume needed for filter coverage, without overloading the aluminum oxide filter (Anodisc, 25 mm diameter, 0.2 μm pore size, Whatman). The subsamples used for FTIR imaging represented 6.4 to 40.6% of the total sample volume (Table 7). Samples were loaded using a 10 mL pipette and a glass funnel to concentrate the sample onto a 10 mm area in diameter. The sample was rinsed with MilliQ® and ethanol to ensure that all the particles were on the filter and not stuck to the pipette or the glass funnel. The filter was placed in a glass petri dish and dried for two days in a drying cabinet/oven at 30 °C. FTIR imaging was done with Hyperion 3000 FTIR microscope with a 64 \times 64 elements FPA detector connected to a Tensor 27 spectrometer (all Bruker) with 6 Scans, a binning factor of 4 and a resolution of 8 cm^{-1} . The resulting data was evaluated via the automated recognition in accordance with Primpke et al. (2017b), with the reference database of Primpke et al. (2018).

Quality control

For quality control, the results of the automated recognition were partly manually reanalyzed in accordance with Primpke et al. (2017b). In short, for each polymer class, randomly selected spectra were compared by expert knowledge to the assigned reference spectrum and the absence/presence of peaks. In this case the calculations from FTIR imaging were within the 95% Confidence Intervals (CI), except for rubber type 3 which was within the 90% CI.

Chapter IV

Results of polymer types, particles per size class and percentage of sample volume used for the loading of the filter were used to calculate total number of particles in the original sample using the following equations:

$N_P = \frac{n_p}{f_V}$	Eq. 2.1
$N_{dw} = \frac{(N_{P1} + N_{P2} + N_{P3})}{m_S}$	Eq. 2.2

The number of particles per phase in the phase-separation (N_P) was calculated with Equation 2.1 with n_P as the numbers of determined particles on the filter and f_V as the fraction (%) of the total sample used. The sum of the particles in each phase (N_{Px}) was divided by the estimated dry weight (dw) (m_S) of the sampled sediments to convert counts to concentration (particles kg^{-1} dw). N_{P3} (Eq 2.4) signifies that up to three subsamples of phase separation were used (St5).

To estimate the errors of scaling and sample preparation the Gaussian propagation of uncertainty was used:

$\Delta N_P = \sqrt{\left(\frac{n_P}{-f_V^2} \Delta f_V\right)^2 + \left(\frac{1}{f_V} \Delta n_P\right)^2}$	Eq. 2.3
$\Delta N_{DW} = \sqrt{\left(\frac{(N_{P1} + N_{P2} + N_{P3})}{-m_S^2} \Delta m_S\right)^2 + \left(\frac{1}{m_S} \Delta N_{P1}\right)^2 + \left(\frac{1}{m_S} \Delta N_{P2}\right)^2 + \left(\frac{1}{m_S} \Delta N_{P3}\right)^2}$	Eq. 2.4

For the error of the sample fraction (Δf_V) an individual error per sample was calculated assuming an error of 0.1 mL during sample filtration. For the error of particle numbers (Δn_P), an average error of 5% for the derived particle numbers by automated recognition was applied. For determination of the error of the sample mass (Δm_S) the given error for dry weight (see Table 7) and the individual error of the subsamples (ΔN_{Px}) was used. To adjust for the lack of a blank sample the lowest number of particles found in a subsample was added to ΔN_{Px} . In practice, this meant that we treated all the particles found in the fraction with the lowest number of identified particles (St 11, water phase) as if they were only due to lab-contamination, and this number of particles were subtracted from all the other samples, which can be considered a conservative approach.

Statistics

Possible differences in the assemblages of polymers among sites were assessed by use of permutational multivariate analysis of variance (PERMANOVA) (Anderson, 2001; Anderson & Walsh, 2013) with Bray Curtis distance metric, 9999 permutations and correcting the

Chapter IV

significance level for multiple testing by sequential Bonferroni (Holm, 1979). Polymer abundance ($\text{MP kg}^{-1} \text{ dw}$) were first transformed to percentage per size class and compared using each size class as a data point for the site.

Results and Discussion

Site characteristics and MP concentrations

This study investigated MP in sediments from Byfjorden, near the city of Bergen (population ~275 000), where sewage and wastewater was released with only primary treatment (grit separation and coarse filtering >1mm) for decades. The sample characteristics and MP particle counts are shown in Table 7.

Concentrations in sediments (MP kg⁻¹ dw) are shown in Table 7 and Figure 19 A-C. Polymer types and size class distribution of MP (11–500 µm) are shown in Figure 20. Tables with details of polymer types and particle numbers per size class are included in the supplementary material (Table S22).

The results show that the maximum concentration of MP smaller than 500 µm followed the expected deposition patterns based on knowledge of historic sediment grain size, total organic matter (TOM), and ocean currents for the sites (Kvalø et al., 2014; Kvalø et al., 2015; Kvalø et al., 2016), as well as distance to the discharge sites. The highest MP concentration was found at the discharge site (Kvr1), which had highly noticeable influence of untreated sewage at the time of sampling. Although a high MP input from wastewater was expected, the shallow Kvr1 (35 m depth) had coarser sediments than the deep sites, indicating stronger currents and less settling of debris. The second highest concentration of MP was found at the deep St4 (333 m depth). St4 is where the surface water running south meets the deeper inflow of water running north. This produces a back-eddy or gyre with slow moving water where conditions favorable for deposition of debris, as seen throughout years of benthic monitoring. The slow bottom currents are reflected by the moderately high organic content (Table 7) and dominantly fine sediments, which has been typical for this site (Table 7) (Kvalø et al., 2016). The southern site St5 (322 m) is close to the large sewage discharge point at (Lyraneset), and is positioned between city of Bergen, the old wharfs and maritime industry on the southern bank, and the populated island Askøy. However, St5 had a lower concentration of MP than St4, coarser sediments and lower TOM. This was likely due to the episodic events of inflow of deep water, moving the top sediment layer northeast towards St4. The sediment properties at St5 reflected stronger currents and less settling of debris at St5 than in the more open parts of the fjord (Table 7) (Kvalø et al., 2016). St11 in the northern part of the fjord, upstream of the sewage outlets, had the lowest number of MP of all sites. The sediments at St11 was mostly fine, with TOM higher than St5 and Kvr1 (Table 7), which indicated favorable conditions for deposition of fine particles. St11 is furthest from the city, and the surface water moving south over this station is likely to contain less plastic since it comes from a less populated area. The results,

indicated that organic matter content and grain size is related to MP concentrations, which supports findings by Maes et al. (2017b) and Vianello et al. (2013).

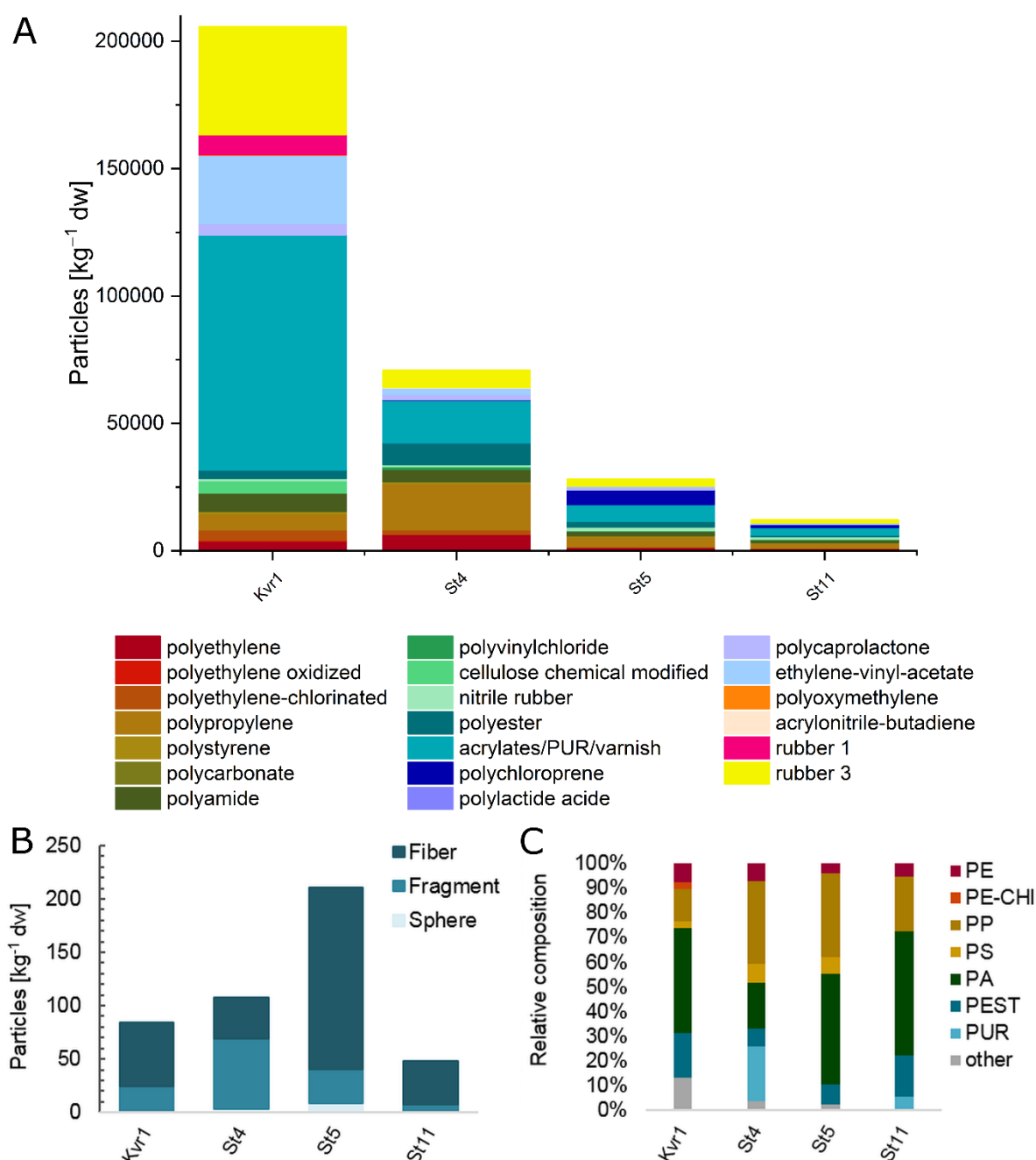


Figure 19: MP in sediments from Byfjorden (Norway) April 2015. Polymer distribution and MP concentration $\text{kg}^{-1} \text{ dw}$ for particles 11–500 μm (A). MP concentrations $\text{kg}^{-1} \text{ dw}$ and shapes of particles >500 μm (B). Relative contribution of synthetic polymers per station for particles >500 μm (C). The group “Other” includes Styrene Acrylonitrile, Expanded polystyrene, Polymethyl(methyl)acrylate and Polyvinyl Chloride.

At the site near the main wastewater outlet for the city, on the southern bank (Lyr2) the influence of untreated sewage was noticeable at the time of sampling. Due to the nature of this sample, flooding after reaction with ZnCl_2 and subsequent blocked filters during isolation lead

to severe losses of sample material. For this reason, the sample from Lyr2 was disregarded for the quantitative analysis. It was clear from the initial separation that the sample contained visually identifiable plastic materials, where glitter particles were among the most conspicuous.

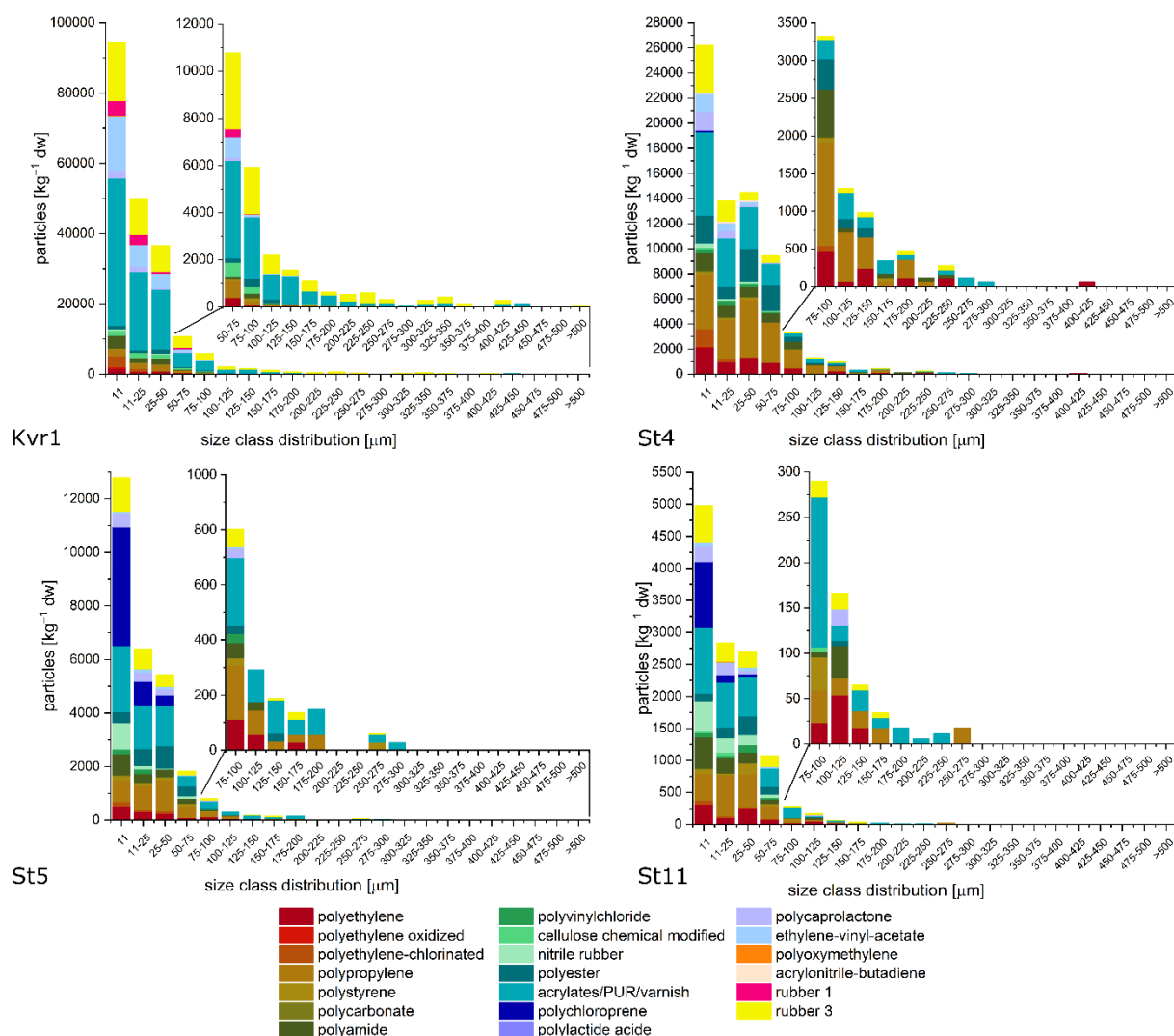


Figure 20: Concentration (MP kg⁻¹ dw), polymer composition and size class distribution of MP (11–500 μm) in the top-layer (0–1 cm) of sediments from Byfjorden (Norway), April 2015.

Size distribution and polymer types

From the FTIR imaging analyses of particles 11–500 μm it was clear that smaller particle sizes were dominant in numbers (Figure 20), which corresponds to previous studies (Shim & Thompson, 2015; Bergmann et al., 2017). For all sites, MP under 100 μm made up 95–97% of the total < 500 μm, and the MP < 25 μm made up 56.3–70.1% of the total. There were over all few MP in the size classes 300–500 μm (Figure 20, and Supplementary Table S22).

Twenty different polymers types were identified in this study using FTIR imaging. Additionally, polytetrafluoroethylen (PTFE/Teflon) and silicone were found among the MP >500 μm , but since these polymers were believed to come from the MPSS, valves and tubes used in the lab, they were excluded. In comparison, 18 polymer types were identified in Arctic samples after ZnCl_2 separation (Bergmann et al., 2017), and ten polymers were found in the Lagoon of Venice, where saline solution was used for density separation (Vianello et al., 2013). Among the polymers were polyamide/nylon (PA), PET and PVC that have densities higher than 1.2 kg dm^{-3} , and would thus not float in saturated saline. At the discharge site (Kvr1) the six most frequent polymers, which made up 88.8 % of the total were Polyurethane/acrylate varnish (PUR/Acr: 44.7%), rubber type 3 (R3: 20.6%), ethylene-vinyl-acetate (EVA: 13%), rubber type 1 (R1: 3.8%), polyamide (PA: 3.4%) and polypropylene (PP: 3.2%). At St4, the top six polymers which made up 86% of the total were PP (25.5%), PUR/Acr (23.6%), Polyester (PEST: 12%), R3 (9.6%), PE (9%) and PA (6.6%). At St5 the top seven polymers which made up 85.8% of the total were PUR/Acr (23.7%), polychloroprene (PChl: 20.4%), PP (13.3%), R3 (7%), PEST (8.2%), PA (5.9%) and PE (4.8%). At the most distant site, St11, the seven polymers which made up 81.8% of the total at St11 were PUR/Acr (23.6%), followed by PP (15.4%), R3 (10.8%), (PChl: 9.8%), PA (8.2%), PE (6.9%) and PEST (5.7%). The total number of MP at St11 amounted to less than six percent of the total at Kvr1.

In sum for all sites, eight polymers comprised 87.7% of the total particle counts. By far the most numerous polymer particle at all sites was PUR/Acr resins which comprised 37.3% of the total, followed by R3 (16.8%), PP (9.5%), EVA (9.3%), PA (4.5%), PEST (4.7%), PE (3.9%) and PChl (2.2%).

Comparing the polymer assemblages by PERMANOVA, including particles 11–500 μm from FTIR imaging and separating between size classes, showed that there was a significant difference between the polymer assembly at the discharge point and the deposition sites, while there were no statistical differences in polymer composition or relative abundance among the deposition sites (Table 8).

Table 8: Comparison of polymers from the sites St4, St5, St11 and Kvr1. The upper half of the table shows F-values (in bold) and the lower half shows statistical significance (in italic) (** $p < 0.01$) from PERMANOVA. A significant result indicates a difference between the sites. p-values are adjusted for multiple testing.

F value <i>p-value</i>	St4	St5	St11	Kvr1
St4	-	1,653	0,9181	12,7**
St5	<i>0.1457</i>	-	0,2759	8,923**
St11	<i>0.4332</i>	<i>0.9295</i>	-	7,371**
Kvr1	<i>1E-05</i>	<i>2E-05</i>	<i>2E-05</i>	-

Polyurethane acrylic resins is a diverse group of polymer blends with different specific gravities (Osswald et al., 2006). PUR/Acr resins are commonly used for paints and boat varnish. The presence of PUR/Acr at the discharge site supports its land-based source. Rubber Type 3 (R3) is mainly ethylene propylene diene monomer (EPDM) rubber used for a variety of land based applications such as seals, waterhoses and electrical insulation. PP and PE are the most demanded plastic materials commonly used in packaging and single use plastics (Plastics Europe), and are for that reason frequently encountered in the environment (Mintenig et al., 2017) and in surface water and beach-samples (Morét-Ferguson et al., 2010; Browne et al., 2011; Maes et al., 2017b).

The low proportion of PP and PE at the wastewater discharge site and relatively low percentage at the deep deposition sites in Byfjorden indicates that these polymers do not readily deposit on the ocean floor after release. PEST is commonly used for synthetic clothing, but here made up less than 2% of the total MP at all sites. Fibers of PA/Nylon may have come from land based (clothes) and marine sources, (ropes, nets and aquaculture). Polychloroprene (neoprene) was among the top polymers at St5 and St11 but was found in very small numbers at Kvr1 and St4, which indicates a source close to St5. Polycaprolactone was present at all sites. Polycaprolactone is termed a biodegradable plastic under anaerobic conditions (Tokiwa et al., 2009), yet it was widely distributed in the urban fjord system.

The sewage discharge site Kvr1 was the only site where polylactide acid, chemically modified cellulose, chlorinated polyethylene and rubber type 1 (acrylonitrile butadiene) were found, indicating that these polymers were discharged with wastewater and did not readily disperse to the deposition sites.

Car-tire abrasion and run-off from roads is estimated as the main source of MP to the Norwegian environment (MEPEX, 2016), thus Styrene Butadiene Rubber (SBR) was expected in the samples. SBR has a density of 1.7–2.5 (Vogelsang et al., 2018) and it is possible that ZnCl_2 is not dense enough (1.78 kg dm^{-3}) to separate the SBR from the sediments. Moreover, FTIR imaging in transmission and reflectance mode does not successfully identify SBR in car-tire rubber, as the SBR is vulcanized to Carbon Black. This study does therefore not conclude regarding the seeming absence of car-tire rubber in the samples. Investigations of car-tire rubber in environmental samples should take the mentioned limitations into consideration.

Particles larger than 500 μm

We examined by Attenuated Total Reflectance FTIR (ATR-FTIR) a total of 429 particles >500 μm that were retained after *n*-hexane/ NaCl separation. One hundred and eighty-eight (188) of the particles (43.8 %) were identified as synthetic polymers, excluding fragments of PTFE and silicone, which may come from lab-equipment. Pictures of MP of some of the most

typical polymers are shown in Figure 21 for reference. Polyamide (polyamide and nylon combined) was the dominant polymer type and fibers was the dominant shape among the MP >500 μm . The concentrations of MP >500 μm ranged from 48 kg^{-1} dw at St11 to maximum 211 kg^{-1} dw at St5 (Figure 19, Table 7). Some of the particles which were suspected to be synthetic from visual cues were not identified as plastic after FTIR and expert investigation of spectra (see Supplementary Material, Figure S22). A summary table of numbers, polymer types and shapes of identified polymers >500 μm is shown in Supplementary material (Table S23). It is highly time consuming to do ATR FTIR with manual validation of FTIR spectra, and only spectra from particles with HQ >600 were manually checked. This made the cut-off of HQ >600 likely to cause an underestimation of synthetic particles (>500 μm). Supplementary material (Figure S23) shows some of the excluded particles which were highly likely synthetic and anthropogenic, judging from color and texture, but had HQ <600, and were not identified as synthetic by ATR-FTIR investigation with the current cut-off.

Interpreting the results, the concentrations and polymer composition of “large” MP > 500 μm (Figure 19. B) did not present the same picture of MP distribution as the “small” MP (11–500 μm , Figure 19 A). According to the analysis of the particles >500 μm , St5 had the highest MP concentration, with PA-fibers as the dominant polymer type (Figure 19 B). This did not correspond to results from MP 11–500 μm (Figure 19 A), where Kvr1 had the highest concentration, and PUR/Acr was the dominant polymer type. Polychloroprene, which was highly abundant among the smaller size classes (<100 μm) at St5, was not found as MP >500 μm . In sum, the MP >500 μm (kg^{-1} dw) made up 0.04%, 0.15%, 0.74% and 0.39% of the total at Kvr1, St4, St5 and St11, respectively.

Based on the current results, we argue the importance of quantifying particles below 100 μm for a full understanding and representative description of MP in sediment samples.

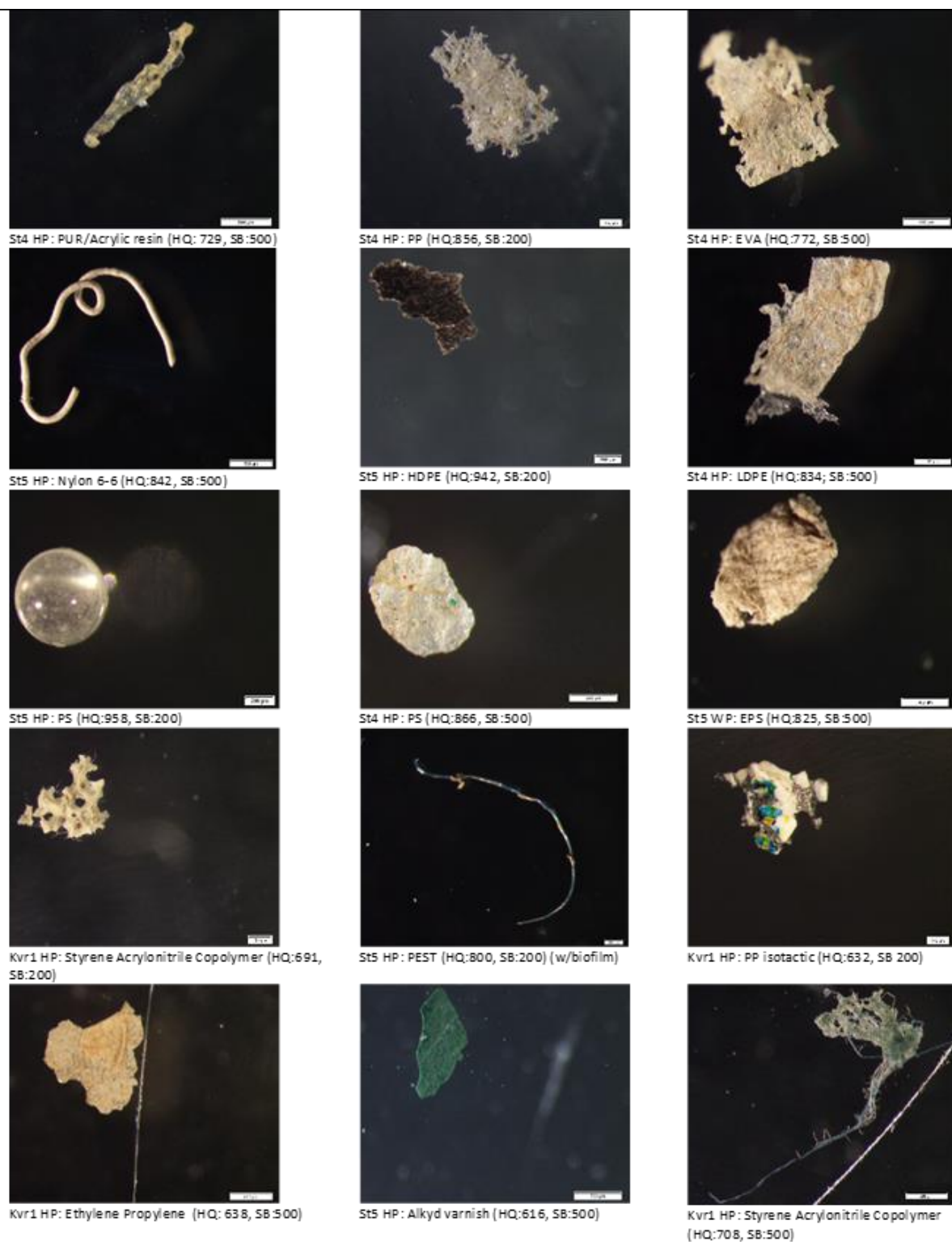


Figure 21: Representative images of MP > 500 µm, from Byfjorden (Bergen, Norway). Station name and separation-phase in which the particle was found is given. HP= Hexane Phase, WP = Water Phase; Hit Quality (HQ) >700/1000 or (>600/1000- manually validated); SB= scalebar (µm).

Pre-selection of synthetic polymers by phase separation

Debris, such as indigestible coal and silt, which remained in the sample after density separation and enzymatic digestion, was settled out of suspension by phase-separation using salt-solution/*n*-hexane for all samples as a final step. During phase separation, fibers often remained suspended at the top of the water-phase or in the transition zone, thus loss of fibers may occur if the water phase would be discarded (Figure 18). Careful release of the settled material may be sufficient to reduce the amount of coal and silt while retaining most of the MP in both the saturated salt solution and the hexane-phase. Identification of particles in the separate phases showed that pre-selection of polymers using *n*-hexane was promising and may be of assistance in reducing debris and sample volumes before further processing and identification. Heavy polymers, such as PET (1.4 kg dm^{-3}) remained floating in the hexane-phase. The automated counting after FTIR imaging showed that the *n*-hexane phase retained 69 to 87% of the synthetic polymers (11–500 μm), and also removed much of the coal, silt and organic particles (Figure 18, Figure 22, Supplementary Figure S21). However, not all synthetic materials are attracted to the *n*-hexane phase, such as road wear particles and artificial soccer-turf pellets made of car-tire rubber. This might be due to surface properties as well as density of mixed polymers such as car-tire rubber. Although there is potential for improvement, the phase separation shows promise as pre-selection of a number of polymer particles with concurrent removal of interfering and resilient particles before further identification.

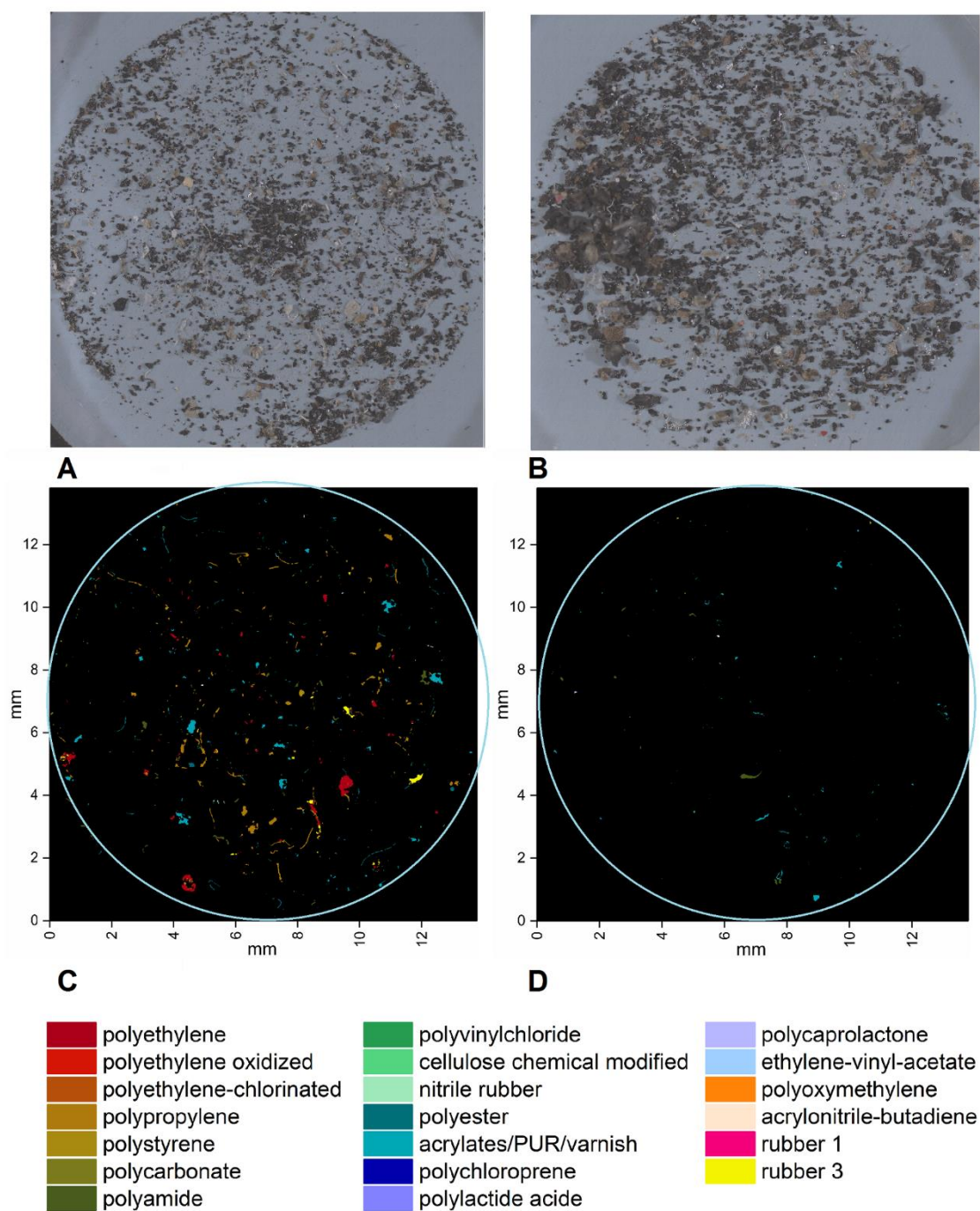


Figure 22: Pictures of Anodisc filters before FPA-FTIR imaging (top) and the corresponding False Color Plots of identified synthetic polymers (bottom) after FPA-FTIR imaging. The blue circle indicates the approximate circumference of the sample on the filter. The results of phase separation using saturated NaCl solution: n-hexane (1:1) is shown for St4 only, as the Hexane Phase (A, C) and the waterphase (B,D). For the Hexane Phase, 6.4% (7 mL) of the total sample volume was loaded, and for the water phase 8.7% (8mL) was loaded on the Anodisc filter. (For the other sites, see Supplementary Figure S21).

MP distribution may be influenced by size

The results from this study indicate that variations in MP concentrations follow expected patterns of deposition, based on knowledge of the fjord current systems, and historic patterns of deposition of organic matter. Coastal water enters Byfjorden from South-west through the strait south of the island Askøy, flowing northward along the east of the fjord from the city center (Graphical abstract, Figure 17). The inflowing water runs faster as it enters through the narrow part of the fjord south at St5 and slows down as the fjord opens up in the city harbor near St4. Seasonal inflow of heavy oceanic bottom water from the west over the fjord sill will wash away the top sediment layer at St5, moving the sediments towards St4. The processes involved, which may also be responsible for the transport of small MP are described in (Puig et al., 2014). It may seem from this study that the larger PA fibers are not as easily moved by the currents as the smaller MP. A brackish fjord brings water from north to south into Byfjorden, as surface water (Figure 17). This water is coming from a less populated area without large wastewater treatment plants. Dominant sources of MPs into the fjord system is therefore presumed to be mainly the urban wastewater discharges, surface run-off and marine activities in the harbor.

Comparison of results with other sediments studies

The MP concentrations reported by this study can only in part be compared to previous studies, due to differences in methods and reported size classes. This is a recurring challenge in MP studies, as also noted by Bergmann et al. (2017) who used methods that are comparable to this study investigating Arctic sediments. Using the MPSS for density separation, ATR-FTIR and FTIR imaging to determine MP down to 11 μm , Bergmann et al. (2017) found 18 polymer types with a mean concentration of $4356 \pm 675 \text{ MP kg}^{-1} \text{ dw}$ ($n=9$), and a maximum of $6594.56 \text{ MP kg}^{-1} \text{ dw}$. Similar to this study, 99% of MP particles in the Arctic were under 150 μm and 78 % were $\leq 25 \mu\text{m}$. The identification of the small MP may be due to the efficiency of the MPSS for density separation and extraction. Bergmann et al. (2017) similarly report lower numbers of MP with increasing size, and MP $>500 \mu\text{m}$ of maximum 9.43 MP kg^{-1} . This supports the current finding that the larger particles are fewer in numbers, less dispersed by ocean currents, and not comparable to the MP abundance and composition of the smaller size classes in the sediments.

In a Belgian study of harbor sediments (Claessens et al., 2011), density separation with saline was followed by filtering over a 38 μm mesh and identification of polymers by FTIR. The study reported a mean of $166.7 \pm 92.1 \text{ MP kg}^{-1} \text{ dw}$ and a maximum of $391 \pm 32.6 \text{ MP kg}^{-1} \text{ dw}$ from approximately 1 kg of sediments. The actual size of the identified particles was not included, which makes further comparisons to the current study difficult. However, if particles of 38 μm

were efficiently identified, the concentration of MP in the Belgian Harbors is low compared to the current study.

Maes et al. (2017b) reported a mean of 421 MP kg⁻¹ dw in 27 samples from Belgium, France and the UK. The particles were visually identified as plastic by light microscopy, and the majority of particles were larger than 355 µm. At three of the investigated sites no MP were identified. The maximum concentration reported for the Belgian harbor was 3146 particles kg⁻¹ dw. In light of our finding that 95–97% of the deposited particles were under 100 µm, we think that the reported mean probably is underestimating the MP concentration at these sites. Comparing to the concentrations of MP over 355 µm in the current study, the results indicate that total MP concentration in the Belgian harbor may be much higher than in Bergen. Moreover, the study reported mainly fibers and spheres, and no fragments or flakes. This could be a result of the manual selection of particles, which would favor the selection of certain particle shapes (Lavers et al., 2016). Moreover, as sediments are highly heterogeneous, extraction of a 25 gram sediment sample and back calculating to MP kg⁻¹ dw may not give a representative picture of the sites.

The MAREANO project at the Norwegian Continental Shelf (NCS) reported concentrations of MP >100 µm from the Norwegian continental shelf. The highest concentration reported by MAREANO was 391 MP kg⁻¹ dw of sizes up to 450 µm (Jensen & Cramer, 2017). This is comparable to the lowest levels at St11 which had 319 MP kg⁻¹ dw of sizes 100–500 µm, but less than the highest concentration 3759 MP kg⁻¹ dw of particles 100–500 µm at St4 (Supplementary Table S22). The similarity between MP concentrations on the NCS and the urban site St11 in this study is interesting and warrants investigation of transport and settling of MP along the Norwegian coast.

Matsuguma et al. (2017) reported a max of 5385 MP kg⁻¹ dw (particle size 315–1000 µm) and a mean of 1900 MP kg⁻¹ dw in a shallow canal in Tokyo Bay, and 100 MP kg⁻¹ dw of similar size in the Gulf of Thailand. Judging from the dominance of smaller particles in the current as well as previous studies, (Bergmann et al., 2017; Mintenig et al., 2017), the total MP concentrations in the Tokyo Bay canal is likely to have been much higher if investigations of MP <100 µm had been included.

Vianello et al. (2013) investigated MP in sediments in the Lagoon of Venice and reported a maximum of 2175 MP kg⁻¹ dw (30–500 µm) after triple extraction of 250 gram sediment with saturated saline, followed by identification by µ-FTIR. Despite the fine resolution FTIR-identification, the reported concentrations are much lower than the current study. This may be due to the density separation method using saline, which limits extraction of particles heavier than 1.2 kg dm⁻³.

In a study investigating sediments from the Irish Continental shelf, cores taken from four sections down to 3.5 cm sediment depth were extracted by dry sieving of particles $>250\text{ }\mu\text{m}$, and identified by visual means and FTIR (Martin et al., 2017). The sixty-two identified MP particles ($250\text{ }\mu\text{m}$ – 5 mm) were believed to be an underrepresentation of the likely total MP concentration, but the study recommended investigating sections down to 5 cm depth. The current study investigated the top 0–1 cm sediment layer, which is common for chemical analyses, following the Water Framework Directive. It might be that despite bioturbation, sampling of the top layer has led to a higher concentration per kg sediments than if older and deeper layers had been included.

There is an obvious need to proceed by using with similar sampling, extraction and identification methods, to be able to compare concentrations across studies, as also highlighted by (Löder & Gerds, 2015).

Sources of error

Most current MP studies are limited by the lack of standardization and replicates, which prevents results with uncertainty estimates. As replicate sampling may not always be possible, errors should be targeted by a propagation of uncertainty, which was performed in this study. All the uncertainties derived for our samples including lack of blank-analysis, as well as subsampling, back-calculations and the use of single replicates were addressed within the propagation of uncertainty. Despite the mentioned limitations, the study demonstrates an ability to differentiate between high and low concentrations and detect variations in polymer composition that indicate local sources and sedimentation patterns. The maximum uncertainty is 60 % at St11, which has the lowest number of particles. The reported MP concentrations are given with an error estimate taking these uncertainties into account, and we thus believe that the concentration, size distribution and the polymers found is a reasonable representation of MP at these sites.

Losses or contamination

Every procedure with the sample open to air and every transfer of the sample during processing increases the chance of contamination and losses. Losses of particles smaller than $30\text{ }\mu\text{m}$ may have occurred due to the filter mesh size, and the size class $< 30\text{ }\mu\text{m}$ can therefore not be considered to be a quantitative measure. However, particles are known to be trapped on the filter by attachment to other particles. Validation by Raman has identified even higher numbers of smaller MP than FPA-FTIR (Cabernard et al., 2018), indicating that even smaller particles are in fact trapped.

Centrifugation, which was applied in this study, is likely to have caused some loss of MP, even after two extractions of the pellet with ZnCl_2 . Investigation of the pellet after centrifugation did

indeed show that some spheres and fragments fell out of suspension. Thus slow centrifugation to remove heavy debris such as sand and silt is not recommended.

There may also be losses of MP due to insufficient extraction by ZnCl_2 in the MPSS. Although some particles of car-tire rubber and road paints are extracted by using the MPSS, such polymers have also been found to remain in the remaining sediments after extraction by the MPSS (unpublished observation), and thus observations of these particles can only be considered a qualitative measurement.

Some use of plastic materials in the lab is unavoidable, such as gloves for protection from ZnCl_2 . This may have contributed to nitrile particles in the samples. However, nitrile may also be present in wastewater, from sources such as health care or research facilities. The contribution from nitrile makes up 0.3–7.4% of total number of MP kg^{-1} dw, with a maximum of 1238 MP kg^{-1} dw at St5, with the smaller size fractions as dominant (Supplementary material, Table S22). Dust is also unavoidable in a lab-area, unless a closed system or high-pressure ventilated room is available. In consideration of this problem, all samples were covered and equipment rinsed thoroughly in MilliQ® immediately before use to reduce the effects of exposure to dust.

A small number of the identified particles $>500 \mu\text{m}$ resembled fragments from blue bottle tops, which has previously been known to contaminate liquids and samples during storage and handling (Gerdt pers. comm.). Other PP particles identified in this study do however not resemble contamination from the lab-environment (Figure 21). All samples were treated enzymatically in the same run and transported in the same type of flasks with PP lids. The content of MP together with PP varied strongly between the samples, supporting that the results represent actual differences among the sites. Also visually, the properties of the PP fragments indicates several different sources (Suppl. Figure S22). Silicone and PTFE found among fragments $>500 \mu\text{m}$ may stem from abrasion of laboratory equipment, and were therefore excluded from results (Suppl. Figure S22).

Subsampling

Sediments are heterogeneous, and a single small sample may not be representative of a site. Multiplying MP concentrations in extracts from a small sample to achieve a concentration kg^{-1} dw gives potentially large errors (see also Equation 2.4), and sample size should thus be as large as possible. During standardized benthic monitoring programs, it is common procedure to analyze pooled samples from three grabs to represent one site. It is feasible to perform extraction of MP from such pooled sediment samples. The MPSS can hold 4 kg of sediments, but with the high MP and organic content in fjords, this is not a necessary or practical sample size. A volume of 200–400 grams of pooled sample may be representative,

and may allow the loading of the entire resulting extract onto the filter after purification, thus eliminating errors related to subsampling. Reporting both sample volume, weight, surface area and depth sampled would allow comparison across studies, and is recommended.

Treatment effects

Microscopy of MP >500 μm showed weathered and fragile looking PUR/Acr particles with embedded coal particles. According to the FTIR imaging all the PUR/Acr particles were smaller than 300 μm . Gentle extraction, and short durations of ultra-sonication in order to maintain the integrity of brittle particles is suggested.

Limitations of visual identification

Many early studies have used visual identification or hot needle tests to identify synthetic polymers. It has been previously shown that visual identification is a limitation to the identification of even large particles (Hidalgo-Ruz et al., 2012; Lavers et al., 2016). For small and weathered particles, visual identification is even more difficult. Löder and Gerdtz (2015), discuss likely overestimation of MP by visual methods, as many biopolymers have a shiny, smooth or regular appearance resembling synthetic polymers (Figure 23). Dekiff et al. (2014) similarly found no correlation between the amount of visual debris (>1mm) and small microplastics (<1mm). Microscopy in combination with identification by ATR FTIR in this study also show how particles positively identified as synthetic polymers can be weathered, discolored and cracked, looking like organic material, which would make them inconspicuous and likely to be overlooked (*i.e.* LDPE, Figure 21).

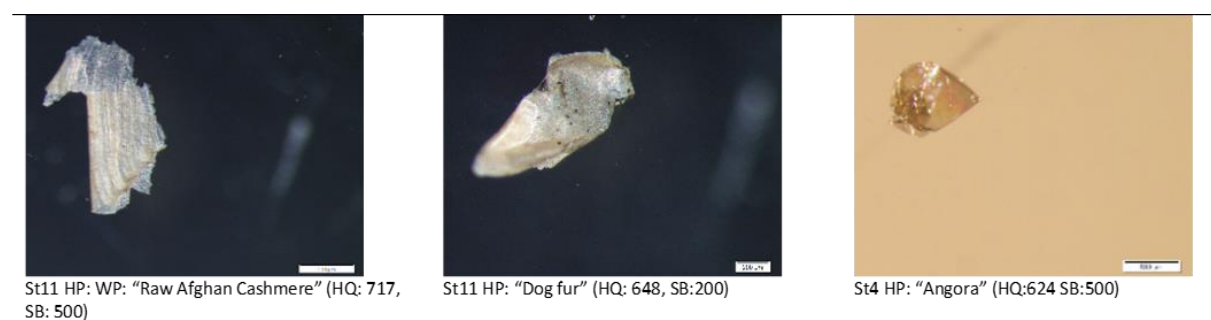


Figure 23: Natural polymers visually similar to plastics. The FTIR library suggests origin of polymers based on best fit, though they are more likely marine biopolymers.

One challenge with the identification of plastic by FTIR is composite materials, as they may be identified as one polymer on one side, and another polymer on the other. Embedded coal or silt particles in for example PUR/Acr resins would sometimes give uncertain hits (<600), while visually they had great similarity to particles with HQ 600 (Figure 21, top row). The particles had a spotted grey and brown uneven surface and soft appearance, and could easily be overlooked by visual selection. In conclusion, visual identification is inadequate to provide a

secure scientific basis for comparisons across studies, trend-analyses or risk assessments, as it may result in both under and overestimating MP concentrations, subjective results and possible misinterpretation of the actual MP status. The *n*-hexane/saltwater phase separation method may here be useful as an unbiased pre-selection before further identification, based on attraction to *n*-hexane rather than visual cues. This may help sorting MP from organic material, reducing interference with further analyses.

Need for evaluation of concentration ranges

The EU-WFD aims to obtain good ecological and chemical status for coastal recipients, thus frequent and standardized monitoring is performed. When threshold levels are reached, mitigating measures are considered. However, since plastic is not defined as an environmental pollutant, monitoring of plastic concentrations has not been included in mandatory monitoring programs, and knowledge of levels and distribution in various environmental compartments is therefore lacking. There are no definitions of “moderate” or “high concentrations” of MP and thus no thresholds exist for the onset of mitigating measures. This study shows that concentrations may vary several orders of magnitude over relatively short distances. The ecological effects of the documented concentrations remain to be investigated, and large knowledge gaps must be closed before safe threshold concentrations for MP can be established. Developing knowledge about the location of MP deposition sites, the range of environmental MP concentrations and the risks associated with such concentrations is necessary to perform risk assessments of present and future MP concentrations.

Sources

The major sources of MP to the selected sites are expected to be the sewage outlets (Magnusson, 2014; Duckett & Repaci, 2015; Horton et al., 2017a). Norway has a “combined system” of household sewage and surface run-off going through the wastewater treatment plants (Magnusson, 2014; McCormick et al., 2014; MEPEX, 2014; Mintenig et al., 2017). The recipient area in Bergen now receives discharge from approximately 200 000 person equivalents, estimated to contribute 1–1.6 tons of MP per year from personal care products alone. However, this does not account for long-range transport or production of secondary MP from degradation of large plastic items at sea, varnish and paints from marine vessels or other marine sources, implying that the amounts released may be much greater.

Long-range transported particles that have acquired a biofilm during oceanic transport may enter the sheltered fjord system and settle to the bottom in calm waters, whereas recently discharged, buoyant particles may be transported out of the fjord system before a biofilm forms. This effect is also indicated by preliminary distribution modelling from Byfjorden (Helge Avlesen pers. comm.) and is discussed in MEPEX (2014), but deserves further investigation. We cannot

ascertain the origin of the MP based on polymer composition. Investigating the occurrence of MP in the water masses of the fjord system with increasing distance from the urban center might provide information about sources of MP from urban areas versus long-range transport, and their environmental fate and distribution.

Conclusion

Quantitative analysis of MP particles in marine sediments in an urban recipient has been performed and describes characteristics of polymer composition, MP size classes and concentration ranges from discharge to deposition sites. The concentrations and distribution follow predictable patterns according to known discharge sites. Factors such as current systems, sediment grain size and deposition of organic matter can be used to indicate favorable deposition sites for MP for monitoring purposes.

This investigation supports previous studies reporting that the highest number of particles are among the size classes below 100 μm , and that the distribution patterns differ in small MP (<500 μm) and large MP, where small MP seem to be deposited at sites with weak currents. Efforts should be made to report concentrations for the smaller sizes (<100 μm) to gain a full picture of MP contamination. Unbiased methods that do not rely on visual identification or manual sorting of particles is essential, as many particles of confirmed synthetic material are inconspicuous in appearance. A novel phase separation using organic solvent and a salt solution used as a non-biased pre-selection to reduce the amount of interfering and resilient debris before further identification, may be useful.

Reporting the particles as size classes allows comparison to other studies, where data on MP size are available, and provides a reference for mapping MP concentration ranges in marine sediments. A frequent or regular sampling regime will permit timelines of MP accumulation in the urban recipient, and may further serve to evaluate any effects of mitigating measures such as secondary treatment of wastewater or improvements in waste management.

Understanding the concentration range, relevant concentrations and dominant polymers is vital for future risk assessments and toxicity studies of relevant polymers.

Acknowledgments

Thanks to June Helen Gudmestad and Nora Bjerkli (University of Bergen) for excellent lab-assistance. Thanks also to Gunnar Bratbak and Antonio Pagarete (University of Bergen), Gaute Velle, Eivind Bastesen, Helge Avlesen and Jessica L. Ray at Uni Research (NORCE) for contributions, discussions and practical help, and to former colleagues at Uni Research for

Chapter IV

sampling. Special thanks to Anne S. Cornell at the Bergen Municipality Water- and Sewage department for participation in the project.

The study was funded by the Norwegian RFFV (project #258890), Bergen Municipality and Uni Research, now NORCE Norwegian Research Centre, Deutsche Bundesstiftung Umwelt (DBU). The German Federal Ministry of Education and Research funded parts of the Project BASEMAN - Defining the baselines and standards for microplastics analyses in European waters; BMBF grant 03F0734A.

General Discussion

Already back in 2004 Richard Thompson and colleagues raised the question "Where is all the plastic?" considering the steadily increasing global production of plastics and consequently input in the marine environment (Thompson et al., 2004). Since then most studies focused on MP floating on the oceans surfaces (e.g. C3zar et al., 2014; Eriksen et al., 2014; Law et al., 2014). This topic was further addressed by Erik van Sebille and colleagues, who made an inventory of the floating MP all over the globe (van Sebille et al., 2015). Based on results of 11854 plankton net surface-trawls conducted from 1971 to 2013, and three different oceanographic models, they estimated $15\text{--}51 \times 10^{12}$ MP ($300\text{--}5000 \mu\text{m}$) floating in the world's oceans, weighing $93\text{--}236 \times 10^3$ Mt (van Sebille et al., 2015). Taking into consideration that in 2010 alone $4.8\text{--}12.7 \times 10^6$ Mt have supposedly entered the oceans, this amount only presents around 1% of what is floating as MP on the ocean surface (Jambeck et al., 2015; van Sebille et al., 2015). This discrepancy again raises the question where all the plastics are which are not accounted for at the sea surface. Other compartments like the water column, beaches, sublittoral sediments, atmosphere, cryosphere and biota need to be considered. Since less than 50% of the globally produced plastics have a density which would allow them to float in seawater (Kedzierski et al., 2017), a considerable amount of the missing plastics is suspected to be held in marine sediments. Hence, this thesis aimed to shed some light onto this question concerning the southern North Sea by analyzing MP (including PWs – **Chapter III**) in surface water and sediment samples (**Chapter I**). Furthermore, focusing on the potential of marine sediments to accumulate MP, the results from the southern North Sea (**Chapter I**) were compared to an analog study on MP in sediments of an urban Norwegian fjord (**Chapter IV**). Since several characteristics are playing a role in the behavior of MP once they have entered the oceans, another contribution was the analysis of the weathering status of MP identified in the surface water and sediment samples from the southern North Sea (**Chapter II**). In the following the outcome of the previous chapters are discussed in a general context and results will be compared to other studies analyzing MP in marine surface waters and sublittoral sediments. Another contribution of this thesis is in the form of method development and optimization, which will briefly be discussed with respect to a harmonization of methods.

Transport and Pathways - From the land to the shore and beyond

Land-based sources are considered to contribute significantly to the amount of MP in the oceans. Figure 24 shows a selection of possible sources and pathways related to land-based input but also ocean-based input.

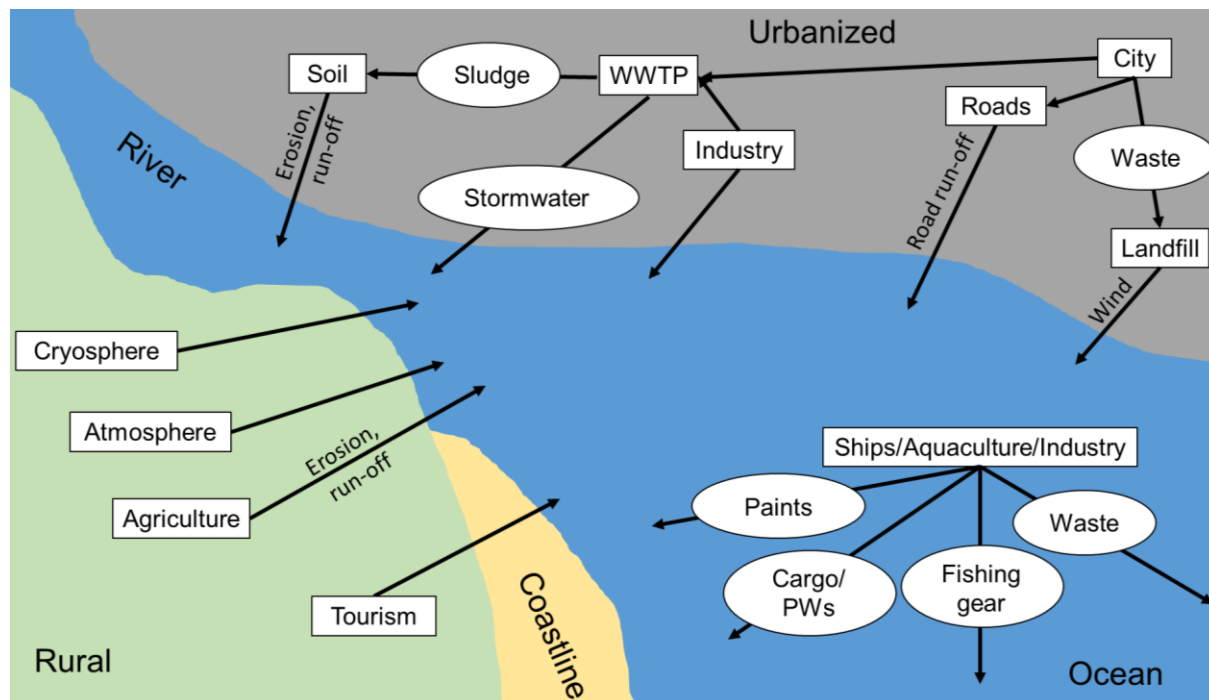


Figure 24: Potential sources and transport pathways of (micro)plastics to the ocean. WWTP: wastewater treatment plant; PWs: paraffin waxes. Modified from Horton et al. (2017b) and Horton and Dixon (2018).

Rivers are considered to be a major entry pathway for plastics into the marine environment (Schmidt et al., 2017). When considering the potential river load, the catchment area is decisive, and a selection of important factors to take into account are the size of the area, whether it is urbanized or rural, and point sources such as specific plastic-related industries. Schmidt et al. (2017) estimated an average annual input of $0.47\text{--}2.75 \times 10^6$ Mt of (micro)plastics based on data sets from 57 rivers. One of the main riverine discharge areas of the North Sea is the Rhine-Meuse delta. As stated in **Chapter I** of this thesis, the two stations situated in the vicinity of this river delta differed significantly from the other stations concerning their polymer composition. For the Meuse, Mintenig et al. (2020) found MP concentrations of $1.77\text{--}13.81 \times 10^2$ particles m^{-3} and respectively $0.16\text{--}11.53 \times 10^3$ particles m^{-3} in one of its tributaries, the Dommel, in a size range of $20\text{--}5000$ μm . In the Meuse, the dominating polymer types were rubbers, PE, PP and acrylates/PUR/varnish (Mintenig et al., 2020). These polymer types were, except PE, also the dominating ones in the surface water and sediment samples close to the river delta (**Chapter I**). For the Rhine Mani et al. (2015) found average MP concentrations of 4.96 particles m^{-3} ($300\text{--}5000$ μm), mainly consisting of PS-based spheres, all along the Rhine from Basel (CH) to Rotterdam (NL). In a subsequent study, focusing solely on these

microbeads, which had been most abundant in the Rhine-Ruhr area (DE), concentrations ranged between 0.05–8.3 beads m⁻³ (300–5000 µm) (Mani et al., 2015; Mani et al., 2019a). Furthermore, Klein et al. (2015) found MP concentrations of up to 3.76×10^3 particles kg⁻¹ (63–5000 µm) in river shore sediments and Mani et al. (2019c) of up to 11.07×10^3 particles kg⁻¹ (11–5000 µm) in midstream sediments of the Rhine, respectively. Considering that, according to Hurley et al. (2018b), flooding events can export around 70% of the MP load in the river bed, riverine sediments might only serve as temporary sinks. The dominating (70%) polymer type in the Rhine midstream sediments was identified as acrylates/PUR/varnish by Mani et al. (2019c) which in turn was also the dominating polymer type in the surface water samples closest to the Rhine-Meuse delta and very abundant in the sediments at the same locations (**Chapter I**). Thus, also MP retained in river sediments need to be considered as contributing to the MP input into the North Sea or oceans in general.

Once having reached the ocean, MP might float on the surface. For the North Sea, the horizontal transport of floating MP at the sea surface is mainly driven by winds and surface currents (Thiel et al., 2011). Hence, potential accumulation zones are hypothesized to form under calm weather conditions at the coastal frontal zones, e.g. the East Frisian Front and the North Frisian Front, or local gyres, e.g. the German Bight Gyre (Thiel et al., 2011). In accordance to this, the polymer compositions of surface water samples taken along the West and East Frisian Islands, as presented in **Chapter I**, were quite similar among each other but differed significantly when compared to samples taken closer to the English Channel. However, Neumann et al. (2014) modelled the particle transport in the southern North Sea and found a very high seasonal and also short term variability. Thus, the results from North Sea surface water samples need to be considered a snapshot in time.

While MP float at the sea surface, they are subjected to several influencing factors. One of these is wind mixing (Kukulka et al., 2012). Thus, MP can be found not only at the sea surface but in varying concentrations also in the underlying water column (e.g. Reisser et al., 2015; Egger et al., 2020; Tekman et al., 2020), where they are still subjected to horizontal transport. However, recently Allen et al. (2020) detected MP in the ocean surface boundary layer and suggested that sea spray can act as a source for atmospheric MP. Consequently, the horizontal transport can also take place in the air, and the ocean can act as a source for MP.

Apart from the wind, another influencing environmental factor is UV-radiation, which is strongest close to the sea surface. This process of weathering leads to photooxidation at the material surface of the particle, leading to cracks, thus increasing the roughness and the surface area and consequently making the surface brittle (Ter Halle et al., 2016; Andrady, 2017). This embrittlement, combined with mechanical stress, e.g. through wind and waves,

leads to the fragmentation of the MP. The fragmentation processes are very complex and not yet fully understood. Thus, Ter Halle et al. (2016) investigated several MP collected from the surface of the North Atlantic gyre and found that flat pieces were more photooxidized on one side and overgrown with biofilm on the other, while small cubic MP were equally oxidized on all sides, indicating a rolling movement. They further hypothesized that the small cubic MP would fragment faster than the flat ones. Andrady (2017) proposed in this context the fragmentation via surface ablation, which is caused by increasing oxidation and consequently swelling behavior of a thin material surface layer to a point where the surface is shedding a large number of small, thin and oxidized particles leaving behind the parent-particle with a relatively unoxidized surface. This hypothesis could be reinforced in this thesis (**Chapter II**) since the average carbonyl index of PE and PP of small sizes (11–500 μm), 0.07 and 0.06, respectively, was higher than the one for large MP (500–5000 μm), 0.03 and 0.02, respectively. In conclusion, the weathering status can have an influence on the sinking behavior since it changes the size and material surface (Kowalski et al., 2016; Rummel et al., 2017; Karlsson et al., 2018). Consequently, the apparent density of plastics increases with increasing degradation (Kowalski et al., 2016; Rummel et al., 2017; Karlsson et al., 2018).

A third factor is biofouling. Although biofilm growth will increase the apparent density of the MP particle, it does not necessarily result in the immediate sinking of the particle. Biofilms on plastics have been reported on floating MP by a multitude of studies (e.g. Lobelle & Cunliffe, 2011; Zettler et al., 2013; Kirstein et al., 2016). Additionally, biofilm formation might even increase the buoyancy of MP that have an initially higher density than seawater. Hence the impact of biofilm growth on the vertical transport is considered to be far more complex (Rummel et al., 2017).

Moreover, MP, or particles in general, rarely occur as freely dispersed particles in the marine environment but rather are merged with organic and inorganic particulate matter into marine aggregates. This explains the presence of MP smaller than the mesh size used for sampling in this thesis (100 μm , **Chapter I**) and the presence of polymer types, which have a theoretical density higher than seawater. The ready incorporation of MP into marine aggregates has been shown, (e.g. Long et al., 2015; Long et al., 2017; Möhlenkamp et al., 2018; Porter et al., 2018). The latter two studies confirmed that low-density polymers like PE become incorporated in marine aggregates and increase the sinking rates of these plastic types. Taking into consideration that in the marine environment the available particulate matter consists of a great variety of organic and inorganic materials, stressed the complexity of this interaction. MP have also been shown to be ingested by marine copepods (e.g. Cole et al., 2016). The incorporated MP then alter the sinking behavior of the egested fecal pellets. Along these lines, Cole et al. (2016) showed a decrease in sinking velocities of fecal pellets from 86.4 m d^{-1} to 38.3 m d^{-1} .

when PS beads were incorporated. In consequence, marine snow, including fecal pellets and marine aggregates, can act as vectors for MP, even low-density polymers, to be transported to the seafloor (Long et al., 2015; Katija et al., 2017; Long et al., 2017; Möhlenkamp et al., 2018; Porter et al., 2018). This hypothesis is corroborated by the findings of this thesis (**Chapter I & IV**) by recording that low density polymer types like PE and PP, combined contributed 15% and 13%, respectively, to the polymer composition of sublittoral sediments.

As previously mentioned, several particle properties influence sinking behavior, e.g. density of the polymer, shape and size, as well as external forcing parameters, e.g. seawater density, seabed topography, flow velocity, turbulence, and pressure (Ballent et al., 2013; Kowalski et al., 2016; Chubarenko et al., 2018a; Pohl et al., 2020). Considering these parameters, Ballent et al. (2013) tested the sinking behavior of plastic pellets of approx. 5 mm diameter and densities around 1.06 g cm^{-3} in seawater of slightly lower density. Furthermore, they tested the effect of turbulence on LDPE particles of different size and shape and found that pellets were less susceptible to turbulence than large, irregular shaped particles like fibers and films (Ballent et al., 2013). Kowalski et al. (2016) conducted a series of sinking experiments with MP ranging from 0.3 to 3.6 mm of six different polymer types, thus densities, and shapes. They confirmed that sinking velocities increase with particle size and that the shape, i.e. flatness, is a decisive factor. Instead of a steady fall, which would be expected from spherical particles, flakes, flat cylinders and fibers are inclined to rotations, oscillations and tumbles (Kowalski et al., 2016; Chubarenko et al., 2018a).

Furthermore, there are also other, oceanographic, processes that can transport MP into deeper waters, e.g. saline subduction, offshore convection, and dense shelf water cascading (Ballent et al., 2013; Woodall et al., 2014). Even though vertical settling of MP from surface accumulation zones, like recently been shown by Egger et al. (2020), is considered the main route to the seafloor, a recent study by Kane et al. (2020) has shown that the ultimate spatial distribution at the seabed is driven by near-bed thermohaline currents (bottom currents). Hence, the transport of MP is complex and suitable locations for regular monitoring campaigns not easily defined.

Spatial distribution of MP as a basis for monitoring

All these aforementioned factors influence the spatial distribution of MP in the oceans. Historically, most studies target MP floating on the sea surface since these are more easily accessible. Figure 25 provides a selection of studies focusing on MP concentrations in surface and sub-surface waters. Apart from the sampling location, the sampling method, e.g. Manta trawl, neuston net, plankton net, pump or filtration system with the respective mesh size is noted. The average sampled volume is indicated, if provided, as well as the analyzed size

range. Utilized filter or mesh sizes ranged from 10–50 μm ($n=3$) over 51–150 μm ($n=8$), 151–250 μm ($n=4$), 251–350 μm ($n=4$) to 451–550 μm ($n=3$). Approximately half of the studies ($n=10$) provided the average sampled volume, which ranges from 0.3 m^3 (Tekman et al., 2020) to 614 m^3 (de Lucia et al., 2014). Most of the selected studies ($n=18$) applied spectroscopic methods, i.e. FTIR or Raman, to verify at least a subset of visually pre-selected MP. A few of these studies ($n=3$), contributed to in this thesis work, even utilized FPA-based FTIR imaging or automated single-particle exploration (SPE) coupled to μRaman to analyze small MP (11–500 μm) independently from visual pre-selection (Cabernard et al., 2018; Lorenz et al., 2019; Tekman et al., 2020).

Figure 25 shows that, while not conclusively so, there is a tendency that studies using a smaller size limit for sampling and identification detect more particles. This is most notably when comparing studies conducted in the same oceanographic region. For the central western Mediterranean, for example, Suaria et al. (2016), sampling with a 200- μm net and analyzing MP down to 200 μm , found average concentrations one order of magnitude higher than de Lucia et al. (2014), sampling with a 500- μm net and analyzing MP down to 500 μm . A similar observation can be made from studies focusing on the English Channel and the North Sea. While Maes et al. (2017b) sampled with a 333- μm net and reported an average MP concentration of 0.14 particles m^{-3} , not specifying the analyzed size range, Lindeque et al. (2020), sampling with a net with the same mesh size, reported a concentration of 4 particles m^{-3} (11–5000 μm). In turn, when sampling with a 100- μm net, Lindeque et al. (2020) reported an average MP concentration of 10 particles m^{-3} (11–5000 μm), which is the same order of magnitude as reported in this thesis in **Chapter I** (27 particles m^{-3} , 11–5000 μm). In general, very few studies on marine surface waters have included MP down to 11 μm in their analysis. Cabernard et al. (2018) analyzed a subset of the samples analyzed in this thesis (station 2, 5, 7, 20, 21, 23, and 24 in **Chapter I**) with SPE- μRaman and found for the size range of 10–5000 μm MP concentrations of 38–2621 particles m^{-3} . These were an order of magnitude higher than the ones recorded in this thesis (5–245 particles m^{-3} , **Chapter I** Supplement Table S4). Cabernard et al. (2018) ascribed this difference to the analysis technique and identification approach, which might indicate that SPE- μRaman has an advantage in automatic identification, especially of small-sized MP.

General Discussion

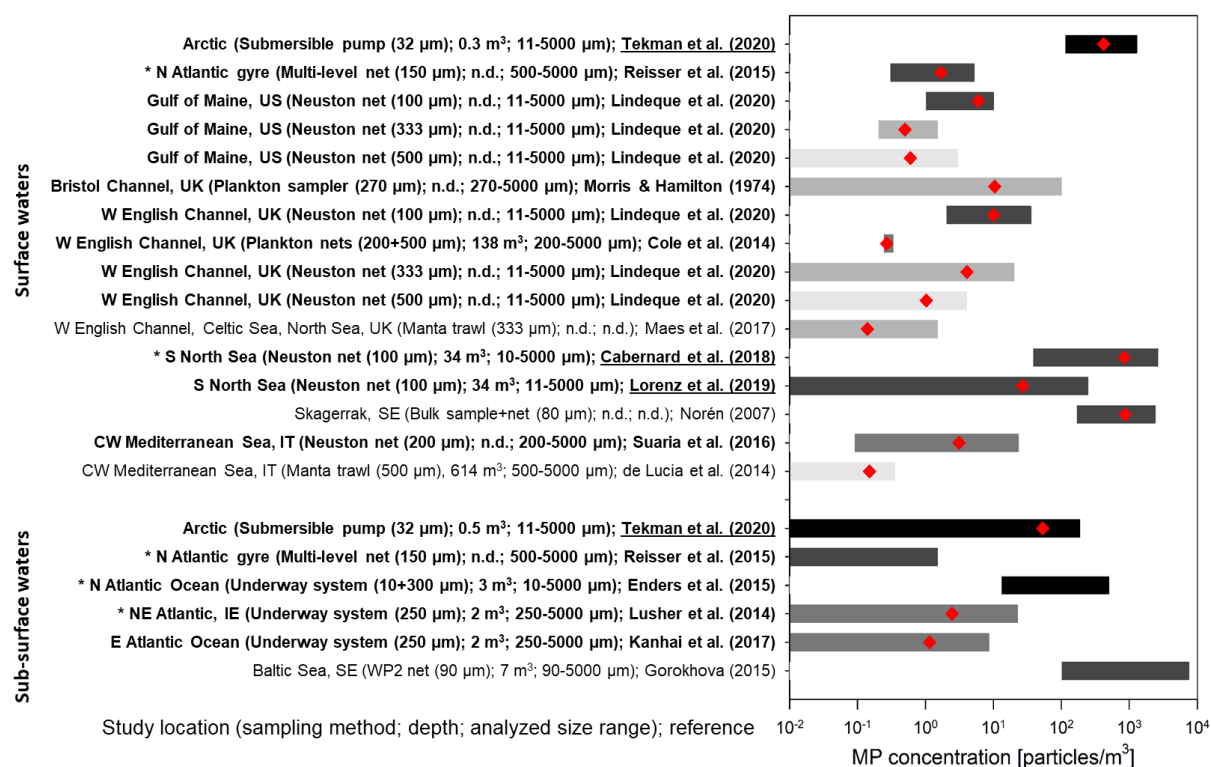


Figure 25: A selection of studies having analyzed the concentration of microplastics (MP) in surface waters (upper part) and sub-surface waters (bottom part). The bars show the recorded range of MP concentrations and the red diamonds mark the mean concentrations in particles per m³. The studies are grouped according to the oceanographic region. The greyscale of the bars refers to the mesh size used from 10–50 µm (black) over 50–150 µm, 150–250 µm, 250–350 µm to 450–550 µm (light grey). Studies highlighted in bold applied spectroscopic techniques like (µ)ATR-FTIR or µRaman (additionally marked with *) to verify at least a subset of the putative MP. The underlined studies applied additionally analysis techniques like µFTIR imaging or SPE-µRaman (marked with *) for small MP (<500 µm), which are independent of any visual pre-selection.

Another study analyzing MP in size range 10–5000 µm also with Raman spectroscopy and presented in Figure 25, has been done by Enders et al. (2015). They found MP concentrations of 13–501 particles m⁻³ with the highest concentration recorded in the English Channel and the second highest in the North Sea close to the English Channel (approx. 400 particles m⁻³). This is in the same order of magnitude as the highest concentration (245 particles m⁻³) recorded in this thesis (**Chapter I**), found at a station near the English Channel as well. The slightly higher concentration might be explained by the sampling setup since Enders et al. (2015) used a pumping system with 10-µm filters. In the framework of this thesis (**Chapter I**) a net with 100 µm mesh size was used, hence MP concentrations in the size range 11–100 µm (on average 26.4 ± 53 particles m⁻³, see Supplement General Discussion Table S24) should be considered as semi-quantitative and are likely higher than recorded in this thesis.

Another study, by Tekman et al. (2020), used a pumping system as well with 30-µm filters and recorded MP in size range of 11–5000 µm in Arctic surface waters showing that the lowest MP

concentration (113–262 particles m^{-3}) in these waters was in the same order of magnitude as the highest in the southern North Sea (245 particles m^{-3} , **Chapter I**) and that the highest (1287 particles m^{-3}) was even one order of magnitude higher. The discrepancy might for one be explained again with the smaller mesh size of the sampling equipment or, as indicated by Tekman et al. (2020) by the Arctic Ocean being an accumulation zone for MP pollution.

Another issue for inter-study comparison is the reporting unit. Some studies provide concentrations in MP per m^3 , others abundances in MP per km^2 and some both. As such Hajbane and Pattiaratchi (2017) found one order of magnitude higher mean MP abundances in Australian estuarine and nearshore surface waters (1.6×10^4 and $2.2 \times 10^4 \text{ km}^{-2}$, respectively), than offshore ($0.5 \times 10^4 \text{ km}^{-2}$). They used a 333- μm Manta trawl and identified MP in the size range 333–5000 μm . When comparing their results to the North Sea water samples considering only MP in the size-range 300–5000 μm , the mean MP abundance is with $2.5 \times 10^4 \text{ km}^{-2}$ comparable to the nearshore abundance in Australian surface waters (Supplement General Discussion Table S25). However, in this thesis (**Chapter I**), MP were sampled with a 100- μm mesh and analyzed down to 11 μm in size. Hence, the average MP abundance in the size range 11–5000 μm is two orders of magnitude higher ($2.7 \times 10^6 \text{ km}^{-2}$). This example highlights the benefits and importance of acquiring high-resolution data, i.e. size distribution and providing metadata, e.g. the sampled water volume and surface area that allow for the conversion of MP per m^3 to MP per km^2 and vice versa, to facilitate comparison between different studies.

As elaborated on in the previous section, MP are subjected to vertical transport in the water column and eventually settle to the seafloor due to their apparent density being higher than the surrounding seawater, inclusion in marine aggregates or fecal pellets or vertical transport mechanisms like downwelling (Ballent et al., 2013; Möhlenkamp et al., 2018). Thus, the seafloor is considered a major sink for MP pollution (Woodall et al., 2014). Figure 26 shows a selection of studies focusing on MP in sublittoral sediments, applying to some extent comparable methods as in the framework of this thesis. Apart from the sampling location, the sampling method, i.e. Van Veen grab ($n=9$), Box/Multiple Corer ($n=7$), divers ($n=1$), the sampled sediment surface depth (all within the uppermost 10 cm), and the targeted size range of the analyzed MP is given. Furthermore, the studies have been clustered according to the analyzed sample amount, ranging between $<0.1 \text{ kg}$ and $>1 \text{ kg}$, and color-coded based on the density of the used separation fluid.

Among these studies presented in Figure 26, the highest average concentration of MP in sublittoral sediments ($7.9 \times 10^4 \text{ particles kg}^{-1}$) was recorded in an urban Norwegian fjord, which results were presented in this thesis (**Chapter IV**). The next highest average MP

General Discussion

concentrations were recorded in Arctic sublittoral sediments with 4.4×10^3 (Bergmann et al., 2017) and 4.7×10^3 particles kg^{-1} (Tekman et al., 2020), respectively. In the same order of magnitude are the average MP concentrations that were reported from the Portuguese Continental shelf (3.3×10^3 particles kg^{-1}) by Frias et al. (2016) and the Venice Lagoon (1.4×10^3 particles kg^{-1}) by Vianello et al. (2013). In the southern North Sea (**Chapter I**) only the highest concentration (1.2×10^3 particles kg^{-1}) was in this same order of magnitude while the average concentration was lower by factor 10 (2.2×10^2 particles kg^{-1}).

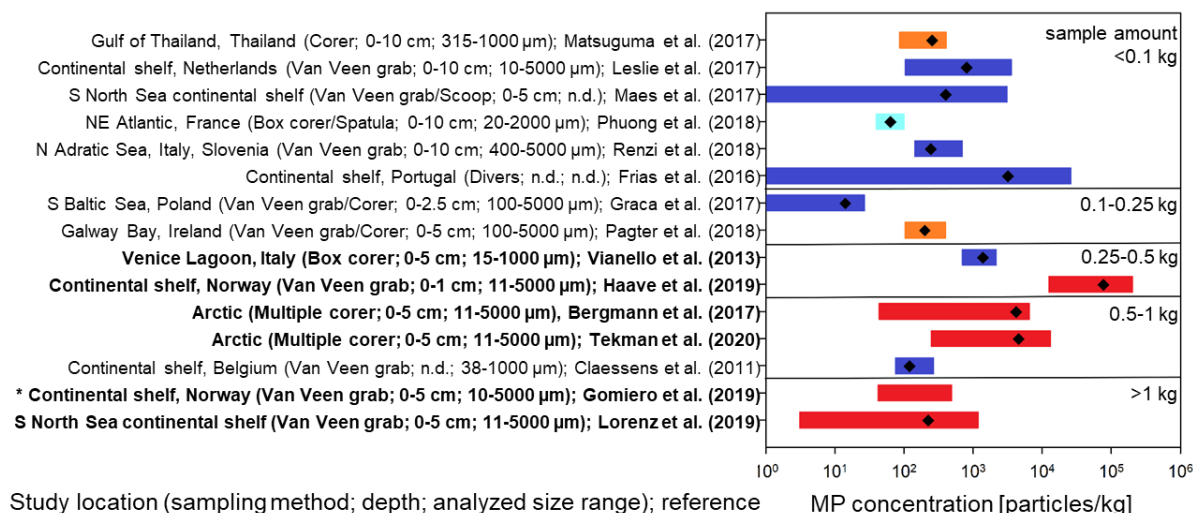


Figure 26: A selection of studies having analyzed the abundance of microplastics (MP) in sublittoral sediments. The bars show the recorded range of MP concentrations and the black diamonds mark the mean concentrations in particles/kg dry weight (dw) sediment. The studies are sorted according to the analyzed sediment dw from <0.1 kg to >1 kg. The different colors refer to the density of the separation solution used: light blue: $\rho=1.0 \text{ g/cm}^3$ (MilliQ water), blue: $\rho=1.2 \text{ g/cm}^3$ (NaCl), orange: $\rho=1.4\text{--}1.6 \text{ g/cm}^3$ (NaI, SPT), red: $\rho=1.7\text{--}1.8 \text{ g/cm}^3$ (ZnCl_2). Studies highlighted in bold applied analysis techniques like μFTIR imaging or Pyrolysis-GC-MS (marked with *, concentration in $\mu\text{g/kg}$) which are independent of a visual pre-selection of the small MP (<500 μm).

As highlighted in **Chapter I & III**, the North Sea presents a very dynamic system with a strong anthropogenic influence. Furthermore, the Norwegian Coastal Current presents a mayor run-off directed northwards from the northern North Sea, potentially influencing the Norwegian coast and thus areas like the Norwegian fjord (i.e. Byfjorden) presented in **Chapter IV**. In contrast to the southern North Sea, this fjord, being more narrow but less shallow, presents a far less dynamic system but with a likewise heavily anthropogenic influence. Moreover, fjords are considered to have the greatest sediment trapping efficiency compared to other coastal sedimentary environments (Harris, 2020). This might be one explanation for the difference in MP concentration by factor 100. Another reason might be the untreated wastewater discharges the fjord received for over a year. Both of these studies presented in this thesis in **Chapter I & IV**, however, provide very comprehensive data in terms of size range and distribution and polymer composition. High-resolution data, as presented in this thesis, allows for better

comparisons among studies. It becomes quite apparent that the MP concentration varies a lot concerning the targeted size range. Several studies have noted that size distribution follows an exponential curve with increasing particle numbers following decreasing particle size (e.g. Enders et al., 2015; Cabernard et al., 2018). It has been highlighted in this thesis (**Chapter I & IV**) that not only MP concentrations are higher for small MP (11–500 μm), but also the polymer diversity is increased, and the polymer composition sometimes differs significantly from large MP (500–5000 μm). This observation has also been confirmed by other studies, analyzing a variety of environmental matrixes like Arctic sediments (Bergmann et al., 2017; Tekman et al., 2020), the water column of the Arctic Ocean (Tekman et al., 2020), river sediments (Mani et al., 2019c), river surface water (Mintenig et al., 2020), stormwater pond surface water (Liu, F. et al., 2019a), and wastewater treatment plants (Mintenig et al., 2017).

Figure 27 includes a selection of studies that applied spectroscopic methods, i.e. FTIR (n=17) and Raman (n=1), to identify the polymer composition in (marine) surface waters and sediments. The polymer types are color-coded based on the polymer group they belong to, e.g. orange for elastomers like nitrile rubber or polychloroprene, light green for "biopolymers", which are considered as bio-based or biodegradable plastics like rayon or polylactic acid, and grey for other thermoplastics like ethylene vinyl acetate or polyoxymethylene.

In general, PE and PP are dominating polymer types in surface waters. Especially in the Mediterranean and the Yellow Sea, they made up more than 50% of the polymer composition (Suaria et al., 2016; Vianello et al., 2018; Jiang et al., 2020). In Arctic surface waters, PA was the dominating polymer type, which might be attributed to high fishing activities (Tekman et al., 2020). The polymer composition recorded in this thesis for the southern North Sea (**Chapter I**) coincides well with the one recorded in other studies focusing on the Northeast Atlantic (Enders et al., 2015) and the English Channel (Lindeque et al., 2020) and is defined by PP, PE, PEST, PS, PA, PVC and acrylates/PUR/varnish. As noted before, also the polymer composition recorded in the Meuse river (Mintenig et al., 2020) is similar to the one in the southern North Sea (**Chapter I**). This might confirm that both, the oceanic input through the English Channel and the riverine input, contribute to the MP load in the North Sea. The detection of PWs was explicitly only mentioned by one of the studies presented in Figure 27. Suaria et al. (2016) reported 0.8% of the identified polymers to be PWs. In this thesis (**Chapter III**), PWs were analyzed separately, and the highest abundance was found at the same station that exhibited the highest concentration of MP. However, for the other stations, the results did not coincide. As such, the station with the second highest MP concentration was further offshore while PWs were mainly detected in the English Channel and close to the coast.

In sublittoral sediments of the Adriatic Sea (Vianello et al., 2013) and the Northeast Atlantic (Phuong et al., 2018) PP and PE appear to be the dominant polymer types. In the Arctic Ocean, these are further accompanied by PA and several rubber types (Bergmann et al., 2017; Tekman et al., 2020). In the Norwegian fjord (**Chapter IV**), the southern North Sea (**Chapter I**) and the Rhine river (Mani et al., 2019c) PP and PP are present in sediments but play a minor role in contrast to acrylates/PUR/varnish, several rubbers, PEST and PA. However, so far, only a few studies present detailed information on the polymer composition in surface water and sediment samples which hampers a valid comparison.

General Discussion

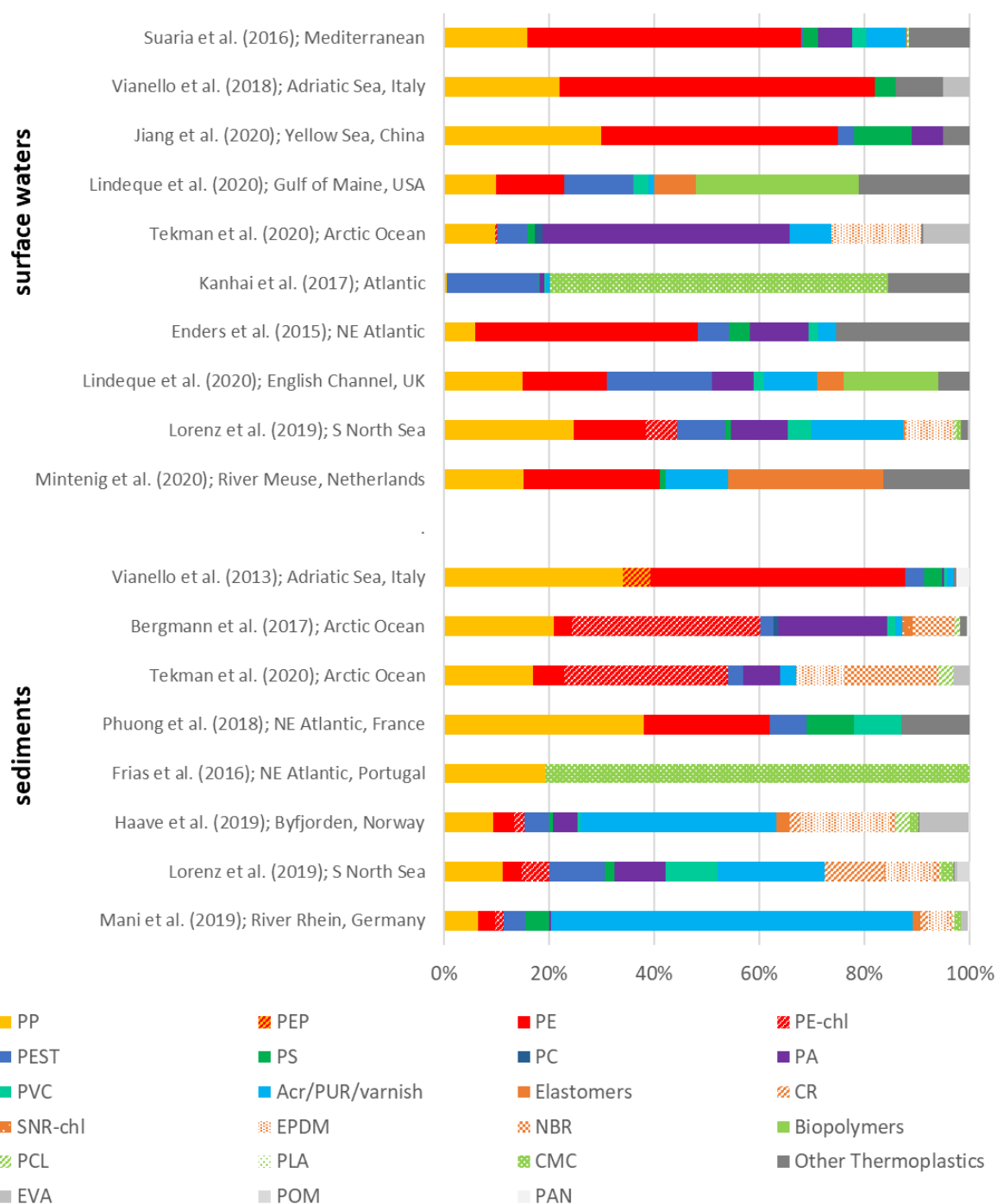


Figure 27: Polymer composition of a selection of studies that identified microplastics in surface waters and sublittoral sediments with spectroscopic methods as percentage per polymer type. PP: polypropylene, PEP=poly(ethylene-propylene), PE(-chl)=polyethylene (chlorinated), PEST=polyester/polyethylene terephthalate, PS=polystyrene, PC=polycarbonate, PA=polyamide, PVC=polyvinyl chloride, Acr/PUR/varnish=acrylates/polyurethanes/varnish and paints, CR=polychloroprene, SNR-chl=polyisoprene chlorinated, EPDM=ethylene-propylene-diene monomer, NBR=nitrile rubber, PCL=polycaprolactone, PLA=polylactid acids, CMC=chemically modified cellulose/rayon, EVA=ethylene vinyl acetate, POM=polyoxymethylene, PAN=polyacrylonitrile.

This shows that the comprehensive analysis of MP in various environmental matrixes improves significantly the comparability and also the quality and reliability of the data.

Considering high-quality data and comparative studies, it all comes down to harmonization of methods and SOPs.

Down the rabbit hole of method harmonization and standardization

In the previous section, it was made apparent that results from different studies have to be considered carefully in the context of the applied methods and the targeted size range. Therefore, as stated above, the key to a successful inter-study comparison is the utilization of standardized or at least harmonized methods. In the following section, the methods utilized in this thesis will be briefly discussed in this context and their ability to provide reliable data.

Sampling

Commonly, nets of varying mesh size are deployed to sample MP accumulated on the sea surface. The mesh size hereby affects the maximum volume that can be filtered in a given time before the mesh becomes clogged and the lower size limit of the retained particles (Löder & Gerdt, 2015). However, as has been discussed in **Chapter I** and the corresponding Supplement, as well as in the first section of the General Discussion, it can be assumed that most of the MP are not freely dispersed but rather trapped in aggregates. Furthermore, Colton et al. (1974) pointed out already that as soon as the net starts to clog during sampling it will inevitably also collect particles smaller than the given mesh size. Thus, it seems reasonable to assume that many small sized MP therefore are collected by a net of 100- μm mesh size, regardless.

In a recent study, Lindeque et al. (2020) showed that concentrations for MP collected with 100- μm nets were 2.5 times higher than for MP collected with 333- μm nets and even 10 times higher compared to 500- μm nets, respectively. To see if this correlation also continues below 100 μm other sampling techniques need to be pursued like pump systems with integrated filters of smaller mesh size like has been done by a few studies (e.g. Enders et al., 2015; Rist et al., 2020; Tekman et al., 2020). However, with a decrease in mesh size during sampling the sample volume will most likely need to be decreased as well since the general particle load also of biogenic and inorganic material will increase and hamper subsequent sample processing. This leads to another issue, namely, what is the right and representative sample volume. According to Bruge et al. (2020), a sample volume of 35 m^3 for river water with MPs concentrations of 1–4 particles m^{-3} was deemed sufficient when sampling with a 330- μm mesh size net. Thus, the MP concentrations presented in **Chapter I** can be considered as representative since on average 34 m^3 of surface water were sampled at each station with a net of even smaller mesh size (i.e. 100 μm). Regarding the water column, pumping systems

become more and more commonly used (e.g. Liu, F. et al., 2019a; Zobkov et al., 2019; Rist et al., 2020; Tekman et al., 2020), which usually do not allow for volumes this large to be sampled. Maximum sample volumes vary between 0.5 m³ (Tekman et al., 2020), 3.5 m³ (Zobkov et al., 2019), 16 m³ (Liu, K. et al., 2019b), and 2378 m³ (Choy et al., 2019). In a recent study, Liu, K. et al. (2019b) showed that a sample volume of at least 8 m³ could be deemed representative when considering MP down to 60 µm in size since the concentration of MP fibers and fragments did not differ significantly between 8 and 16 m³.

For sampling of sublittoral sediments, the use of grabs is most common, followed by corers, and has been deemed suitable (Gerdtz, 2019). In this thesis, a Van Veen grab was used for sampling, and the sediment surface was sampled to a depth of 1 cm (**Chapter IV**) or 5 cm (**Chapter I**), with the latter being recommended by Frias et al. (2018). So far, no clear recommendation on appropriate sample amounts for sublittoral sediments exist. According to Koelmans et al. (2019), the representativeness of a sample is related to the limit of detection and the targeted particle size range. For North Sea sediments in this thesis (**Chapter I**), the lowest MP concentration in the size range 11–5000 µm has been 3 particles kg⁻¹, deeming a sample of 1 kg (dw) sediment sufficient, transferring the requirements proposed by Bruge et al. (2020) from water volume to sediment weight. Since in **Chapter I** of this thesis, reported sediment dw ranged between 1.3 and 1.8 kg, the results could be considered representative. For the fjord sediments, presented in **Chapter IV**, the lowest MP concentration in the same size range was 10⁴ times higher thus deeming the lower analyzed sample amount (0.25–0.5 kg (dw) sediment) representative as well.

Sample processing

Apart from the sampling equipment, also the mesh or pore size of filters that are used during sample preparation needs to be considered when determining the size fraction, which can be analyzed quantitatively. The nominal mesh size of the stainless steel filters used in the context of this thesis (**Chapter I & IV**) has been 20 µm and 30 µm, respectively. This allowed for the quantitative detection of MP >20/30 µm in sediment samples and the semi-quantitative detection in the surface water samples.

Regarding sediment sample processing, the removal of the inorganic matrix via density separation is the most crucial step. A great variety of salt solutions with different achievable densities is available for this purpose. Figure 28 shows which polymer types would be positively buoyant in which of these salt solutions. Additionally, to its density, also its health hazard, toxicity and price range should be considered (Frias et al., 2018). Early recommendations by Hanke et al. (2013) suggested the use of a concentrated NaCl solution due to it being inexpensive, readily available, and non-toxic. However, due to the low density

that can be reached, NaCl does not facilitate the separation of polymer types with a density higher than 1.2 g cm^{-3} . Hence, Frias et al. (2018) recommended in the framework of the BASEMAN project, apart from NaCl, the use of sodium tungstate dihydrate ($\text{Na}_2\text{WO}_4 \cdot 2\text{H}_2\text{O}$), which can achieve a higher density (e.g. 1.4 g cm^{-3}), is less expensive than other tungstate solutions and less toxic than the slightly cheaper ZnCl_2 . In the studies presented here in **Chapter I & IV**, a ZnCl_2 solution of $1.7\text{--}1.8 \text{ g cm}^{-3}$ was used, since it presented at that time a good compromise between cost and efficiency (Löder & Gerdt, 2015; Coppock et al., 2017). According to Kedzierski et al. (2017), ZnCl_2 solution of $1.7\text{--}1.8 \text{ g cm}^{-3}$ would allow extracting 93–98% of the polymer mass fraction produced in Europe (Figure 28). With regard to its health hazard, great care has been taken to protect the operator and to prevent spillage. Furthermore, the ZnCl_2 solution was successfully recycled repeatedly via filtration, which has recently been supported by Rodrigues et al. (2020).

Considering that the representativeness of a sample increases with the analyzed sample volume, especially considering the patchy distribution in sediments, the analysis of large sample amounts ($\sim 1 \text{ kg}$) is recommended. Thus, devices like the commercially available MPSS (HydroBios) for the density separation method have their advantage and consequently have been used in this thesis (**Chapter I & IV**) and several other studies (e.g. Imhof et al., 2012; Imhof et al., 2016; K  ppler et al., 2016; Bergmann et al., 2017; Bord  s et al., 2019; Tekman et al., 2020). Such devices can therefore be deemed suitable for a harmonized protocol. Nevertheless, for monitoring purposes, the dimension of the MPSS is quite extensive and its use quite time demanding since only one sample can be processed at a time. As a consequence, other modifications to this design, like the new separator, developed at the Alfred Wegener Institute on Helgoland in the context of this thesis (Patents DE 10 2016 008 966 A1 and EP 3 272 421 A1) might become more suitable in future studies (Gerdt, 2019).

For the sample treatment to remove the biogenic organic matter, several maceration treatments, i.e. acidic, alkaline, oxidative, and enzymatic, can be used. When choosing a suitable treatment method with regard to harmonization between studies and potential for monitoring purposes, some factors need to be considered, i.e. time demand, cost, effectiveness, and destructiveness. Considering time demand, acidic treatments are usually fast, while alkaline treatments can take several days (e.g. Karami et al., 2017). Oxidative treatments can take several days (e.g. Nuelle et al., 2014) but the time demand can be decreased by catalyzing the reaction like it is done with iron sulfate for the Fenton reaction (Tagg et al., 2017). Enzymatic treatments might take a couple of hours (Cole et al., 2014) or days (L  der et al., 2017) depending on the number of enzymatic steps included and the amount of biogenic organic matter. The use of special enzymes might be the most expensive option. However, the cost can be reduced by using enzyme-blends (Piarulli et al., 2019) or

technical grade enzymes (Löder & Gerdt, 2015; Löder et al., 2017). Figure 29 clearly shows the benefits of using an enzymatic maceration since it exhibits high removal efficiencies (97–98%) with at the same time having no negative impact on the synthetic polymers (Cole et al., 2014; Löder et al., 2017; von Friesen et al., 2019). When additionally combined with an oxidative treatment (e.g. H₂O₂, Fenton) it presents the most effective but also least destructive approach to remove the environmental matrix (e.g. Löder et al., 2017; Liu, F. et al., 2019b). Furthermore, this approach by Löder et al. (2017), which has been optimized and successfully applied during the framework of this thesis (**Chapter I & IV**), has been adopted by a growing number of studies for a variety of environmental matrixes (e.g. Cabernard et al., 2018; Liu, F. et al., 2019a; Liu, F. et al., 2019b; Mintenig et al., 2020; Tekman et al., 2020).

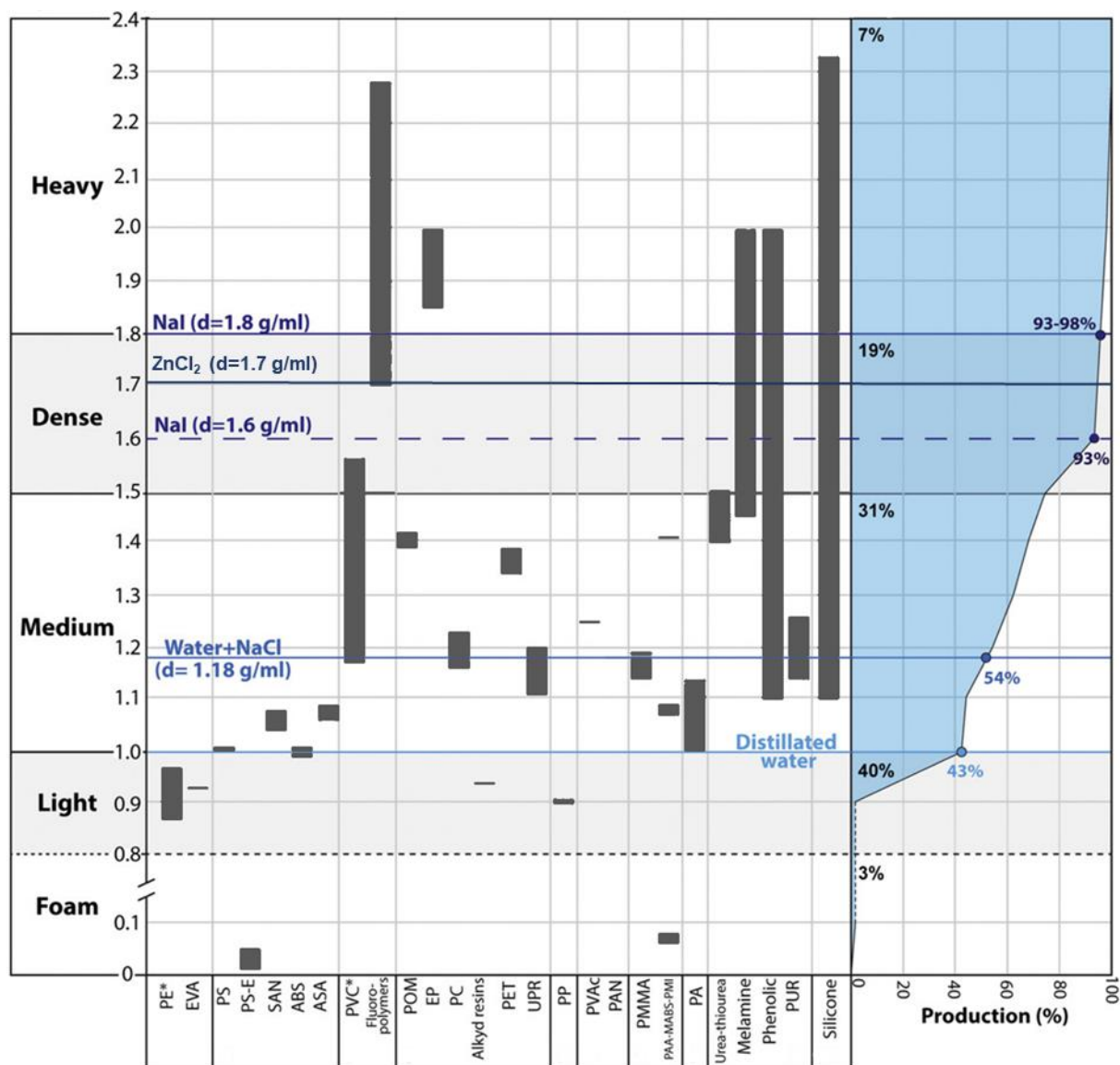


Figure 28: Specific density and related mass European production. The vertical lines highlight what percentage of the European plastics production can be extracted with density solutions of varying density. Modified from Kedzierski et al. (2017).

For the works in this thesis, (**Chapter I, IV** and exemplarily **III**) the purified samples had to be transferred to a filter, suitable for the analysis using FPA-based FTIR imaging, concentrated in an area as small as possible to reduce the required analysis time (Löder et al., 2015). To avoid overloading these filters, which would hamper the FTIR analysis in transmission mode, subsamples had to be transferred onto the filters. To define the right amount of this subsample the utilization of the FlowCam was introduced in the framework of this thesis and has since been applied in several other studies (Bergmann et al., 2017; Cabernard et al., 2018; Bergmann et al., 2019; Mani et al., 2019c; Tekman et al., 2020).

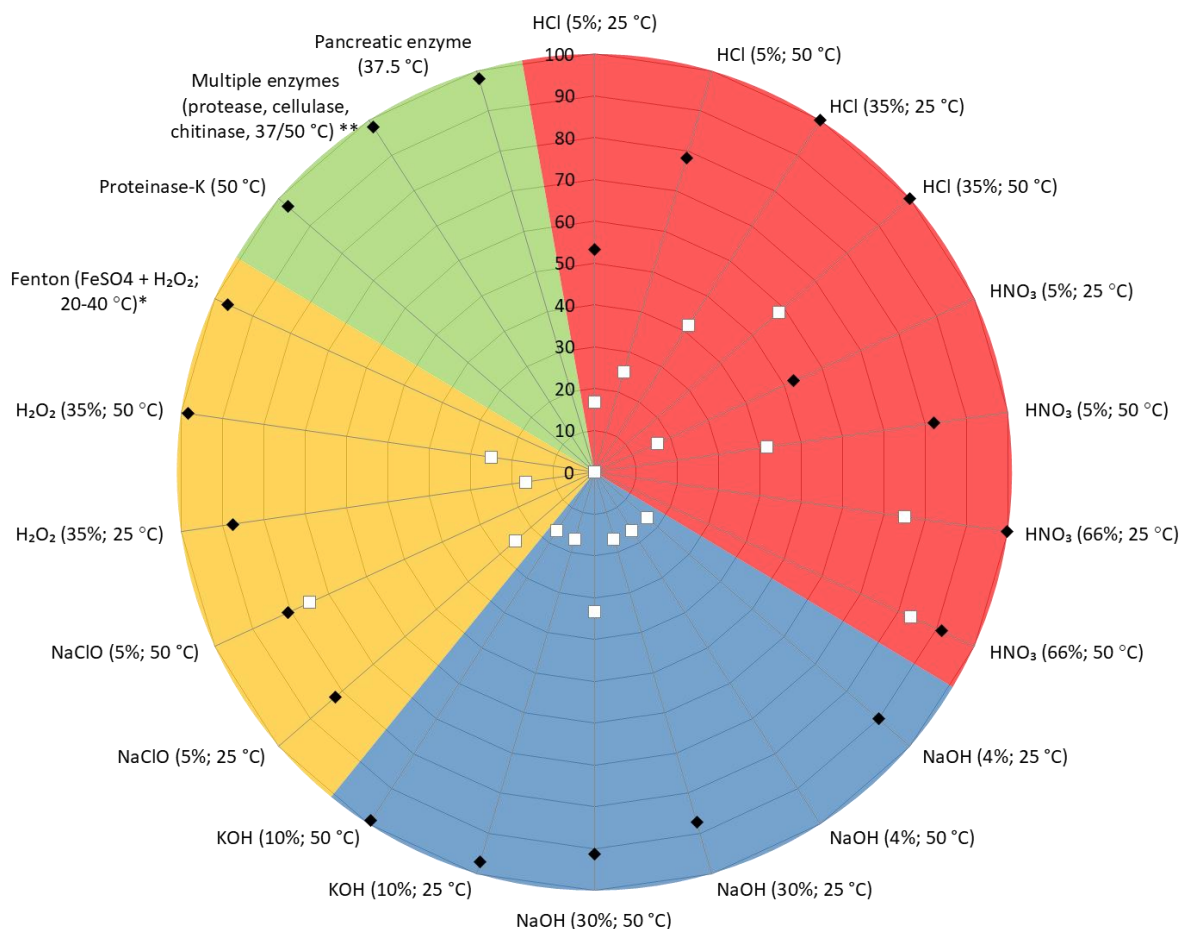


Figure 29: Comparison of different sample treatment methods according to their effectiveness (black diamonds, in%) and the maximum percentage of microplastics negatively affected by it (white squares, considering 12 polymer types). Methods marked with * were only tested for 8 polymer types and marked with ** were only tested for polyethylene. Differently colored sectors represent the different maceration categories: red=acidic, blue=alkaline, yellow=oxidative, green=enzymatic. Modified from Hamm et al. (2018) (based on Karami et al., 2017; Löder et al., 2017; von Friesen et al., 2019).

Identification and quantification

The solely visual identification of MP is deemed insufficient, which is especially true when it comes to assessing the small-sized MP. According to Andrade et al. (2020), FTIR spectroscopy is the most widely accepted analytical technique for MP analysis. A considerable benefit of a chemical identification is the identification of individual polymer types based on comparison to a database containing verified polymer spectra. This identification of polymer types might even allow, to some extent, for source tracking. As, for example, alkyd resins are utilized as a binder in industrial paints (Filella, 2015) and have been, along with paints based on acrylates or PUR, identified in several studies (e.g. Imhof et al., 2016; Mani et al., 2019c; Tagg et al., 2019; Tekman et al., 2020). In this thesis (**Chapter I & IV**), they have been identified as well in the acrylates/PUR/varnish cluster. Paint chips can stem from ship maintenance and cleaning (Turner, 2010; Filella, 2015).

Another benefit of FTIR spectroscopy, as stated by Andrade et al. (2020), is that it allows for the assessment of an increase of oxygenized moieties and thus the weathering status of MP extracted from environmental matrixes as has been shown in this thesis (**Chapter II**). Furthermore, this weathering status will affect surface properties like hydrophobicity, which, in turn, might make the particle more accessible for adsorption of chemicals and biofilm formation and hence more appealing for uptake by organisms (Rummel et al., 2017; Bråte et al., 2018). Considering this impact on uptake by organisms and on the sinking behavior, it is crucial to assess the weathering status of environmentally weathered MP. As the results of this thesis (**Chapter II**) have shown, MP extracted from environmental matrixes are weathered to some extent. This was also confirmed by other studies that analyzed the carbonyl index of MP, i.e. PE and PP, in surface waters. In one of these, Ter Halle et al. (2017b) analyzed PE micro- and mesoplastics collected from North Atlantic surface waters. They recorded mean carbonyl indices of 0.7 and no significant difference between the two size categories. Vianello et al. (2018) reported that 23% of PE particles identified in Adriatic Sea surface waters were oxidized with similar values for the carbonyl index ranging between 0.34 and 0.75. In this thesis (**Chapter II**), the carbonyl index for PE particles (11–5000 μm) collected in the surface water of the southern North Sea did not exceed 0.5. However, in all three studies, the carbonyl index for PE was calculated differently. While Vianello et al. (2018) calculated the ratio of the carbonyl band height at 1712 cm^{-1} to the methylene band at 1468 cm^{-1} , Ter Halle et al. (2017b) considered the ratio of the integrated areas in a wavenumber region ($1780\text{--}1600\text{ cm}^{-1}$ for carbonyl groups and $1490\text{--}1420\text{ cm}^{-1}$ for methylene groups). In the context of this thesis (**Chapter II**) also the ratio of the areas for carbonyl groups compared to methylene groups as reference was used, but with a slightly narrower wavenumber region for the carbonyl groups ($1800\text{--}1700\text{ cm}^{-1}$) and a slight shift for the methylene groups ($1480\text{--}1400\text{ cm}^{-1}$). Brandon et al. (2016) attempted to quantify the exposure time of HDPE, LDPE and PP particles collected with a manta trawl in the Northeast Pacific Ocean by comparing their carbonyl indices to particles of the same polymer type that were experimentally weathered for up to 36 months. For both PE types, the majority of the collected MP showed carbonyl indices in the same range as the experimentally weathered ones. For oceanic PP particles, this trend was less clear and most carbonyl indices exceeded the experimentally weathered ones. However, as hypothesized in the surface ablation model by Andrady (2017), which was reinforced by the results of this thesis (**Chapter II**), the progressing oxidation at the surface of a particle will result in the ablation of a thin oxidized layer that, after being shed, leaves an unoxidized surface behind, which in turn makes the task of estimating the exposure time of MP in the marine environment far more complex.

Considering that particle size and shape influences the ingestion behavior of organisms (Lehtiniemi et al., 2018) as well as the sinking behavior of MP (Ballent et al., 2013; Chubarenko et al., 2018a), knowledge of particle related data is of great value, especially for exposure studies. To date exposure studies usually utilize only a limited number of polymer types (e.g. PS, PE) of a narrow size range and preferably regular shape (i.e. beads) (Kögel et al., 2020). When considering these restrictions, the concentrations used in these studies are by far exceeding environmental realism. Furthermore, in most experimental studies, pristine MP are used. However, Bråte et al. (2018) recently showed that Mediterranean mussels (*Mytilus galloprovincialis*) ingested significantly more weathered PE beads than virgin ones. Hence, an analysis technique which allows for the identification of the chemical properties (e.g. synthetic or natural origin, weathering status) as well as the size and shape (i.e. proper elongation factor), ideally with a high degree of automatization, is crucial. This can best be achieved by combining image analysis with a microscopy-based spectroscopic method, e.g. FTIR imaging and μ Raman mapping is of great importance (Anger et al., 2018; Anger et al., 2019; Primpke et al., 2019; Vianello et al., 2019; Brandt et al., 2020; Primpke et al., 2020a; Primpke et al., 2020b).

In contrast to this, Pyr-GC-MS gives mass concentrations related data, which is in turn more suitable for budgeting MP mass fluxes. This analysis is also suitable to analyze tire wear treads (Lachowicz et al., 2012; Unice et al., 2013), which is not possible with FTIR spectroscopy due to the high content of carbon black that leads to total absorbance of the spectra (Kole et al., 2017). Furthermore, GC-MS methods can provide additional information on additives and POPs and are highly suitable to identify PWs, as was shown in this thesis (**Chapter III**).

Recently, however, Simon et al. (2018) presented a method to estimate mass related data from particle concentration and size distribution related data obtained by FTIR imaging. This mass estimation has been applied in several recent studies (e.g. Liu, F. et al., 2019a; Liu, F. et al., 2019b; Olesen et al., 2019; Vianello et al., 2019; Mintenig et al., 2020) and is an integrated feature in the freely available software siMPle (Primpke et al., 2020b). The provided mass estimation can, to some extent improve comparisons between studies using thermal degradation rather than a spectroscopic methods. Nevertheless, both techniques should still be considered complementary.

QA/QC and reporting of data

Another important aspect of standardization is quality assurance and control (QA/QC). In this regard, Hanke et al. (2013) pointed out in the MSFD monitoring guidelines that confidence in data collection would increase with validated and accredited methods and inter-laboratory studies. This topic of lacking QA/QC in MP studies has been acknowledged by Filella (2015). Recently, an attempt to strengthening the issue of QA/QC has been made by Hermesen et al.

(2018) and Koelmans et al. (2019). They proposed key aspects that need to be considered during MP analysis and reporting of data and introduced a scoring system to evaluate the reliability and validity of studies, taking several studies on MP in biota (Hermsen et al., 2018) as well as in drinking and wastewater as examples (Koelmans et al., 2019). This scoring system can also be applied to the two studies presented in this PhD thesis assessing MP in the southern North Sea (**Chapter I**) and the Byfjorden (**Chapter IV**). Both studies scored positively with 15 or 13 points out of 18, respectively (Table 9).

Table 9: Scoring of the two studies presented in this thesis (**Chapter I & IV**) based on specific quality criteria defined by Hermsen et al. (2018) and Koelmans et al. (2019).

Criteria	Lorenz et al. (2019)	Haave et al. (2019)
Sampling methods	2	2
Sample size	2	2
Sample processing and storage	1	1
Laboratory preparation	2	2
Clean air conditions	2	1
Negative control	2	1
Positive control	0	0
Sample treatment	2	2
Polymer identification	2	2
Sum	15	13

For the study presented in **Chapter I**, no positive controls were performed, i.e. recovery experiments (-2), and samples were stored in PVC containers but providing blanks for that (-1). The study presented in **Chapter IV** did not include positive controls neither (-2), and samples were stored in bottles with PP cap but providing blanks for this (-1). Furthermore, the work was not done in a laminar flow cabinet, but several blank filters for airborne contamination were done and revealed no visible contamination (-1). Finally, only one blank was processed within the study (-1). In both studies, it was necessary to extrapolate the concentrations based on the measured subsamples to the entire sample normalized to 1 kg dw sediment or 1 m³ filtered surface water, respectively. However, both studies performed an error propagation for calculation of particle concentrations to estimate the errors originating from this required extrapolation to increase the quality of the data.

Moreover, Koelmans et al. (2019) pointed out that the exhaustive reportage on method details is another important aspect related to QA/QC. In a recent attempt to further harmonization in the field of MP research, Cowger et al. (2020a) published reporting guidelines, which were contributed to by many experts of the respective scientific community. In this context, the size range targeted during sampling, sample processing and analysis plays an essential role.

Hence, Frias and Nash (2019) pointed out that results on MP abundances should be reported in three size categories which reflect current sampling, processing and analysis techniques best and would allow for better comparability. These size categories are 1–100 μm , 100–350 μm and 350–5000 μm . As pointed out in the inter-study comparison, the comprehensive analysis of MP presented in this thesis allows for the reporting of the results for all of these size categories (Supplement General Discussion Table S24–26). However, the results of this study have shown that reporting the size distribution in even finer resolved size classes improves the comparability further. Analysis tools like the recently developed and freely available siMPle software provide even the accurate size of each particle and any categorization into appropriate size classes can be done in retrospect Primpke et al. (2020b). This consequently improves, apart from the comparability, also the quality and reliability of the data and thus, provides valuable information for exposure studies under realistic scenarios.

Conclusion

This thesis provides the first comprehensive analysis of MP in a size range of 11 to 5000 μm in surface waters and sublittoral sediments of the southern North Sea as well as sublittoral sediments of a Norwegian fjord in an urbanized area. The application of state-of-the-art methods for sample processing and analysis with spectroscopic techniques supplied polymer composition and size distribution of MP down to 11 μm in size. Here, I showed that large MP (500–5000 μm) exhibited lower concentrations as well as different and less diverse polymer compositions than small MP (11–500 μm). Furthermore, more than 95% of MP in sediments and 86% in surface waters, respectively, were smaller than 100 μm . This implies that future monitoring campaigns should include also small MP (<500 μm) to gain a realistic view of the actual MP pollution in the marine environment. Average as well as highest MP concentrations detected in the Norwegian fjord exceeded the respective ones in the southern North Sea sediments by factor 100. This result can be explained by a temporarily high input of MP through the discharge of untreated wastewater as well as stronger accumulation in the fjord system. Both areas, however, showed a similar polymer composition dominated by paint-related polymer types, rubbers, PP, PEST and PA confirming that size and polymer type are driving forces in the vertical transport of MP. Polymer composition in southern North Sea surface waters differed significantly from sediments with low-density polymer types such as PP and PE representing more than a third of the polymer composition. The carbonyl indices of these two polymer types also differed significantly between surface water and sediment samples. When considering the entire recorded spectral range (3600–1250 cm^{-1}) for small MP (11–500 μm), the difference was less prominent. Still, the spectra of naturally weathered MP of four different polymer types (PE, PP, PS, and PVC) differed significantly from pristine reference spectra. The wavenumber region which is characteristic for carbonyl groups (1750–1650 cm^{-1}) showed to be a good indicator for weathering, but the wavenumber region characteristic for hydroxyl groups (3500–3200 cm^{-1}) displayed some potential as well.

Concerning the spatial distribution of MP in the southern North Sea, MP concentrations as well as polymer compositions differed significantly between the central southern North Sea and the regions closer to the English Channel and the Rhine-Meuse-delta. While MP concentrations in surface waters were highest where influenced by oceanic and riverine input, the highest MP concentrations in sediments were detected further in the central part of the southern North Sea, possibly indicating a northeasterly transport and accumulation in the sediments there. However, to confirm this assumption, the water column needs to be investigated to resolve vertical transport. For the Norwegian fjord, sampling stations with high concentrations coincided with closeness to discharge sites and areas of increased deposition marking this fjord as a suitable area for monitoring purposes.

Conclusion

This thesis additionally highlighted that the lack of SOPs hampers inter-study comparisons. Differences in methodologies might overshadow differences in MP concentrations recorded by previous studies. This issue applies to the analyzed sample volume (i.e. representativeness of the sample), the targeted size range (i.e. lower size cut-off during sampling, sample processing or analysis), sample treatment (e.g. density of solution used for MP extraction, maceration agents to remove the biogenic organic matter), and the analytical method (e.g. visual identification only vs (semi)automatic chemical identification).

For analysis of MP in a size range from 11 to 5000 μm , ATR-FTIR spectroscopy combined with μFTIR imaging could be deemed suitable to provide detailed particle-related data. Along with large MP (500–5000 μm), floating PWs of the same size range could be collected successfully utilizing a MP-sampling net (100 μm mesh size) and a subsequent fractionation with a 500- μm stainless steel mesh. The analysis of PWs with ATR-FTIR spectroscopy provided promising results for individual particles but should be complemented by GC-MS analyses, to gain a more detailed chemical fingerprint and unambiguous identification of PWs.

Once MP have entered the marine environment, it becomes challenging if not impossible, to remove them, due to their small size. With regard to the known sources and pathways, there are several more suitable points of vantage, such as improving waste management, WWTP facilities, and recycling capabilities.

Outlook – Old and new challenges to face

The long and winding road to monitoring strategies

A main outcome of the JPI-Oceans BASEMAN project has been along the line of this thesis that small MP (<500 µm) are more numerous than large MP and that it is thus crucial to focus environmental surveillance in the marine environment on these small MP (Gerdt, 2019). Up to date European authorities concerned with this task of monitoring MP still need to commit to this task entirely. However, JPI-Oceans reacted to this conclusion and the new projects, accepted for the subsequent call, target also smaller MP and nanoplastics (JPI-Oceans, 2020).

The behavior of small MP (<500 µm) in the marine environment

As stated by Ballent et al. (2013), the knowledge on the distribution of MP, especially in the water column and deep-sea sediments, is still scarce due to resource-intensive sampling methods. Some knowledge gaps might, however, be bridged by modelling approaches. Hence, as much information on particle properties from MP extracted from diverse environmental matrices, and consequently their hydrodynamic behavior, are required to predict transport from land-based sources across the global marine environment even to remote areas. Thus, one of the recently launched new JPI-Oceans projects is concerned with the "Fluxes and Fate of Microplastics in Northern European Waters" (FACTS). This project addresses the spatial distribution of MP from the southern North Sea to the arctic Barents Sea on different temporal scales (JPI-Oceans, 2020). Furthermore, it focusses on the whole water column from the surface boundary layer to the sea bed and aims to improve the comprehension of the horizontal and vertical transport of MP. Moreover, the detection and quantification of nanoplastics are addressed as well.

Nanoplastics – Smaller particles but not smaller challenges

Nanoplastics (1–1000 nm) have been shown to form during the degradation of plastics under laboratory conditions (Lambert & Wagner, 2016) and are thus expected to occur and accumulate in the marine environment. So far only a limited number of studies have attempted to characterize nanoplastics in natural samples (Ter Halle et al., 2017a; Materić et al., 2020) since sampling and sample processing are major challenges (Mintenig et al., 2018; Li, P. et al., 2020). Due to their minuscule size, nanoplastics can hardly be sampled utilizing conventional filtration, which would require filters with very narrow pore sizes which in turn would clog rather quickly, depending on the sampled matrix. To overcome this, Ter Halle et al. (2017a) concentrated the colloidal fraction (1 nm to 1 µm) of 1 L of seawater by ultrafiltration. In a similar approach Mintenig et al. (2018) utilized crossflow ultrafiltration to concentrate over 600 L surface water of a freshwater system into a sample volume of 0.4 L. Recently, Hildebrandt et al. (2019) presented cross flow centrifugation as a potential method to sample

liquid matrices for MP down to 1 μm . Subsequently, they successfully evaluated this method with metal-doped nanoplastics ($\sim 160\text{ nm}$) and river water (Hildebrandt et al., 2020). Another big challenge is the identification and quantification of nanoplastics. Chemical analysis techniques commonly applied for MP identification, such as FTIR and Raman microspectroscopy, have detection limits of one to several μm . Other methods like dynamic light scattering (DLS) can be used to quantify and characterize particle size distribution in the nm range but do not provide information about the polymer type. Hence, Ter Halle et al. (2017a) combined DLS with a bulk-analysis of the sample via Py-GC-MS, which provides mass-related data related to the polymer types, and noted that the sample volume needs to be sufficiently large ($>5\text{ L}$) to determine the chemical composition reliably. However, this approach does not provide the chemical composition of the individual nanoplastics. There exist some promising techniques which allow the spectroscopic analysis of single nanoplastics (Primpke et al., 2020a). One approach is the application of Raman tweezers which enabled the identification of individual particles down to 50 nm in seawater (Gillibert et al., 2019). Another approach is to combine atomic force microscopy (AFM) with spectroscopy or utilizing nano-FTIR and IR-sSNOM (scattering-type nearfield optical microscope). Meyns et al. (2019) demonstrated that the latter has the potential to successfully identify polymers when linked with analysis software such as siMPle. Despite these advances, the collection and unambiguous identification of nanoplastics from environmental matrixes is still in its infancy.

Supplement

The Supplement contains five subsections, one for each Chapter I to IV and one for the General Discussion.

Supplementary material for Chapter I

Spatial distribution of microplastics in sediments and surface waters of the southern North Sea

Claudia Lorenz, Lisa Roscher, Melanie S. Meyer, Lars Hildebrandt, Julia Prume, Martin G. J. Löder, Sebastian Primpke, Gunnar Gerdts

Paragraphs (6), figures (13) and tables (11) describing the sampling, sample processing and analysis in greater detail as well as presenting result for the statistical analysis

Paragraph S1 on sampling

At each of the 24 stations, when deploying as well as removing the net, the coordinates were registered along with the readout of the flowmeter revolutions. According to Maes et al. (2017b) and Rivers et al. (2019) the number of revolutions multiplied with the impeller constant (0.3) equals the trawled distance in meters. The trawled surface area was obtained by multiplying the results by the width of the net (0.3 m). The sampled water volume was determined by multiplying these results by the sampled depth when assuming that two-thirds of the net were submerged ($\frac{2}{3} \times 0.15$ m). The samples were stored in 1-L bottles (polyvinyl chloride, Kautex Textron GmbH & Co KG, Bonn, Germany). One surface water samples taken at station 12 got lost before analysis and the sediment sample taken at station 17 contained considerably less material than the other sediment samples and was therefore regarded not being representative. This resulted in 46 samples that were analyzed, 23 for each environmental compartment.

Supplement Chapter I

Table S1: Sampling stations and dates with corresponding geographic coordinates of Heincke cruise He430 in 2014. Water volume is given in m³ and water depth of sediment grabs in m as well as corresponding dry weight of sampled sediments in kg. The water volume which passed through a neuston net (100 µm) with a net opening of 0.15 m × 0.3 m was determined using a mechanical flowmeter. The number of revolutions between start and end were multiplied by the impeller constant (0.3) to get the trawled distance, which was then multiplied by the cross-sectional area (net opening which was submerged up to two-thirds) to refer to the sampled surface water volume in m³.

Station	Sampling date	Latitude	Longitude	Start flow	End flow	Filtered volume	Water depth	Sediment dry weight
He430		N	E			m ³	m	kg
1	31.07.2014	53.8233	7.7205	116	4196	36.72	12	1.533
2	31.07.2014	53.7768	7.2843	14307	18811	40.54	14	1.606
3	01.08.2014	53.7477	6.9983	27785	32918	46.20	9	1.558
4	01.08.2014	53.7117	6.6443	44964	49904	44.46	13	1.693
5	01.08.2014	53.6542	6.2797	57773	60027	20.29	18	1.630
6	02.08.2014	53.5985	5.9223	69737	73636	35.09	19	1.498
7	02.08.2014	53.5567	5.6315	79553	82291	24.64	20	1.410
8	02.08.2014	53.4647	5.2093	90190	94067	34.89	17	1.595
9	03.08.2014	53.3127	4.8022	6098	10650	40.97	15	1.615
10	03.08.2014	53.1108	4.5613	21496	25452	35.60	22	1.592
11	03.08.2014	52.8595	4.4040	36757	39892	28.22	18	1.670
12	04.08.2014	52.4178	4.3308	48928	50815	16.98	16	1.629
13	04.08.2014	52.1380	3.9762	60724	63436	24.41	18	1.564
14	04.08.2014	51.8508	3.5287	75349	77072	15.51	19	1.561
15	05.08.2014	51.5272	3.1500	88855	93351	40.46	19	1.658
16	05.08.2014	51.2442	2.4547	5090	7595	22.55	23	1.474
17	05.08.2014	51.0615	1.8448	18521	22866	39.11	27	n.a.
18	06.08.2014	50.4678	1.1512	34366	38201	34.52	17	1.605
19	06.08.2014	51.5217	2.4323	50202	53856	32.89	36	1.631
20	07.08.2014	52.1865	2.8847	68072	72088	36.14	35	1.770
21	07.08.2014	53.0363	3.2312	86128	91828	51.30	29	1.553
22	08.08.2014	53.9690	3.1873	6434	11630	46.76	33	1.765
23	08.08.2014	54.8682	3.4092	23308	28819	49.60	37	1.309
24	09.08.2014	55.8118	3.6403	40820	44337	31.65	49	1.636

Paragraph S1 on contamination prevention and quality assurance

Equipment made of glass or metal was used if not stated otherwise. If use of plastics was necessary, as few as possible different polymer types were used: polyvinyl chloride (PVC; Kautex bottles for sampling), silicone (tubings, sealing), polypropylene (PP; pleated cartridge filters) and polytetrafluorethylene (PTFE; sealing, squeeze bottle).

All applied chemicals etc. were filtered before usage over 0.2 μm (GTTP, polycarbonate), enzymes and sodium dodecyl sulfate (SDS) over 0.45 μm (cellulose nitrate) or 1.2 μm (GF/F glass fiber) filters to remove particles.

All processes involving exposed samples were performed in a laminar flow cabinet (ScanLaf Fortuna 1800, LaboGene, Lillerød, Denmark). Furthermore, a Dustbox (DB1000, G4 prefiltration, HEPA-H14 final filtration, $Q=950\text{ m}^3\text{ h}^{-1}$, Möcklinghoff Lufttechnik, Gelsenkirchen, Germany) had been installed in every laboratory to reduce airborne contamination with fibers.

All equipment was rinsed with Milli-Q (0.22 μm filtered water, Millipore) before usage.

Samples were processed in batches and for each batch a procedural blank, consisting of 1 L of Milli-Q (surface water samples) or 1 L of zinc chloride (ZnCl_2) solution (sediment samples) was run in parallel to the samples. In total six blanks ($n=4$ for sediment, $n=2$ for surface water) were processed. At the end, the final results from the sample analysis were corrected for their accompanying blank.

Paragraph S2 on density separation of sediment samples

The MicroPlastic Sediment Separator (MPSS, HydroBios Apparatebau GmbH, Kiel, Germany) (Imhof et al., 2012) was filled with filtered (10 μm stainless steel and 1 μm PP pleated cartridge filters, Wolftechnik Filtersysteme GmbH & Co. KG, Weil der Stadt, Germany) ZnCl_2 solution (density $>1.7\text{ g cm}^{-3}$, Carl Roth, Karlsruhe, Germany) to the top dividing chamber. The rotor at the bottom was left running for 30 min, then turned off. The handle of the ball valve was moved to remove any entrapped air and the MPSS was left standing to allow any present plastic particles to concentrate in the upper chamber. After 3–4 hours the ball valve was closed, approximately 3 L of ZnCl_2 solution drained and the separated liquid containing potential cross contamination stored. Periodically these “pre-samples” were analyzed to access whether contaminating plastic types were also present in high numbers in the actual samples or not. This was not the case.

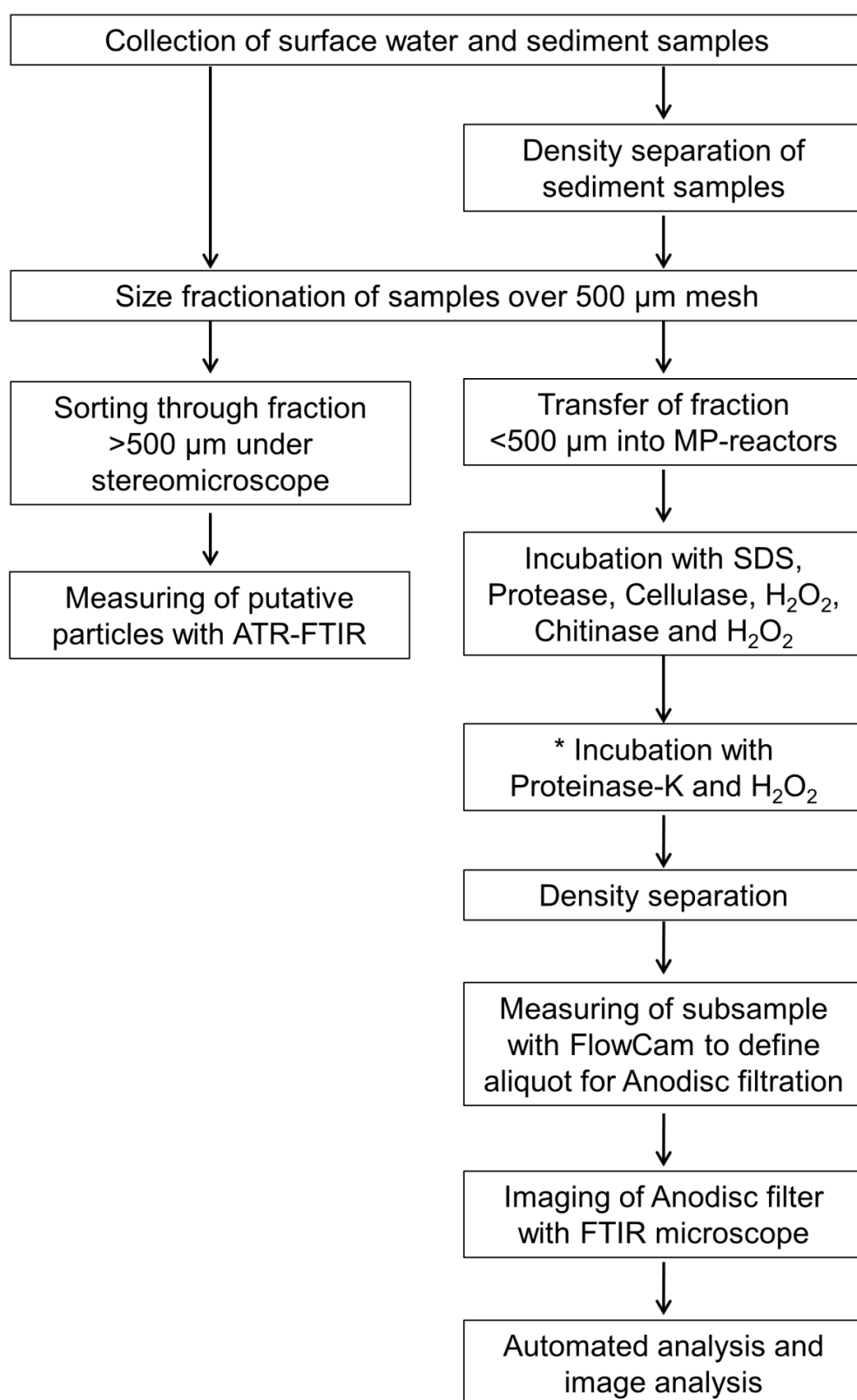


Figure S1: Schematic flowchart of sample processing. Marked steps (*) are optional based on sample condition



Figure S2: Microplastic (MP) reactors

Paragraph S3 on enzymatic-oxidative treatment of <500 μm fraction

Sample fractions containing all particles <500 μm were transferred into the Microplastic (MP) reactors (Gerdt, 2017). The MP reactors (Figure S2a) consist of a stainless steel tube with flanges at each end. At the bottom a 20- μm stainless steel filter (Haver & Boecker OHG, Oelde, Germany) was attached with six screws between two silicone sealing rings and a metal plate with an opening (Figure S2b). When the samples were concentrated on the bottom filter, the reactors were sealed at the bottom with a silicone plug and 300 mL of SDS (10%, Carl Roth, Karlsruhe, Germany) were introduced from the top. The reactors were then closed by attaching another 20- μm stainless steel filter between two sealing rings and an elbow piece with a valve at the top part (Figure S2c) that could be connected to a membrane pump to apply pressure or vacuum. The MP reactors were then incubated for 24 h in a shaking incubator (Infors AG, Bottmingen, Switzerland) at 50 °C (Figure S2d). Next, the SDS was removed via pressure filtration and the samples rinsed by alternatingly introducing Milli-Q from the bottom through vacuum filtration and removing it by applying pressure. The enzymatic digestion followed the protocol by Löder et al. (2017). As first enzymatic step a treatment with 50 mL of the technical

grade enzyme Protease-A01 (EC 3.4.21.62, ASA Spezialenzyme GmbH, Wolfenbüttel, Germany) in 250 mL of tris(hydroxymethyl)aminomethane buffer (Tris, 0.1 M, pH 9.0) was applied. Next enzymatic treatment was done with 61 mL Cellulase TXL (EC 3.2.14, ASA Spezialenzyme GmbH, Wolfenbüttel, Germany) in 250 mL of sodium acetate buffer (NaOAc, 0.1 M, pH 4.5) for 24 h at 40 °C and repeated three times. The enzyme-buffer-solutions were exchanged by filtering off the old solution and filtering in the new one with several Milli-Q rinsing steps in between. Before the last enzymatic treatment samples were incubated with 30 mL hydrogen peroxide (H₂O₂, 35%, Carl Roth, Karlsruhe, Germany) at 37 °C for maximum 24 h to improve the efficiency of the chitinase treatment. For this 1 mL of chitinase (EC 3.2.1.14, ASA Spezialenzyme GmbH, Wolfenbüttel, Germany) was added to 25 mL of NaOAc-buffer (0.1 M, pH 5.5) and transferred into the MP reactor from the opened top. The samples were incubated in the MP reactors with chitinase at 37 °C for 96 h. Subsequently the chitinase was removed and a second treatment with 30 mL of H₂O₂ at 37 °C for maximum 5 h was applied. Finally, the bottom filters with the concentrated, treated samples were removed and samples transferred with Milli-Q into 100-mL glass bottles with glass stoppers.

If visible material remained on the filter these were placed in a beaker with Milli-Q and subjected to ultrasonication for up to five times three minutes at 215 W/35 kHz (Sonorex RK514; Bandelin Electronic GmbH & Co. KG, Berlin, Germany).

Paragraph S4 on FlowCam measurement and Anodisc filtration

To determine the sample volume that could be concentrated on the measuring aluminum oxide filter (0.2 µm, Anodisc, Whatman, GE Healthcare, Chicago, United States) a FlowCam (Portable Version IV, Fluid Imaging Technologies, Scarborough, Maine, United States) was used. Therefore, triplicates of 1 mL per sample each were introduced into the FlowCam and all particles between 10–500 µm counted and their surface area recorded (Bergmann et al., 2017). Based on these measurements the surface area of all particles combined was determined per mL and related to the surface area where the sample was concentrated onto an Anodisc (diameter of 13 mm). This allowed for defining the subsample volume that could be used from each sample to cover the Anodisc with particles without overloading it, which would hamper a good spectral analysis in transmission mode. The volumes of these subsamples along with the analyzed proportion are presented in Table S2.

Supplement Chapter I

Table S2: Analyzed subsample volume and sample proportion for each station and matrix

sampling station	compartment	sample volume	total sample volume	volume used for μ FTIR	analyzed proportion
	sediment	kg (dw)	mL	mL	
	surface water	m ³	mL	mL	
1	sediment	1.533	81.3	28.5	0.3504
	surface water	36.7	92.7	15.0	0.1458
2	sediment	1.606	74.9	45.0	0.6011
	surface water	40.5	75.6	55.4	0.7324
3	sediment	1.558	92.6	17.3	0.1864
	surface water	46.2	84.5	5.8	0.0605
4	sediment	1.693	70.2	50.0	0.7123
	surface water	44.5	101.5	17.3	0.1705
5	sediment	1.630	96.8	38.9	0.4014
	surface water	20.3	99.0	10.4	0.1050
6	sediment	1.498	87.8	34.1	0.3885
	surface water	35.1	105.0	33.2	0.3162
7	sediment	1.410	92.0	46.7	0.5073
	surface water	24.6	82.9	4.6	0.0555
8	sediment	1.595	78.9	56.9	0.7214
	surface water	34.9	100.2	11.6	0.1157
9	sediment	1.615	94.8	63.6	0.6713
	surface water	41.0	96.5	1.4	0.0145
10	sediment	1.592	107.5	20.0	0.1860
	surface water	35.6	93.5	12.5	0.1338
11	sediment	1.670	100.8	75.6	0.7499
	surface water	28.2	79.9	30.0	0.2524
12	sediment	1.629	92.6	20.0	0.2159
	surface water	n.a.	n.a.	n.a.	n.a.
13	sediment	1.564	95.8	41.3	0.4313
	surface water	24.4	94.9	20.0	0.2347
14	sediment	1.561	112.7	84.5	0.7495
	surface water	15.5	94.0	1.3	0.0122
15	sediment	1.658	106.9	57.0	0.5333
	surface water	40.5	95.9	10.0	0.1042
16	sediment	1.474	110.3	45.0	0.4080
	surface water	22.5	98.5	3.4	0.0345
17	sediment	n.a.	n.a.	n.a.	n.a.
	surface water	39.1	100.7	27.4	0.2721
18	sediment	1.605	110.4	82.8	0.7499
	surface water	34.5	97.6	3.8	0.0389
19	sediment	1.631	79.6	60.0	0.7542
	surface water	32.9	97.3	12.7	0.0617
20	sediment	1.770	60.4	40.0	0.6623
	surface water	36.1	104.6	4.1	0.0329
21	sediment	1.553	96.1	42.3	0.4398
	surface water	51.3	108.3	6.3	0.0582
22	sediment	1.765	108.9	15.6	0.1433
	surface water	46.8	88.4	1.5	0.0153
23	sediment	1.309	93.0	10.0	0.1075
	surface water	49.6	98.6	4.6	0.0467
24	sediment	1.636	91.0	50.0	0.5495
	surface water	31.7	91.1	52.4	0.5753

Paragraph S5 on manual spectra evaluation

Four sediment and four surface water samples were selected that contained as many different polymers as possible. From these eight samples all spectra of synthetic polymers were evaluated based on criteria presented by Primpke et al. (2018) to establish specific thresholds to safely identify MPs for this data set (confidence interval of 95%). For natural polymers, e.g. cellulose, proteins and chitin, a maximum of 2000 spectra per sample were evaluated to reduce the time demand. The established thresholds are presented in SI Table S3. These were used for the final image analysis providing data on the particle counts, polymer types and size distribution of the MPs in the samples.

Table S3: Thresholds of hit quality (max. 2000) defined by manual spectra evaluation

Polymer cluster	Hit quality threshold
polyethylene	600
polyethylene oxidized	600
polyethylene-chlorinated	1000
polypropylene	600
polystyrene	600
polycarbonate	800
polyamide	600
polyvinyl chloride	680
chemically modified cellulose	600
nitrile rubber	600
polyester	750
acrylates/polyurethanes/varnish	600
animal fur	600
plant fibers	850
sand	740
polysulfone	600
polyetheretherketon	600
polychloroprene	600
chitin	600
polyisoprene chlorinated	600
polylactide acide	600
polycaprolactone	600
ethylene-vinyl-acetate	1270
polyimide	600
polyoxymethylene	600
polybutadiene	600
acrylonitrile-butadiene	600
rubber type 1	600
rubber type 2	600
charcoal	600
coal	600
rubber type 3	1100

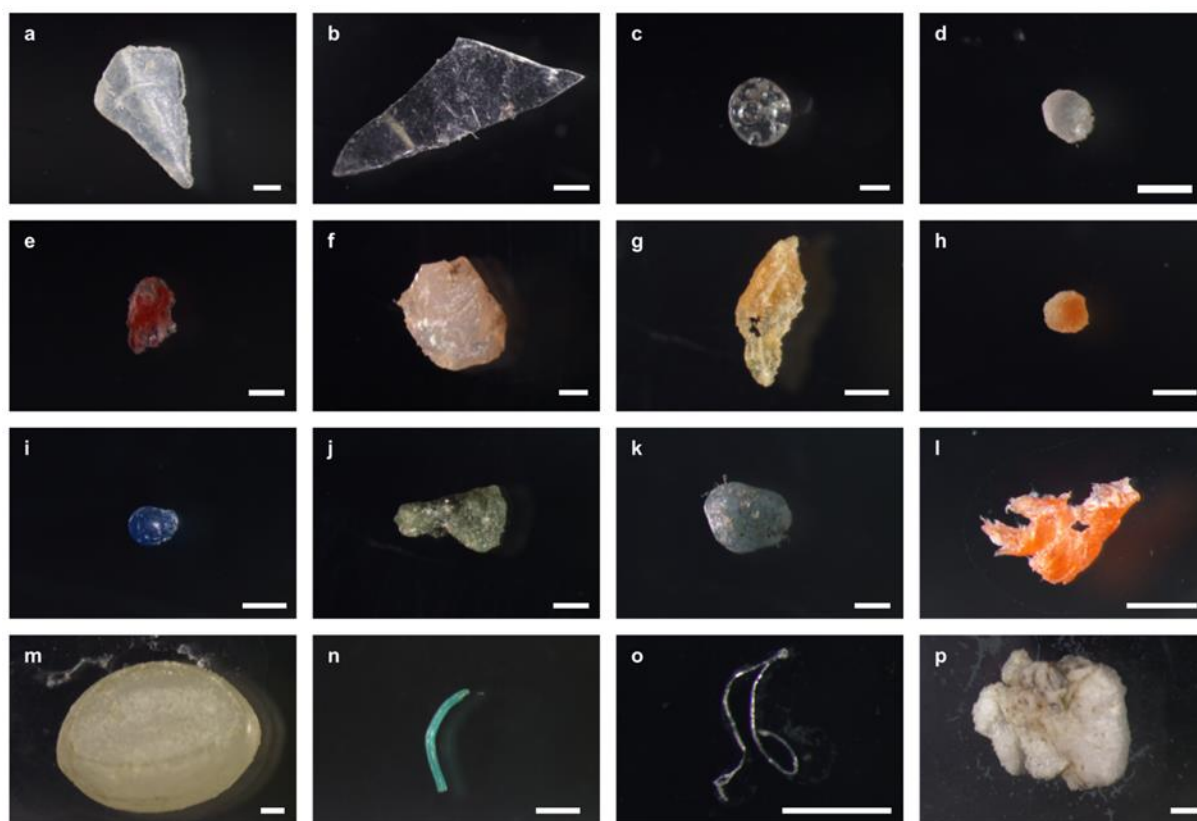


Figure S3: Selection of identified microplastics >500 μm . Particles were extracted from surface water samples of station 23 (a–e), 21 (f–k), 2 (l), 4 (m–n), and 9 (o–p). They were identified as polyethylene (a, d–f, h–k, m), polypropylene (b, g, n), polymethylmethacrylate (c), polyvinyl chloride (l), polyester (o), and polystyrene (p). Scale bar: 500 μm

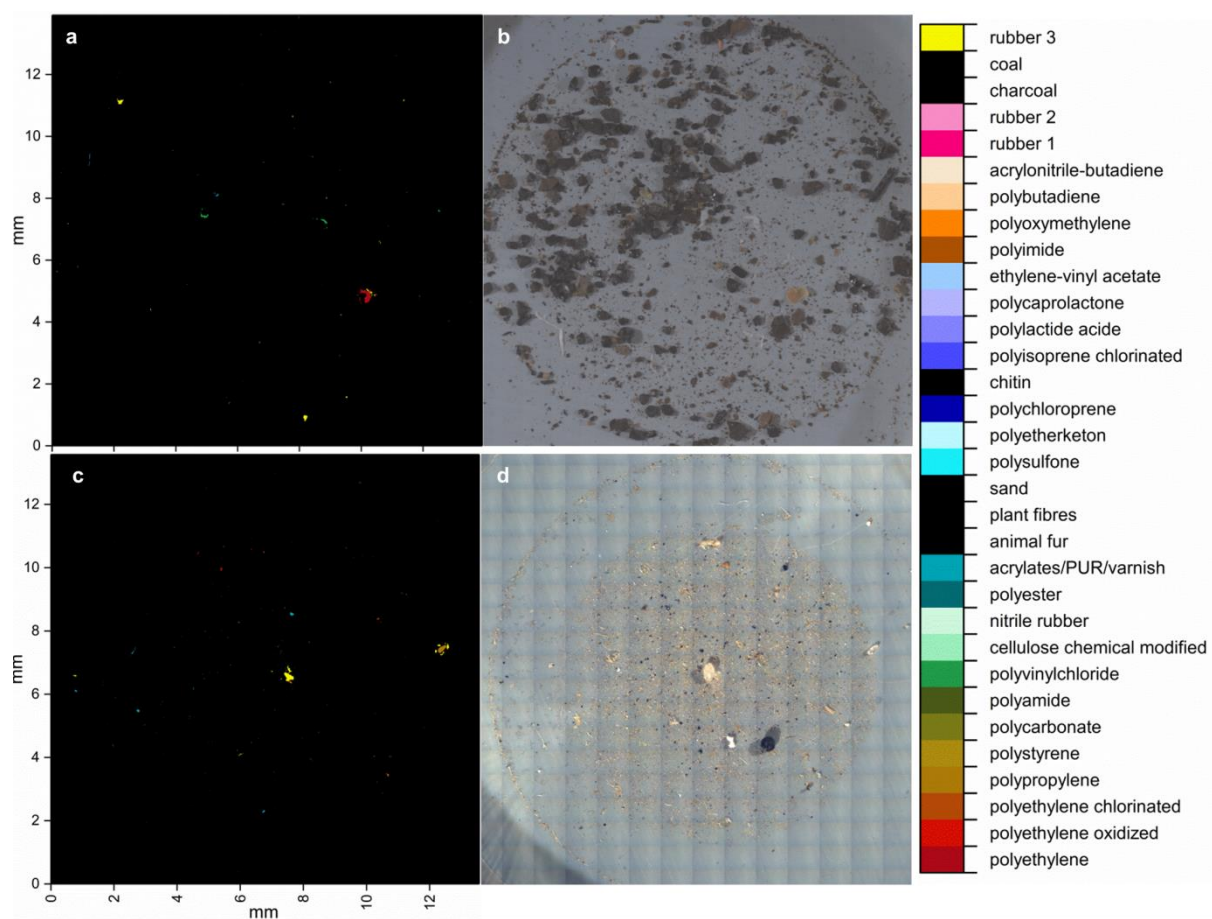


Table S4: Number of microplastic (MP) particles per station in sediments (MP concentration in particles per kg dry weight and abundance in particles per m²) and surface waters (MP concentration in particles per m³ and L and abundance in particles per m² and km²).

Station	Distance to coast	Latitude	Longitude	Elevation	Sediment dry weight	MP concentration	MP abundance	MP surface water	Sampled area	MP concentration	MP concentration	MP abundance	MP abundance
He430	km	N	E	m	kg	particles kg ⁻¹	particles m ⁻²	m ³	km ²	particles m ⁻³	particles L ⁻¹	particles m ⁻²	particles km ⁻²
1	6.7	53.82333	7.72050	-12	1.533	271.42	922.84	36.72	3.67E-04	5.34	0.01	0.53	5.34E+05
2	6	53.77683	7.28433	-14	1.606	288.87	982.15	40.50	4.05E-04	25.17	0.03	2.51	2.51E+06
3	6.4	53.74767	6.99833	-9	1.558	309.60	1052.63	46.20	4.62E-04	6.21	0.01	0.62	6.21E+05
4	5.4	53.71167	6.64433	-13	1.693	119.16	405.15	44.46	4.45E-04	22.85	0.02	2.28	2.28E+06
5	7.5	53.65417	6.27967	-18	1.630	217.27	738.70	20.30	2.03E-04	8.44	0.01	0.84	8.45E+05
6	7.6	53.59850	5.92233	-19	1.498	318.40	1082.57	35.09	3.51E-04	58.56	0.06	5.86	5.86E+06
7	5.3	53.55667	5.63150	-20	1.410	98.49	334.86	24.60	2.46E-04	7.89	0.01	0.79	7.88E+05
8	6.3	53.46467	5.20933	-17	1.595	120.51	409.73	34.89	3.49E-04	11.58	0.01	1.16	1.16E+06
9	8	53.31267	4.80217	-15	1.615	38.72	131.66	40.97	4.10E-04	3.51	0.00	0.35	3.51E+05
10	6.7	53.11083	4.56133	-22	1.592	539.41	1833.98	35.60	3.56E-04	3.33	0.00	0.33	3.33E+05
11	8	52.85950	4.40400	-18	1.670	2.79	9.50	28.22	2.82E-04	2.81	0.00	0.28	2.81E+05
12	7.1	52.41783	4.33083	-16	1.629	255.44	868.50	16.98	1.70E-04	n.a.	n.a.	n.a.	n.a.
13	6.8	52.13800	3.97617	-18	1.564	140.45	477.51	24.41	2.44E-04	0.31	0.00	0.03	3.08E+04
14	6.5	51.85083	3.52867	-19	1.561	33.56	114.11	15.51	1.55E-04	63.19	0.06	6.32	6.32E+06
15	8.4	51.52717	3.15000	-19	1.658	77.06	262.01	40.46	4.05E-04	0.24	0.00	0.02	2.37E+04
16	8	51.24417	2.45467	-23	1.474	22.24	75.62	22.55	2.25E-04	8.90	0.01	0.89	8.90E+05
17	8.5	51.06150	1.84483	-27	n.a.	n.a.	n.a.	39.11	3.91E-04	16.43	0.02	1.64	1.64E+06
18	14.5	50.46783	1.15117	-17	1.605	88.69	301.53	34.52	3.45E-04	5.32	0.01	0.53	5.32E+05
19	28	51.52167	2.43233	-37	1.631	106.47	362.00	32.89	3.29E-04	0.49	0.00	0.05	4.93E+04
20	38	52.18650	2.88467	-35	1.770	149.62	508.71	36.10	3.61E-04	245.37	0.25	24.51	2.45E+07
21	52	53.03633	3.23117	-29	1.553	137.31	466.85	51.30	5.13E-04	21.82	0.02	2.18	2.18E+06
22	67	53.96900	3.18733	-33	1.765	628.92	2138.34	46.76	4.68E-04	0.06	0.00	0.01	6.42E+03
23	104	54.86817	3.40917	-37	1.309	1188.80	4041.92	49.60	4.96E-04	101.85	0.10	10.18	1.02E+07
24	156	55.81183	3.64033	-49	1.636	239.90	815.65	31.70	3.17E-04	5.11	0.01	0.51	5.11E+05
					Mean	234.48	797.24	34.56	3.46E-04	27.16	0.03	2.72	2.72E+06
					SD	254.28	864.56	9.79	9.80E-05	52.52	0.05	5.25	5.25E+06
					Min	2.79	9.50	15.51	1.55E-04	0.06	0.00	0.01	6.42E+03
					Max	1188.80	4041.92	51.30	5.13E-04	245.37	0.25	24.51	2.45E+07

Supplement Chapter I

Table S5: PERMANOVA for 46 samples (23 sediment, 23 surface water) based on Hellinger distance resemblance matrix and square root transformed relative abundance data of polymer types.

d.F.: degrees of freedom, SS: sums of squares, MS: mean squares

¹ Significant results ($P(\text{perm}) < 0.001$) are highlighted in bold. P-values were obtained by using Type I sums of squares and 999 permutations.

Sources of variation	d.F.	SS	MS	Pseudo-F	$P(\text{perm})^1$	Sq.root
Sample type	1	1.4354	1.4354	4.4493	0.001	0.21996
Residuals	44	14.195	0.32261			0.56799
Total	45	15.63				

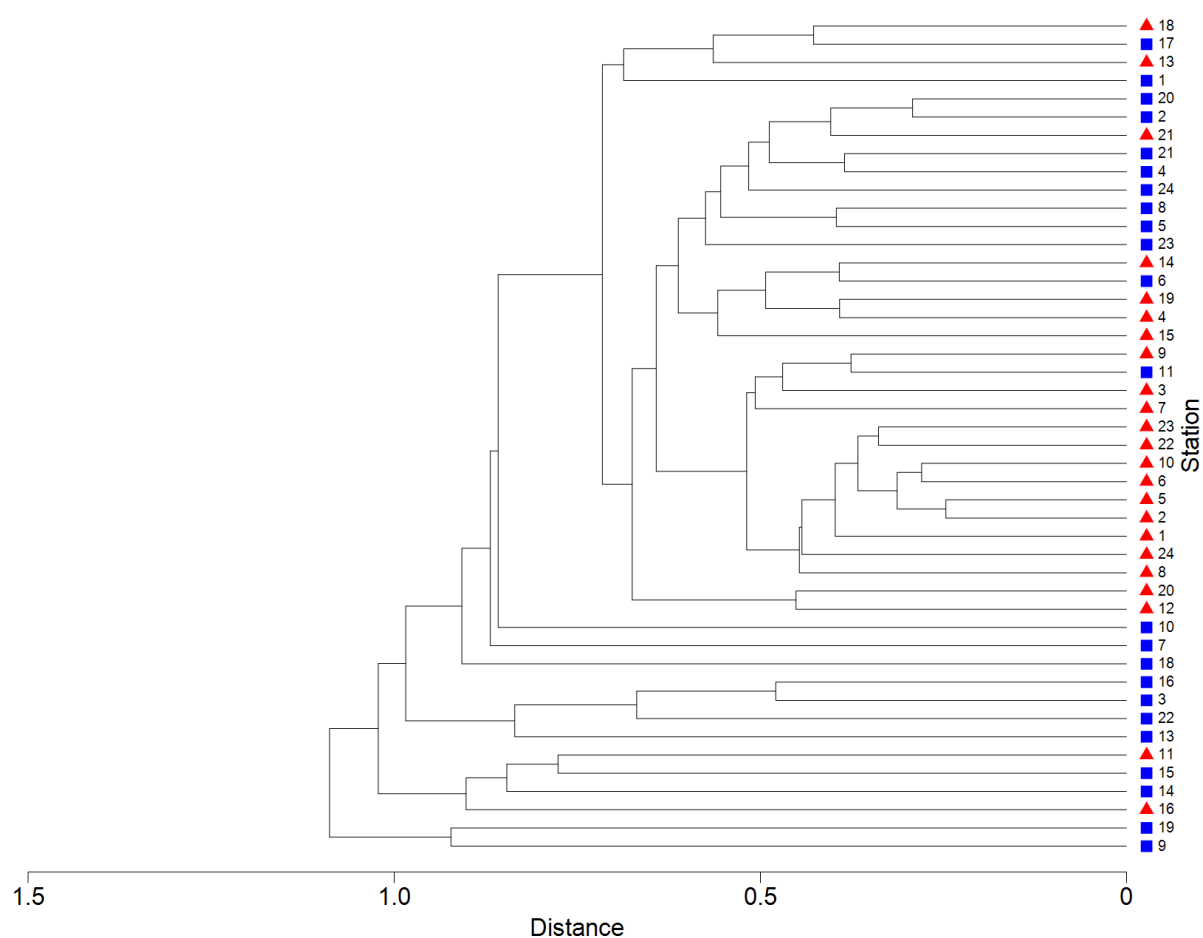


Figure S5: Cluster analysis of square root transformed relative abundances of polymer types based on Hellinger distance resemblance matrix and group average. Red triangles depict sediment samples and blue squares depict surface water samples.

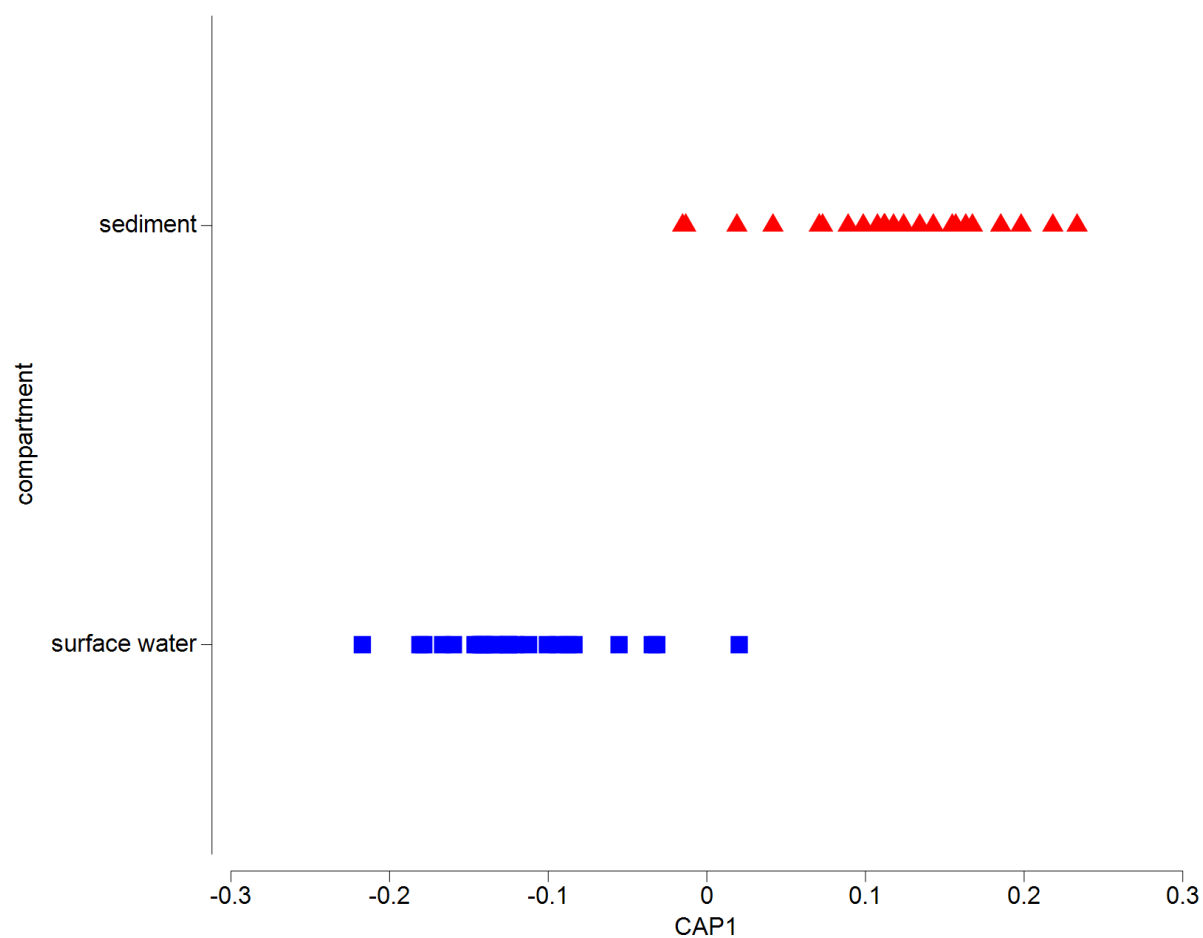


Figure S6: Canonical analysis of principal coordinates (CAP) on polymer types with separation of two a priori groups (sediment and surface water). Analysis is based on Hellinger distances calculated from square root transformed relative abundances of polymer types with correlation values of $\delta=0.891$ using $m=14$ principal coordinate axes. Red triangles refer to sediment samples and blue squares refer to surface water samples.

Supplement Chapter I

Table S6: ANOVA for polymer richness and diversity based on Shannon-Wiener index H' .

Variable	Unit	Average Sediment (S)	Average Surface water (W)	Intercept	Factor	Error	Total
Richness	N	11.0	7.2	SS	3816.5	164.5	589.9
				MS	3816.5	164.5	13.4
				F	284.7	12.3	
				p	0.000	0.001	
Shannon- Wiener index H'	-	1.830	1.332	SS	115.0	2.8	10.1
				MS	115.0	2.8	0.2
				F	500.6	12.4	
				p	0.000	0.001	

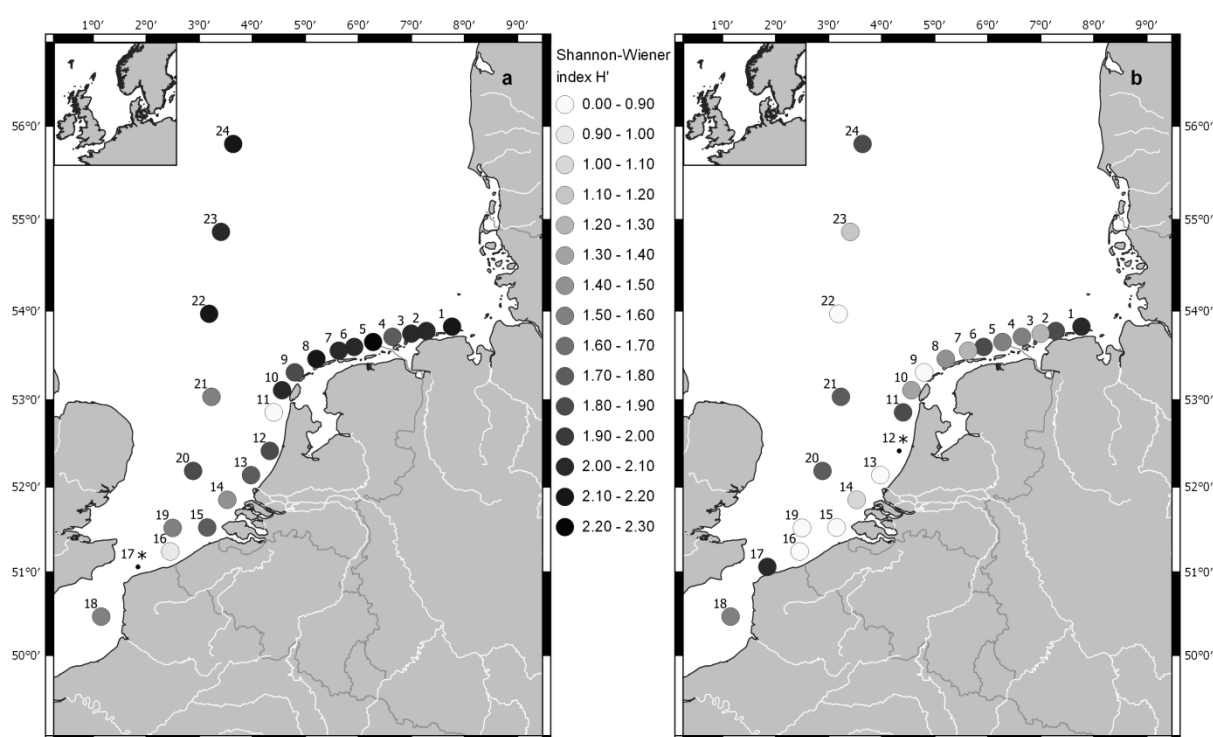


Figure S7: Spatial distribution of the polymer diversity based on Shannon-Wiener index H' . Stations where no sample was analyzed are marked with *.

Supplement Chapter I

Table S7: ANOVA for individual polymer types, ¹ unit: arcsine-square root (%)

Polymer	Average ¹			Intercept	Factor	Error	Total
	sediment (s)	surface water (w)			(w/s)		
PE	0.167	0.313	SS	2.649	0.243	1.464	1.707
			MS	2.649	0.243	0.033	
			F	79.622	7.298		
			p	0.000	0.010		
PE oxidized	0.012	0.034	SS	0.024	0.006	0.324	0.329
			MS	0.024	0.006	0.007	
			F	3.263	0.763		
			p	0.078	0.387		
PE chlorinated	0.194	0.161	SS	1.451	0.013	1.285	1.297
			MS	1.451	0.013	0.029	
			F	49.711	0.440		
			p	0.000	0.510		
PP	0.319	0.471	SS	7.184	0.268	2.693	2.961
			MS	7.184	0.268	0.061	
			F	117.368	4.376		
			p	0.000	0.042		
PS	0.100	0.051	SS	0.263	0.027	0.391	0.418
			MS	0.263	0.027	0.009	
			F	29.613	3.030		
			p	0.000	0.089		
PC	0.003	0.003	SS	0.001	0.000	0.012	0.012
			MS	0.001	0.000	0.000	
			F	1.999	0.001		
			p	0.164	0.973		
PA	0.258	0.238	SS	2.824	0.005	2.638	2.643
			MS	2.824	0.005	0.060	
			F	47.103	0.080		
			p	0.000	0.779		
PVC	0.281	0.135	SS	1.987	0.243	1.338	1.581
			MS	1.987	0.243	0.030	
			F	65.348	8.002		
			p	0.000	0.007		
CMC	0.043	0.034	SS	0.068	0.001	0.761	0.762
			MS	0.068	0.001	0.017	
			F	3.958	0.049		
			p	0.053	0.827		
nitrile rubber	0.072	0.003	SS	0.066	0.055	0.190	0.245
			MS	0.066	0.055	0.004	
			F	15.252	12.715		
			p	0.000	0.001		
PEST	0.301	0.233	SS	3.272	0.053	1.848	1.900
			MS	3.272	0.053	0.042	
			F	77.911	1.254		
			p	0.000	0.269		
acrylates/PUR/ varnish	0.448	0.357	SS	7.457	0.096	3.760	3.856
			MS	7.457	0.096	0.085	
			F	87.268	1.129		
			p	0.000	0.294		

Supplement Chapter I

Table S7 continued

PSU	0.004	0.000	SS	0.000	0.000	0.007	0.007
			MS	0.000	0.000	0.000	
			F	1.000	1.000		
			p	0.323	0.323		
polychloroprene	0.245	0.003	SS	0.704	0.672	1.517	2.189
			MS	0.704	0.672	0.034	
			F	20.419	19.494		
			p	0.000	0.000		
polyisoprene chlorinated	0.005	0.000	SS	0.000	0.000	0.011	0.011
			MS	0.000	0.000	0.000	
			F	1.000	1.000		
			p	0.323	0.323		
polycaprolactone	0.038	0.035	SS	0.062	0.000	0.164	0.164
			MS	0.062	0.000	0.004	
			F	16.534	0.023		
			p	0.000	0.881		
EVA	0.038	0.021	SS	0.040	0.003	0.169	0.172
			MS	0.040	0.003	0.004	
			F	10.431	0.891		
			p	0.002	0.350		
POM	0.119	0.007	SS	0.185	0.144	0.243	0.387
			MS	0.185	0.144	0.006	
			F	33.547	26.108		
			p	0.000	0.000		
acrylonitrile- butadiene	0.005	0.000	SS	0.000	0.000	0.011	0.011
			MS	0.000	0.000	0.000	
			F	1.000	1.000		
			p	0.323	0.323		
rubber type 1	0.017	0.020	SS	0.016	0.000	0.077	0.077
			MS	0.016	0.000	0.002	
			F	8.960	0.088		
			p	0.005	0.768		
rubber type 2	0.000	0.010	SS	0.001	0.001	0.017	0.018
			MS	0.001	0.001	0.000	
			F	2.713	2.713		
			p	0.107	0.107		
rubber type 3	0.253	0.222	SS	2.594	0.011	1.916	1.927
			MS	2.594	0.011	0.044	
			F	59.552	0.249		
			p	0.000	0.620		

Supplement Chapter I

Table S8: PERMANOVA for 46 samples (23 sediment, 23 surface water) based on Hellinger distance resemblance matrix and square root transformed relative abundance data of size classes.

d.F.: degrees of freedom, SS: sums of squares, MS: mean squares

¹ Significant results (P (perm) <0.001) are highlighted in bold. P-values were obtained by using Type I sums of squares and 999 permutations.

Sources of variation	d.F.	SS	MS	Pseudo-F	P(perm) ¹	Sq.root
Sample type	1	0.966	0.966	4.120	0.001	0.178
Residuals	44	10.318	0.235			0.484
Total	45	11.284				

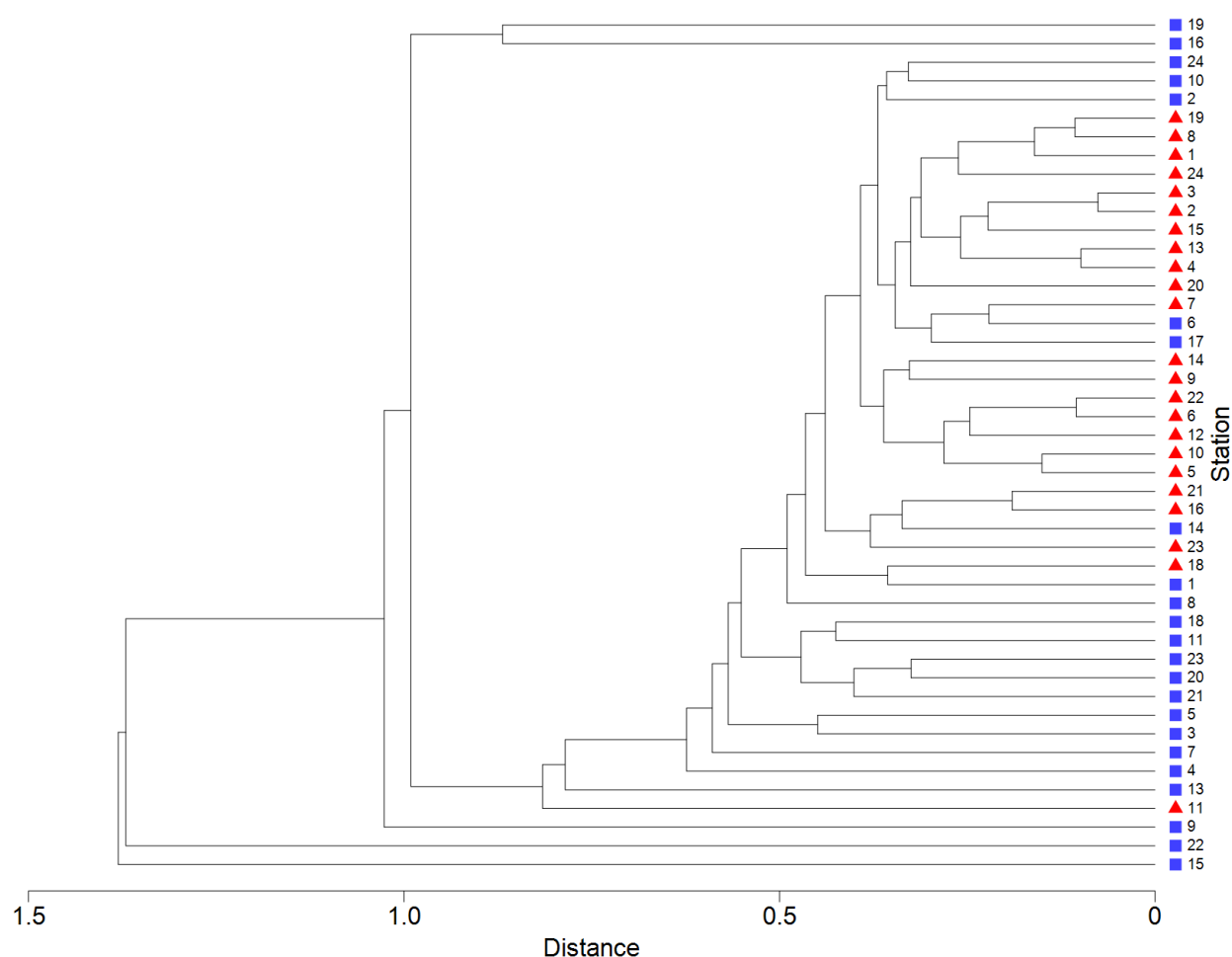


Figure S8: Cluster analysis of square root transformed relative abundances of size classes based on Hellinger distance resemblance matrix and group average. Red triangles depict sediment samples and blue squares depict surface water samples.

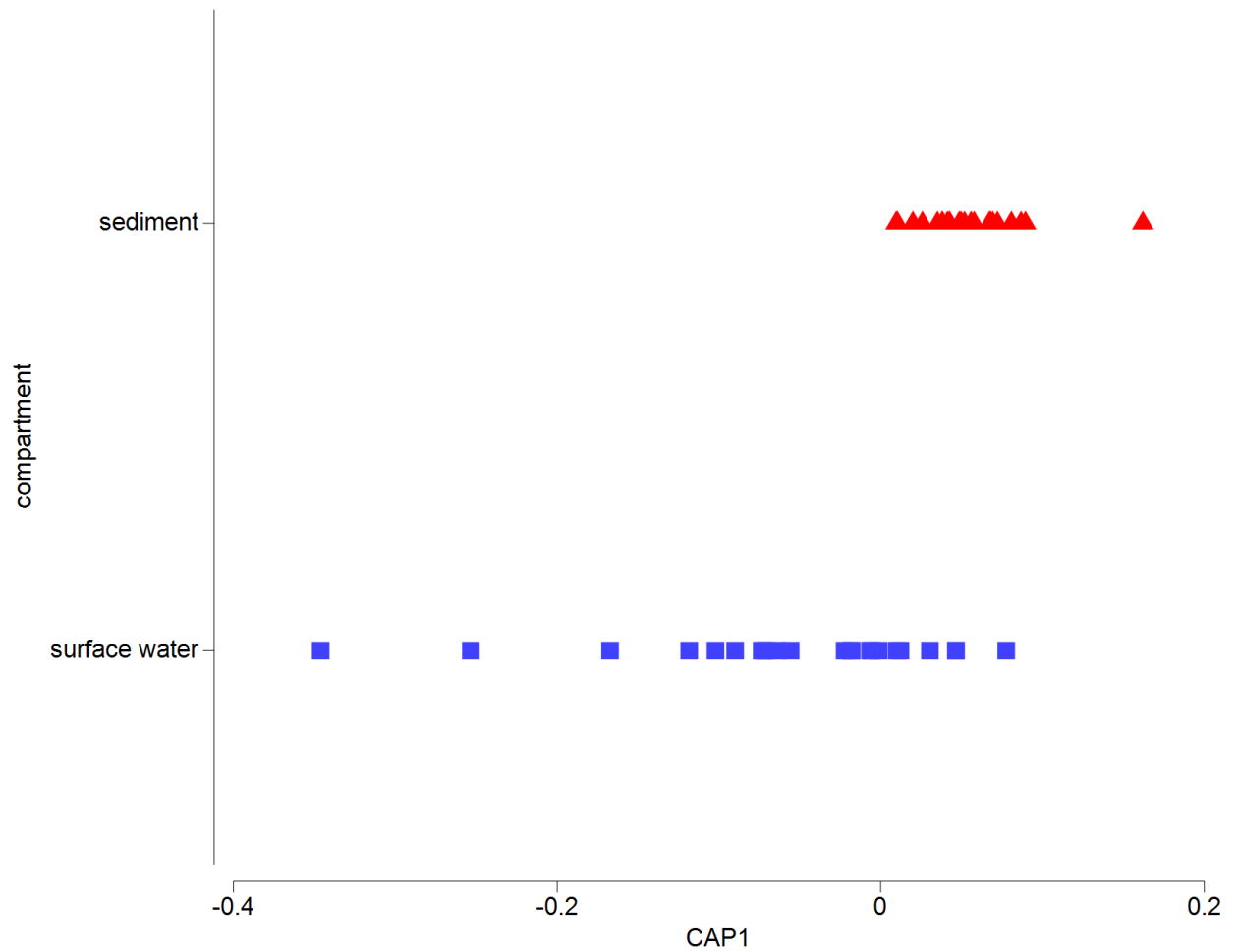


Figure S9: Canonical analysis of principal coordinates (CAP) on size classes with separation of two a priori groups (sediment and surface water). Analysis is based on Hellinger distances calculated from square root transformed size class abundance data with correlation values of $\delta=0.61$ using $m=5$ principal coordinate axes. Red triangles refer to sediment samples and blue squares refer to surface water samples.

Supplement Chapter I

Table S9: ANOVA for individual size classes

¹ unit: arcsine-square root (%)

Size class µm	Average ¹			Intercept	Factor (w/s)	Error	Total
	sediment (s)	surface water (w)					
11	0.691	0.655	SS	20.834	0.015	3.550	3.565
			MS	20.834	0.015	0.081	
			F	258.211	0.181		
			p	0.000	0.673		
11–25	0.511	0.478	SS	11.247	0.013	2.224	2.236
			MS	11.247	0.013	0.051	
			F	222.548	0.249		
			p	0.000	0.620		
25–50	0.456	0.333	SS	7.153	0.173	0.976	1.149
			MS	7.153	0.173	0.022	
			F	322.542	7.799		
			p	0.000	0.008		
50–75	0.281	0.161	SS	2.242	0.166	0.927	1.093
			MS	2.242	0.166	0.021	
			F	106.420	7.899		
			p	0.000	0.007		
75–100	0.123	0.110	SS	0.626	0.002	0.427	0.429
			MS	0.626	0.002	0.010	
			F	64.456	0.186		
			p	0.000	0.669		
100–125	0.070	0.045	SS	0.154	0.007	0.235	0.242
			MS	0.154	0.007	0.005	
			F	28.838	1.321		
			p	0.000	0.257		
125–150	0.073	0.066	SS	0.223	0.001	0.334	0.335
			MS	0.223	0.001	0.008	
			F	29.326	0.088		
			p	0.000	0.768		
150–175	0.020	0.099	SS	0.164	0.071	2.427	2.498
			MS	0.164	0.071	0.055	
			F	2.968	1.281		
			p	0.092	0.264		
175–200	0.008	0.012	SS	0.004	0.000	0.039	0.039
			MS	0.004	0.000	0.001	
			F	4.919	0.178		
			p	0.032	0.676		
200–225	0.003	0.007	SS	0.001	0.000	0.013	0.014
			MS	0.001	0.000	0.000	
			F	3.981	0.713		
			p	0.052	0.403		
225–250	0.011	0.006	SS	0.003	0.000	0.039	0.039
			MS	0.003	0.000	0.001	
			F	3.657	0.336		
			p	0.062	0.565		

Supplement Chapter I

Table S9 continued

250–275	0.005	0.010	SS	0.003	0.000	0.032	0.032
			MS	0.003	0.000	0.001	
			F	3.890	0.433		
			p	0.055	0.514		
275–300	0.006	0.000	SS	0.000	0.000	0.010	0.010
			MS	0.000	0.000	0.000	
			F	2.086	2.086		
			p	0.156	0.156		
300–325	0.000	0.003	SS	0.000	0.000	0.005	0.006
			MS	0.000	0.000	0.000	
			F	1.000	1.000		
			p	0.323	0.323		
325–350	0.000	0.010	SS	0.001	0.001	0.025	0.026
			MS	0.001	0.001	0.001	
			F	1.887	1.887		
			p	0.176	0.176		
375–400	0.000	0.005	SS	0.000	0.000	0.011	0.011
			MS	0.000	0.000	0.000	
			F	1.000	1.000		
			p	0.323	0.323		
425–450	0.000	0.004	SS	0.000	0.000	0.006	0.006
			MS	0.000	0.000	0.000	
			F	1.524	1.524		
			p	0.224	0.224		
500–1000	0.000	0.013	SS	0.002	0.002	0.017	0.019
			MS	0.002	0.002	0.000	
			F	4.936	4.936		
			p	0.031	0.031		
1000–1500	0.000	0.053	SS	0.032	0.032	0.361	0.394
			MS	0.032	0.032	0.008	
			F	3.947	3.947		
			p	0.053	0.053		
1500–2000	0.000	0.046	SS	0.024	0.024	0.361	0.386
			MS	0.024	0.024	0.008	
			F	2.970	2.970		
			p	0.092	0.092		
2000–2500	0.000	0.057	SS	0.037	0.037	0.358	0.396
			MS	0.037	0.037	0.008	
			F	4.589	4.589		
			p	0.038	0.038		
2500–3000	0.000	0.026	SS	0.008	0.008	0.037	0.045
			MS	0.008	0.008	0.001	
			F	9.045	9.045		
			p	0.004	0.004		

Supplement Chapter I

Table S9 continued

3000–3500	0.001	0.012	SS	0.002	0.001	0.014	0.015
			MS	0.002	0.001	0.000	
			F	6.298	3.787		
			p	0.016	0.058		
3500–4000	0.000	0.004	SS	0.000	0.000	0.005	0.006
			MS	0.000	0.000	0.000	
			F	1.416	1.416		
			p	0.240	0.240		
4000–4500	0.000	0.023	SS	0.006	0.006	0.074	0.080
			MS	0.006	0.006	0.002	
			F	3.492	3.492		
			p	0.068	0.068		
4500–5000	0.004	0.016	SS	0.005	0.002	0.033	0.035
			MS	0.005	0.002	0.001	
			F	6.166	2.498		
			p	0.017	0.121		

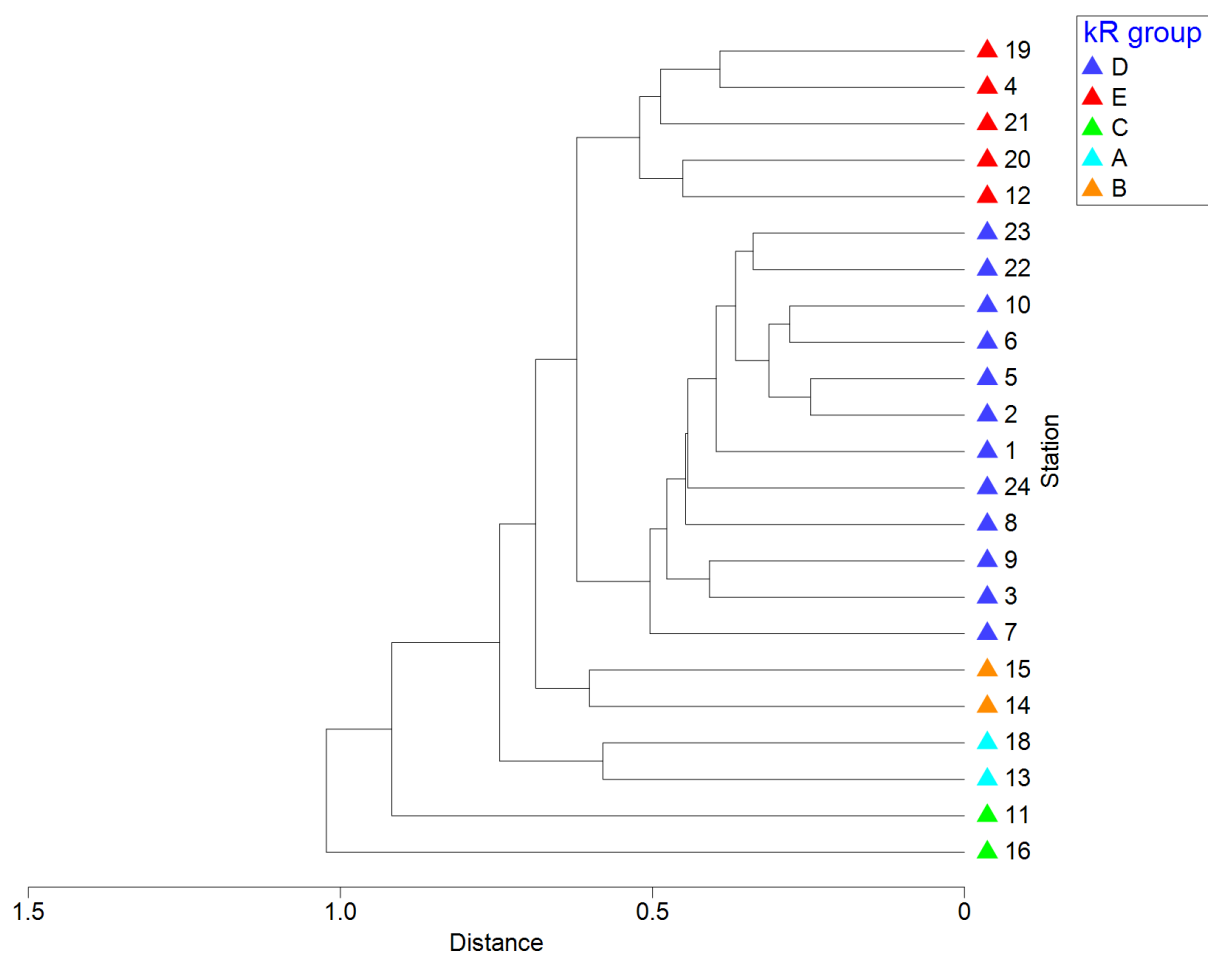


Figure S10: Cluster analysis of sediment samples based on Hellinger distance resemblance matrix of square root transformed relative abundances of polymer types. Triangles of different colors in the legend represent the five different groups (A–E) defined via kR-clustering.

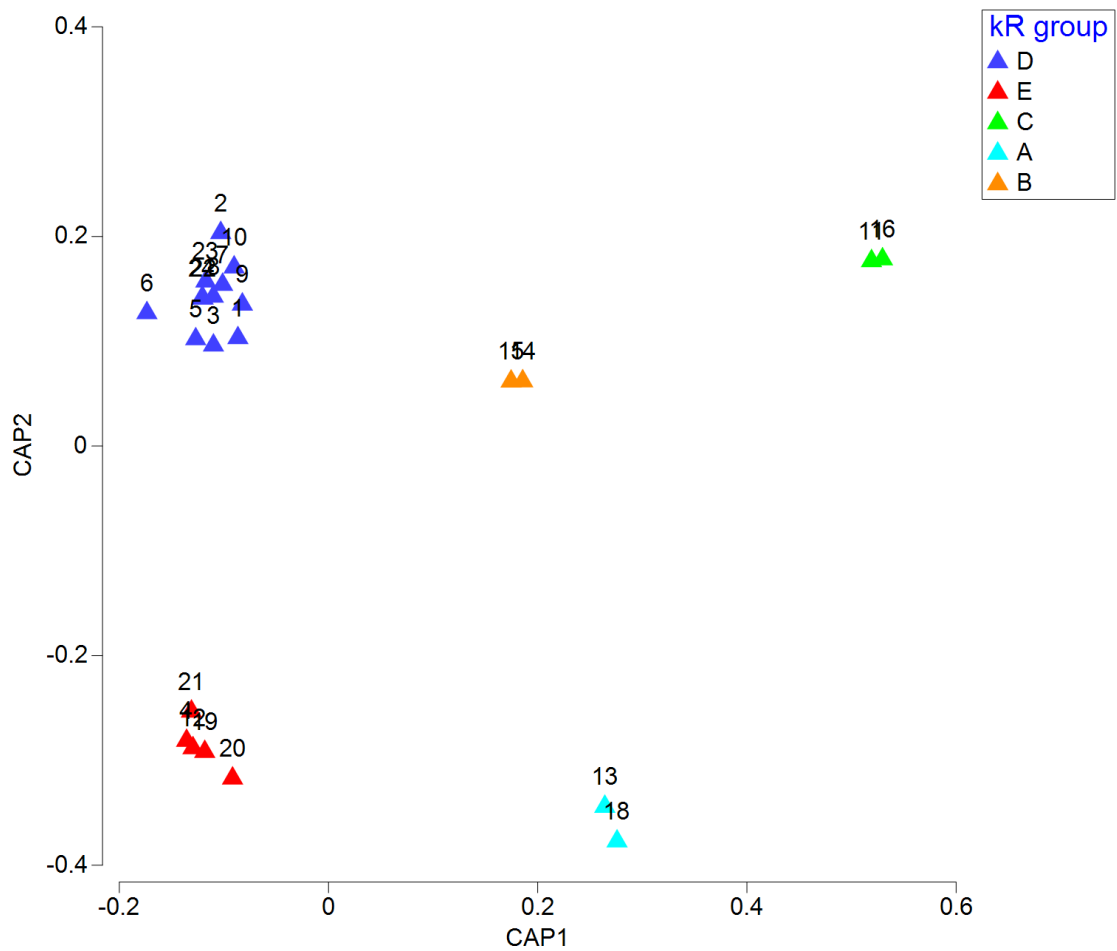


Figure S11: Canonical analysis of principal coordinates (CAP). Separation of five a priori groups (A–E, triangles of different colors in the legend) based on kR-clustering of Hellinger distances calculated from square root transformed relative abundances of polymer types for sediment samples with correlation values of $\delta_1=0.996$, $\delta_2=0.993$, $\delta_3=0.985$, and $\delta_4=0.931$, using $m=17$ principal coordinate axes.

Table S10: ANOVA and post-hoc Tukey HSD test on polymer composition in sediment samples. Polymers, which were not present or had no variance were not considered: polysulfone, polyisoprene chlorinated, acrylonitrile-butadiene, and rubber type 2.

¹ unit: arcsine-square root (%)

Polymer	Average ¹ kR group					Intercept ¹ kR group		Factor ¹ kR group	Error	Total	Tukey HSD test kR group				
	D	E	C	A	B						D	E	C	A	B
PE					SS	0.314	0.070	0.128	0.197		D				
					MS	0.314	0.017	0.007			E				
	0.182	0.177	0.000	0.239	F	44.322	2.456				C				
					p	0.000	0.083				A				
PE oxidized					SS	0.001	0.001	0.021	0.023		D				
					MS	0.001	0.000	0.001			E				
	0.014	0.021	0.000	0.000	F	0.576	0.277				C				
					p	0.458	0.889				A				
PE chlorinated					SS	0.236	0.173	0.187	0.360		D				
					MS	0.236	0.043	0.010			E				
	0.267	0.168	0.000	0.107	F	22.646	4.156				C				
					p	0.000	0.015				A				
PP					SS	1.236	0.070	0.399	0.469		D				
					MS	1.236	0.017	0.022			E				
	0.316	0.402	0.194	0.291	F	55.773	0.789				C				
					p	0.000	0.547				A				
PS					SS	0.102	0.031	0.142	0.173		D				
					MS	0.102	0.008	0.008			E				
	0.117	0.091	0.000	0.150	F	12.957	0.970				C				
					p	0.002	0.448				A				
PC					SS	0.000	0.000	0.006	0.006		D				
					MS	0.000	0.000	0.000			E				
	0.007	0.000	0.000	0.000	F	0.076	0.196				C				
					p	0.785	0.937				A				

Table S10 continued

PA	SS	0.438	0.438	0.683	0.305	0.988	D	0.007	0.007	0.001	0.003	0.002
	MS	0.438	0.171	0.017			E					
	F	25.821	10.058				C	0.001	0.001			
	p	0.000	0.000	0.000			A	0.003	0.003			
							B	0.002	0.002			
PVC	SS	0.665	0.171	0.467	0.638		D					
	MS	0.665	0.043	0.026			E					
	F	25.633	1.647				C					
	p	0.000	0.206				A					
							B					
CMC	SS	0.136	0.443	0.136	0.580		D	0.000	0.000			
	MS	0.136	0.111	0.008			E	0.000	0.000			
	F	17.992	14.648				C	0.000	0.000			
	p	0.000	0.000	0.000			A	0.000	0.000	0.000	0.000	
							B	0.000	0.000			
nitrile rubber	SS	0.094	0.038	0.146	0.185		D					
	MS	0.094	0.010	0.008			E					
	F	11.623	1.183				C					
	p	0.003	0.352				A					
							B					
PEST	SS	1.354	0.051	0.550	0.602		D					
	MS	1.354	0.013	0.031			E					
	F	44.290	0.420				C					
	p	0.000	0.792				A					
							B					
acrylates/PUR/varnish	SS	4.224	0.620	0.157	0.777		D	0.000	0.000			
	MS	4.224	0.155	0.009			E	0.000	0.000			
	F	484.661	17.775				C	0.000	0.000	0.001	0.004	
	p	0.000	0.000				A	0.001	0.001			
							B	0.004	0.004			
polychloroprene	SS	0.123	1.261	0.252	1.513		D	0.000	0.001	0.001	0.001	0.001
	MS	0.123	0.315	0.014			E	0.000	0.000			
	F	8.814	22.552				C	0.001	0.001			
	p	0.008	0.000				A	0.001	0.001			
							B	0.001	0.001			

Table S10 continued

polycaprolactone	SS	0.006	0.015	0.050	0.066	D
	MS	0.006	0.004	0.003		E
	F	2.175	1.381			C
	p	0.158	0.280			A
						B
EVA	SS	0.019	0.015	0.079	0.094	D
	MS	0.019	0.004	0.004		E
	F	4.268	0.849			C
	p	0.054	0.512			A
						B
POM	SS	0.337	0.053	0.176	0.229	D
	MS	0.337	0.013	0.010		E
	F	34.396	1.358			C
	p	0.000	0.288			A
						B
rubber type 1	SS	0.005	0.005	0.021	0.025	D
	MS	0.005	0.001	0.001		E
	F	4.136	0.992			C
	p	0.057	0.437			A
						B
rubber type 3	SS	0.824	0.619	0.178	0.798	D
	MS	0.824	0.155	0.010		E
	F	83.065	15.619			C
	p	0.000	0.000			A
						B
						0.015 0.007
						0.015 0.007
						0.002 0.000
						0.002 0.001
						0.002 0.000 0.001

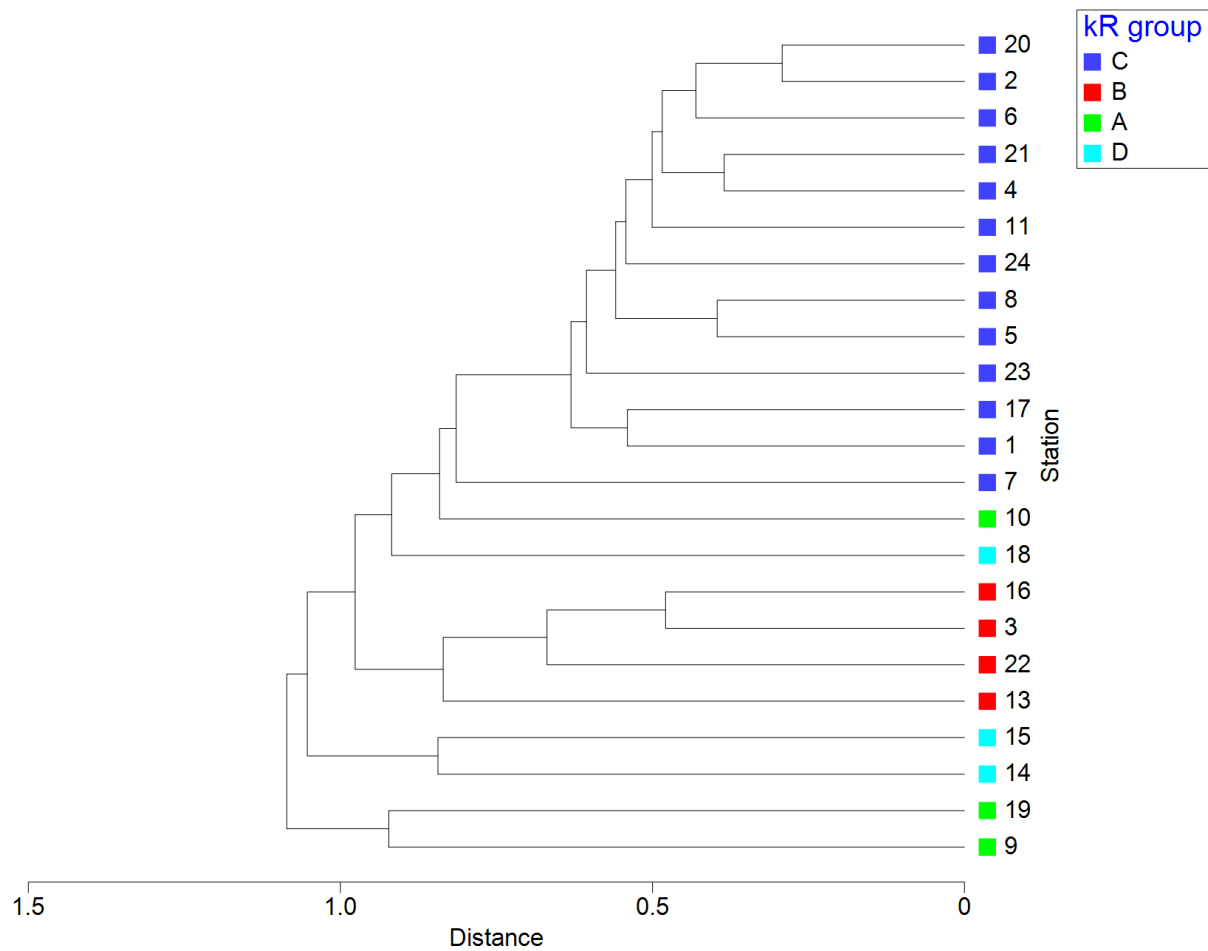


Figure S12: Cluster analysis of surface water samples based on Hellinger distance resemblance matrix of square root transformed relative abundances of polymer types. Triangles of different colors in the legend represent the four different groups (A–D) defined via kR-clustering.

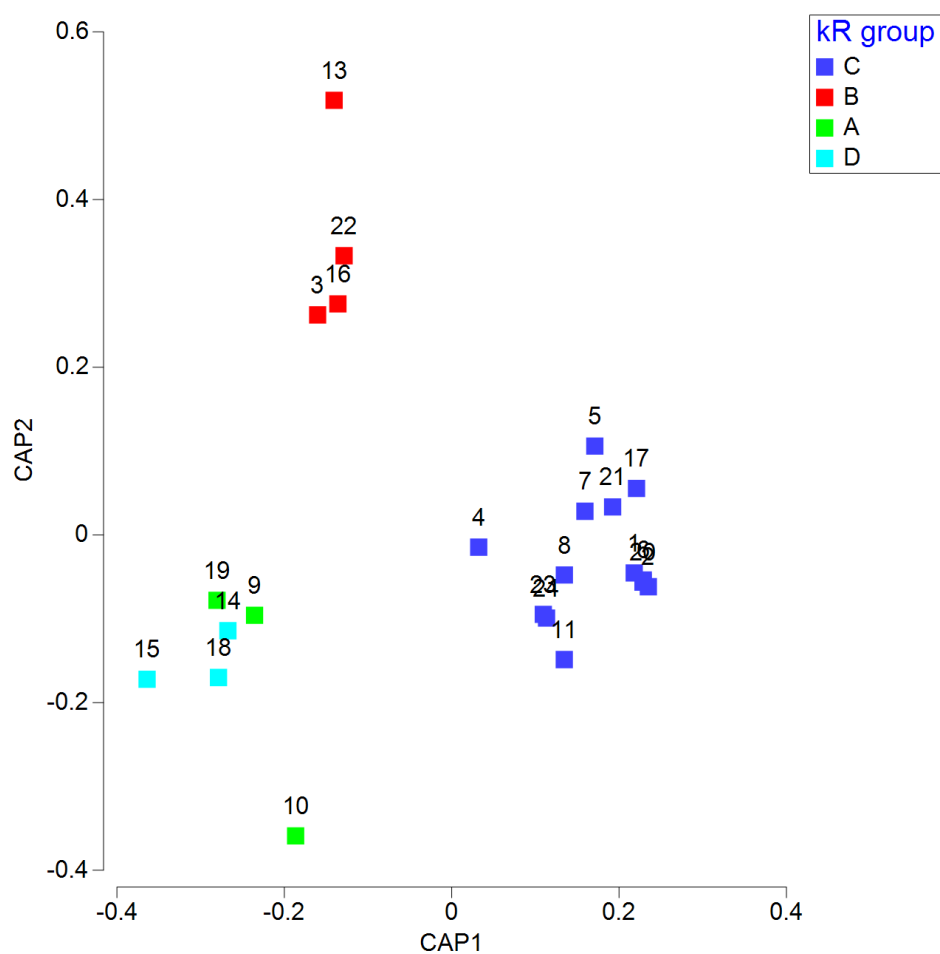


Figure S13: Canonical analysis of principal coordinates (CAP). Separation of four a priori groups (A–D, triangles of different colors in the legend) based on kR-clustering of Hellinger distances calculated from square root transformed relative abundances of polymer types for surface water samples with correlation values of $\delta_1=0.970$, $\delta_2=0.901$, and $\delta_3=0.811$, using $m=5$ principal coordinate axes.

Table S11: ANOVA and post-hoc Tukey HSD test on polymer composition in surface water samples. Polymers which were not present or had no variance were not considered: polysulfone, polyisoprene chlorinated, and acrylonitrile-butadiene.

¹ unit: arcsine-square root (%)

Polymer	Average ¹ kR group				Intercept	Factor	Error	Total	Tukey HSD test kR group			
	C	B	A	D		kR group			C	B	A	D
PE				SS	2.248	0.442	0.825	1.267	C			
				MS	2.248	0.147	0.043		B		0.037	
	0.356	0.472	0.000	F	51.799	3.395			A	0.037		
				p	0.000	0.039			D			
PE oxidized				SS	0.026	0.020	0.281	0.301	C			
				MS	0.026	0.007	0.015		B			
	0.060	0.000	0.000	F	1.789	0.459			A			
				p	0.197	0.714			D			
PE chlorinated				SS	0.595	0.372	0.552	0.924	C			
				MS	0.595	0.124	0.029		B		0.027	
	0.191	0.000	0.405	F	20.481	4.261			A	0.027		0.041
				p	0.000	0.018			D		0.041	
PP				SS	5.113	0.680	1.544	2.224	C			
				MS	5.113	0.227	0.081		B			
	0.396	0.561	0.867	F	62.922	2.791			A			
				p	0.000	0.068			D			
PS				SS	0.061	0.029	0.189	0.218	C			
				MS	0.061	0.010	0.010		B			
	0.042	0.015	0.056	F	6.116	0.973			A			
				p	0.023	0.426			D			
PC				SS	0.000	0.000	0.005	0.005	C			
				MS	0.000	0.000	0.000		B			
	0.006	0.000	0.000	F	0.895	0.229			A			
				p	0.356	0.875			D			
PA				SS	1.298	0.439	1.211	1.650	C			
				MS	1.298	0.146	0.064		B			
	0.350	0.000	0.175	F	20.366	2.296			A			
				p	0.000	0.110			D			

Table S11 continued

PVC	SS	0.420	0.265	0.435	0.700	C	
	MS	0.420	0.088	0.023		B	0.037
	F	18.353	3.862			A	0.040
	p	0.000	0.026			D	0.037 0.040
CMC	SS	0.027	0.021	0.160	0.181	C	
	MS	0.027	0.007	0.008		B	
	F	3.204	0.822			A	
	p	0.089	0.498			D	
nitrile rubber	SS	0.000	0.000	0.005	0.005	C	
	MS	0.000	0.000	0.000		B	
	F	0.895	0.229			A	
	p	0.356	0.875			D	
PEST	SS	1.247	0.949	0.297	1.246	C	0.000
	MS	1.247	0.316	0.016		B	0.000
	F	79.691	20.205			A	0.000
	p	0.000	0.000			D	0.000
acrylates/PUR/ varnish	SS	2.928	1.053	1.930	2.983	C	
	MS	2.928	0.351	0.102		B	0.029
	F	28.829	3.455			A	
	p	0.000	0.037			D	0.029
polychloroprene	SS	0.000	0.000	0.004	0.004	C	
	MS	0.000	0.000	0.000		B	
	F	0.895	0.229			A	
	p	0.356	0.875			D	
polycaprolactone	SS	0.029	0.022	0.076	0.098	C	
	MS	0.029	0.007	0.004		B	
	F	7.135	1.829			A	
	p	0.015	0.176			D	
EVA	SS	0.010	0.015	0.059	0.074	C	
	MS	0.010	0.005	0.003		B	
	F	3.210	1.607			A	
	p	0.089	0.221			D	
POM	SS	0.001	0.001	0.013	0.014	C	
	MS	0.001	0.000	0.001		B	
	F	1.920	0.492			A	
	p	0.182	0.692			D	

Table S11 continued

rubber type 1						SS	0.009	0.007	0.045	0.052	C
						MS	0.009	0.002	0.002		B
		0.036	0.000	0.000	0.000	F	4.037	1.035			A
						p	0.059	0.399			D
rubber type 2						SS	0.002	0.002	0.016	0.017	C
						MS	0.002	0.001	0.001		B
		0.017	0.000	0.000	0.000	F	2.588	0.664			A
						p	0.124	0.585			D
rubber type 3						SS	1.134	0.873	0.246	1.118	C
						MS	1.134	0.291	0.013		B
		0.393	0.000	0.000	0.000	F	87.688	22.484			A
						p	0.000	0.000			D
											0.000
											0.000
											0.000
											0.000

□

Paragraph S6 on discussion of methodology**Sampling**

For sampling of surface waters the application of nets vs. pumps is a frequently discussed issue (Löder & Gerdt, 2015; Conkle et al., 2018). The advantage of nets is a larger sampling volume which is of advantage when analyzing samples from areas not considered eminent accumulation zones or with unknown status. The disadvantage is that a lower size limit is set already at an early state. A mesh size of 100 μm , as has been used in this study, might provide a good compromise. We acknowledge that in surface water samples MP <100 μm might be underestimated because of the chosen net mesh size. Nevertheless, the detection of a high amount of MP <100 μm confirms the hypotheses that MP are readily entrapped in aggregates when phytoplankton is present, which has been shown by a number of studies (Long et al., 2015; Long et al., 2017; Möhlenkamp et al., 2018). Additionally, the stagnation pressure and clogging of the net after some time will also facilitate entrapping of smaller sized particles. Of course, sampling with (in-situ) pumps would overcome this bias through mesh sizes of nets. On the other hand sampling with nets also allows for sampling of a larger surface area which might present an advantage in regard to the heterogeneous distribution of MP. In this context, the use of a flowmeter was recently recommended to determine the water volume that actually passed through the net and combine this with the width of the net to determine the sampled surface area (Suaria et al., 2016; Maes et al., 2017b; Rivers et al., 2019).

To sample sublittoral sediments, commonly grabs or corers are used (Löder & Gerdt, 2015). When aiming for undisturbed sediment horizons and depth profile, the use of multiple corers is recommended, while grabs enable sampling of larger volumes of the sediment surface (Löder & Gerdt, 2015). Martin et al. (2017) showed that most MP are present in the upper 3.5 ± 0.5 cm of sublittoral sediments and recommended, as more precautionary approach, to sample the upper 5 cm as it has been done in this study with a Van-Veen grab.

For sample storage Kautex bottles, made of PVC with a PE containing lid, have been used, to avoid sample loss, since glass containers would be heavier and are very fragile with regard to freezing and transport. Analyses of blank samples confirmed that there was no considerable introduction of PVC and PE by these.

Sample processing

The MPSS was used because it showed high recovery rates of $95.5 \pm 1.8\%$ (Imhof et al., 2012) and has already been successfully applied in other studies on deep sea sediments (Bergmann et al., 2017) and sediments from a Norwegian fjord (Haave et al., 2019).

During the density separation in separation funnels it was noteworthy that, especially in surface water samples, there was a high concentration of diatom shells. Since these are supposed to float in surface waters, they also float in the ZnCl_2 solution and could only be removed more or less sufficiently by prolonging the density separation to up to seven days. Any method to break them down (e.g. ultrasonication, hydrofluoric acid) would result in disintegration of the MP as well. Therefore, the long lasting density separation was the most reasonable option. An improvement in purification, especially of surface water samples, would increase the aliquoted volume, which would further increase representativeness of the analyzed subsample.

Furthermore, we acknowledge that the lower size limit for processed sediment samples was $20\ \mu\text{m}$, defined by the stainless steel filters used. Contrary to this, the lower size limit for surface water was theoretically $100\ \mu\text{m}$ during sampling and $20\ \mu\text{m}$ during processing. This has to be considered to contribute, at least to a small amount, to the lower numbers of MP in surface water samples when compared to sediments.

Analysis and evaluation

The identification of polymers followed the adaptable database design published by Primpke et al. (2018). Polymers were arranged in 32 clusters based on how good they are to differentiate and only marginally overlaying with each other. Consequently, polymers like polyester (PEST) and polyethylene terephthalate (PET) whose spectra are quite similar have been grouped into one cluster PEST (Primpke et al., 2018). For convenience particles and fibers identified as PEST or PET in the $>500\ \mu\text{m}$ fraction were assigned to PEST as broader term, as well.

Since the significant wave numbers to identify polytetrafluoroethylene (PTFE) lie outside the investigated range (due to IR transparency of Anodiscs (Löder et al., 2015)), PTFE could not be identified in the sample fraction $<500\ \mu\text{m}$. Furthermore, PTFE particles $>500\ \mu\text{m}$ were detected in the procedural blanks. The MPSS contains PTFE in the sealing of the ball valve, which might shed during density separation when moving the ball valve. Consequently, any particles $>500\ \mu\text{m}$ identified as PTFE by ATR-FTIR were excluded from the results.

In terms of time demand for analysis, the use of a 4x objective and without binning instead of 15x objective and 4×4 binning would reach a similar resolution and would reduce the time demand for a measurement by one third (4 h instead of 12 h) (Sebastian Primpke, personal communication). The use of a newly developed analysis software, the MPhunter software

(Aalborg University, Denmark), might further decrease analysis time (Liu, F. et al., 2019a). Both measures would allow for the analysis of more samples per filter, which would increase representativeness.

Supplementary material for Chapter II

Assessing the weathering status of marine microplastics in the southern North Sea – A multivariate approach

Claudia Lorenz, Sebastian Primpke, Gunnar Gerdtz

Paragraphs (1), figures (5) and tables (8) describing the spectral data collection and presenting results for the statistical analysis.

Paragraph S7: Spectral data collection

For particles in a size range of 500 to 5000 μm spectra were recorded in a wavenumber range of 4000–400 cm^{-1} with a resolution of 4 cm^{-1} and 32 co-added scans with an attenuated total reflectance (ATR)-FTIR unit with a diamond crystal coupled to a Tensor 27 spectrometer (Bruker Optik GmbH). Whenever possible, three spectra were recorded for each particle. A particle was considered as positively identified when at least one of the three measurements showed a hit quality >700 (hit quality ranging between 0 and 1000) or for a hit quality between 600 and 700, when the correct identity was confirmed by expert knowledge.

Particles from 11 to 500 μm in size were analyzed via imaging with a FTIR-microscope (Hyperion 3000) coupled to a spectrometer (Tensor 27) equipped with a 15x objective and a focal plane array (FPA) detector (all Bruker Optik GmbH). Complete filter areas of 185 mm^2 were imaged and spectra were recorded in transmittance mode with 6 scans in the wavenumber range of 3600–1250 cm^{-1} with a resolution of 8 cm^{-1} and 4x4 binning. Background spectra were recorded on the same filter in an area free of sample material with 32 scans in the same wave number range with 4x4 binning. FTIR imaging data was evaluated using an automated analysis (Primpke et al., 2017b) with the reference database design by Primpke et al. (2018). Quality assurance was done and thresholds for hit quality defined (Lorenz et al., 2019).

Table S12: Results of the pairwise multiple comparisons (Dunn's test) for carbonyl indices of polyethylene (PE) and polypropylene (PP) regarding sampled compartment (surface water and sediment).

Comparison	Differences of ranks	Q	p
PE sediment vs PP sediment	3080.557	13.68	<0.05
PE sediment vs PP surface water	2315.582	11.6	<0.05
PE sediment vs PE surface water	2106.34	10.51	<0.05
PE surface water vs PP sediment	974.217	7.89	<0.05
PE surface water vs PP surface water	209.242	3.167	<0.05
PP surface water vs PP sediment	764.975	6.27	<0.05

Table S13: Results of Kruskal-Wallis test for median carbonyl indices of polyethylene (PE) and polypropylene (PP) regarding size classes in the sampled compartments.

Compartment	PE				PP			
	n	H	dF	p	n	H	dF	p
Surface water	4822	2008.96	12	<0.001	5684	1901.94	11	<0.001
Sediment	301	18.20	4	0.001	884	186.17	6	<0.001

Table S14: Results of multiple pairwise comparison for mean carbonyl indices of size classes, which were significantly different based on Kruskal-Wallis test. a=11 µm, b=11–25 µm, c=25–50 µm, d=50–75 µm, e=75–100 µm, f=100–125 µm, g=125–150 µm, h=150–175 µm, i=175–200 µm, j=200–225 µm, k=225–250 µm, l=250–275 µm, m=275–300 µm, o=325–350 µm, q=375–400 µm.

Comparison	PE surface water			PE sediment			PP surface water			PP sediment		
	Differences of ranks	Q	p < 0.05	Differences of ranks	Q	p < 0.05	Differences of ranks	Q	p < 0.05	Differences of ranks	Q	p < 0.05
a vs. b	344.703	2.006	n.t.	34.476	1.217	n.t.	34.229	0.14	n.t.	23.089	0.361	n.t.
a vs. c	813.017	5.349	yes	65.102	2.817	yes	284.954	1.287	n.t.	7.095	0.119	n.t.
a vs. d	520.259	3.443	yes	4.84	0.235	n.t.	252.666	1.17	n.t.	53.192	0.896	n.t.
a vs. e	283.664	1.912	n.t.				70.027	0.324	n.t.	71.053	1.131	n.t.
a vs. f	172.226	1.134	no				464.021	2.096	no	47.17	0.758	n.t.
a vs. g	816.204	5.183	yes				1475.283	6.407	yes	322.922	5.176	yes
a vs. h	1291.504	7.371	yes				122.582	0.529	n.t.			
a vs. i	1028.299	6.63	yes				354.037	1.441	n.t.			
a vs. j	863.725	5.679	yes									
a vs. k	7.31	0.0483	n.t.									
a vs. l	1801.567	12.163	yes									
a vs. m				21.698	1.11	n.t.						
a vs. o												
a vs. q	1153.953	8.231	yes				1924.22	8.872	yes			
b vs. c	468.314	3.584	yes				1848.888	8.813	yes			
b vs. d	175.556	1.355	n.t.	30.627	1.176	n.t.	250.726	1.55	n.t.	30.184	0.907	n.t.
b vs. e	61.039	0.483	n.t.	39.316	1.651	no	218.438	1.417	n.t.	76.281	2.315	n.t.
b vs. f	516.93	3.963	yes				104.256	0.674	n.t.	94.141	2.421	no
b vs. g	1160.907	8.474	yes				429.792	2.658	n.t.	70.258	1.851	n.t.
b vs. h	946.801	6.029	yes				1441.054	8.297	yes	299.834	7.852	yes
b vs. i	1373.002	10.229	yes				88.354	0.503	n.t.			
b vs. j	519.022	3.969	yes				388.266	2.004	n.t.			
b vs. k	352.013	2.711	no									
b vs. l	2146.27	17.019	yes									
b vs. m				12.778	0.557	n.t.						
b vs. o												
b vs. q	1498.656	12.841	yes				1958.448	12.59	yes	1883.116	12.943	yes

Table S14 continued

c vs. d	292.758	2.875	n.t.	69.942	4.05	yes	32.288	0.285	n.t.	46.097	1.978	n.t.
c vs. e	529.353	5.413	yes				354.981	3.115	no	63.957	2.055	n.t.
c vs. f	985.244	9.574	yes				179.066	1.453	n.t.	40.075	1.338	n.t.
c vs. g	1629.221	14.663	yes				1190.329	8.589	yes	330.018	10.909	yes
c vs. h	478.487	3.542	yes				162.372	1.15	n.t.			
c vs. i	1841.316	17.099	yes				638.991	3.921	yes			
c vs. j	50.708	0.491	n.t.									
c vs. k	820.327	8.029	yes									
c vs. l	2614.584	26.849	yes									
c vs. m				43.404	2.706	no	318.832	3.316	n.t.			
c vs. o	1966.97	23.18	yes				2209.174	19.203	yes			
c vs. q	236.595	2.455	no				2133.842	21.12	yes			
d vs. e	692.485	6.819	yes				322.694	3.136	n.t.	17.861	0.58	n.t.
d vs. f	1336.463	12.165	yes				211.354	1.869	n.t.	6.022	0.203	n.t.
d vs. g	771.246	5.754	yes				1222.616	9.43	yes	376.114	12.581	yes
d vs. h	1548.558	14.555	yes				130.084	0.982	n.t.			
d vs. i	343.466	3.368	no				606.704	3.903	yes			
d vs. j	527.569	5.234	yes									
d vs. k	2321.826	24.199	yes									
d vs. l				26.538	2.195	n.t.	286.544	3.463	n.t.			
d vs. m												
d vs. o	1674.212	20.121	yes				2176.886	20.91	yes			
d vs. q	455.891	4.676	yes				2101.554	23.78	yes			
e vs. f	1099.868	10.364	yes				534.048	4.69	yes	23.883	0.662	n.t.
e vs. g	1007.84	7.693	yes				1545.31	11.857	yes	393.975	10.847	yes
e vs. h	1311.963	12.796	yes				192.61	1.446	n.t.			
e vs. i	580.061	5.922	yes				284.01	1.82	n.t.			
e vs. j	290.974	3.008	n.t.									
e vs. k	2085.231	22.752	yes									
e vs. l												
e vs. o	1437.617	18.381	yes				36.149	0.431	n.t.			
e vs. q	1463.731	10.854	yes				1854.193	17.667	yes			
f vs. g	856.073	7.97	yes				1778.861	19.904	yes			
f vs. h	1035.952	10.053	yes				1011.262	7.301	yes	370.092	10.476	yes
f vs. i	164.917	1.619	n.t.				341.438	2.419	n.t.			
f vs. j	1629.341	16.783	yes				818.058	5.022	yes			
f vs. k												
f vs. l							497.899	5.185	yes			

☐

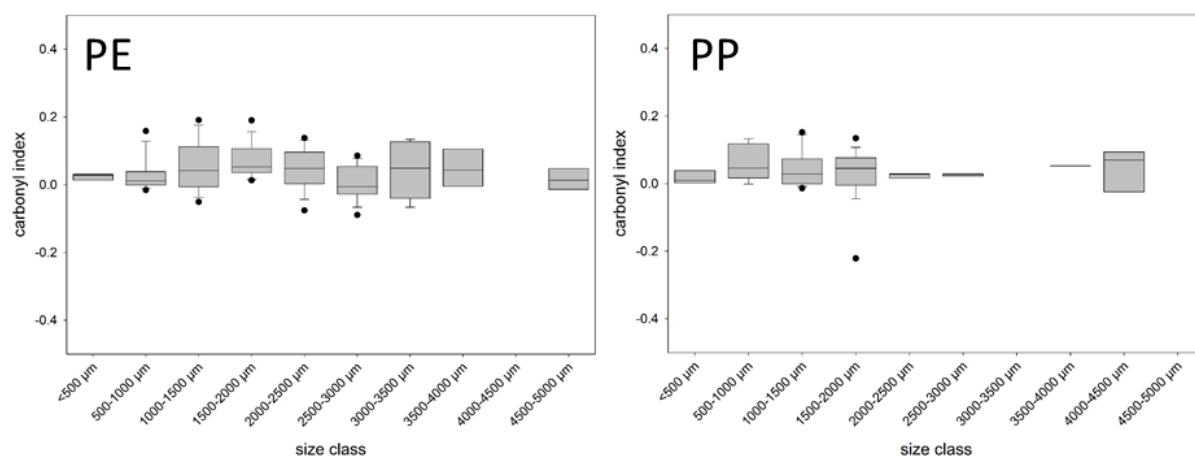


Figure S14: Box plots for the carbonyl indices of large microplastics (500–5000 µm) for polyethylene (PE) and polypropylene (PP) identified in surface water samples. All outliers, plotted as black dots, represent the 5th and 95th percentiles.

Supplement Chapter II

Table S15: Results of multiple pairwise comparison for mean carbonyl indices of size classes (500–5000 μm), which were significantly different based on Kruskal-Wallis test for polyethylene (PE) particles detected in surface water samples. a=500–1000 μm , b=1000–1500 μm , c=1500–2000 μm , d=2000–2500 μm , e=2500–3000 μm , f=3000–3500 μm , g=3500–4000 μm , i=4500–5000 μm , Z= <500 μm .

Comparison	PE surface water			
	Differences of ranks	Q	p < 0.05	
a vs. b	24.254	1.845	n.t.	
a vs. c	61.201	4.001	n.t.	
a vs. d	20.622	1.325	n.t.	
a vs. e	33.428	1.847	n.t.	
a vs. f	17.989	0.753	n.t.	
a vs. g	18.906	0.582	n.t.	
a vs. i	10.719	0.376	n.t.	
a vs. Z	2.406	0.0053	n.t.	
b vs. c	36.946	2.396	n.t.	
b vs. d	3.632	0.232	n.t.	
b vs. e	57.682	3.169	no	
b vs. f	6.265	0.261	n.t.	
b vs. g	5.348	0.164	n.t.	
b vs. i	34.973	1.224	n.t.	
b vs. Z	21.848	0.485	n.t.	
c vs. d	40.579	2.316	n.t.	
c vs. e	94.628	4.777	yes	
c vs. f	43.212	1.714	n.t.	
c vs. g	42.295	1.263	n.t.	
c vs. i	71.92	2.427	no	
c vs. Z	58.795	1.285	n.t.	
d vs. e	54.05	2.701	n.t.	
d vs. f	2.633	0.104	n.t.	
d vs. g	1.716	0.0511	n.t.	
d vs. i	31.341	1.053	n.t.	
d vs. Z	18.216	0.397	n.t.	
e vs. f	51.417	1.905	n.t.	
e vs. g	52.333	1.502	n.t.	
e vs. i	22.708	0.728	n.t.	
e vs. Z	35.833	0.766	n.t.	
f vs. g	0.917	0.024	n.t.	
f vs. i	28.708	0.824	n.t.	
f vs. Z	15.583	0.316	n.t.	
g vs. i	29.625	0.718	n.t.	
g vs. Z	16.5	0.306	n.t.	
i vs. Z	13.125	0.254	n.t.	

Supplement Chapter II

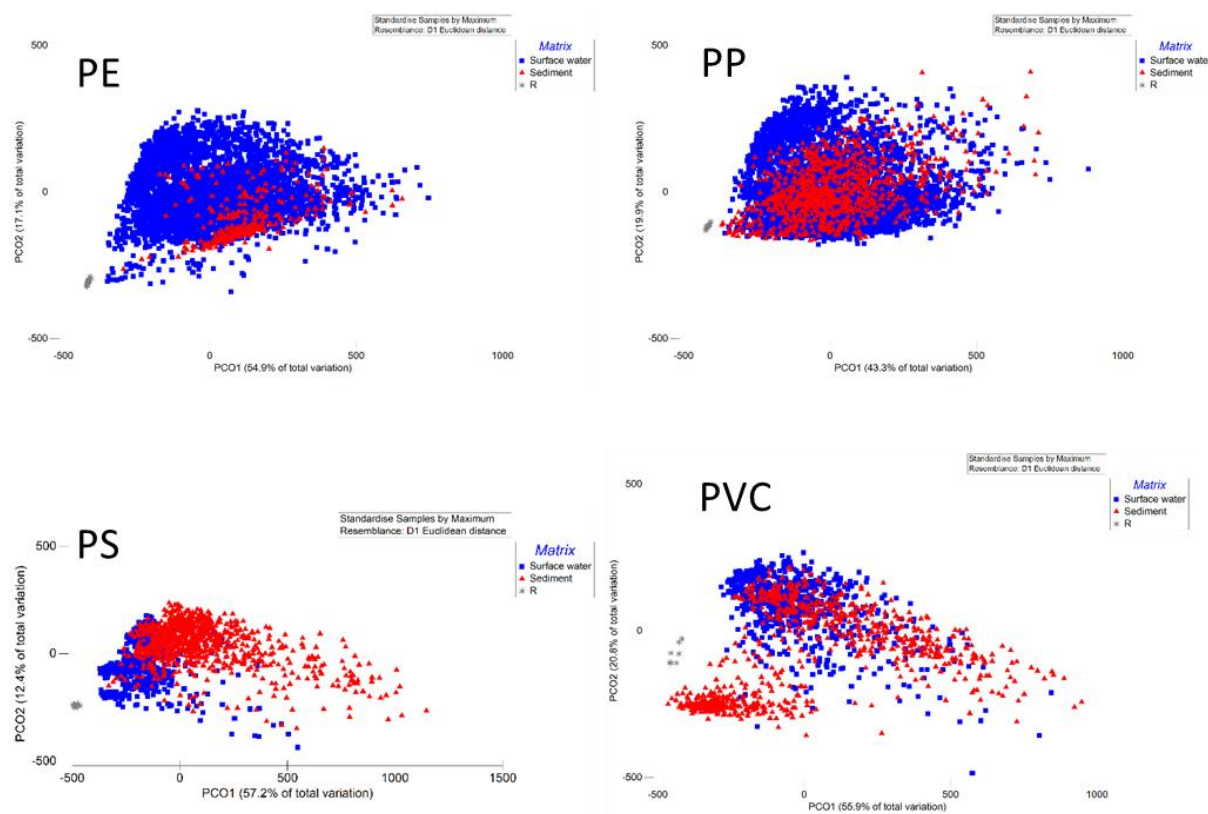


Figure S15: PCoA results for spectra of four polymer types regarding analyzed compartment, surface water (blue), sediment (red) and reference (grey) for four polymer types. PE=polyethylene, PP=polypropylene, PS=polystyrene, PVC=polyvinyl chloride.

Supplement Chapter II

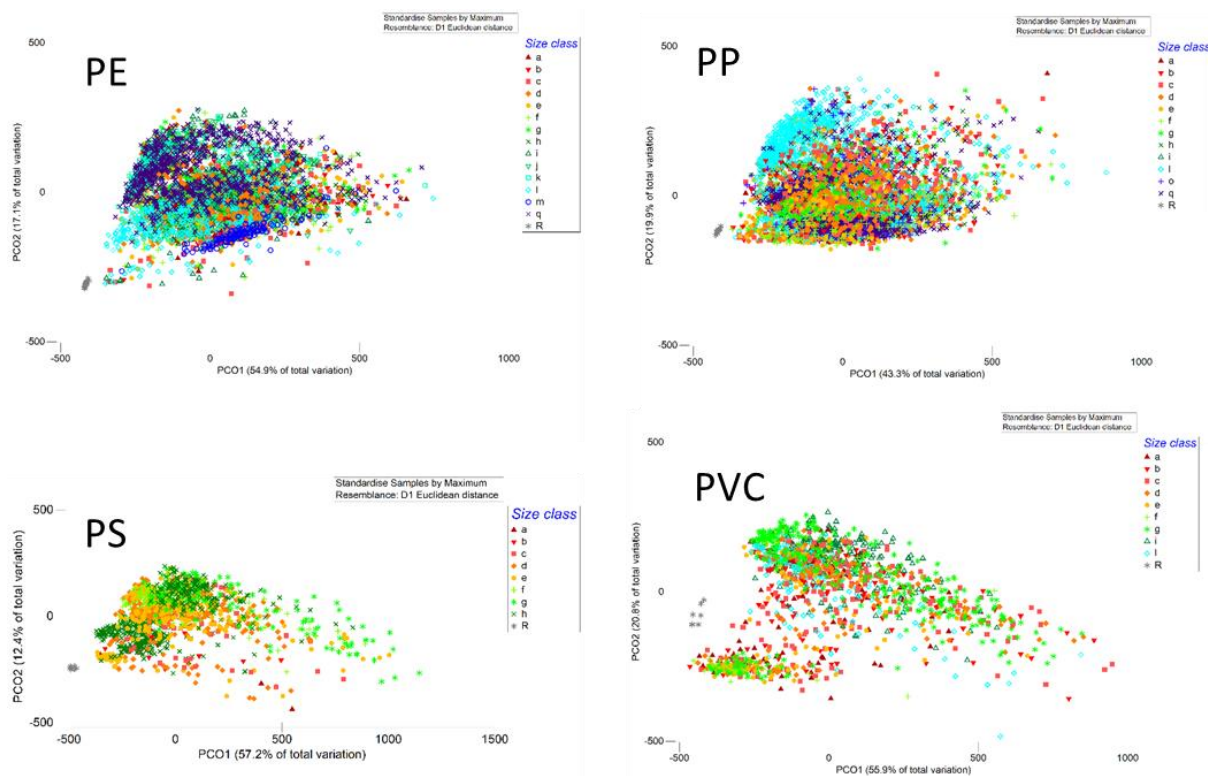


Figure S16: PCoA results for spectra of four polymer types regarding analyzed size classes and the reference (grey) for four polymer types. PE=polyethylene, PP=polypropylene, PS=polystyrene, PVC=polyvinyl chloride. a=11 μm , b=11-25 μm , c=25-50 μm , d=50-75 μm , e=75-100 μm , f=100-125 μm , g=125-150 μm , h=150-175 μm , i=175-200 μm , j=200-225 μm , k=225-250 μm , l=250-275 μm , m=275-300 μm , o=325-350 μm , q=375-400 μm , R=reference.

Table S16: SIMPER results for polyethylene (PE) with contributions >0.5% and contributions >1% highlighted in grey.

Surface water & sediment: av. sq. distance = 150000.03

Wavenumber (cm^{-1})	Surface water av. value	Sediment av. value	Av. sq. distance	Sq. distance/SD	Contribution %	Cum. %
1602.308	8.33	35.6	1030	1.2	0.69	0.69
1606.123	8.57	35.8	1030	1.2	0.68	1.37
1609.938	8.79	35.8	1010	1.2	0.68	2.05
1598.493	8.12	35.2	1010	1.19	0.68	2.72
1613.753	8.95	35.5	988	1.21	0.66	3.38
1594.677	8	34.5	974	1.18	0.65	4.03
1617.568	9.08	35	944	1.2	0.63	4.66
1590.863	7.98	33.7	921	1.16	0.61	5.27
1621.383	9.2	34.1	876	1.19	0.58	5.86
1587.047	7.99	33	868	1.15	0.58	6.43
1583.233	7.91	32	813	1.15	0.54	6.98
1625.198	9.34	32.9	781	1.16	0.52	7.5
1579.417	7.69	30.6	749	1.14	0.5	8

Supplement Chapter II

Table S16 continued

Surface water & reference: av. sq. distance = 362336.92

Wavenumber (cm ⁻¹)	Surface water av. value	Reference av. value	Av. sq. distance	Sq. distance/SD	Contribution %	Cum. %
2941.379	84.5	11.1	5530	3.61	1.53	1.53
2945.194	80.8	7.86	5500	3.2	1.52	3.05
2949.009	77.3	6.37	5250	2.81	1.45	4.5
2937.564	87.6	16	5240	3.84	1.45	5.94
2952.824	74.3	6.06	4920	2.47	1.36	7.3
2865.079	83.2	14.4	4850	3.52	1.34	8.64
2868.894	81.8	13.3	4830	3.33	1.33	9.97
2872.708	81.7	13.9	4740	3.33	1.31	11.28
2956.639	71.5	5.67	4630	2.21	1.28	12.56
2876.524	82.8	15.9	4600	3.45	1.27	13.82
2933.749	89.6	23	4550	3.64	1.26	15.08
2861.264	85.7	19.1	4540	3.68	1.25	16.33
2880.339	84.4	19.5	4330	3.54	1.19	17.53
2960.454	68	4.8	4310	2.04	1.19	18.72
2884.154	85.9	23.9	3940	3.52	1.09	19.81
2964.269	63.6	3.7	3900	1.91	1.08	20.88
2830.743	72.4	13.3	3680	2.44	1.02	21.9
2834.559	77.2	18.6	3580	2.69	0.99	22.89
2826.928	67.9	10.2	3540	2.24	0.98	23.87
2857.448	88.3	29.8	3510	3.36	0.97	24.84
2929.934	90.8	32.5	3500	3.14	0.97	25.8
2887.969	86.9	28.9	3470	3.35	0.96	26.76
2968.084	58.8	2.67	3450	1.81	0.95	27.71
2823.113	63.8	8.09	3320	2.1	0.92	28.63
2819.298	60.2	6.64	3090	2.01	0.85	29.48
2971.899	54	1.84	3000	1.72	0.83	30.31
2891.784	87.8	34	2990	3.1	0.82	31.13
2838.374	82	28.6	2970	2.82	0.82	31.95
2815.483	57.2	5.57	2870	1.94	0.79	32.74
2811.668	54.4	4.74	2670	1.88	0.74	33.48
2975.714	49.7	1.24	2590	1.66	0.72	34.2
2895.599	88.7	39.1	2550	2.88	0.7	34.9
2807.853	52	4.08	2490	1.84	0.69	35.59
2804.038	49.7	3.54	2320	1.81	0.64	36.23
2979.529	45.9	0.824	2250	1.63	0.62	36.85
2926.119	91.3	45.9	2160	2.45	0.6	37.44
2800.223	47.5	3.07	2150	1.78	0.59	38.04
2899.414	89.6	44.6	2120	2.59	0.58	38.62
2796.408	45.3	2.66	1980	1.76	0.55	39.17
2983.344	42.7	0.549	1970	1.61	0.54	39.71
2792.593	43.1	2.29	1820	1.73	0.5	40.21

Supplement Chapter II

Table S16 continued

Sediment & reference: av. sq. distance = 442992.77

Wavenumber (cm ⁻¹)	Sediment av. value	Reference av. value	Av. sq. distance	Sq. distance/SD	Contribution %	Cum. %
2941.379	80.8	11.1	5010	3.21	1.13	1.13
2945.194	76.6	7.86	4890	3.02	1.1	2.23
2937.564	84.3	16	4800	3.35	1.08	3.32
2949.009	72.9	6.37	4600	2.71	1.04	4.35
2952.824	69.5	6.06	4220	2.4	0.95	5.31
2933.749	86.7	23	4200	3.18	0.95	6.25
2956.639	65.8	5.67	3830	2.15	0.86	7.12
2865.079	74.3	14.4	3750	2.49	0.85	7.97
2861.264	78.5	19.1	3690	2.62	0.83	8.8
2868.894	72.1	13.3	3640	2.38	0.82	9.62
2872.708	71.4	13.9	3480	2.29	0.79	10.41
2960.454	61.6	4.8	3450	1.96	0.78	11.18
2876.524	72.2	15.9	3330	2.27	0.75	11.94
2929.934	88.1	32.5	3220	2.71	0.73	12.66
2880.339	74.3	19.5	3170	2.3	0.72	13.38
2857.448	84.1	29.8	3080	2.61	0.69	14.07
2964.269	57	3.7	3050	1.82	0.69	14.76
2884.154	76.8	23.9	2950	2.34	0.67	15.43
2887.969	79.4	28.9	2690	2.33	0.61	16.04
2968.084	52.1	2.67	2640	1.72	0.6	16.63
2891.784	81.8	34	2420	2.29	0.55	17.18
2971.899	47.6	1.84	2260	1.69	0.51	17.69

Supplement Chapter II

Table S17: SIMPER results for polypropylene (PP) with contributions >0.5%.

Surface water & reference: av. sq. distance = 287151.93

Wavenumber (cm ⁻¹)	Surface water av. value	Reference av. value	Av. sq. distance	Sq. distance/SD	Contribution %	Cum. %
2971.899	69.6	21	2550	1.93	0.89	0.89
2975.714	59.8	13.3	2380	1.68	0.83	1.71
2968.084	78.8	32.4	2280	2.2	0.8	2.51
2937.564	84.7	40	2090	2.54	0.73	3.97
2857.448	67.5	23.9	2090	1.7	0.73	4.7
2853.634	66	22.7	2110	1.58	0.73	3.24
2979.529	51.1	8.55	2040	1.48	0.71	5.41
2849.819	68.2	26.2	2000	1.55	0.7	6.1
2826.928	57.4	16.5	1900	1.44	0.66	6.76
2846.003	72.8	31.5	1870	1.76	0.65	7.42
2941.379	85.6	44.4	1800	2.37	0.63	8.67
2823.113	51.4	11.8	1810	1.31	0.63	8.05
2830.743	65.5	26.1	1740	1.55	0.61	9.28
2983.344	44.2	5.59	1710	1.36	0.6	9.88
2861.264	72.1	33	1680	1.74	0.59	10.46
2819.298	47.3	9.34	1680	1.24	0.59	11.05
2933.749	86.4	46.7	1660	2.39	0.58	11.63
2964.269	85.6	46.5	1630	2.18	0.57	12.19
2887.969	79	40.5	1610	1.94	0.56	12.75
2815.483	44.4	7.85	1580	1.19	0.55	13.3
2891.784	79.5	41.7	1560	1.92	0.54	13.85
2884.154	79.4	41.7	1550	1.92	0.54	14.39
2842.188	77.4	40.3	1510	1.84	0.53	14.91
2811.668	42.3	6.84	1490	1.17	0.52	15.43
2987.159	39.1	3.73	1450	1.29	0.5	15.94

Sediment & reference: av. sq. distance = 300065.37

Wavenumber (cm ⁻¹)	Sediment av. value	Reference av. value	Av. sq. distance	Sq. distance/SD	Contribution %	Cum. %
2971.899	64.9	21	2140	1.68	0.71	0.71
2968.084	76.2	32.4	2060	2	0.69	1.4
2853.634	63.4	22.7	1990	1.31	0.66	2.06
2975.714	54.1	13.3	1900	1.44	0.63	2.7
2937.564	81.8	40	1880	2.02	0.63	4.58
2857.448	64	23.9	1890	1.35	0.63	3.33
2849.819	65.7	26.2	1890	1.31	0.63	3.96
2846.003	69.3	31.5	1670	1.44	0.56	5.14
2964.269	85.8	46.5	1630	2.29	0.54	5.68
2941.379	83.1	44.4	1620	1.99	0.54	6.22
2979.529	45.3	8.55	1580	1.29	0.53	6.75
2933.749	84.2	46.7	1520	2	0.51	7.26

Supplement Chapter II

Table S18: SIMPER results for polystyrene (PS) with contributions >0.5%.

Surface water & reference av. sq. distance = 289681.73

Wavenumber (cm ⁻¹)	Surface water av. value	Reference av. value	Av. sq. distance	Sq. distance/SD	Contribution %	Cum. %
2941.379	74.1	22.2	2860	2.2	0.99	0.99
2945.194	67.7	16.3	2840	2.01	0.98	1.97
2949.009	62.1	11.6	2770	1.81	0.95	2.92
2937.564	80.8	29.6	2760	2.42	0.95	3.88
2952.824	57	8.08	2640	1.65	0.91	4.79
2933.749	86.6	38	2470	2.71	0.85	6.49
2853.634	66.4	19.1	2470	1.7	0.85	5.64
2849.819	68.3	21.2	2460	1.69	0.85	7.34
2956.639	52.1	5.41	2430	1.53	0.84	8.18
2857.448	61.8	15.5	2380	1.64	0.82	9
3036.754	62.1	16.7	2290	1.66	0.79	9.79
3074.905	55.8	10.8	2270	1.56	0.78	12.14
3071.09	56	11	2260	1.59	0.78	12.92
3067.274	59.6	14.6	2250	1.7	0.78	15.25
3052.014	59.2	14.2	2250	1.66	0.78	13.7
3040.569	56.3	11.5	2270	1.49	0.78	11.36
2899.414	72	26.5	2250	1.93	0.78	14.47
2895.599	67.3	21.8	2270	1.77	0.78	10.57
2891.784	63.1	18.3	2230	1.63	0.77	16.79
2861.264	56.7	12.1	2230	1.57	0.77	17.56
2846.003	64.8	20.1	2240	1.66	0.77	16.02
3078.72	58	13.7	2210	1.53	0.76	19.85
3055.83	64.6	19.9	2210	1.73	0.76	19.09
3048.199	54.8	10.6	2200	1.53	0.76	20.61
3044.385	53.7	9.62	2220	1.43	0.76	18.32
3063.459	64.6	20.5	2140	1.78	0.74	23.57
2960.454	47.2	3.58	2140	1.45	0.74	22.83
2903.229	77.1	32.3	2160	2.11	0.74	21.35
2887.969	59.6	15.9	2150	1.54	0.74	22.09
3059.645	67.1	23.6	2100	1.76	0.73	24.3
2929.934	91.1	46.3	2100	2.86	0.72	25.02
3082.535	58.5	16	2050	1.48	0.71	26.44
2884.154	56.6	14	2050	1.5	0.71	27.14
2865.079	52.5	9.77	2050	1.5	0.71	25.73
3032.939	70	27	2010	1.9	0.69	27.84
2907.044	82	38.5	2000	2.31	0.69	28.53
3086.35	54	12.6	1960	1.43	0.68	29.2
2880.339	53.8	12.2	1950	1.5	0.67	29.88
2868.894	50.2	8.92	1920	1.48	0.66	30.54
2876.524	51.4	10.6	1880	1.49	0.65	31.19
2872.708	50	9.38	1860	1.48	0.64	31.83
3013.864	53.8	13.4	1830	1.58	0.63	32.46
2842.188	55.8	15.5	1820	1.62	0.63	33.09
3017.679	64	23.4	1810	1.79	0.62	33.71
2964.269	42.4	2.33	1810	1.43	0.62	34.34
2910.859	86.1	45	1790	2.48	0.62	34.95
2926.119	93.7	52.6	1770	2.81	0.61	35.57
3090.165	46.3	7.25	1740	1.4	0.6	36.17
1491.672	61.6	100	1700	1.47	0.59	36.75
3010.049	47.9	9.53	1690	1.41	0.58	37.34
3006.234	46.8	9.49	1610	1.36	0.55	37.89
2914.674	89.7	50.7	1600	2.68	0.55	38.44
2922.304	94.1	55.5	1580	2.73	0.54	38.99
3002.419	47.2	10.6	1550	1.35	0.53	39.52
2968.084	38.3	1.52	1510	1.47	0.52	40.56
2918.489	92.6	54.6	1520	2.8	0.52	40.04

Supplement Chapter II

Table S18 continued

3093.98	40.3	4.33	1480	1.39	0.51	41.07
2998.604	44.6	8.98	1450	1.42	0.5	41.58
Sediment & reference: av. sq. distance = 614135.28						
Wavenumber (cm ⁻¹)	Sediment av. value	Reference av. value	Av. sq. distance	Sq. distance/SD	Contribution %	Cum. %
2949.009	81.5	11.6	4970	3.96	0.81	0.81
2952.824	77.2	8.08	4890	3.54	0.8	1.61
2945.194	84.9	16.3	4780	4.22	0.78	2.38
3074.905	77.8	10.8	4640	2.92	0.76	3.9
2956.639	72.8	5.41	4660	3.15	0.76	3.14
3044.385	76.3	9.62	4610	2.9	0.75	4.65
3040.569	78.2	11.5	4590	3	0.75	5.4
3071.09	77.4	11	4560	2.99	0.74	6.14
3048.199	76.4	10.6	4480	2.92	0.73	6.87
3078.72	78.9	13.7	4400	2.95	0.72	7.59
2960.454	68.5	3.58	4370	2.75	0.71	8.3
3067.274	79	14.6	4280	3.13	0.7	10.4
3052.014	78.9	14.2	4330	3.04	0.7	9
2941.379	87.2	22.2	4290	4.07	0.7	9.7
3036.754	81	16.7	4250	3.2	0.69	11.09
2861.264	75.1	12.1	4100	2.99	0.67	11.76
3082.535	78.5	16	4050	2.93	0.66	13.08
3055.83	82.3	19.9	4020	3.1	0.66	14.39
2865.079	72.1	9.77	4030	2.84	0.66	13.74
2857.448	78.3	15.5	4070	3.09	0.66	12.42
3086.35	74.6	12.6	3990	2.78	0.65	15.69
2964.269	64.2	2.33	4000	2.47	0.65	15.04
2887.969	77.9	15.9	3970	3.02	0.65	16.99
2868.894	70.7	8.92	3970	2.68	0.65	16.34
3010.049	71	9.53	3940	2.62	0.64	20.85
2891.784	80.4	18.3	3960	3.24	0.64	17.63
2884.154	75.8	14	3950	2.87	0.64	18.28
2880.339	73.8	12.2	3950	2.77	0.64	19.56
2876.524	72.1	10.6	3940	2.63	0.64	20.2
2872.708	70.9	9.38	3950	2.59	0.64	18.92
2853.634	80.7	19.1	3920	3.12	0.64	21.48
3090.165	68.2	7.25	3900	2.45	0.63	22.12
3063.459	81.9	20.5	3880	3.16	0.63	23.38
3013.864	74.5	13.4	3890	2.71	0.63	22.75
3006.234	70.4	9.49	3870	2.58	0.63	24.01
2895.599	82.7	21.8	3820	3.37	0.62	24.64
3059.645	83.7	23.6	3730	3.12	0.61	26.46
3002.419	70.4	10.6	3750	2.48	0.61	25.25
2849.819	81.3	21.2	3740	3.06	0.61	25.85
3093.98	62.9	4.33	3640	2.19	0.59	27.05
2968.084	59.9	1.52	3590	2.32	0.59	28.23
2846.003	78.8	20.1	3590	2.88	0.59	27.64
2998.604	67	8.98	3540	2.39	0.58	28.8
2937.564	88.4	29.6	3540	3.61	0.58	29.38
3097.795	60.6	3.88	3430	2.11	0.56	30.5
2899.414	84.6	26.5	3470	3.36	0.56	29.94
2842.188	72	15.5	3350	2.63	0.55	31.05
3032.939	83.8	27	3320	3.05	0.54	31.59
3017.679	79.1	23.4	3230	2.77	0.53	32.11
3101.61	59.4	4.5	3210	2.11	0.52	32.64
2994.789	60.1	5.1	3190	2.31	0.52	33.68
2971.899	56.2	1.11	3210	2.24	0.52	33.16

Supplement Chapter II

Table S19: SIMPER results for polyvinyl chloride (PVC) with contributions >0.5% and contributions >1% highlighted in grey.

Surface water & sediment: av. sq. distance = 232347.56

Wavenumber (cm ⁻¹)	Surface water av. value	Sediment av. value	Av. sq. distance	Sq. distance/SD	Contribution %	Cum. %
2914.674	81.2	61.1	1850	0.82	0.8	0.8
2918.489	81.1	60.7	1830	0.82	0.79	1.58
2922.304	80.4	59.9	1790	0.82	0.77	3.13
2910.859	79.9	60.5	1790	0.82	0.77	2.36
2926.119	79.2	58.9	1730	0.82	0.75	3.87
2929.934	77.2	57.3	1630	0.82	0.7	4.57
2907.044	76.3	58.3	1600	0.81	0.69	5.26
2933.749	74	55.3	1470	0.81	0.63	5.89
1430.632	75.4	58.5	1390	0.77	0.6	6.49
1327.626	68.5	53	1340	0.81	0.58	7.07
1434.447	73.7	57	1320	0.77	0.57	8.21
1331.441	68.1	52.7	1330	0.81	0.57	7.64
2903.229	70	54.7	1290	0.81	0.56	9.32
1426.817	72.8	57.5	1300	0.78	0.56	8.77
2937.564	70.2	53.1	1290	0.8	0.55	9.87
1323.811	66.6	51.9	1290	0.81	0.55	10.43
1335.256	64.9	50.7	1220	0.81	0.53	10.95
1319.996	63.4	50	1190	0.82	0.51	11.47
1732.018	61.6	47.1	1160	0.76	0.5	11.96

Surface water & reference: av. sq. distance = 315613.46

Wavenumber (cm ⁻¹)	Surface water av. value	Reference av. value	Av. sq. distance	Sq. distance/SD	Contribution %	Cum. %
2926.119	79.2	25.2	3290	1.72	1.04	1.04
2922.304	80.4	26.9	3250	1.7	1.03	2.07
2929.934	77.2	23.7	3210	1.75	1.02	3.09
2918.489	81.1	28.9	3120	1.67	0.99	4.08
2933.749	74	22	3020	1.8	0.96	5.04
2914.674	81.2	30.8	2930	1.65	0.93	5.97
2937.564	70.2	20.1	2780	1.86	0.88	6.85
2910.859	79.9	31.3	2730	1.66	0.86	7.71
2941.379	66.6	18.3	2570	1.9	0.81	8.52
2907.044	76.3	29.4	2510	1.72	0.8	9.32
2945.194	63.5	16.8	2400	1.91	0.76	10.08
2903.229	70	24.8	2290	1.82	0.73	10.81
2949.009	61.1	15.8	2250	1.89	0.71	11.52
1732.018	61.6	31.2	2200	1.17	0.7	12.92
1728.203	61.2	30.4	2210	1.21	0.7	12.22
2952.824	59.3	15.4	2120	1.87	0.67	13.59
2899.414	62	18.9	2040	1.91	0.65	14.24
2956.639	57.9	15.3	2000	1.87	0.63	14.87
1724.388	57.1	26.8	1940	1.2	0.61	15.48
2960.454	57.2	15.7	1890	1.87	0.6	16.08
1735.833	57.3	28.6	1870	1.13	0.59	16.67
2964.269	56.6	16.2	1790	1.87	0.57	17.24
2895.599	53.9	13.5	1780	1.91	0.57	17.8
2968.084	55.7	16.2	1720	1.87	0.54	18.35
2971.899	53.9	15.3	1640	1.85	0.52	19.39
2849.819	45.9	7.23	1640	1.8	0.52	18.87
2853.634	45.5	7.08	1610	1.77	0.51	19.9

Supplement Chapter II

Table S19 continued

Sediment & reference: av. sq. distance = 387291.5

Wavenumber (cm ⁻¹)	Sediment av. value	Reference av. value	Av. sq. distance	Sq. distance/SD	Contribution %	Cum. %
2926.119	58.9	25.2	2220	1.05	0.57	0.57
2922.304	59.9	26.9	2220	1.05	0.57	1.14
2918.489	60.7	28.9	2160	1.07	0.56	1.7
2929.934	57.3	23.7	2140	1.06	0.55	2.26
2914.674	61.1	30.8	2080	1.09	0.54	3.87
1732.018	47.1	31.2	2090	0.94	0.54	2.8
1728.203	47.1	30.4	2090	0.94	0.54	3.33
2933.749	55.3	22	2020	1.08	0.52	4.39
2910.859	60.5	31.3	1990	1.11	0.51	4.91

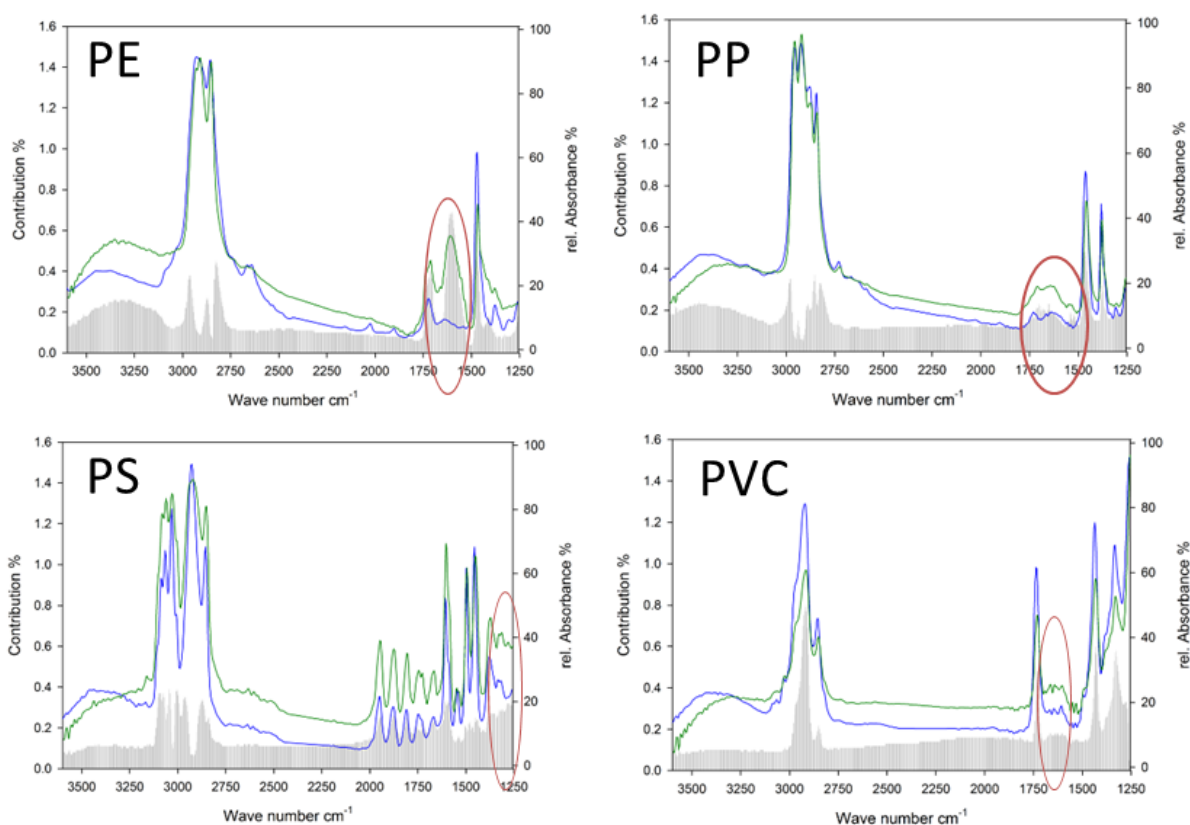


Figure S17: Results of the contribution to the dissimilarities based on SIMPER analysis when comparing the average relative absorbance of surface water (blue) to sediment samples (green) for four polymer types. PE=polyethylene, PP=polypropylene, PS=polystyrene, PVC=polyvinyl chloride.

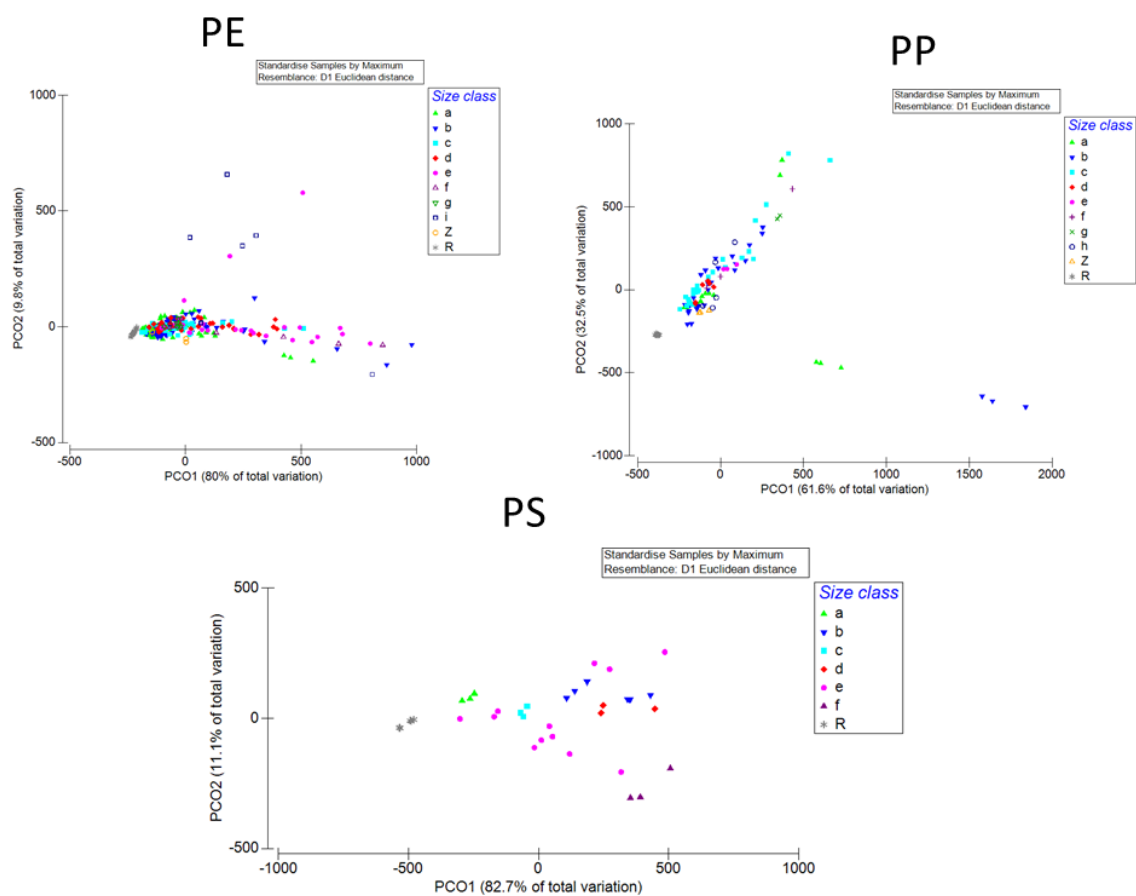


Figure S18: PCoA results for spectra of three polymer types regarding size classes compared to reference spectra (grey). PE=polyethylene, PP=polypropylene, PS=polystyrene.

Supplementary material Chapter III

Paraffin waxes in the southern North Sea

Claudia Lorenz, Michaela Schafberg, Lisa Roscher, Melanie S. Meyer, Sebastian Primpke, Uta R. Kraus, Gunnar Gerdts

Paragraphs (1), figures (2) and tables (2) describing the sample processing, methodology and analysis and presenting examples

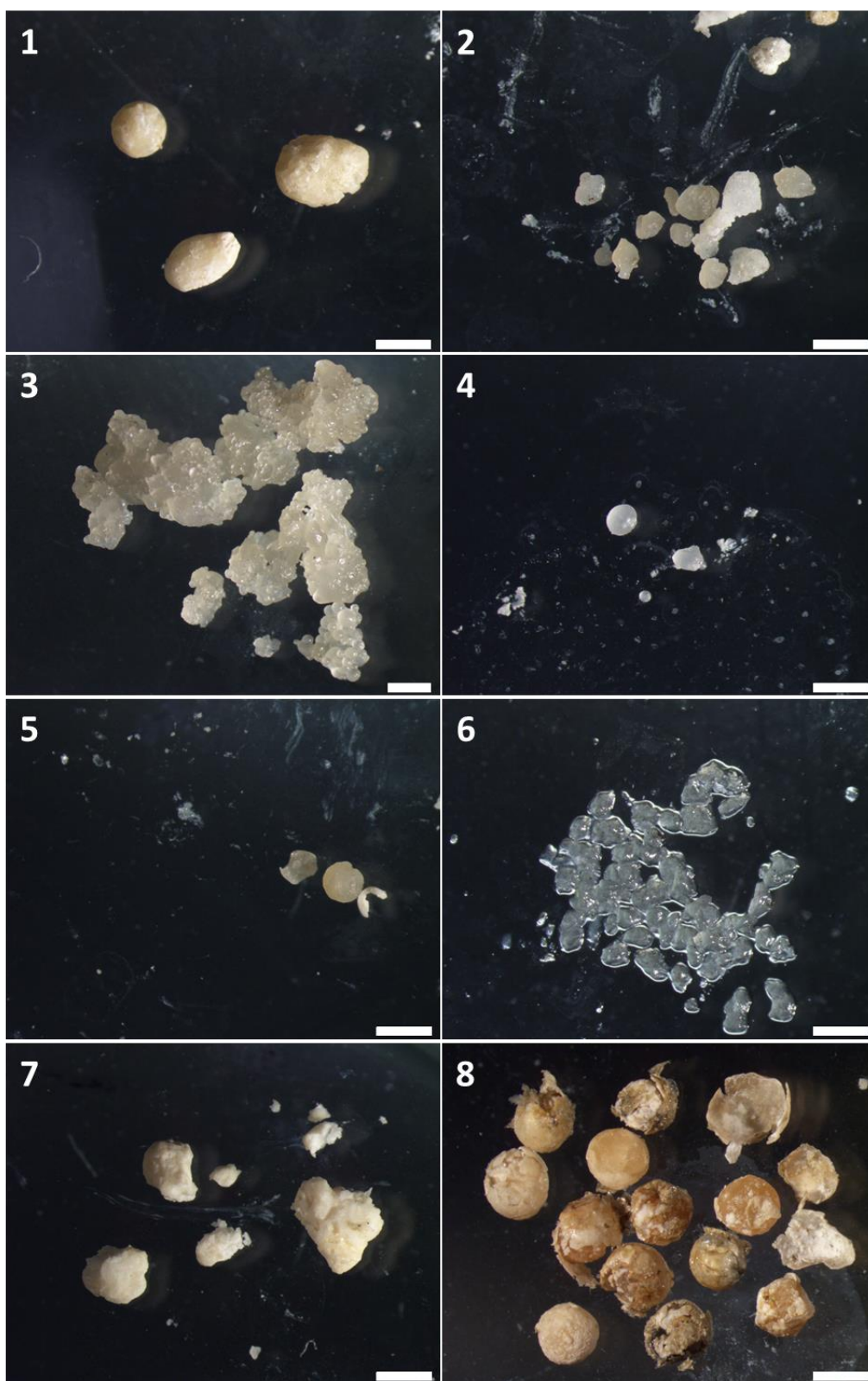


Figure S19: Examples for putative paraffin particles of the eight identified categories. From category 1 to 8: samples from sampling stations 21, 20, 14, 21, 2, 20, 2, 3, situated in the southern North Sea. Scale bar: 1 mm.

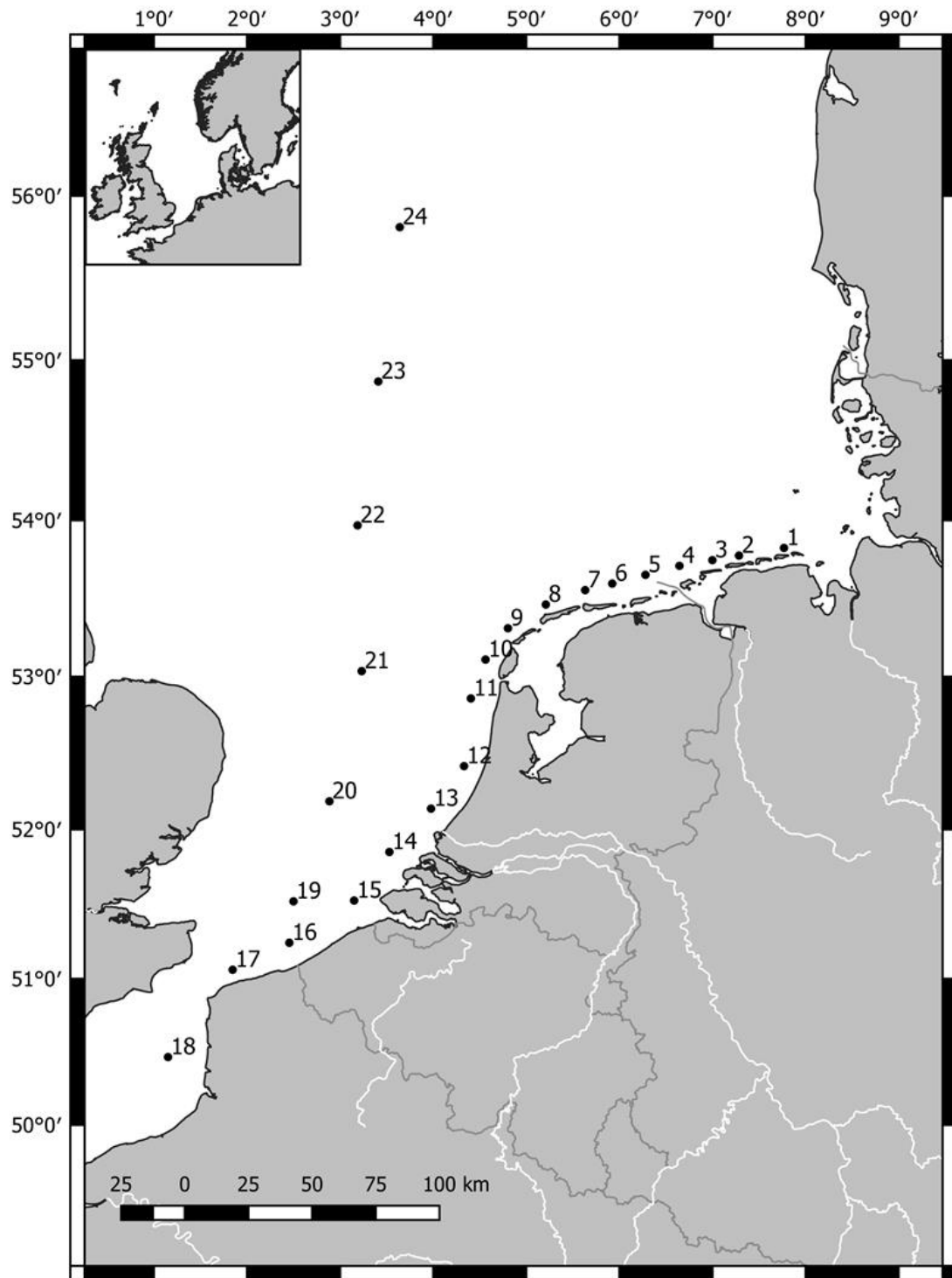


Figure S20: Sampling stations of RV Heincke cruise (He430) in summer 2014. Surface water samples were taken with a 100 µm net for microplastics sampling.

Paragraph S8: Sample processing and analysis using μ FTIR imaging

The sample from station 20 was selected for further analysis of the small size fraction (20–500 μm) based on the large amount of putative paraffin wax (PW) particles in the large size fraction (500–5000 μm). The sample was processed to be analyzed for microplastics in the context of another study by Lorenz et al. (2019). In brief, the purification steps consisted of an enzymatic-oxidative treatment to remove any natural organic matter and a density separation with a dense salt solution to remove any inorganic matrix. Then a sub-sample of 4.1 mL, representing 3.5% of the original prepared and concentrated sample, was filtered onto an aluminum oxide filter (Anodisc, 25 mm diameter, Whatman) and dried at 30 °C in an oven overnight. Subsequently, the filter was placed onto a CaF_2 window and analyzed completely using a μ FTIR imaging system (Hyperion 3000 with a 64 x 64 FPA detector, Tensor 27 spectrometer, Bruker Optics) in transmission mode in a wave number range of 3600–1250 cm^{-1} with 4x binning, a resolution of 8 cm^{-1} and 6 co-added scans. Furthermore, a 3-term Blackman-Harris apodization function with a zero filling factor of 2 was used. A background spectrum was acquired beforehand on the same Anodisc filter in a particle-free area and subtracted via the Opus 7.5 software. All acquired spectra were subjected to an automated database comparison and an image analysis as described by Primpke et al. (2017b) using the free available database by (Primpke et al., 2018).

Table S20: Overview of the solubility of the analyzed samples per sampling station and category. Each sample was solved in n-hexane in duplicate. A poor solubility was marked by streaks or a deposit. ● = both duplicates solved completely, ◇ = only one duplicate solved completely, ○ = both duplicates did not solve completely.

Station	Category 1	Category 2	Category 3	Category 4	Category 5	Category 6	Category 7	Category 8
He430_2		◇		◇	◇		●	
He430_3		◇		●				○
He430_5		◇						
He430_14		●	●					
He430_20		○		○		●		
He430_21	●			●				

Supplement Chapter III

Table S21: GC-FID and GC-MS conditions (modified after Fitz et al. (2017))

Parameters	GC-FID	GC-MS
Hardware and Operation		
Instrument	Agilent 6890N	Agilent 7890
Detector	FID	MS (Agilent 7000C)
Carrier gas	H2	H2
Injection		
Volume [μ L]	1	1
Injection temp. [$^{\circ}$ C]	320	40
Pre-inject. Delay [sec]	1	
Injector type	CIS 4 (Gerstel)	CIS 4 (Gerstel)
Ramp_1 [$^{\circ}$ C/s]		16
Ramp_1_end [$^{\circ}$ C]		150
Hold time [min]		0
Ramp_2 [$^{\circ}$ C/s]		12
Ramp_2_end [$^{\circ}$ C]		350
Hold time [min]		15
Injection mode	solvent vent mode	solvent vent mode
Column		
Name	DB-5	HP-5ms Ultra inert
Length [m]	10	30
Diameter [mm]	0.1	0.25
Film [μ m]	0.1	0.25
Const. Flow [mL/min]	0.92	1.1
Oven program		
Start [$^{\circ}$ C]	40	42
Hold-start [min]	0.7	0.8
Rate_1 [$^{\circ}$ C/min]	30.2	5.5
Rate_1_end [$^{\circ}$ C]	300	325
Hold_1 [min]	2.5	20
Rate_2 [$^{\circ}$ C/min]	15	
Rate_2_End [$^{\circ}$ C]	325	
Hold_end [min]	13.6	
Run time [min]	17	72.3
FID conditions		
Heater [$^{\circ}$ C]	340	
H2 [mL/min]	30	
Air [mL/min]	320	
Makeup [mL/min]	30	
MS conditions		
Scan mode [m/z]		50–450
Scan time [ms]		500
Source Temp [$^{\circ}$ C]		230
Transferline Temp [$^{\circ}$ C]		270

Supplementary material Chapter IV

Different stories told by small and large microplastics in sediments – First report of microplastic concentrations in an urban recipient in Norway

Marte Haave, Claudia Lorenz, Sebastian Primpke, Gunnar Gerdts

Figures (3) and tables (2) presenting results and examples for the analyzed samples

Table S22: Polymer type and size class distribution per site in Byfjorden, Bergen (Norway). Total particles number from FTIR imaging back calculated to 100% sample volume. Concentration given as MP kg⁻¹ dw sediment.

Station: Kvr1																								
Size class	polymer name	polyethylene oxidized										synthetic polymers												Cumulative percent
		polyethylene	polyethylene-chlorinated	polypropylene	polystyrene	polycarbonate	polyamide	polyvinylchloride	cellulose modified	nitrile rubber	polyester	acrylates/PUr/ varnish	polychloroprene	polylactide acide	polycaprolactone	ethylene-vinyl - acetate	polyoxy-methylene	acrylonitrile-butadiene	rubber 1	rubber 3				
11		1631	371	3184	2012	164	15	3677	15	1431	327	989	41885	29	0	2283	15505	134	15	4095	16516	94277	45,8 %	
11-25		632	149	715	1555	178	29	1362	29	1475	29	769	22245	0	0	1563	6092	134	0	2815	10256	50000	70,1 %	
25-50		781	0	44	1787	298	0	1587	0	1116	418	1033	16995	0	0	459	4166	15	0	564	7367	36628	87,9 %	
50-75		383	0	15	705	59	0	132	0	581	15	161	4158	0	0	149	859	0	0	327	3233	10777	93,1 %	
75-100		73	0	0	161	134	0	208	0	283	0	356	2588	0	15	15	88	0	0	15	1995	5931	96,0 %	
100-125		15	0	0	88	0	0	44	0	29	0	149	1052	0	0	0	29	0	0	15	774	2195	97,1 %	
125-150		44	0	0	44	0	0	15	0	15	0	29	1160	0	0	15	15	0	15	0	222	1572	97,8 %	
150-175		29	0	0	73	0	0	0	0	29	0	0	535	0	0	0	0	0	0	0	418	1084	98,4 %	
175-200		15	0	0	29	0	0	0	0	0	0	0	462	0	0	0	0	0	0	0	134	640	98,7 %	
200-225		0	0	0	15	15	0	0	0	0	0	0	208	0	0	0	0	0	0	0	283	520	98,9 %	
225-250		15	0	0	29	0	0	0	0	0	0	0	134	0	0	0	0	0	0	0	418	596	99,2 %	
250-275		15	0	0	0	0	0	0	0	0	0	0	164	0	0	0	0	0	0	0	134	313	99,4 %	
275-300		15	0	0	0	0	0	0	0	0	0	0	15	0	0	0	0	0	0	0	0	29	99,4 %	
300-325		0	0	0	0	0	0	0	0	0	0	0	134	0	0	0	0	0	0	0	149	283	99,5 %	
325-350		0	0	0	0	0	0	0	0	0	0	0	164	0	0	0	0	0	0	0	269	432	99,7 %	
350-375		0	0	0	0	0	0	0	0	0	0	0	0	0	0	0	0	0	0	0	149	149	99,8 %	
375-400		0	0	0	0	0	0	0	0	0	0	0	0	0	0	0	0	0	0	0	0	0	99,8 %	
400-425		0	0	0	0	0	0	0	0	0	0	0	134	0	0	0	0	0	0	0	134	269	99,9 %	
425-450		0	0	0	0	0	0	0	0	0	0	0	134	0	0	0	0	0	0	0	0	134	100,0 %	
450-475		0	0	0	0	0	0	0	0	0	0	0	0	0	0	0	0	0	0	0	0	0	100,0 %	
475-500		0	0	0	0	0	0	0	0	0	0	0	0	0	0	0	0	0	0	0	0	0	100,0 %	
>500		0	0	0	0	0	0	0	0	0	0	0	0	0	0	0	0	0	0	0	29	29	100,0 %	
Sum Kvr1		3647	520	3958	6499	847	44	7024	15	4959	789	3486	92166	29	15	4483	26754	283	29	7831	42480	205859		

Supplement Chapter IV

Station St4

Size class	polymer name	polyethylene	polyethylene oxidized	polyethylene-chlorinated	polypropylene	polystyrene	polycarbonate	polyamide	polyvinylchloride	cellulose modified	nitrile rubber	polyester	acrylates/PUR/ varnish	polychloroprene	polyacide acide	polycaprolactone	ethylene-vinyl -acetate	polyoxy-methylene	acrylonitrile-butadiene	rubber 1	rubber 3	synthetic polymers	Cumulative percent
11		2156	44	1392	4375	180	120	1376	328	120	344	2248	6640	120	0	1464	1448	0	120	0	3727	26200	36,9 %
11-25		960	0	240	3131	180	60	884	404	0	164	960	3859	0	0	584	644	0	120	0	1604	13793	56,3 %
25-50		1320	0	60	4543	224	0	808	224	60	120	2652	3323	0	0	120	284	0	120	0	644	14501	76,7 %
50-75		900	0	0	3240	0	0	764	44	60	44	2024	1727	0	0	104	0	0	0	0	540	9446	90,0 %
75-100		480	0	60	1380	60	0	640	0	0	0	404	240	0	0	0	0	0	0	0	60	3323	94,7 %
100-125		60	0	0	660	0	0	60	0	0	0	120	344	0	0	0	0	0	0	0	60	1304	96,5 %
125-150		240	0	0	420	0	0	0	0	0	0	120	148	0	0	0	0	0	0	0	60	988	97,9 %
150-175		0	0	0	60	60	0	60	0	0	0	0	164	0	0	0	0	0	0	0	0	344	98,4 %
175-200		120	0	0	240	0	0	0	0	0	0	0	60	0	0	0	0	0	0	0	60	480	99,1 %
200-225		0	0	0	60	0	0	60	0	0	0	0	0	0	0	0	0	0	0	0	0	120	99,3 %
225-250		120	0	0	0	0	0	44	0	0	0	0	60	0	0	0	0	0	0	0	60	284	99,7 %
250-275		0	0	0	0	0	0	0	0	0	0	0	120	0	0	0	0	0	0	0	0	120	99,8 %
275-300		0	0	0	0	0	0	0	0	0	0	0	60	0	0	0	0	0	0	0	0	60	99,9 %
300-325		0	0	0	0	0	0	0	0	0	0	0	0	0	0	0	0	0	0	0	0	0	99,9 %
325-350		0	0	0	0	0	0	0	0	0	0	0	0	0	0	0	0	0	0	0	0	0	99,9 %
350-375		0	0	0	0	0	0	0	0	0	0	0	0	0	0	0	0	0	0	0	0	0	99,9 %
375-400		0	0	0	0	0	0	0	0	0	0	0	0	0	0	0	0	0	0	0	0	0	99,9 %
400-425		60	0	0	0	0	0	0	0	0	0	0	0	0	0	0	0	0	0	0	0	60	100,0 %
425-450		0	0	0	0	0	0	0	0	0	0	0	0	0	0	0	0	0	0	0	0	0	100,0 %
450-475		0	0	0	0	0	0	0	0	0	0	0	0	0	0	0	0	0	0	0	0	0	100,0 %
475-500		0	0	0	0	0	0	0	0	0	0	0	0	0	0	0	0	0	0	0	0	0	100,0 %
>500		0	0	0	0	0	0	0	0	0	0	0	0	0	0	0	0	0	0	0	0	0	100,0 %
Sum St4		6415	44	1752	18109	704	180	4695	1000	240	672	8527	16745	120	0	2271	2375	0	360	0	6815	71023	

Supplement Chapter IV

Station St5																								
Size class	polymer name	polyethylene	polyethylene oxidized	polyethylene-chlorinated	polypropylene	polystyrene	polycarbonate	polyamide	polyvinylchloride	cellulose modified	nitrile rubber	polyester	acrylates/PUR/ varnish	polychloroprene	polylactide acide	polycaprolactone	ethylene-vinyl -acetate	polyoxy-methylene	acrylonitrile-butadiene	rubber 1	rubber 3	synthetic polymers	Cumulative percent	
11		527	0	160	825	143	27	797	171	0	980	412	2473	4433	0	523	66	0	0	0	1265	12800	45,5 %	
11-25		302	0	88	902	110	0	330	176	0	137	631	1602	901	0	338	127	0	0	0	0	749	6393	68,2 %
25-50		231	0	94	1187	82	27	269	27	0	27	829	1498	410	0	210	93	0	0	0	0	457	5441	87,6 %
50-75		88	0	0	423	110	0	182	0	0	94	368	391	0	0	0	27	0	0	0	0	148	1832	94,1 %
75-100		110	0	0	198	27	0	55	33	0	0	27	248	0	0	33	6	0	0	0	0	66	803	97,0 %
100-125		55	0	0	88	0	0	33	0	0	0	0	116	0	0	0	0	0	0	0	0	0	292	98,0 %
125-150		0	0	0	33	0	0	0	0	0	0	27	121	0	0	0	0	0	0	0	0	6	187	98,7 %
150-175		27	0	0	27	0	0	0	0	0	0	0	55	0	0	0	0	0	0	0	0	27	137	99,2 %
175-200		0	0	0	55	0	0	0	0	0	0	0	94	0	0	0	0	0	0	0	0	0	149	99,7 %
200-225		0	0	0	0	0	0	0	0	0	0	0	0	0	0	0	0	0	0	0	0	0	0	99,7 %
225-250		0	0	0	0	0	0	0	0	0	0	0	0	0	0	0	0	0	0	0	0	0	0	99,7 %
250-275		0	0	0	0	27	0	0	0	0	0	0	27	0	0	0	0	0	0	0	0	6	60	99,9 %
275-300		0	0	0	0	0	0	0	0	0	0	0	27	0	0	0	0	0	0	0	0	0	27	100,0 %
300-325		0	0	0	0	0	0	0	0	0	0	0	0	0	0	0	0	0	0	0	0	0	0	100,0 %
325-350		0	0	0	0	0	0	0	0	0	0	0	0	0	0	0	0	0	0	0	0	0	0	100,0 %
350-375		0	0	0	0	0	0	0	0	0	0	0	0	0	0	0	0	0	0	0	0	0	0	100,0 %
375-400		0	0	0	0	0	0	0	0	0	0	0	0	0	0	0	0	0	0	0	0	0	0	100,0 %
400-425		0	0	0	0	0	0	0	0	0	0	0	0	0	0	0	0	0	0	0	0	0	0	100,0 %
425-450		0	0	0	0	0	0	0	0	0	0	0	0	0	0	0	0	0	0	0	0	0	0	100,0 %
450-475		0	0	0	0	0	0	0	0	0	0	0	0	0	0	0	0	0	0	0	0	0	0	100,0 %
475-500		0	0	0	0	0	0	0	0	0	0	0	0	0	0	0	0	0	0	0	0	0	0	100,0 %
>500		0	0	0	0	0	0	0	0	0	0	0	0	0	0	0	0	0	0	0	0	0	0	100,0 %
Sum St5		1339	0	341	3738	500	55	1666	408	0	1238	2295	6653	5743	0	1104	319	0	0	0	2723	28122		

Supplement Chapter IV

Station St11																								
Size class	polymer name	polyethylene	polyethylene oxidized	polyethylene-chlorinated	polypropylene	polystyrene	polycarbonate	polyamide	polyvinylchloride	cellulose modified	nitrile rubber	polyester	acrylates/PUR/ varnish	polychloroprene	polylactide acide	polycaprolactone	ethylene-vinyl -acetate	polyoxy-methylene	acrylonitrile-butadiene	rubber 1	rubber 3	synthetic polymers	Cumulative percent	
11		315	0	58	422	65	18	485	71	17	485	108	1031	1031	0	237	68	0	0	0	574	4984	40,9 %	
11-25		105	0	24	640	36	0	229	40	60	221	164	702	119	0	175	17	18	0	0	288	2837	64,1 %	
25-50		255	0	18	513	168	0	171	123	0	150	294	613	42	0	60	53	0	0	0	237	2696	86,2 %	
50-75		76	0	18	191	36	0	75	24	0	47	127	287	0	0	0	24	0	0	0	168	1073	95,0 %	
75-100		24	0	0	36	36	0	6	0	6	0	0	165	0	0	0	0	0	0	0	18	290	97,4 %	
100-125		54	0	0	18	0	0	36	0	0	0	6	17	0	0	18	0	0	0	0	18	166	98,7 %	
125-150		18	0	0	18	0	0	0	0	0	0	0	24	0	0	0	0	0	0	0	6	65	99,3 %	
150-175		0	0	0	18	0	0	0	0	0	0	0	11	0	0	0	0	0	0	0	6	35	99,6 %	
175-200		0	0	0	0	0	0	0	0	0	0	0	18	0	0	0	0	0	0	0	0	18	99,7 %	
200-225		0	0	0	0	0	0	0	0	0	0	0	6	0	0	0	0	0	0	0	0	6	99,8 %	
225-250		0	0	0	0	0	0	0	0	0	0	0	11	0	0	0	0	0	0	0	0	11	99,9 %	
250-275		0	0	0	18	0	0	0	0	0	0	0	0	0	0	0	0	0	0	0	0	18	100,0 %	
275-300		0	0	0	0	0	0	0	0	0	0	0	0	0	0	0	0	0	0	0	0	0	100,0 %	
300-325		0	0	0	0	0	0	0	0	0	0	0	0	0	0	0	0	0	0	0	0	0	100,0 %	
325-350		0	0	0	0	0	0	0	0	0	0	0	0	0	0	0	0	0	0	0	0	0	100,0 %	
350-375		0	0	0	0	0	0	0	0	0	0	0	0	0	0	0	0	0	0	0	0	0	100,0 %	
375-400		0	0	0	0	0	0	0	0	0	0	0	0	0	0	0	0	0	0	0	0	0	100,0 %	
400-425		0	0	0	0	0	0	0	0	0	0	0	0	0	0	0	0	0	0	0	0	0	100,0 %	
425-450		0	0	0	0	0	0	0	0	0	0	0	0	0	0	0	0	0	0	0	0	0	100,0 %	
450-475		0	0	0	0	0	0	0	0	0	0	0	0	0	0	0	0	0	0	0	0	0	100,0 %	
475-500		0	0	0	0	0	0	0	0	0	0	0	0	0	0	0	0	0	0	0	0	0	100,0 %	
>500		0	0	0	0	0	0	0	0	0	0	0	0	0	0	0	0	0	0	0	0	0	100,0 %	
sum st11		847	0	118	1874	341	18	1001	258	82	903	699	2884	1192	0	489	161	18	0	0	1315	12199		

Table S23: Synthetic polymer particles >500 μm as polymer type and shape. Identified by ATR-FTIR. Criteria: Hit Quality Index >700/1000 or manually validated spectrum when >600/1000.

Station	Sphere-PS	Fragment-PS	Fragment-PE	Fragment-PE chl	Fragment-PP	Fragment-PUR	Fragment-other	Fiber-PP	Fiber-PA	Fiber Pest+PET	Fiber-PET	Fiber-PEST	Fiber PE	Fiber other	Sum
Kvr1	0	1	3	1	1	0	6	4	16	7	3	4	0	3	42
St4	1	1	2	0	7	6	1	3	5	2	2	0	0	0	29
St5	4	3	4	0	1	1	2	27	35	12	1	0	1	1	97
St11	0	0	1	0	2	1	0	2	12	5	1	0	1	0	24
Sum	5	5	10	1	11	8	13	36	68	26	7	4	2	4	192

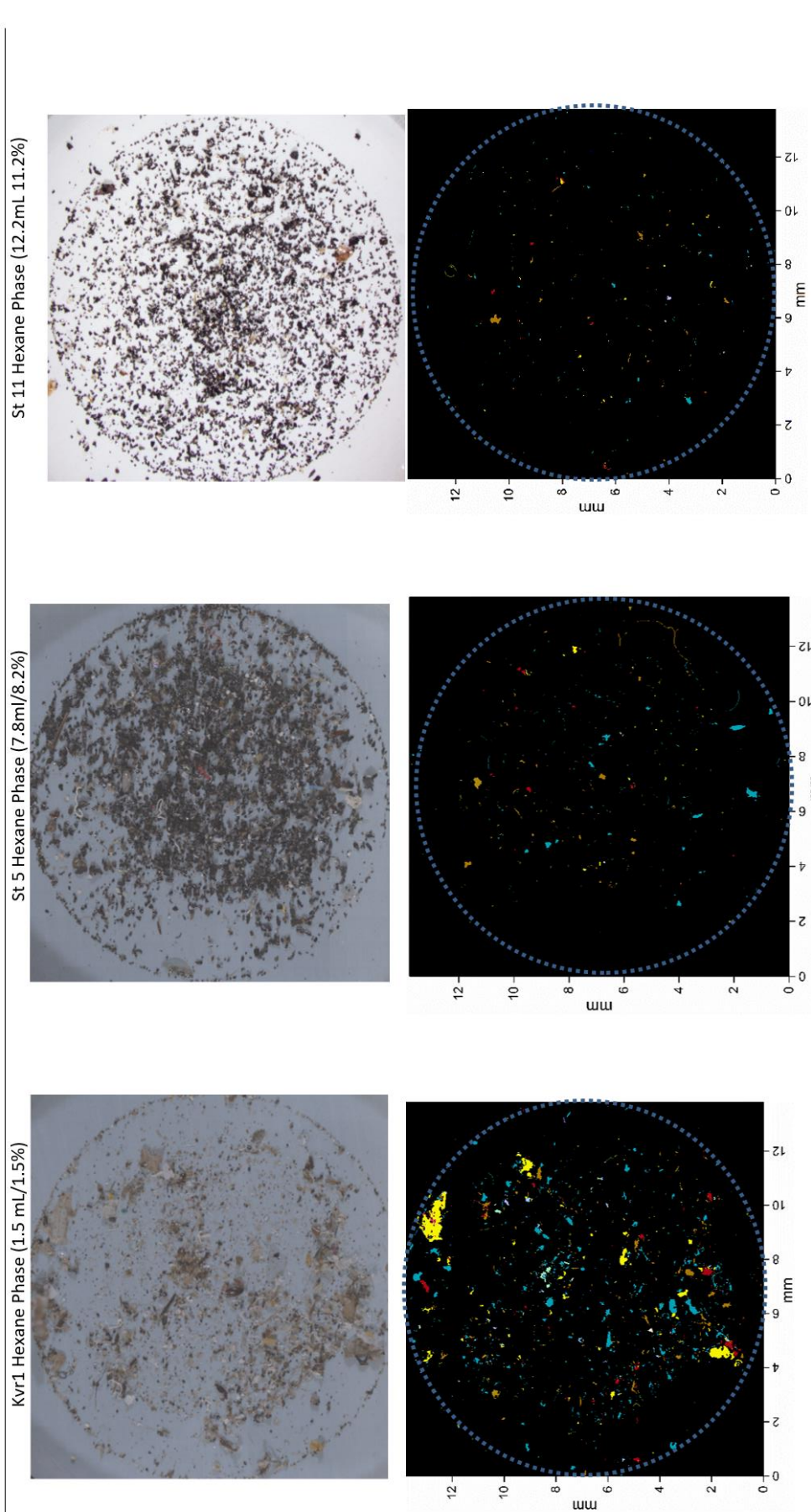


Figure S21: Pictures of Anodisc filters and corresponding False Color Plots (FCP) shows identified polymers following phase separations with n-hexane: NaCl solution (1:1) and FPA μ FTIR identification of retained particles. Colors denote different synthetic polymers. St5 Waterphase bottom is not shown.

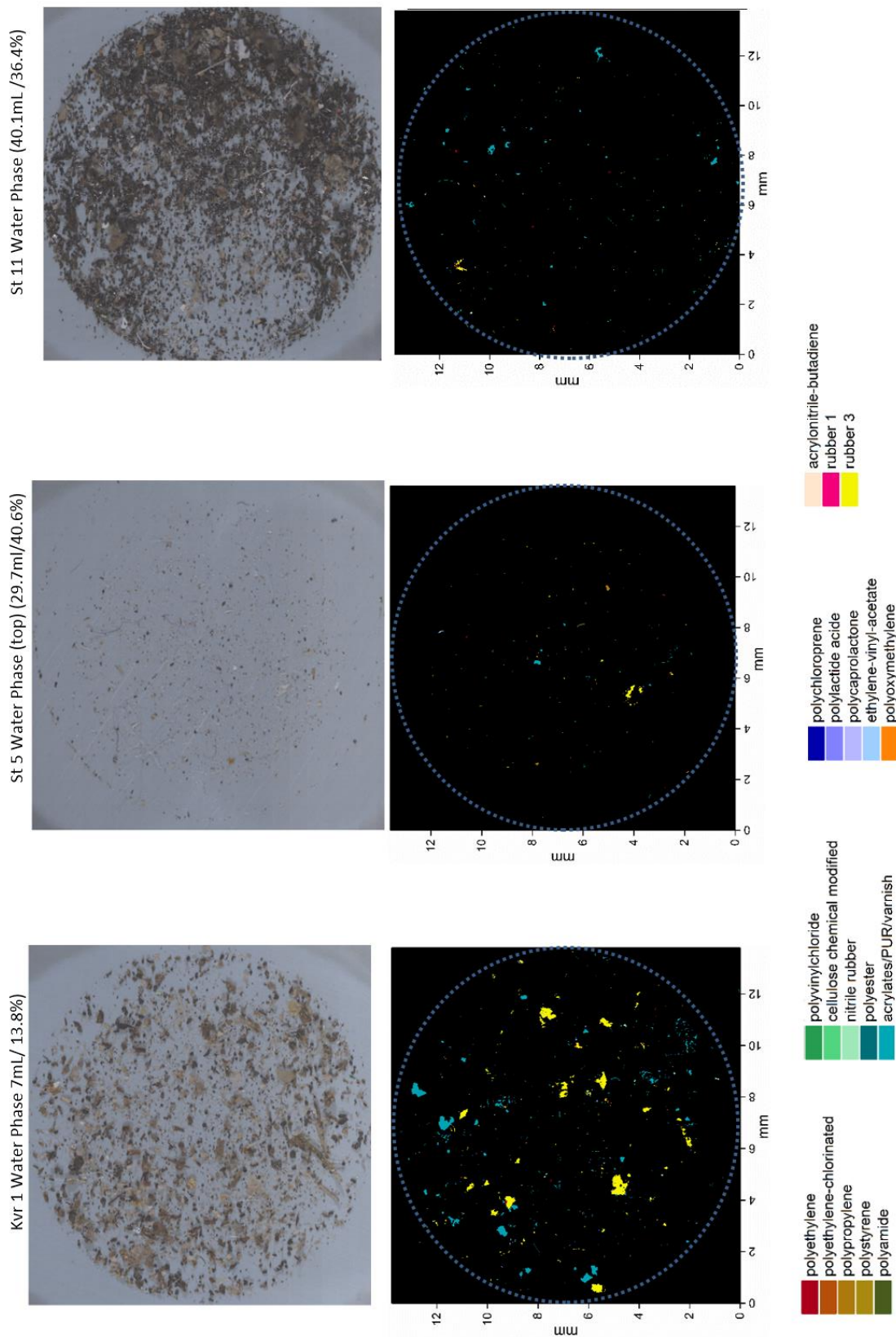


Figure S21 continued: Pictures of Anodisc filters and corresponding False Color Plots (FCP) shows identified polymers following phase separations with n-hexane: NaCl solution (1:1) and FPA μ FTIR identification of retained particles. St5 Waterphase bottom is not shown.

Supplement Chapter IV



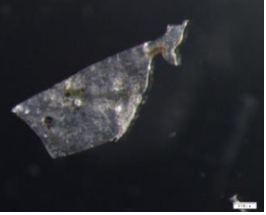

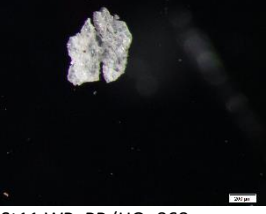
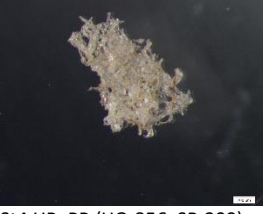

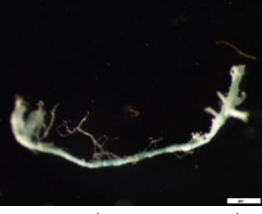
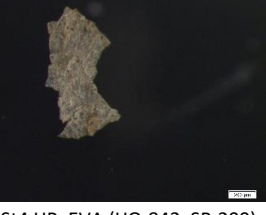
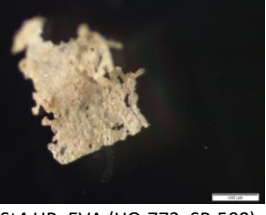
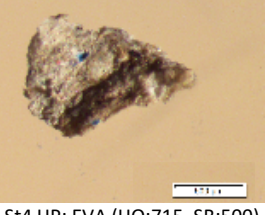


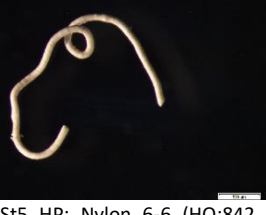




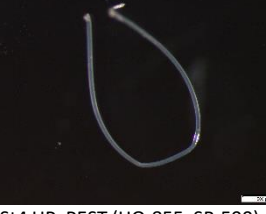



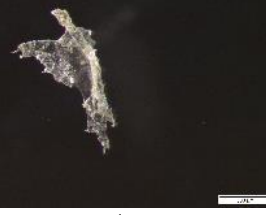
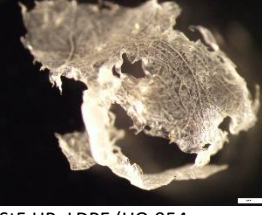
Polyurethanes (PUR)	 St4 HP: PUR/Acrylic resin (HQ: 729, SB:500)	 St4 HP: PUR/Acr varnish (HQ:499*, SB:500)	 St4 HP: PP/PUR-Acr** (HQ:892/559, SB:200)	 St4 HP: PP/PUR/Acr** (HQ: 892/ 552, SB:200)
Polypropylene (PP)	 St11 WP: PP (HQ: 868, SB:200)	 St4 HP: PP (HQ:856, SB:200)	 St5 HP: PP (HQ:850 SB:500)	 St5 HP: PP (HQ:793, SB:500)
Ethyl Vinyl Alcohol (EVA)	 St4 HP: EVA (HQ:842, SB:200)	 St4 HP: EVA (HQ:772, SB:500)	 St4 HP: EVA (HQ:715, SB:500)	 St5 HP: EVA (HQ:700, SB:200)
Polyamide (PA) , nylon and copolyamide (Co-PA)	 St5 HP: Fibre PA-6 (HQ:863, SB:200)	 St5 HP: Nylon 6-6 (HQ:842, SB:500)	 St5 HP: Nylon 6-6 (HQ:860, SB:200)	 St5 HP: Co-PA (HQ:856, SB:500)
Polyester (PEST)	 St5 HP: PEST (HQ:800, SB:200) (w/biofilm)	 St5 HP: PEST (HQ:762, SB:500)	 St4 HP: PEST (HQ:855, SB:500)	 Kvr1 WP: PEST/PET (HQ:804/787, SB:200)
Low Density Polyethylene LDPE	 St11 WP: LDPE (HQ:900, SB:500)	 St4 HP: LDPE (HQ:834; SB:500)	 St4 HP: LDPE (HQ:852, SB:500)	 St5 HP: LDPE (HQ:954, SB:500)

Figure S22: A selection of representative particles from common polymers. * low HQ due to incorporated particles of soot and silt. ** different polymers on each side, both polymers with their respective HQ.

Supplement Chapter IV

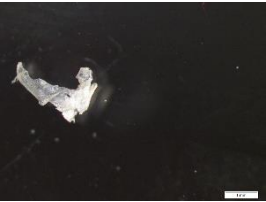
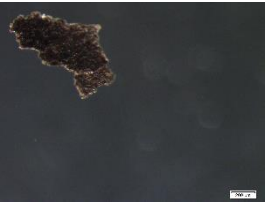
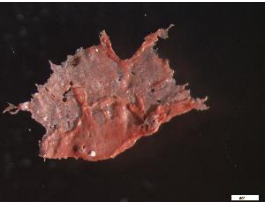
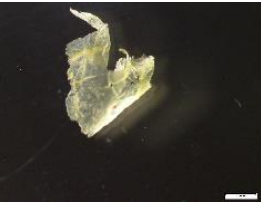



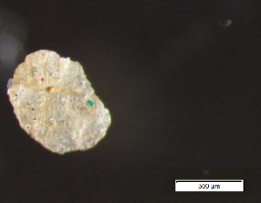


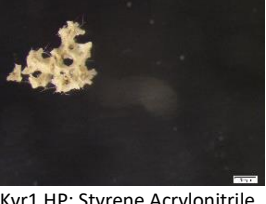
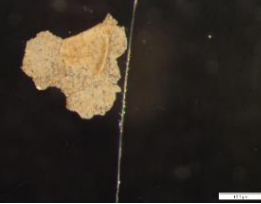
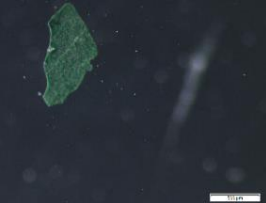
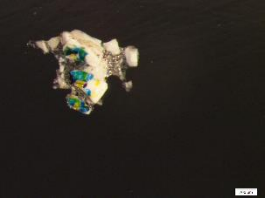
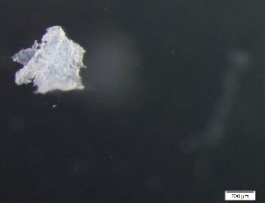
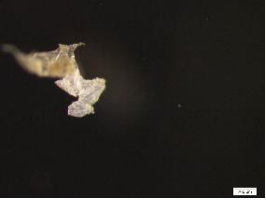
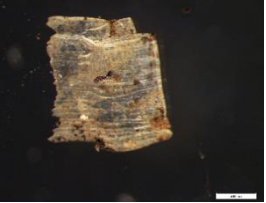
High Density Polyethylene (HDPE)	 St4 HP: HDPE (HQ:949, SB:1mm)	 St5 HP: HDPE (HQ:942, SB:200)	 St4 HP: HDPE (HQ: 901, SB:500)	 St4 HP: HDPE (HQ:907, SB:1mm)
Polystyrene	 St5 HP: PS (HQ:958, SB:200)	 St5 HP: PS (HQ:947, SB:200)	 St4 HP: PS (HQ:925, SB:500)	 St4 HP: PS (HQ:866, SB:500)
Other polymers	 St5 WP: Expanded polystyrene (EPS) (HQ:825, SB:500)	 Kvr1 HP: Styrene Acrylonitrile Copolymer (HQ:708, SB:500)	 Kvr1 HP: Styrene Acrylonitrile Copolymer (HQ:691, SB:200)	 Kvr1 HP: Ethylene Propylene (HQ:638, SB:500)
	 St5 HP: Alkyd varnish (HQ:616, SB:500)	 Kvr1 HP: PP isotactic (HQ:632, SB200)		
Excluded particles	 St4 HP: PTFE/Teflon, (HQ:710, SB:200)	 St5 HP: PTFE/Teflon (HQ:688, SB200)	 St5 HP: Silicone rubber (HQ:856, SB:500)	

Figure S22 continued: A selection of representative particles from common polymers. * low HQ due to incorporated particles of soot and silt. ** different polymers on each side, both polymers with their respective HQ.

Supplement Chapter IV

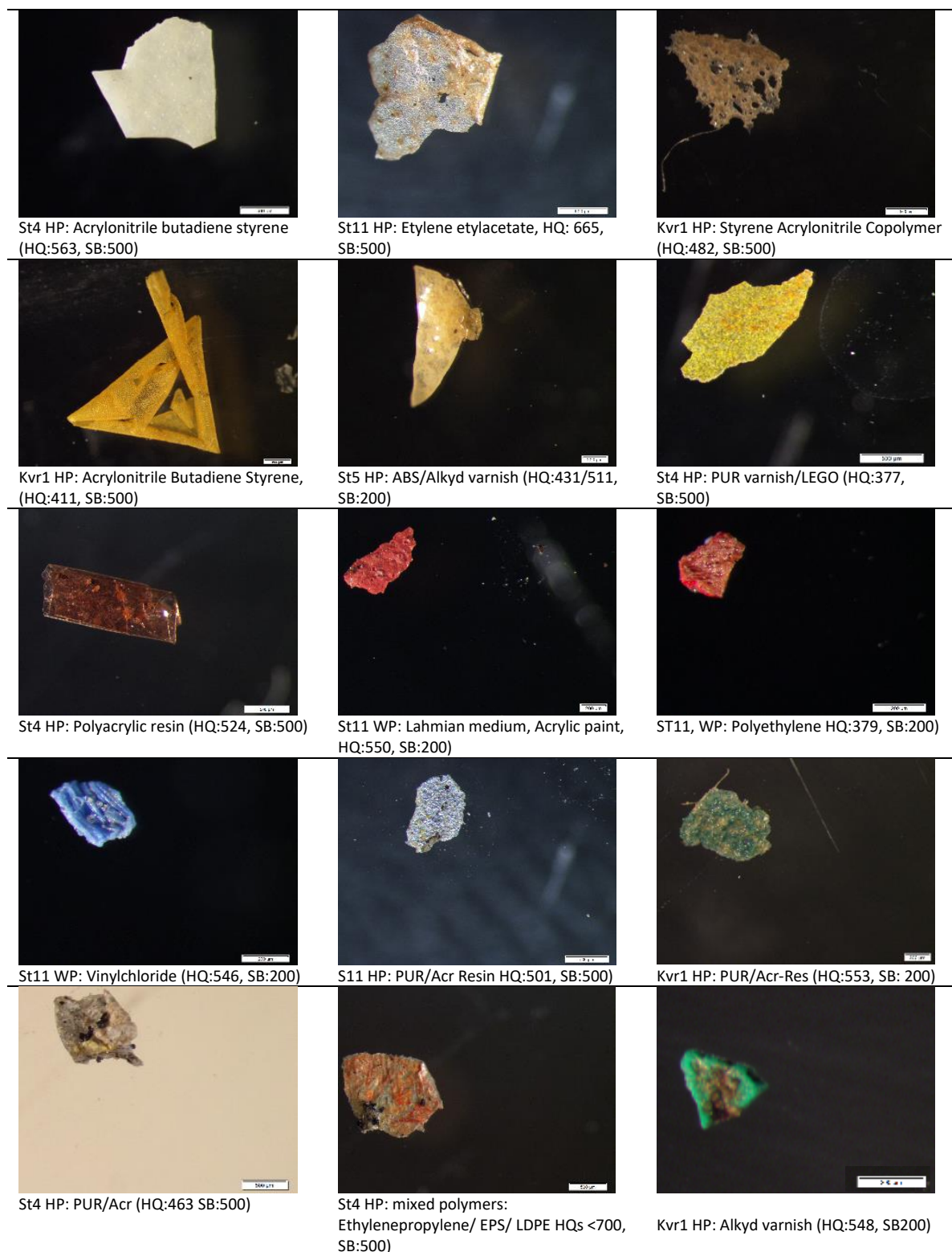


Figure S23: Some examples of MP>500 with HQ>600, thus not classified as MP, of suspected anthropogenic and synthetic origin. Based on visual identification alone, the most colorful of these would be classified as MP, whereas identification based on FTIR Hit Quality as well as manual expert inspection of FTIR spectra excludes them from MP >500 µm

Supplementary material for General Discussion

Tables (3) presenting detailed results related to the General Discussion

Table S24: Number of microplastics per m³ surface water (sampled with a 100 µm net) sorted by size class and station sampled during a cruise with the RV Heincke in 2014 (He430). All values are blank corrected by subtracting the number of microplastics of the same polymer type of each size class identified in the procedural blanks from the sample and extrapolated to m³ sampled surface water.

Size classes	1	2	3	4	5	6	7	8	9	10	11	13	14	15	16	17	18	19	20	21	22	23	24	Sum	Mean	SD	Min	Max
11 µm	2.61	13.22	3.20	8.29	4.64	24.75	2.85	5.20	3.37	1.89	0.86	0.17	21.06	0.00	0.00	5.33	2.23	0.00	148.90	10.95	0.00	67.23	2.43	329.60	14.33	31.98	0.00	148.90
11-25 µm	0.93	6.44	1.41	6.16	0.94	17.25	3.50	0.96	0.00	0.60	0.21	0.00	10.53	0.00	6.33	5.02	1.46	0.46	64.76	6.37	0.00	25.92	1.32	161.17	7.01	13.76	0.00	64.76
25-50 µm	0.93	3.28	0.34	3.39	0.89	9.83	0.73	2.17	0.00	0.21	0.49	0.13	26.33	0.00	1.20	3.59	0.74	0.00	16.82	3.33	0.00	7.34	0.90	82.65	3.59	6.21	0.00	26.33
50-75 µm	0.56	1.06	0.36	1.43	0.47	3.22	0.00	0.96	0.00	0.18	0.11	0.00	5.27	0.00	0.00	0.82	0.74	0.00	8.40	0.32	0.00	0.43	0.19	24.51	1.07	1.97	0.00	8.40
75-100 µm	0.19	0.51	0.36	0.66	0.47	1.53	0.73	0.74	0.00	0.21	0.00	0.00	0.00	0.00	0.00	0.85	0.00	0.00	2.53	0.00	0.00	0.43	0.16	9.37	0.41	0.59	0.00	2.53
100-125 µm	0.00	0.27	0.00	0.26	0.00	0.87	0.00	0.50	0.00	0.21	0.00	0.00	0.00	0.00	0.00	0.35	0.00	0.00	0.00	0.00	0.00	0.00	0.00	2.52	0.11	0.21	0.00	0.87
125-150 µm	0.00	0.07	0.00	0.40	0.47	0.72	0.00	0.74	0.00	0.00	0.00	0.00	0.00	0.00	1.28	0.19	0.00	0.00	0.00	0.34	0.00	0.00	0.05	4.26	0.19	0.33	0.00	1.28
150-175 µm	0.00	0.07	0.36	0.66	0.47	0.00	0.00	0.00	0.00	0.00	0.00	0.00	0.00	0.24	0.00	0.00	0.00	0.00	0.00	0.00	0.00	0.00	0.00	1.79	0.08	0.18	0.00	0.66
175-200 µm	0.00	0.00	0.00	0.40	0.00	0.00	0.00	0.00	0.00	0.00	0.00	0.00	0.00	0.00	0.00	0.09	0.00	0.00	0.84	0.00	0.00	0.00	0.00	1.33	0.06	0.19	0.00	0.84
200-225 µm	0.00	0.03	0.00	0.13	0.00	0.18	0.00	0.00	0.00	0.00	0.00	0.00	0.00	0.00	0.00	0.00	0.00	0.00	0.00	0.00	0.00	0.00	0.00	0.35	0.02	0.04	0.00	0.18
225-250 µm	0.00	0.00	0.00	0.13	0.00	0.00	0.00	0.00	0.00	0.00	0.00	0.00	0.00	0.00	0.00	0.00	0.00	0.00	0.84	0.00	0.00	0.00	0.00	0.97	0.04	0.17	0.00	0.84
250-275 µm	0.00	0.00	0.00	0.26	0.00	0.18	0.00	0.00	0.00	0.00	0.00	0.00	0.00	0.00	0.00	0.09	0.00	0.00	0.00	0.00	0.00	0.00	0.00	0.54	0.02	0.07	0.00	0.26
275-300 µm	0.00	0.00	0.00	0.00	0.00	0.00	0.00	0.00	0.00	0.00	0.00	0.00	0.00	0.00	0.00	0.00	0.00	0.00	0.00	0.00	0.00	0.00	0.00	0.00	0.00	0.00	0.00	0.00
300-325 µm	0.00	0.00	0.00	0.00	0.00	0.00	0.00	0.00	0.00	0.00	0.00	0.00	0.00	0.00	0.00	0.09	0.00	0.00	0.00	0.00	0.00	0.00	0.00	0.09	0.00	0.02	0.00	0.09
325-350 µm	0.00	0.00	0.00	0.13	0.00	0.00	0.00	0.25	0.00	0.00	0.00	0.00	0.00	0.00	0.00	0.00	0.00	0.00	0.00	0.00	0.00	0.00	0.00	0.38	0.02	0.06	0.00	0.25
350-375 µm	0.00	0.00	0.00	0.00	0.00	0.00	0.00	0.00	0.00	0.00	0.00	0.00	0.00	0.00	0.00	0.00	0.00	0.00	0.00	0.00	0.00	0.00	0.00	0.00	0.00	0.00	0.00	0.00
375-400 µm	0.00	0.00	0.00	0.26	0.00	0.00	0.00	0.00	0.00	0.00	0.00	0.00	0.00	0.00	0.00	0.00	0.00	0.00	0.00	0.00	0.00	0.00	0.00	0.26	0.01	0.05	0.00	0.26
400-425 µm	0.00	0.00	0.00	0.00	0.00	0.00	0.00	0.00	0.00	0.00	0.00	0.00	0.00	0.00	0.00	0.00	0.00	0.00	0.00	0.00	0.00	0.00	0.00	0.00	0.00	0.00	0.00	0.00
425-450 µm	0.00	0.00	0.00	0.13	0.00	0.00	0.00	0.00	0.00	0.00	0.00	0.00	0.00	0.00	0.00	0.00	0.00	0.00	0.00	0.00	0.00	0.04	0.00	0.17	0.01	0.03	0.00	0.13
450-475 µm	0.00	0.00	0.00	0.00	0.00	0.00	0.00	0.00	0.00	0.00	0.00	0.00	0.00	0.00	0.00	0.00	0.00	0.00	0.00	0.00	0.00	0.00	0.00	0.00	0.00	0.00	0.00	0.00
475-500 µm	0.00	0.00	0.00	0.00	0.00	0.00	0.00	0.00	0.00	0.00	0.00	0.00	0.00	0.00	0.00	0.00	0.00	0.00	0.00	0.00	0.00	0.00	0.00	0.00	0.00	0.00	0.00	0.00
500-1000 µm	0.00	0.00	0.04	0.04	0.00	0.00	0.00	0.00	0.00	0.00	0.00	0.00	0.00	0.00	0.00	0.00	0.00	0.00	0.39	0.19	0.00	0.10	0.00	0.77	0.03	0.09	0.00	0.39
1000-1500 µm	0.00	0.12	0.00	0.02	0.00	0.00	0.00	0.03	0.00	0.00	0.04	0.00	0.00	0.00	0.04	0.00	0.06	0.00	0.50	0.16	0.02	0.14	0.00	1.13	0.05	0.11	0.00	0.50
1500-2000 µm	0.00	0.07	0.04	0.00	0.00	0.00	0.00	0.00	0.00	0.03	0.00	0.00	0.00	0.00	0.00	0.00	0.00	0.00	0.55	0.08	0.02	0.08	0.03	0.91	0.04	0.11	0.00	0.55
2000-2500 µm	0.00	0.00	0.04	0.00	0.05	0.00	0.00	0.00	0.02	0.00	0.04	0.00	0.00	0.00	0.04	0.00	0.03	0.00	0.50	0.06	0.02	0.04	0.03	0.88	0.04	0.10	0.00	0.50
2500-3000 µm	0.00	0.02	0.02	0.04	0.05	0.00	0.04	0.00	0.10	0.00	0.00	0.00	0.00	0.00	0.00	0.00	0.03	0.00	0.17	0.02	0.00	0.02	0.00	0.51	0.02	0.04	0.00	0.17
3000-3500 µm	0.03	0.00	0.00	0.00	0.00	0.00	0.00	0.03	0.02	0.00	0.00	0.00	0.00	0.00	0.00	0.00	0.00	0.00	0.11	0.02	0.00	0.02	0.00	0.23	0.01	0.02	0.00	0.11
3500-4000 µm	0.00	0.00	0.00	0.00	0.00	0.00	0.00	0.00	0.00	0.00	0.00	0.00	0.00	0.00	0.00	0.00	0.03	0.00	0.06	0.00	0.00	0.00	0.00	0.08	0.00	0.01	0.00	0.06
4000-4500 µm	0.03	0.00	0.00	0.00	0.00	0.00	0.04	0.00	0.00	0.00	0.04	0.00	0.00	0.00	0.00	0.00	0.00	0.03	0.00	0.00	0.00	0.02	0.00	0.15	0.01	0.01	0.00	0.04
4500-5000 µm	0.05	0.00	0.04	0.04	0.00	0.03	0.00	0.00	0.00	0.00	0.04	0.00	0.00	0.00	0.00	0.00	0.00	0.00	0.00	0.00	0.00	0.02	0.00	0.23	0.01	0.02	0.00	0.05
Sum_total	5.34	25.17	6.21	22.85	8.44	58.56	7.89	11.58	3.51	3.33	2.81	0.31	63.19	0.24	8.90	16.43	5.32	0.49	245.37	21.82	0.06	101.85	5.17	624.86	27.17	52.51	0.06	245.37
Sum <500 µm	5.23	24.95	6.02	22.69	8.35	58.53	7.81	11.52	3.37	3.30	2.67	0.31	63.19	0.24	8.81	16.43	5.18	0.46	243.10	21.30	0.00	101.40	5.11	619.96	26.95	52.10	0.00	243.10
Sum >500 µm	0.11	0.22	0.19	0.16	0.10	0.03	0.08	0.06	0.15	0.03	0.14	0.00	0.00	0.00	0.09	0.00	0.14	0.03	2.27	0.53	0.06	0.44	0.06	4.90	0.21	0.46	0.00	2.27
Sum 11-300 µm	5.23	24.95	6.02	22.16	8.35	58.53	7.81	11.28	3.37	3.30	2.67	0.31	63.19	0.24	8.81	16.34	5.18	0.46	243.10	21.30	0.00	101.36	5.11	619.05	26.92	52.10	0.00	243.10
Sum 300-5000 µm	0.11	0.22	0.19	0.69	0.10	0.03	0.08	0.30	0.15	0.03	0.14	0.00	0.00	0.00	0.09	0.09	0.14	0.03	2.27	0.53	0.06	0.48	0.06	5.81	0.25	0.46	0.00	2.27
Sum 11-100 µm	5.23	24.51	5.66	19.92	7.41	56.58	7.81	10.04	3.37	3.09	2.67	0.31	63.19	0.00	7.53	15.61	5.18	0.46	241.41	20.96	0.00	101.36	5.00	607.29	26.40	53.00	0.00	241.41
Sum 100-5000 µm	0.11	0.66	0.55	2.93	1.04	1.98	0.08	1.54	0.15	0.24	0.14	0.00	0.00	0.24	1.37	0.82	0.14	0.03	3.96	0.86	0.06	0.48	0.17	17.56	0.76	1.02	0.00	3.96

Table S25: Number of microplastics per km² surface water (sampled with a 100 µm net) sorted by size class and station sampled during a cruise with the RV Heincke in 2014 (He430). All values are blank corrected by subtracting the number of microplastics of the same polymer type of each size class identified in the procedural blanks from the sample and extrapolated to km² sampled surface water.

Size classes	1	2	3	4	5	6	7	8	9	10	11	13	14	15	16	17	18	19	20	21	22	23	24	Sum	Mean	SD	Min	Max	
11 µm	2.6E+05	1.3E+06	3.2E+05	8.3E+05	4.6E+05	2.5E+06	2.8E+06	5.2E+06	3.4E+05	1.9E+05	1.3E+05	1.7E+04	2.1E+06	0.0E+00	0.0E+00	5.3E+05	2.2E+05	0.0E+00	1.5E+07	0.0E+00	0.0E+00	6.7E+06	2.4E+05	3.3E+07	1.4E+06	3.2E+06	0.0E+00	1.5E+07	
11-25 µm	9.3E+04	6.4E+05	1.4E+05	6.2E+05	9.4E+04	1.7E+06	3.5E+05	9.6E+04	0.0E+00	6.0E+04	8.1E+04	0.0E+00	1.1E+06	0.0E+00	0.0E+00	6.3E+05	1.5E+05	4.6E+04	6.5E+06	1.7E+05	7.0E+05	0.0E+00	1.3E+06	1.6E+07	7.0E+05	1.4E+06	0.0E+00	6.5E+06	
25-50 µm	9.3E+04	3.3E+05	3.4E+04	3.4E+05	8.9E+04	9.8E+05	7.3E+04	2.2E+05	0.0E+00	2.1E+04	4.9E+04	1.3E+04	2.6E+06	0.0E+00	1.2E+05	3.6E+05	7.4E+04	0.0E+00	1.7E+06	3.3E+05	0.0E+00	0.0E+00	7.3E+05	9.0E+04	8.3E+06	3.8E+05	6.2E+05	0.0E+00	2.6E+06
50-75 µm	5.6E+04	1.1E+05	3.8E+04	1.4E+05	4.7E+04	3.2E+05	4.7E+04	1.5E+05	0.0E+00	1.9E+04	1.1E+04	0.0E+00	5.3E+05	0.0E+00	0.0E+00	8.2E+04	7.4E+04	0.0E+00	8.4E+05	3.2E+04	0.0E+00	0.0E+00	4.3E+04	1.9E+04	2.5E+06	4.1E+05	2.0E+05	0.0E+00	8.4E+05
75-100 µm	1.9E+04	5.1E+04	3.8E+04	6.6E+04	4.7E+04	1.5E+05	7.3E+04	7.4E+04	0.0E+00	2.1E+04	0.0E+00	0.0E+00	0.0E+00	0.0E+00	0.0E+00	8.5E+04	0.0E+00	0.0E+00	2.5E+05	0.0E+00	0.0E+00	0.0E+00	4.3E+04	1.6E+04	9.4E+05	1.1E+05	5.9E+04	0.0E+00	2.5E+05
100-125 µm	0.0E+00	2.7E+04	0.0E+00	2.6E+04	0.0E+00	8.7E+04	0.0E+00	5.0E+04	0.0E+00	2.1E+04	0.0E+00	0.0E+00	0.0E+00	0.0E+00	0.0E+00	1.3E+05	3.5E+04	0.0E+00	0.0E+00	0.0E+00	0.0E+00	0.0E+00	0.0E+00	4.3E+05	1.9E+04	2.1E+04	0.0E+00	1.3E+05	
125-150 µm	0.0E+00	6.7E+03	3.8E+04	6.6E+04	4.7E+04	7.2E+04	0.0E+00	7.4E+04	0.0E+00	0.0E+00	0.0E+00	0.0E+00	0.0E+00	0.0E+00	0.0E+00	0.0E+00	0.0E+00	0.0E+00	0.0E+00	0.0E+00	0.0E+00	0.0E+00	0.0E+00	1.8E+05	7.8E+03	1.8E+04	0.0E+00	6.6E+04	
150-175 µm	0.0E+00	0.0E+00	0.0E+00	4.0E+04	0.0E+00	0.0E+00	0.0E+00	0.0E+00	0.0E+00	0.0E+00	0.0E+00	0.0E+00	0.0E+00	0.0E+00	0.0E+00	0.0E+00	0.0E+00	0.0E+00	0.0E+00	0.0E+00	0.0E+00	0.0E+00	0.0E+00	1.3E+05	5.8E+03	1.9E+04	0.0E+00	8.4E+04	
175-200 µm	0.0E+00	3.4E+03	0.0E+00	1.3E+04	0.0E+00	1.8E+04	0.0E+00	0.0E+00	0.0E+00	0.0E+00	0.0E+00	0.0E+00	0.0E+00	0.0E+00	0.0E+00	0.0E+00	0.0E+00	0.0E+00	0.0E+00	0.0E+00	0.0E+00	0.0E+00	0.0E+00	3.5E+04	1.5E+03	4.5E+03	0.0E+00	1.8E+04	
200-225 µm	0.0E+00	0.0E+00	0.0E+00	0.0E+00	0.0E+00	0.0E+00	0.0E+00	0.0E+00	0.0E+00	0.0E+00	0.0E+00	0.0E+00	0.0E+00	0.0E+00	0.0E+00	0.0E+00	0.0E+00	0.0E+00	0.0E+00	0.0E+00	0.0E+00	0.0E+00	0.0E+00	9.7E+04	4.2E+03	1.7E+04	0.0E+00	8.4E+04	
225-250 µm	0.0E+00	0.0E+00	0.0E+00	0.0E+00	0.0E+00	0.0E+00	0.0E+00	0.0E+00	0.0E+00	0.0E+00	0.0E+00	0.0E+00	0.0E+00	0.0E+00	0.0E+00	0.0E+00	0.0E+00	0.0E+00	0.0E+00	0.0E+00	0.0E+00	0.0E+00	0.0E+00	5.4E+04	2.3E+03	6.5E+03	0.0E+00	2.6E+04	
250-275 µm	0.0E+00	0.0E+00	0.0E+00	0.0E+00	0.0E+00	0.0E+00	0.0E+00	0.0E+00	0.0E+00	0.0E+00	0.0E+00	0.0E+00	0.0E+00	0.0E+00	0.0E+00	0.0E+00	0.0E+00	0.0E+00	0.0E+00	0.0E+00	0.0E+00	0.0E+00	0.0E+00	0.0E+00	0.0E+00	0.0E+00	0.0E+00	0.0E+00	0.0E+00
275-300 µm	0.0E+00	0.0E+00	0.0E+00	0.0E+00	0.0E+00	0.0E+00	0.0E+00	0.0E+00	0.0E+00	0.0E+00	0.0E+00	0.0E+00	0.0E+00	0.0E+00	0.0E+00	0.0E+00	0.0E+00	0.0E+00	0.0E+00	0.0E+00	0.0E+00	0.0E+00	0.0E+00	0.0E+00	0.0E+00	0.0E+00	0.0E+00	0.0E+00	0.0E+00
300-325 µm	0.0E+00	0.0E+00	0.0E+00	0.0E+00	0.0E+00	0.0E+00	0.0E+00	0.0E+00	0.0E+00	0.0E+00	0.0E+00	0.0E+00	0.0E+00	0.0E+00	0.0E+00	0.0E+00	0.0E+00	0.0E+00	0.0E+00	0.0E+00	0.0E+00	0.0E+00	0.0E+00	0.0E+00	0.0E+00	0.0E+00	0.0E+00	0.0E+00	0.0E+00
325-350 µm	0.0E+00	0.0E+00	0.0E+00	0.0E+00	0.0E+00	0.0E+00	0.0E+00	0.0E+00	0.0E+00	0.0E+00	0.0E+00	0.0E+00	0.0E+00	0.0E+00	0.0E+00	0.0E+00	0.0E+00	0.0E+00	0.0E+00	0.0E+00	0.0E+00	0.0E+00	0.0E+00	0.0E+00	0.0E+00	0.0E+00	0.0E+00	0.0E+00	0.0E+00
350-375 µm	0.0E+00	0.0E+00	0.0E+00	0.0E+00	0.0E+00	0.0E+00	0.0E+00	0.0E+00	0.0E+00	0.0E+00	0.0E+00	0.0E+00	0.0E+00	0.0E+00	0.0E+00	0.0E+00	0.0E+00	0.0E+00	0.0E+00	0.0E+00	0.0E+00	0.0E+00	0.0E+00	0.0E+00	0.0E+00	0.0E+00	0.0E+00	0.0E+00	0.0E+00
375-400 µm	0.0E+00	0.0E+00	0.0E+00	0.0E+00	0.0E+00	0.0E+00	0.0E+00	0.0E+00	0.0E+00	0.0E+00	0.0E+00	0.0E+00	0.0E+00	0.0E+00	0.0E+00	0.0E+00	0.0E+00	0.0E+00	0.0E+00	0.0E+00	0.0E+00	0.0E+00	0.0E+00	0.0E+00	0.0E+00	0.0E+00	0.0E+00	0.0E+00	0.0E+00
400-425 µm	0.0E+00	0.0E+00	0.0E+00	0.0E+00	0.0E+00	0.0E+00	0.0E+00	0.0E+00	0.0E+00	0.0E+00	0.0E+00	0.0E+00	0.0E+00	0.0E+00	0.0E+00	0.0E+00	0.0E+00	0.0E+00	0.0E+00	0.0E+00	0.0E+00	0.0E+00	0.0E+00	0.0E+00	0.0E+00	0.0E+00	0.0E+00	0.0E+00	0.0E+00
425-450 µm	0.0E+00	0.0E+00	0.0E+00	0.0E+00	0.0E+00	0.0E+00	0.0E+00	0.0E+00	0.0E+00	0.0E+00	0.0E+00	0.0E+00	0.0E+00	0.0E+00	0.0E+00	0.0E+00	0.0E+00	0.0E+00	0.0E+00	0.0E+00	0.0E+00	0.0E+00	0.0E+00	0.0E+00	0.0E+00	0.0E+00	0.0E+00	0.0E+00	0.0E+00
450-475 µm	0.0E+00	0.0E+00	0.0E+00	0.0E+00	0.0E+00	0.0E+00	0.0E+00	0.0E+00	0.0E+00	0.0E+00	0.0E+00	0.0E+00	0.0E+00	0.0E+00	0.0E+00	0.0E+00	0.0E+00	0.0E+00	0.0E+00	0.0E+00	0.0E+00	0.0E+00	0.0E+00	0.0E+00	0.0E+00	0.0E+00	0.0E+00	0.0E+00	0.0E+00
475-500 µm	0.0E+00	0.0E+00	0.0E+00	0.0E+00	0.0E+00	0.0E+00	0.0E+00	0.0E+00	0.0E+00	0.0E+00	0.0E+00	0.0E+00	0.0E+00	0.0E+00	0.0E+00	0.0E+00	0.0E+00	0.0E+00	0.0E+00	0.0E+00	0.0E+00	0.0E+00	0.0E+00	0.0E+00	0.0E+00	0.0E+00	0.0E+00	0.0E+00	0.0E+00
500-1000 µm	0.0E+00	1.2E+04	4.3E+03	4.5E+03	0.0E+00	0.0E+00	0.0E+00	0.0E+00	0.0E+00	0.0E+00	0.0E+00	0.0E+00	0.0E+00	0.0E+00	0.0E+00	0.0E+00	0.0E+00	0.0E+00	0.0E+00	0.0E+00	0.0E+00	0.0E+00	0.0E+00	0.0E+00	0.0E+00	0.0E+00	0.0E+00	0.0E+00	0.0E+00
1000-1500 µm	0.0E+00	0.0E+00	0.0E+00	0.0E+00	0.0E+00	0.0E+00	0.0E+00	0.0E+00	0.0E+00	0.0E+00	0.0E+00	0.0E+00	0.0E+00	0.0E+00	0.0E+00	0.0E+00	0.0E+00	0.0E+00	0.0E+00	0.0E+00	0.0E+00	0.0E+00	0.0E+00	0.0E+00	0.0E+00	0.0E+00	0.0E+00	0.0E+00	0.0E+00
1500-2000 µm	0.0E+00	0.0E+00	0.0E+00	0.0E+00	0.0E+00	0.0E+00	0.0E+00	0.0E+00	0.0E+00	0.0E+00	0.0E+00	0.0E+00	0.0E+00	0.0E+00	0.0E+00	0.0E+00	0.0E+00	0.0E+00	0.0E+00	0.0E+00	0.0E+00	0.0E+00	0.0E+00	0.0E+00	0.0E+00	0.0E+00	0.0E+00	0.0E+00	0.0E+00
2000-2500 µm	0.0E+00	0.0E+00	0.0E+00	0.0E+00	0.0E+00	0.0E+00	0.0E+00	0.0E+00	0.0E+00	0.0E+00	0.0E+00	0.0E+00	0.0E+00	0.0E+00	0.0E+00	0.0E+00	0.0E+00	0.0E+00	0.0E+00	0.0E+00	0.0E+00	0.0E+00	0.0E+00	0.0E+00	0.0E+00	0.0E+00	0.0E+00	0.0E+00	0.0E+00
2500-3000 µm	0.0E+00	0.0E+00	0.0E+00	0.0E+00	0.0E+00	0.0E+00	0.0E+00	0.0E+00	0.0E+00	0.0E+00	0.0E+00	0.0E+00	0.0E+00	0.0E+00	0.0E+00	0.0E+00	0.0E+00	0.0E+00	0.0E+00	0.0E+00	0.0E+00	0.0E+00	0.0E+00	0.0E+00	0.0E+00	0.0E+00	0.0E+00	0.0E+00	0.0E+00
3000-3500 µm	2.7E+03	0.0E+00	0.0E+00	0.0E+00	0.0E+00	0.0E+00	0.0E+00	0.0E+00	0.0E+00	0.0E+00	0.0E+00	0.0E+00	0.0E+00	0.0E+00	0.0E+00	0.0E+00	0.0E+00	0.0E+00	0.0E+00	0.0E+00	0.0E+00	0.0E+00	0.0E+00	0.0E+00	0.0E+00	0.0E+00	0.0E+00	0.0E+00	0.0E+00
3500-4000 µm	0.0E+00	0.0E+00	0.0E+00	0.0E+00	0.0E+00	0.0E+00	0.0E+00	0.0E+00	0.0E+00	0.0E+00	0.0E+00	0.0E+00	0.0E+00	0.0E+00	0.0E+00	0.0E+00	0.0E+00	0.0E+00	0.0E+00	0.0E+00	0.0E+00	0.0E+00	0.0E+00	0.0E+00	0.0E+00	0.0E+00	0.0E+00	0.0E+00	0.0E+00
4000-4500 µm	2.7E+03	0.0E+00	0.0E+00	0.0E+00	0.0E+00	0.0E+00	0.0E+00	0.0E+00	0.0E+00	0.0E+00	0.0E+00	0.0E+00	0.0E+00	0.0E+00	0.0E+00	0.0E+00	0.0E+00	0.0E+00	0.0E+00	0.0E+00	0.0E+00	0.0E+00	0.0E+00	0.0E+00	0.0E+00	0.0E+00	0.0E+00	0.0E+00	0.0E+00
4500-5000 µm	5.4E+03	0.0E+00	4.3E+03	4.5E+03	0.0E+00	2.8E+03	0.0E+00	0.0E+00	0.0E+00	0.0E+00	3.5E+03	0.0E+00	0.0E+00	0.0E+00	0.0E+00	0.0E+00	0.0E+00	0.0E+00	0.0E+00	0.0E+00	0.0E+00	0.0E+00	0.0E+00	0.0E+00	0.0E+00	0.0E+00	0.0E+00	0.0E+00	0.0E+00
Sum_total	5.3E+05	2.5E+06	6.2E+05	2.3E+06	8.4E+05	5.9E+06	7.9E+05	1.2E+06	3.5E+05	3.3E+05	2.8E+05	3.1E+04	6.3E+06	2.4E+04	8.9E+05	1.6E+06	5.3E+05	4.9E+04	2.5E+07	2.2E+06	6.4E+03	1.0E+07	5.2E+05	6.2E+07	2.7E+06	5.3E+06	6.4E+03	2.5E+07	
Sum <500 µm	5.2E+05	2.5E+06	6.0E+05	2.3E+06	8.3E+05	5.9E+06	7.8E+05	1.2E+06	3.4E+05	3.3E+05	2.7E+05	3.1E+04	6.3E+06	2.4E+04	8.8E+05	1.6E+06	5.2E+05	4.6E+04	2.4E+07	2.1E+06	0.0E+00	1.0E+07	5.1E+05	6.2E+07	2.7E+06	5.2E+06	0.0E+00	2.4E+07	
Sum >500 µm	1.1E+04	2.2E+04	1.9E+04	1.6E+04	9.9E+03	2.8E+03	8.1E+03	5.7E+03	1.5E+04	2.8E+03	1.4E+04	0.0E+00	0.0E+00	0.0E+00	8.9E+03	0.0E+00	1.4E+04	3.0E+03	2.3E+05	5.3E+04	6.4E+03	4.4E+04	6.3E+03	4.9E+05	2.1E+04	4.8E+04	0.0E+00	2.4E+05	
Sum 11-300 µm	5.2E+05	2.5E+06																											

Table S26: Number of microplastics per kg dry weight sediment (sampled with Van Veen grab) sorted by size class and station sampled during a cruise with the RV Heincke in 2014 (He430). All values are blank corrected by subtracting the number of microplastics of the same polymer type of each size class identified in the procedural blanks from the sample and extrapolated to kg (dry weight) sediment.

Size classes	1	2	3	4	5	6	7	8	9	10	11	12	13	14	15	16	18	19	20	21	22	23	24	Sum	Mean	SD	Min	Max
11 µm	165.54	156.86	164.93	55.08	115.50	160.97	39.09	59.68	11.05	307.60	0.00	138.38	45.25	3.42	18.47	4.92	29.70	39.00	69.96	67.04	380.29	677.79	125.96	2836.51	123.33	151.05	0.00	677.79
11-25 µm	44.84	43.11	79.22	31.74	52.87	73.23	17.46	34.76	8.30	118.98	0.40	53.35	46.86	10.69	10.93	9.60	29.70	31.70	33.57	35.13	141.83	219.58	57.22	1191.19	51.79	48.96	0.40	219.58
25-50 µm	30.49	55.95	37.89	18.24	39.73	54.99	26.56	18.25	11.07	76.51	0.60	42.20	32.79	12.82	21.72	4.39	22.02	22.76	31.57	20.49	83.07	206.13	34.48	904.70	39.33	40.84	0.60	206.13
50-75 µm	14.46	16.58	13.78	9.12	6.11	17.18	8.39	2.61	3.69	15.84	1.80	5.28	12.70	5.56	15.43	1.66	4.98	8.13	6.83	13.17	15.82	49.76	10.01	258.88	11.26	9.60	1.66	49.76
75-100 µm	10.52	5.18	6.89	2.49	3.06	6.87	1.40	0.87	2.77	19.85	0.00	10.55	1.27	0.21	8.24	0.00	0.83	0.81	4.27	0.00	3.96	0.00	3.34	93.37	4.06	4.66	0.00	19.85
100-125 µm	1.86	3.11	3.44	2.49	0.00	0.00	1.40	0.87	0.00	0.00	0.00	0.00	1.48	0.00	1.13	1.66	0.00	0.81	1.71	1.46	0.00	7.11	2.22	30.76	1.34	1.62	0.00	7.11
125-150 µm	1.86	2.07	3.44	0.00	0.00	5.16	2.80	1.74	0.92	0.00	0.00	2.84	0.00	0.85	1.13	0.00	0.00	1.63	0.00	3.96	21.32	3.34	53.06	2.31	4.32	0.00	21.32	3.34
150-175 µm	1.86	0.00	0.00	0.00	0.00	0.00	0.00	1.74	0.00	0.00	0.00	0.00	0.00	0.00	0.00	0.00	0.00	1.63	0.85	0.00	0.00	0.00	1.11	7.19	0.31	0.62	0.00	1.86
175-200 µm	0.00	0.00	0.00	0.00	0.00	0.00	0.00	0.00	0.00	0.00	0.00	2.84	0.00	0.00	0.00	0.00	0.00	0.00	0.85	0.00	0.00	0.00	0.00	3.70	0.16	0.60	0.00	2.84
200-225 µm	0.00	0.00	0.00	0.00	0.00	0.00	0.00	0.00	0.00	0.00	0.00	0.00	0.00	0.00	0.00	0.00	0.00	0.00	0.00	0.00	0.00	0.00	1.11	1.11	0.05	0.23	0.00	1.11
225-250 µm	0.00	0.00	0.00	0.00	0.00	0.00	0.00	0.00	0.92	0.00	0.00	0.00	0.00	0.00	0.00	0.00	0.83	0.00	0.00	0.00	0.00	0.00	0.00	1.75	0.08	0.25	0.00	0.92
250-275 µm	0.00	0.00	0.00	0.00	0.00	0.00	1.40	0.00	0.00	0.00	0.00	0.00	0.00	0.00	0.00	0.00	0.00	0.00	0.00	0.00	0.00	0.00	0.00	1.40	0.06	0.29	0.00	1.40
275-300 µm	0.00	0.00	0.00	0.00	0.00	0.00	0.00	0.00	0.00	0.00	0.00	0.00	0.00	0.00	0.00	0.00	0.00	0.00	0.00	0.00	0.00	1.11	8.22	0.36	1.46	0.00	7.11	1.11
300-325 µm	0.00	0.00	0.00	0.00	0.00	0.00	0.00	0.00	0.00	0.00	0.00	0.00	0.00	0.00	0.00	0.00	0.00	0.00	0.00	0.00	0.00	0.00	0.00	0.00	0.00	0.00	0.00	0.00
325-350 µm	0.00	0.00	0.00	0.00	0.00	0.00	0.00	0.00	0.00	0.00	0.00	0.00	0.00	0.00	0.00	0.00	0.00	0.00	0.00	0.00	0.00	0.00	0.00	0.00	0.00	0.00	0.00	0.00
350-375 µm	0.00	0.00	0.00	0.00	0.00	0.00	0.00	0.00	0.00	0.00	0.00	0.00	0.00	0.00	0.00	0.00	0.00	0.00	0.00	0.00	0.00	0.00	0.00	0.00	0.00	0.00	0.00	0.00
375-400 µm	0.00	0.00	0.00	0.00	0.00	0.00	0.00	0.00	0.00	0.00	0.00	0.00	0.00	0.00	0.00	0.00	0.00	0.00	0.00	0.00	0.00	0.00	0.00	0.00	0.00	0.00	0.00	0.00
400-425 µm	0.00	0.00	0.00	0.00	0.00	0.00	0.00	0.00	0.00	0.00	0.00	0.00	0.00	0.00	0.00	0.00	0.00	0.00	0.00	0.00	0.00	0.00	0.00	0.00	0.00	0.00	0.00	0.00
425-450 µm	0.00	0.00	0.00	0.00	0.00	0.00	0.00	0.00	0.00	0.00	0.00	0.00	0.00	0.00	0.00	0.00	0.00	0.00	0.00	0.00	0.00	0.00	0.00	0.00	0.00	0.00	0.00	0.00
450-475 µm	0.00	0.00	0.00	0.00	0.00	0.00	0.00	0.00	0.00	0.00	0.00	0.00	0.00	0.00	0.00	0.00	0.00	0.00	0.00	0.00	0.00	0.00	0.00	0.00	0.00	0.00	0.00	0.00
475-500 µm	0.00	0.00	0.00	0.00	0.00	0.00	0.00	0.00	0.00	0.00	0.00	0.00	0.00	0.00	0.00	0.00	0.00	0.00	0.00	0.00	0.00	0.00	0.00	0.00	0.00	0.00	0.00	0.00
500-1000 µm	0.00	0.00	0.00	0.00	0.00	0.00	0.00	0.00	0.00	0.00	0.00	0.00	0.00	0.00	0.00	0.00	0.00	0.00	0.00	0.00	0.00	0.00	0.00	0.00	0.00	0.00	0.00	0.00
1000-1500 µm	0.00	0.00	0.00	0.00	0.00	0.00	0.00	0.00	0.00	0.00	0.00	0.00	0.00	0.00	0.00	0.00	0.00	0.00	0.00	0.00	0.00	0.00	0.00	0.00	0.00	0.00	0.00	0.00
1500-2000 µm	0.00	0.00	0.00	0.00	0.00	0.00	0.00	0.00	0.00	0.00	0.00	0.00	0.00	0.00	0.00	0.00	0.00	0.00	0.00	0.00	0.00	0.00	0.00	0.00	0.00	0.00	0.00	0.00
2000-2500 µm	0.00	0.00	0.00	0.00	0.00	0.00	0.00	0.00	0.00	0.00	0.00	0.00	0.00	0.00	0.00	0.00	0.00	0.00	0.00	0.00	0.00	0.00	0.00	0.00	0.00	0.00	0.00	0.00
2500-3000 µm	0.00	0.00	0.00	0.00	0.00	0.00	0.00	0.00	0.00	0.00	0.00	0.00	0.00	0.00	0.00	0.00	0.00	0.00	0.00	0.00	0.00	0.00	0.00	0.00	0.00	0.00	0.00	0.00
3000-3500 µm	0.00	0.00	0.00	0.00	0.00	0.00	0.00	0.00	0.00	0.63	0.00	0.00	0.00	0.00	0.00	0.00	0.00	0.00	0.00	0.00	0.00	0.00	0.00	0.63	0.03	0.13	0.00	0.63
3500-4000 µm	0.00	0.00	0.00	0.00	0.00	0.00	0.00	0.00	0.00	0.00	0.00	0.00	0.00	0.00	0.00	0.00	0.00	0.00	0.00	0.00	0.00	0.00	0.00	0.00	0.00	0.00	0.00	0.00
4000-4500 µm	0.00	0.00	0.00	0.00	0.00	0.00	0.00	0.00	0.00	0.00	0.00	0.00	0.00	0.00	0.00	0.00	0.00	0.00	0.00	0.00	0.00	0.00	0.00	0.00	0.00	0.00	0.00	0.00
4500-5000 µm	0.00	0.00	0.00	0.00	0.00	0.00	0.00	0.00	0.00	0.00	0.00	0.00	0.00	0.00	0.00	0.00	0.62	0.00	0.00	0.00	0.00	0.00	0.00	0.62	0.03	0.13	0.00	0.62
Sum_total	271.42	288.87	309.60	119.16	217.27	318.40	98.49	120.51	38.72	539.41	2.79	255.44	140.45	33.56	77.06	22.24	88.69	106.47	149.62	137.31	628.92	1188.80	239.90	5393.10	234.48	254.28	2.79	1188.80
Sum <500 µm	271.42	288.87	309.60	119.16	217.27	318.40	98.49	120.51	38.72	538.78	2.79	255.44	140.45	33.56	77.06	22.24	88.06	106.47	149.62	137.31	628.92	1188.80	239.90	5391.85	234.43	254.27	2.79	1188.80
Sum >500 µm	0.00	0.00	0.00	0.00	0.00	0.00	0.00	0.00	0.00	0.63	0.00	0.00	0.00	0.00	0.00	0.00	0.62	0.00	0.00	0.00	0.00	0.00	0.00	1.25	0.05	0.18	0.00	0.63
Sum 11-300 µm	271.42	288.87	309.60	119.16	217.27	318.40	98.49	120.51	38.72	538.78	2.79	255.44	140.45	33.56	77.06	22.24	88.06	106.47	149.62	137.31	628.92	1188.80	239.90	5391.85	234.43	254.27	2.79	1188.80
Sum 300-5000 µm	0.00	0.00	0.00	0.00	0.00	0.00	0.00	0.00	0.00	0.63	0.00	0.00	0.00	0.00	0.00	0.00	0.62	0.00	0.00	0.00	0.00	0.00	0.00	1.25	0.05	0.18	0.00	0.63

References

- Allen, S., Allen, D., Moss, K., Le Roux, G., Phoenix, V. R., & Sonke, J. E. (2020). Examination of the ocean as a source for atmospheric microplastics. *PLOS ONE*, 15(5), e0232746. doi:<https://doi.org/10.1371/journal.pone.0232746>
- Anderson, M. J. (2001). A new method for non-parametric multivariate analysis of variance. *Austral Ecology*, 26(1), 32-46. doi:<https://doi.org/10.1111/j.1442-9993.2001.01070.pp.x>
- Anderson, M. J., & Walsh, D. C. I. (2013). PERMANOVA, ANOSIM, and the Mantel test in the face of heterogeneous dispersions: What null hypothesis are you testing? *Ecological Monographs*, 83(4), 557-574. doi:<https://doi.org/10.1890/12-2010.1>
- Anderson, M. J., & Willis, T. J. (2003). Canonical analysis of principal coordinates: a useful method of constrained ordination for ecology. *Ecology*, 84(2), 511-525.
- Andrade, J. M., Ferreira, B., López-Mahía, P., & Muniategui-Lorenzo, S. (2020). Standardization of the minimum information for publication of infrared-related data when microplastics are characterized. *Marine Pollution Bulletin*, 154, 111035. doi:<https://doi.org/10.1016/j.marpolbul.2020.111035>
- Andrady, A. L. (1994). Assessment of Environmental Biodegradation of Synthetic Polymers. *Journal of Macromolecular Science, Part C*, 34(1), 25-76. doi:<http://dx.doi.org/10.1080/15321799408009632>
- Andrady, A. L. (2009). *Fate of Plastics Debris in the Marine Environment*. Paper presented at the Proceedings of the International Research Workshop on the Occurrence, Effects, and Fate of Microplastic Marine Debris. Sept 9-11, 2008. NOAA Technical Memorandum NOS-OR&R-30.
- Andrady, A. L. (2011). Microplastics in the marine environment. *Marine Pollution Bulletin*, 62(8), 1596-1605. doi:<http://dx.doi.org/10.1016/j.marpolbul.2011.05.030>
- Andrady, A. L. (2017). The plastic in microplastics: A review. *Marine Pollution Bulletin*, 119(1), 12-22. doi:<https://doi.org/10.1016/j.marpolbul.2017.01.082>
- Anger, P. M., Prechtel, L., Elsner, M., Niessner, R., & Ivleva, N. P. (2019). Implementation of an open source algorithm for particle recognition and morphological characterisation for microplastic analysis by means of Raman microspectroscopy. *Analytical Methods*, 11(27), 3483-3489. doi:<http://dx.doi.org/10.1039/C9AY01245A>
- Anger, P. M., von der Esch, E., Baumann, T., Elsner, M., Niessner, R., & Ivleva, N. P. (2018). Raman microspectroscopy as a tool for microplastic particle analysis. *TrAC Trends in Analytical Chemistry*, 109, 214-226. doi:<https://doi.org/10.1016/j.trac.2018.10.010>
- Arp, H. P. H., & Knutsen, H. (2020). Could We Spare a Moment of the Spotlight for Persistent, Water-Soluble Polymers? *Environmental Science & Technology*, 54(1), 3-5. doi:<https://doi.org/10.1021/acs.est.9b07089>
- Arthur, C., Baker, J., & Bamford, H. (2009). *Proceedings of the International Research Workshop on the Occurrence, Effects and Fate of Microplastic Marine Debris*. Sept 9-11, 2008. NOAA Technical Memorandum NOS-OR&R-30. Retrieved from <https://marinedebris.noaa.gov/proceedings-international-research-workshop-microplastic-marine-debris>
- Avio, C. G., Gorbi, S., & Regoli, F. (2015). Experimental development of a new protocol for extraction and characterization of microplastics in fish tissues: First observations in commercial species from Adriatic Sea. *Marine Environmental Research*, 111, 18-26. doi:<http://dx.doi.org/10.1016/j.marenvres.2015.06.014>
- Bagaev, A., Mizyuk, A., Khatmullina, L., Isachenko, I., & Chubarenko, I. (2017). Anthropogenic fibres in the Baltic Sea water column: Field data, laboratory and numerical testing of their motion. *Science of the Total Environment*, 599, 560-571. doi:<https://dx.doi.org/10.1016/j.scitotenv.2017.04.185>
- Ballent, A., Pando, S., Purser, A., Juliano, M. F., & Thomsen, L. (2013). Modelled transport of benthic marine microplastic pollution in the Nazaré Canyon. *Biogeosciences*, 10(12), 7957-7970. doi:<https://doi.org/10.5194/bg-10-7957-2013>

References

- Behr, A., & Seidenstricker, T. (2017). *Einführung in die Chemie nachwachsender Rohstoffe: Vorkommen, Konversion, Verwendung*: Springer.
- Bergmann, M., Mützel, S., Primpke, S., Tekman, M. B., Trachsel, J., & Gerdts, G. (2019). White and wonderful? Microplastics prevail in snow from the Alps to the Arctic. *Science Advances*, 5(8), eaax1157. doi:<http://dx.doi.org/10.1126/sciadv.aax1157>
- Bergmann, M., Wirzberger, V., Krumpen, T., Lorenz, C., Primpke, S., Tekman, M. B., & Gerdts, G. (2017). High quantities of microplastic in Arctic deep-sea sediments from the HAUSGARTEN Observatory. *Environmental Science & Technology*, 51(19), 11000-11010. doi:<https://doi.org/10.1021/acs.est.7b03331>
- Besseling, E., Wegner, A., Foekema, E. M., van den Heuvel-Greve, M. J., & Koelmans, A. A. (2013). Effects of Microplastic on Fitness and PCB Bioaccumulation by the Lugworm *Arenicola marina* (L.). *Environmental Science & Technology*, 47(1), 593-600. doi:<http://dx.doi.org/10.1021/es302763x>
- Bordós, G., Urbányi, B., Micsinai, A., Kriszt, B., Palotai, Z., Szabó, I., Hantosi, Z., & Szoboszlai, S. (2019). Identification of microplastics in fish ponds and natural freshwater environments of the Carpathian basin, Europe. *Chemosphere*, 216, 110-116. doi:<https://doi.org/10.1016/j.chemosphere.2018.10.110>
- Brahney, J., Hallerud, M., Heim, E., Hahnenberger, M., & Sukumaran, S. (2020). Plastic rain in protected areas of the United States. *Science*, 368(6496), 1257-1260. doi:<https://doi.org/10.1126/science.aaz5819>
- Brandon, J., Goldstein, M., & Ohman, M. D. (2016). Long-term aging and degradation of microplastic particles: Comparing in situ oceanic and experimental weathering patterns. *Marine Pollution Bulletin*, 110(1), 299-308. doi:<http://dx.doi.org/10.1016/j.marpolbul.2016.06.048>
- Brandt, J., Bittrich, L., Fischer, F., Kanaki, E., Tagg, A., Lenz, R., Labrenz, M., Brandes, E., Fischer, D., & Eichhorn, K.-J. (2020). High-Throughput Analyses of Microplastic Samples Using Fourier Transform Infrared and Raman Spectrometry. *Applied Spectroscopy*, 0(0), 0003702820932926. doi:<https://doi.org/10.1177/0003702820932926>
- Browne, M. A., Crump, P., Niven, S. J., Teuten, E., Tonkin, A., Galloway, T., & Thompson, R. (2011). Accumulation of Microplastic on Shorelines Worldwide: Sources and Sinks. *Environmental Science & Technology*, 45(21), 9175-9179. doi:<http://dx.doi.org/10.1021/es201811s>
- Bruge, A., Dhamelincourt, M., Lancelot, L., Monperrus, M., Gasperi, J., & Tassin, B. (2020). A first estimation of uncertainties related to microplastic sampling in rivers. *Science of the Total Environment*, 718, 137319. doi:<https://doi.org/10.1016/j.scitotenv.2020.137319>
- Bråte, I. L. N., Blázquez, M., Brooks, S. J., & Thomas, K. V. (2018). Weathering impacts the uptake of polyethylene microparticles from toothpaste in Mediterranean mussels (*Mytilus galloprovincialis*). *Science of the Total Environment*, 626, 1310-1318. doi:<https://doi.org/10.1016/j.scitotenv.2018.01.141>
- Bundesinstitut für Risikobewertung (BfR). (2009). Fragen und Antworten zu Glycidol-Fettsäureestern. Retrieved from https://www.bfr.bund.de/de/fragen_und_antworten_zu_glycidol_fettsaeureestern-29220.html
- Cabernard, L., Roscher, L., Lorenz, C., Gerdts, G., & Primpke, S. (2018). Comparison of Raman and Fourier Transform Infrared Spectroscopy for the Quantification of Microplastics in the Aquatic Environment. *Environmental Science & Technology*, 52(22), 13279-13288. doi:<https://doi.org/10.1021/acs.est.8b03438>
- Carpenter, E. J., Anderson, S. J., Harvey, G. R., Miklas, H. P., & Peck, B. B. (1972). Polystyrene Spherules in Coastal Waters. *Science*, 178(4062), 749-750. doi:<http://dx.doi.org/10.1126/science.178.4062.749>
- Carpenter, E. J., & Smith, K. L., Jr. (1972). Plastics on the Sargasso sea surface. *Science*, 175(4027), 1240-1241. doi:<https://doi.org/10.1126/science.175.4027.1240>

References

- Catarino, A. I., Thompson, R., Sanderson, W., & Henry, T. B. (2016). Development and optimization of a standard method for extraction of microplastics in mussels by enzyme digestion of soft tissues. *Environmental Toxicology and Chemistry*, n/a-n/a. doi:<https://dx.doi.org/10.1002/etc.3608>
- CEN. (2012). CEN/TR 15522-2:2012: Oil spill identification. Waterborne petroleum and petroleum products. Part 2: Analytical methodology and interpretation of results based on GC-FID and GC-MS low resolution analyses. In (pp. 138). Brussels: European Committee for Standardisation
- Choy, C. A., Robison, B. H., Gagne, T. O., Erwin, B., Firl, E., Halden, R. U., Hamilton, J. A., Katija, K., Lisin, S. E., Rolsky, C., & S. Van Houtan, K. (2019). The vertical distribution and biological transport of marine microplastics across the epipelagic and mesopelagic water column. *Scientific Reports*, 9(1), 7843. doi:<https://doi.org/10.1038/s41598-019-44117-2>
- Chubarenko, I. P., Esiukova, E., Bagaev, A., Isachenko, I., Demchenko, N., Zobkov, M., Efimova, I., Bagaeva, M., & Khatmullina, L. (2018a). Chapter 6 - Behavior of Microplastics in Coastal Zones. In E. Y. Zeng (Ed.), *Microplastic Contamination in Aquatic Environments* (pp. 175-223): Elsevier.
- Chubarenko, I. P., Esiukova, E. E., Bagaev, A. V., Bagaeva, M. A., & Grave, A. N. (2018b). Three-dimensional distribution of anthropogenic microparticles in the body of sandy beaches. *Science of the Total Environment*, 628-629, 1340-1351. doi:<https://doi.org/10.1016/j.scitotenv.2018.02.167>
- Claessens, M., Meester, S. D., Landuyt, L. V., Clerck, K. D., & Janssen, C. R. (2011). Occurrence and distribution of microplastics in marine sediments along the Belgian coast. *Marine Pollution Bulletin*, 62(10), 2199-2204. doi:<http://dx.doi.org/10.1016/j.marpolbul.2011.06.030>
- Claessens, M., Van Cauwenberghe, L., Vandegehuchte, M. B., & Janssen, C. R. (2013). New techniques for the detection of microplastics in sediments and field collected organisms. *Marine Pollution Bulletin*, 70(1-2), 227-233. doi:<http://dx.doi.org/10.1016/j.marpolbul.2013.03.009>
- Clarke, K. R. (1993). Non-parametric multivariate analyses of changes in community structure. *Australian Journal of Ecology*, 18(1), 117-143. doi:<https://doi.org/10.1111/j.1442-9993.1993.tb00438.x>
- Clarke, K. R., & Gorley, R. N. (2015). *PRIMER v7: User Manual/Tutorial*. Retrieved from Plymouth: http://updates.primer-e.com/primer7/manuals/User_manual_v7a.pdf
- Cole, M. (2016). A novel method for preparing microplastic fibers. *Scientific Reports*, 6, 34519. doi:<http://dx.doi.org/10.1038/srep34519>
- Cole, M., Lindeque, P., Halsband, C., & Galloway, T. S. (2011). Microplastics as contaminants in the marine environment: A review. *Marine Pollution Bulletin*, 62(12), 2588-2597. doi:<http://dx.doi.org/10.1016/j.marpolbul.2011.09.025>
- Cole, M., Lindeque, P. K., Fileman, E., Clark, J., Lewis, C., Halsband, C., & Galloway, T. S. (2016). Microplastics Alter the Properties and Sinking Rates of Zooplankton Faecal Pellets. *Environmental Science & Technology*, 50(6), 3239-3246. doi:<http://dx.doi.org/10.1021/acs.est.5b05905>
- Cole, M., Webb, H., Lindeque, P. K., Fileman, E. S., Halsband, C., & Galloway, T. S. (2014). Isolation of microplastics in biota-rich seawater samples and marine organisms. *Scientific Reports*, 4, 1 - 8. doi:<https://doi.org/10.1038/srep04528>
- Collard, F., Gilbert, B., Eppe, G., Parmentier, E., & Das, K. (2015). Detection of Anthropogenic Particles in Fish Stomachs: An Isolation Method Adapted to Identification by Raman Spectroscopy. *Archives of Environmental Contamination and Toxicology*, 69(3), 331-339. doi:<http://dx.doi.org/10.1007/s00244-015-0221-0>
- Colton, J. B., Knapp, F. D., & Burns, B. R. (1974). Plastic particles in surface waters of Northwestern Atlantic. *Science*, 185(4150), 491-497. doi:<https://doi.org/10.1126/science.185.4150.491>

References

- Conkle, J. L., Báez Del Valle, C. D., & Turner, J. W. (2018). Are we underestimating microplastic contamination in aquatic environments? *Environmental Management*, 61(1), 1-8. doi:<https://doi.org/10.1007/s00267-017-0947-8>
- Connors, K. A., Dyer, S. D., & Belanger, S. E. (2017). Advancing the quality of environmental microplastic research. *Environmental Toxicology and Chemistry*, 36(7), 1697-1703. doi:<http://dx.doi.org/10.1002/etc.3829>
- Coppock, R. L., Cole, M., Lindeque, P. K., Queirós, A. M., & Galloway, T. S. (2017). A small-scale, portable method for extracting microplastics from marine sediments. *Environmental Pollution*, 230, 829-837. doi:<https://doi.org/10.1016/j.envpol.2017.07.017>
- Corcoran, P. L., Norris, T., Ceccanese, T., Walzak, M. J., Helm, P. A., & Marvin, C. H. (2015). Hidden plastics of Lake Ontario, Canada and their potential preservation in the sediment record. *Environmental Pollution*, 204, 17-25. doi:<http://dx.doi.org/10.1016/j.envpol.2015.04.009>
- Costa, M. F., & Duarte, A. C. (2017). Microplastics Sampling and Sample Handling. *Comprehensive Analytical Chemistry*, 75, 25-47. doi:<http://dx.doi.org/10.1016/bs.coac.2016.11.002>
- Courtene-Jones, W., Quinn, B., Murphy, F., Gary, S. F., & Narayanaswamy, B. E. (2017). Optimisation of enzymatic digestion and validation of specimen preservation methods for the analysis of ingested microplastics. *Analytical Methods*, 9(9), 1437-1445. doi:<http://dx.doi.org/10.1039/C6AY02343F>
- Cowger, W., Booth, A. M., Hamilton, B. M., Thaysen, C., Primpke, S., Munno, K., Lusher, A. L., Dehaut, A., Vaz, V. P., Liboiron, M., Devriese, L. I., Hermabessiere, L., Rochman, C., Athey, S. N., Lynch, J. M., De Frond, H., Gray, A., Jones, O. A. H., Brander, S., Steele, C., Moore, S., Sanchez, A., & Nel, H. (2020a). Reporting Guidelines to Increase the Reproducibility and Comparability of Research on Microplastics. *Applied Spectroscopy*, 0(0), 0003702820930292. doi:<https://doi.org/10.1177/0003702820930292>
- Cowger, W., Gray, A., Christiansen, S. H., De Frond, H., Deshpande, A., Hermabessiere, L., Lee, E., Mill, L., Munno, K., Ossmann, B., Pittroff, M., Rochman, C., Sarau, G., Tarby, S., & Primpke, S. (2020b). EXPRESS: Critical Review of Processing and Classification Techniques for Images and Spectra in Microplastic Research. *Applied Spectroscopy*, 0(0), 0003702820929064. doi:<https://doi.org/10.1177/0003702820929064>
- Cózar, A., Echevarría, F., González-Gordillo, J. I., Irigoien, X., Úbeda, B., Hernández-León, S., Palma, Á. T., Navarro, S., García-de-Lomas, J., Ruiz, A., Fernández-de-Puelles, M. L., & Duarte, C. M. (2014). Plastic debris in the open ocean. *Proceedings of the National Academy of Sciences*, 111(28), 10239-10244. doi:<https://doi.org/10.1073/pnas.1314705111>
- Crawford, C. B., & Quinn, B. (2017a). 4 - Physiochemical properties and degradation. In C. B. Crawford & B. Quinn (Eds.), *Microplastic Pollutants* (pp. 57-100): Elsevier.
- Crawford, C. B., & Quinn, B. (2017b). 5 - Microplastics, standardisation and spatial distribution. In C. B. Crawford & B. Quinn (Eds.), *Microplastic Pollutants* (pp. 101-130): Elsevier.
- Crawford, C. B., & Quinn, B. (2017c). 6 - The interactions of microplastics and chemical pollutants. In C. B. Crawford & B. Quinn (Eds.), *Microplastic Pollutants* (pp. 131-157): Elsevier.
- Crawford, C. B., & Quinn, B. (2017d). 9 - Microplastic separation techniques. In C. B. Crawford & B. Quinn (Eds.), *Microplastic Pollutants* (pp. 203-218): Elsevier.
- Crawford, C. B., & Quinn, B. (2017e). 10 - Microplastic identification techniques. In C. B. Crawford & B. Quinn (Eds.), *Microplastic Pollutants* (pp. 219-267): Elsevier.
- Crichton, E. M., Noel, M., Gies, E. A., & Ross, P. S. (2017). A novel, density-independent and FTIR-compatible approach for the rapid extraction of microplastics from aquatic sediments. *Analytical Methods*, 9(9), 1419-1428. doi:<http://dx.doi.org/10.1039/C6AY02733D>

References

- CROW. (2019). Polymer Properties Database. Retrieved from <http://polymerdatabase.com/home.html>
- da Costa, J. P. (2018). Micro- and nanoplastics in the environment: Research and policymaking. *Current Opinion in Environmental Science & Health*, 1, 12-16. doi:<https://doi.org/10.1016/j.coesh.2017.11.002>
- Dagevos, J. J., Hougee, M., Van Franeker, J. A., Wenneker, B., Van Loon, W. M. G. M., & Oosterbaan, L. (2013). OSPAR Beach Litter Monitoring in the Netherlands. *North Sea Foundation, Utrecht*, 1 - 28.
- de Lucia, G. A., Caliani, I., Marra, S., Camedda, A., Coppa, S., Alcaro, L., Campani, T., Giannetti, M., Coppola, D., Cicero, A. M., Panti, C., Baini, M., Guerranti, C., Marsili, L., Massaro, G., Fossi, M. C., & Matiddi, M. (2014). Amount and distribution of neustonic micro-plastic off the western Sardinian coast (Central-Western Mediterranean Sea). *Marine Environmental Research*, 100, 10-16. doi:<http://dx.doi.org/10.1016/j.marenvres.2014.03.017>
- de Lucia, G. A., Vianello, A., Camedda, A., Vani, D., Tomasetti, P., Coppa, S., Palazzo, L., Amici, M., Romanelli, G., Zampetti, G., Cicero, A. M., Carpentieri, S., Di Vito, S., & Matiddi, M. (2018). Sea Water Contamination in the Vicinity of the Italian Minor Islands Caused by Microplastic Pollution. *Water*, 10(8), 1108. Retrieved from <http://www.mdpi.com/2073-4441/10/8/1108>
- De Witte, B., Devriese, L., Bekaert, K., Hoffman, S., Vandermeersch, G., Cooreman, K., & Robbens, J. (2014). Quality assessment of the blue mussel (*Mytilus edulis*): Comparison between commercial and wild types. *Marine Pollution Bulletin*, 85(1), 146-155. doi:<http://dx.doi.org/10.1016/j.marpolbul.2014.06.006>
- Dehaut, A., Cassone, A.-L., Frère, L., Hermabessiere, L., Himber, C., Rinnert, E., Rivière, G., Lambert, C., Soudant, P., Huvet, A., Duflos, G., & Paul-Pont, I. (2016). Microplastics in seafood: Benchmark protocol for their extraction and characterization. *Environmental Pollution*, 215, 223-233. doi:<http://dx.doi.org/10.1016/j.envpol.2016.05.018>
- Dekiff, J. H., Remy, D., Klasmeier, J., & Fries, E. (2014). Occurrence and spatial distribution of microplastics in sediments from Norderney. *Environmental Pollution*, 186(0), 248-256. doi:<http://dx.doi.org/10.1016/j.envpol.2013.11.019>
- Desa, U. (2016). Transforming our world: The 2030 agenda for sustainable development.
- Dixon, T. J., & Dixon, T. R. (1983). Marine litter distribution and composition in the North Sea. *Marine Pollution Bulletin*, 14(4), 145-148. doi:[http://dx.doi.org/10.1016/0025-326X\(83\)90068-1](http://dx.doi.org/10.1016/0025-326X(83)90068-1)
- Dobretsov, S. (2010). Marine biofilms. In S. Dürr & J. C. Thomason (Eds.), *Biofouling* (pp. 123-136): John Wiley & Sons Inc.
- Doyle, M. J., Watson, W., Bowlin, N. M., & Sheavly, S. B. (2011). Plastic particles in coastal pelagic ecosystems of the Northeast Pacific ocean. *Marine Environmental Research*, 71(1), 41-52. doi:<http://dx.doi.org/10.1016/j.marenvres.2010.10.001>
- Dris, R., Gasperi, J., Mirande, C., Mandin, C., Guerrouache, M., Langlois, V., & Tassin, B. (2017). A first overview of textile fibers, including microplastics, in indoor and outdoor environments. *Environmental Pollution*, 221, 453-458. doi:<http://dx.doi.org/10.1016/j.envpol.2016.12.013>
- Dris, R., Gasperi, J., Rocher, V., Saad, M., Renault, N., & Tassin, B. (2015). Microplastic contamination in an urban area: a case study in Greater Paris. *Environmental Chemistry* 12(5), 592-599. doi:<http://dx.doi.org/10.1071/EN14167>
- Dubaish, F., & Liebezeit, G. (2013). Suspended Microplastics and Black Carbon Particles in the Jade System, Southern North Sea. *Water, Air, & Soil Pollution*, 224(2), 1352-1359. doi:<https://doi.org/10.1007/s11270-012-1352-9>
- Duckett, P. E., & Repaci, V. (2015). Marine plastic pollution: using community science to address a global problem. *Marine and Freshwater Research*, 66(8), 665-673. doi:<http://dx.doi.org/10.1071/MF14087>
- Duncan, E. M., Broderick, A. C., Fuller, W. J., Galloway, T. S., Godfrey, M. H., Hamann, M., Limpus, C. J., Lindeque, P. K., Mayes, A. G., Omeyer, L. C. M., Santillo, D., Snape, R.

References

- T. E., & Godley, B. J. (2019). Microplastic ingestion ubiquitous in marine turtles. *Global Change Biology*, 25(2), 744-752. doi:<https://doi.org/10.1111/gcb.14519>
- Dwivedi, A. P., Ghosal, G., & Belkhole, P. (2017). Studies in Properties of Microcrystalline and Paraffin Waxes with the Help of Gas Chromatography (GC), DSC, FT-IR and by Conventional Methods. *International Journal of Scientific Research in Science, Engineering and Technology*, 3, 922-929.
- Dümichen, E., Eisentraut, P., Bannick, C. G., Barthel, A.-K., Senz, R., & Braun, U. (2017). Fast identification of microplastics in complex environmental samples by a thermal degradation method. *Chemosphere*, 174(Supplement C), 572-584. doi:<https://doi.org/10.1016/j.chemosphere.2017.02.010>
- Dümichen, E., Eisentraut, P., Celina, M., & Braun, U. (2019). Automated thermal extraction-desorption gas chromatography mass spectrometry: A multifunctional tool for comprehensive characterization of polymers and their degradation products. *Journal of Chromatography A*, 1592, 133-142. doi:<https://doi.org/10.1016/j.chroma.2019.01.033>
- EFSA, Panel o. C. i. t. F. C. (2016). Presence of microplastics and nanoplastics in food, with particular focus on seafood. *EFSA Journal*, 14(6), e04501. doi:<https://doi.org/10.2903/j.efsa.2016.4501>
- Egger, M., Sulu-Gambari, F., & Lebreton, L. (2020). First evidence of plastic fallout from the North Pacific Garbage Patch. *Scientific Reports*, 10(1), 7495. doi:<https://doi.org/10.1038/s41598-020-64465-8>
- Emeis, K.-C., van Beusekom, J., Callies, U., Ebinghaus, R., Kannen, A., Kraus, G., Kröncke, I., Lenhart, H., Lorkowski, I., Matthias, V., Möllmann, C., Pätsch, J., Scharfe, M., Thomas, H., Weisse, R., & Zorita, E. (2015). The North Sea — A shelf sea in the Anthropocene. *Journal of Marine Systems*, 141, 18-33. doi:<https://doi.org/10.1016/j.jmarsys.2014.03.012>
- Enders, K., Lenz, R., Stedmon, C. A., & Nielsen, T. G. (2015). Abundance, size and polymer composition of marine microplastics $\geq 10 \mu\text{m}$ in the Atlantic Ocean and their modelled vertical distribution. *Marine Pollution Bulletin*, 100(1), 70-81. doi:<http://dx.doi.org/10.1016/j.marpolbul.2015.09.027>
- Eriksen, M., Lebreton, L. C. M., Carson, H. S., Thiel, M., Moore, C. J., Borerro, J. C., Galgani, F., Ryan, P. G., & Reisser, J. (2014). Plastic Pollution in the World's Oceans: More than 5 Trillion Plastic Pieces Weighing over 250,000 Tons Afloat at Sea. *PLOS ONE*, 9(12), e111913. doi:<http://dx.doi.org/10.1371%2Fjournal.pone.0111913>
- Eriksen, M., Liboiron, M., Kiessling, T., Charron, L., Alling, A., Lebreton, L., Richards, H., Roth, B., Ory, N. C., Hidalgo-Ruz, V., Meerhoff, E., Box, C., Cummins, A., & Thiel, M. (2018). Microplastic sampling with the AVANI trawl compared to two neuston trawls in the Bay of Bengal and South Pacific. *Environmental Pollution*, 232, 430-439. doi:<https://doi.org/10.1016/j.envpol.2017.09.058>
- Erni-Cassola, G., Gibson, M. I., Thompson, R. C., & Christie-Oleza, J. A. (2017). Lost, but Found with Nile Red: A Novel Method for Detecting and Quantifying Small Microplastics (1 mm to 20 μm) in Environmental Samples. *Environmental Science & Technology*, 51(23), 13641-13648. doi:<https://doi.org/10.1021/acs.est.7b04512>
- Erni-Cassola, G., Zadjelovic, V., Gibson, M. I., & Christie-Oleza, J. A. (2019). Distribution of plastic polymer types in the marine environment; A meta-analysis. *Journal of Hazardous Materials*, 369, 691-698. doi:<https://doi.org/10.1016/j.jhazmat.2019.02.067>
- Esiukova, E. (2017). Plastic pollution on the Baltic beaches of Kaliningrad region, Russia. *Marine Pollution Bulletin*, 114(2), 1072-1080. doi:<http://dx.doi.org/10.1016/j.marpolbul.2016.10.001>
- EU Commission. (2018). *Communication from the Commission to the European Parliament, The council, The European Economic and Social Committee and the committee of the regions - A European Strategy for Plastics in a Circular Economy*. (COM/2018/028 final, Document 52018DC0028). Retrieved from <https://eur-lex.europa.eu/legal-content/en/ALL/?uri=CELEX%3A52018DC0028>

References

- European Chemicals Agency (ECHA). Bis(2-ethylhexyl) sebacate. Retrieved from <https://echa.europa.eu/de/substance-information/-/substanceinfo/100.004.145>
- European Commission. (2017). *Commission Decision (EU) 2017/848 of 17 May 2017 laying down criteria and methodological standards on good environmental status of marine waters and specifications and standardised methods for monitoring and assessment, and repealing Decision 2010/477/EU (Text with EEA relevance.)*. Retrieved from <http://data.europa.eu/eli/dec/2017/848/oj>
- European Parliament Council. (2008). Directive 2008/56/EC of the European Parliament and of the Council of 17 June 2008 establishing a framework for community action in the field of marine environmental policy (Marine Strategy Framework Directive). 1 - 22.
- Felsing, S., Kochleus, C., Buchinger, S., Brennholt, N., Stock, F., & Reifferscheid, G. (2018). A new approach in separating microplastics from environmental samples based on their electrostatic behavior. *Environmental Pollution*, 234, 20-28. doi:<https://doi.org/10.1016/j.envpol.2017.11.013>
- Fernando, S. S., Christensen, P. A., Egerton, T. A., & White, J. R. (2007). Carbon dioxide evolution and carbonyl group development during photodegradation of polyethylene and polypropylene. *Polymer Degradation and Stability*, 92(12), 2163-2172. doi:<https://doi.org/10.1016/j.polymdegradstab.2007.01.032>
- Filella, M. (2015). Questions of size and numbers in environmental research on microplastics: methodological and conceptual aspects. *Environmental Chemistry* 12(5), 527-538. doi:<https://doi.org/10.1071/EN15012>
- Fischer, M., & Scholz-Böttcher, B. M. (2017). Simultaneous Trace Identification and Quantification of Common Types of Microplastics in Environmental Samples by Pyrolysis-Gas Chromatography–Mass Spectrometry. *Environmental Science & Technology*, 51(9), 5052-5060. doi:<http://dx.doi.org/10.1021/acs.est.6b06362>
- Fischer, M., & Scholz-Böttcher, B. M. (2019). Microplastics analysis in environmental samples – recent pyrolysis-gas chromatography-mass spectrometry method improvements to increase the reliability of mass-related data. *Analytical Methods*, 11(18), 2489-2497. doi:<http://dx.doi.org/10.1039/C9AY00600A>
- Fitz, N., Kienhuis, P., Tolosa, I., Blaga, C., de Bruyn, R., & Kraus, U. (2017). *Usability of gas chromatography techniques (GC-FID, GC-MS and GC-IRMS) for identification of maritime paraffin wax*. Retrieved from Hamburg and Rostock: https://www.bsh.de/DE/PUBLIKATIONEN/Anlagen/Downloads/Meer_und_Umwelt/Berichte-des-BSH/Berichte-des-BSH_56_en.html
- Foekema, E. M., De Grijter, C., Mergia, M. T., van Franeker, J. A., Murk, A. J., & Koelmans, A. A. (2013). Plastic in North Sea Fish. *Environmental Science & Technology*, 47(15), 8818-8824. doi:<http://dx.doi.org/10.1021/es400931b>
- Frangoulis, C., Belkhiria, S., Goffart, A., & Hecq, J.-H. (2001). Dynamics of Copepod Faecal Pellets in Relation to a Phaeocystis Dominated Phytoplankton Bloom: Characteristics, Production and Flux. *Journal of Plankton Research*, 23(1), 75-88. doi:<http://dx.doi.org/10.1093/plankt/23.1.75>
- Frère, L., Paul-Pont, I., Moreau, J., Soudant, P., Lambert, C., Huvet, A., & Rinnert, E. (2016). A semi-automated Raman micro-spectroscopy method for morphological and chemical characterizations of microplastic litter. *Marine Pollution Bulletin*, 113(1), 461-468. doi:<http://dx.doi.org/10.1016/j.marpolbul.2016.10.051>
- Frias, J. P. G. L., Gago, J., Otero, V., & Sobral, P. (2016). Microplastics in coastal sediments from Southern Portuguese shelf waters. *Marine Environmental Research*, 114, 24-30. doi:<http://dx.doi.org/10.1016/j.marenvres.2015.12.006>
- Frias, J. P. G. L., & Nash, R. (2019). Microplastics: Finding a consensus on the definition. *Marine Pollution Bulletin*, 138, 145-147. doi:<https://doi.org/10.1016/j.marpolbul.2018.11.022>
- Frias, J. P. G. L., Otero, V., & Sobral, P. (2014). Evidence of microplastics in samples of zooplankton from Portuguese coastal waters. *Marine Environmental Research*, 95(Supplement C), 89-95. doi:<https://doi.org/10.1016/j.marenvres.2014.01.001>

References

- Frias, J. P. G. L., Pagter, E., Nash, R., O'Connor, I., Carretero, O., Filgueiras, A., Viñas, L., Gago, J., Antunes, J., Bessa, F., Sobral, P., Goruppi, A., Tirelli, V., Pedrotti, M. L., Suaria, G., Aliani, S., Lopes, C., Raimundo, J., Caetano, M., & Gerds, G. (2018). *Standardised protocol for monitoring microplastics in sediments. JPI-Oceans BASEMAN project*. doi:<https://doi.org/10.13140/RG.2.2.36256.89601/1>
- Fries, E., Dekiff, J. H., Willmeyer, J., Nuelle, M.-T., Ebert, M., & Remy, D. (2013). Identification of polymer types and additives in marine microplastic particles using pyrolysis-GC/MS and scanning electron microscopy. *Environmental Science: Processes & Impacts*, 15(10), 1949-1956. doi:<http://dx.doi.org/10.1039/C3EM00214D>
- Gago, J., Filgueiras, A., Pedrotti, M. L., Suaria, G., Tirelli, V., Andrade, J., Frias, J., Nash, R., O'Connor, I., Lopes, C., Caetano, M., Raimundo, J., Carretero, O., Viñas, L., Antunes, J., Bessa, F., Sobral, P., Goruppi, A., Aliani, S., Palazzo, L., de Lucia, G. A., Camedda, A., Muniategui, S., Grueiro, G., Fernandez, V., & Gerds, G. (2018). *Standardised protocol for monitoring microplastics in seawater. JPI-Oceans BASEMANproject*. Retrieved from https://www.researchgate.net/publication/330931801_Standardised_protocol_for_monitoring_microplastics_in_seawater
- Galgani, F., Fleet, D., Van Franeker, J., Katsanevakis, S., Maes, T., Mouat, J., Oosterbaan, L., Poitou, I., Hanke, G., Thompson, R., Amato, E., Birkun, A., & Janssen, C. (2010). Marine Strategy Framework Directive, Task Group 10 Report, Marine Litter *JRC Scientific and Technical Reports*, 1 - 57. doi:<https://doi.org/10.2788/86941>
- Galgani, F., Hanke, G., & Maes, T. (2015). Global Distribution, Composition and Abundance of Marine Litter. In M. Bergmann, L. Gutow, & M. Klages (Eds.), *Marine Anthropogenic Litter* (pp. 29-56). Cham: Springer International Publishing.
- Galgani, F., Hanke, G., Werner, S., & De Vrees, L. (2013). Marine litter within the European Marine Strategy Framework Directive. *ICES Journal of Marine Science: Journal du Conseil*, 70(6), 1055-1064. doi:<https://doi.org/10.1093/icesjms/fst122>
- Galgani, F., Leaute, J. P., Moguedet, P., Souplet, A., Verin, Y., Carpentier, A., Goraguer, H., Latrouite, D., Andral, B., Cadiou, Y., Mahe, J. C., Poulard, J. C., & Nerisson, P. (2000). Litter on the Sea Floor Along European Coasts. *Marine Pollution Bulletin*, 40(6), 516-527. doi:[http://dx.doi.org/10.1016/S0025-326X\(99\)00234-9](http://dx.doi.org/10.1016/S0025-326X(99)00234-9)
- Galloway, T. S., Cole, M., & Lewis, C. (2017). Interactions of microplastic debris throughout the marine ecosystem. *Nature Ecology & Evolution*, 1, 0116. doi:<http://dx.doi.org/10.1038/s41559-017-0116>
- Gerds, G. (2017). *Reaktor zur enzymatischen Mazeration biogener Bestandteile einer Partikelprobe und Verwendung des Reaktors* *Reactor for the enzymatic maceration biogenic components of a sample of particles and use of the reactor*. Germany Patent No. DE102016123324B3.
- Gerds, G. (2019). *Defining the Baselines and Standards for Microplastics Analyses in European Waters (JPI-O BASEMAN)*. Retrieved from <http://www.jpi-oceans.eu/sites/jpi-oceans.eu/files/public/Microplastics/JPI%20Oceans%20Final%20Project%20Report%20-%20BASEMAN.pdf>
- GESAMP. (2015). *Sources, fate and effects of microplastics in the marine environment: a global assessment* (90). Retrieved from London: https://ec.europa.eu/environment/marine/good-environmental-status/descriptor-10/pdf/GESAMP_microplastics%20full%20study.pdf
- Gewert, B., Plassmann, M. M., & MacLeod, M. (2015). Pathways for degradation of plastic polymers floating in the marine environment. *Environmental Science: Processes & Impacts*, 17(9), 1513-1521. doi:<http://dx.doi.org/10.1039/C5EM00207A>
- Gillibert, R., Balakrishnan, G., Deshoules, Q., Tardivel, M., Magazzù, A., Donato, M. G., Maragò, O. M., Lamy de La Chapelle, M., Colas, F., Lagarde, F., & Gucciardi, P. G. (2019). Raman Tweezers for Small Microplastics and Nanoplastics Identification in

References

- Seawater. *Environmental Science & Technology*, 53(15), 9003-9013. doi:<https://doi.org/10.1021/acs.est.9b03105>
- Gomiero, A., Øysæd, K. B., Agustsson, T., van Hoytema, N., van Thiel, T., & Grati, F. (2019). First record of characterization, concentration and distribution of microplastics in coastal sediments of an urban fjord in south west Norway using a thermal degradation method. *Chemosphere*, 227, 705-714. doi:<https://doi.org/10.1016/j.chemosphere.2019.04.096>
- Gorokhova, E. (2015). Screening for microplastic particles in plankton samples: How to integrate marine litter assessment into existing monitoring programs? *Marine Pollution Bulletin*, 99(1–2), 271-275. doi:<http://dx.doi.org/10.1016/j.marpolbul.2015.07.056>
- Graca, B., Szewc, K., Zakrzewska, D., Dołęga, A., & Szczerbowska-Boruchowska, M. (2017). Sources and fate of microplastics in marine and beach sediments of the Southern Baltic Sea—a preliminary study. *Environmental Science and Pollution Research* 24(8), 7650-7661. doi:<http://dx.doi.org/10.1007/s11356-017-8419-5>
- Guadagno, L., Naddeo, C., Vittoria, V., Camino, G., & Cagnani, C. (2001). Chemical and morphological modifications of irradiated linear low density polyethylene (LLDPE). *Polymer Degradation and Stability*, 72(1), 175-186. doi:[https://doi.org/10.1016/S0141-3910\(01\)00024-6](https://doi.org/10.1016/S0141-3910(01)00024-6)
- Gulmine, J. V., Janissek, P. R., Heise, H. M., & Akcelrud, L. (2002). Polyethylene characterization by FTIR. *Polymer Testing*, 21(5), 557-563. doi:[http://dx.doi.org/10.1016/S0142-9418\(01\)00124-6](http://dx.doi.org/10.1016/S0142-9418(01)00124-6)
- Gulmine, J. V., Janissek, P. R., Heise, H. M., & Akcelrud, L. (2003). Degradation profile of polyethylene after artificial accelerated weathering. *Polymer Degradation and Stability*, 79(3), 385-397. doi:[http://dx.doi.org/10.1016/S0141-3910\(02\)00338-5](http://dx.doi.org/10.1016/S0141-3910(02)00338-5)
- Guo, X., & Wang, J. (2019). The chemical behaviors of microplastics in marine environment: A review. *Marine Pollution Bulletin*, 142, 1-14. doi:<https://doi.org/10.1016/j.marpolbul.2019.03.019>
- Gutow, L., Ricker, M., Holstein, J. M., Dannheim, J., Stanev, E. V., & Wolff, J.-O. (2018). Distribution and trajectories of floating and benthic marine macrolitter in the south-eastern North Sea. *Marine Pollution Bulletin*, 131, 763-772. doi:<https://doi.org/10.1016/j.marpolbul.2018.05.003>
- Hahladakis, J. N., Velis, C. A., Weber, R., Iacovidou, E., & Purnell, P. (2018). An overview of chemical additives present in plastics: Migration, release, fate and environmental impact during their use, disposal and recycling. *Journal of Hazardous Materials*, 344, 179-199. doi:<https://doi.org/10.1016/j.jhazmat.2017.10.014>
- Hajbane, S., & Pattiaratchi, C. B. (2017). Plastic Pollution Patterns in Offshore, Nearshore and Estuarine Waters: A Case Study from Perth, Western Australia. *Frontiers in Marine Science* 4(63). doi:<https://doi.org/10.3389/fmars.2017.00063>
- Hamm, T., Lorenz, C., & Piehl, S. (2018). *Microplastics in Aquatic Systems – Monitoring Methods and Biological Consequences*. Paper presented at the YOUMARES 8 – Oceans Across Boundaries: Learning from each other, Bremen. https://link.springer.com/chapter/10.1007/978-3-319-93284-2_13
- Hanke, G., Galgani, F., Werner, S., Oosterbaan, L., Nilsson, P., Fleet, D., Kinsey, S., Thomposon, R. C., Palatinus, A., Van Franeker, J. A., Vlachogianni, T., Scoullou, M., Veiga, J. M., Matiddi, M., Alcaro, L., Maes, T., Korpinen, S., Budziak, A., Leslie, H., Gago, J., & Liebezeit, G. (2013). *MSFD GES technical subgroup on marine litter. Guidance on Monitoring of marine litter in European Seas*. Retrieved from Luxembourg: <http://publications.jrc.ec.europa.eu/repository/handle/JRC83985>
- Hanvey, J. S., Lewis, P. J., Lavers, J. L., Crosbie, N. D., Pozo, K., & Clarke, B. O. (2017). A review of analytical techniques for quantifying microplastics in sediments. *Analytical Methods*, 9(9), 1369-1383. doi:<http://dx.doi.org/10.1039/C6AY02707E>
- Harris, P. T. (2020). The fate of microplastic in marine sedimentary environments: A review and synthesis. *Marine Pollution Bulletin*, 158, 111398. doi:<https://doi.org/10.1016/j.marpolbul.2020.111398>

References

- Harrison, J. P., Ojeda, J. J., & Romero-González, M. E. (2012). The applicability of reflectance micro-Fourier-transform infrared spectroscopy for the detection of synthetic microplastics in marine sediments. *Science of the Total Environment*, 416(0), 455-463. doi:<http://dx.doi.org/10.1016/j.scitotenv.2011.11.078>
- Harshvardhan, K., & Jha, B. (2013). Biodegradation of low-density polyethylene by marine bacteria from pelagic waters, Arabian Sea, India. *Marine Pollution Bulletin*, 77(1), 100-106. doi:<https://doi.org/10.1016/j.marpolbul.2013.10.025>
- Hartmann, N. B., Hüffer, T., Thompson, R. C., Hassellöv, M., Verschoor, A., Dagaard, A. E., Rist, S., Karlsson, T., Brennholt, N., Cole, M., Herrling, M. P., Hess, M. C., Ileva, N. P., Lusher, A. L., & Wagner, M. (2019). Are We Speaking the Same Language? Recommendations for a Definition and Categorization Framework for Plastic Debris. *Environmental Science & Technology*, 53(3), 1039-1047. doi:<https://doi.org/10.1021/acs.est.8b05297>
- Haseler, M., Schernewski, G., Balciunas, A., & Sabaliauskaite, V. (2018). Monitoring methods for large micro- and meso-litter and applications at Baltic beaches. *Journal of Coastal Conservation*, 22(1), 27-50. doi:<https://doi.org/10.1007/s11852-017-0497-5>
- Hebner, T. S., & Maurer-Jones, M. A. (2020). Characterizing microplastic size and morphology of photodegraded polymers placed in simulated moving water conditions. *Environmental Science: Processes & Impacts*. doi:<http://dx.doi.org/10.1039/C9EM00475K>
- Hermabessiere, L., Dehaut, A., Paul-Pont, I., Lacroix, C., Jezequel, R., Soudant, P., & Duflos, G. (2017). Occurrence and effects of plastic additives on marine environments and organisms: A review. *Chemosphere*, 182, 781-793. doi:<http://dx.doi.org/10.1016/j.chemosphere.2017.05.096>
- Hermabessiere, L., Himber, C., Boricaud, B., Kazour, M., Amara, R., Cassone, A.-L., Laurentie, M., Paul-Pont, I., Soudant, P., Dehaut, A., & Duflos, G. (2018). Optimization, performance, and application of a pyrolysis-GC/MS method for the identification of microplastics. *Analytical and Bioanalytical Chemistry*. doi:<https://doi.org/10.1007/s00216-018-1279-0>
- Hermesen, E., Mintenig, S. M., Besseling, E., & Koelmans, A. A. (2018). Quality Criteria for the Analysis of Microplastic in Biota Samples: A Critical Review. *Environmental Science & Technology*. doi:10.1021/acs.est.8b01611
- Hidalgo-Ruz, V., Gutow, L., Thompson, R. C., & Thiel, M. (2012). Microplastics in the Marine Environment: A Review of the Methods Used for Identification and Quantification. *Environmental Science & Technology*, 46(6), 3060-3075. doi:<http://dx.doi.org/10.1021/es2031505>
- Hildebrandt, L., Mitrano, D. M., Zimmermann, T., & Präfrock, D. (2020). A Nanoplastic Sampling and Enrichment Approach by Continuous Flow Centrifugation. *Frontiers in Environmental Science*, 8(89). doi:<https://doi.org/10.3389/fenvs.2020.00089>
- Hildebrandt, L., Voigt, N., Zimmermann, T., Reese, A., & Proefrock, D. (2019). Evaluation of continuous flow centrifugation as an alternative technique to sample microplastic from water bodies. *Marine Environmental Research*, 151, 104768. doi:<https://doi.org/10.1016/j.marenvres.2019.104768>
- Hinojosa, I. A., & Thiel, M. (2009). Floating marine debris in fjords, gulfs and channels of southern Chile. *Marine Pollution Bulletin*, 58(3), 341-350. doi:<http://dx.doi.org/10.1016/j.marpolbul.2008.10.020>
- Holm, S. (1979). A Simple Sequentially Rejective Multiple Test Procedure. *Scandinavian Journal of Statistics*, 6(2), 65-70. Retrieved from www.jstor.org/stable/4615733
- Holmström, A. (1975). Plastic films on the bottom of the Skagerrack. *Nature*, 255(5510), 622-623. Retrieved from <http://dx.doi.org/10.1038/255622a0>
- Horton, A. A., & Dixon, S. J. (2018). Microplastics: An introduction to environmental transport processes. *WIREs Water*, 5(2), e1268. doi:10.1002/wat2.1268
- Horton, A. A., Svendsen, C., Williams, R. J., Spurgeon, D. J., & Lahive, E. (2017a). Presence and Abundance of Microplastics in Sediments of Tributaries of the River Thames, UK.

References

- In J. Baztan, B. Jorgensen, S. Pahl, R. C. Thompson, & J.-P. Vanderlinden (Eds.), *Fate and Impact of Microplastics in Marine Ecosystems* (pp. 6-7): Elsevier.
- Horton, A. A., Walton, A., Spurgeon, D. J., Lahive, E., & Svendsen, C. (2017b). Microplastics in freshwater and terrestrial environments: Evaluating the current understanding to identify the knowledge gaps and future research priorities. *Science of the Total Environment*, 586, 127-141. doi:<http://dx.doi.org/10.1016/j.scitotenv.2017.01.190>
- Howarth, M. J. (2001). North Sea Circulation. In J. H. Steele (Ed.), *Encyclopedia of Ocean Sciences (Second Edition)* (pp. 73-81). Oxford: Academic Press.
- Hurley, R. R., Lusher, A. L., Olsen, M., & Nizzetto, L. (2018a). Validation of a Method for Extracting Microplastics from Complex, Organic-Rich, Environmental Matrices. *Environmental Science & Technology*, 52(13), 7409-7417. doi:<https://doi.org/10.1021/acs.est.8b01517>
- Hurley, R. R., Woodward, J. C., & Rothwell, J. J. (2018b). Microplastic contamination of river beds significantly reduced by catchment-wide flooding. *Nature Geoscience*, 11(4), 251-257. doi:<https://doi.org/10.1038/s41561-018-0080-1>
- Haave, M., Lorenz, C., Primpke, S., & Gerds, G. (2019). Different stories told by small and large microplastics in sediment - first report of microplastic concentrations in an urban recipient in Norway. *Marine Pollution Bulletin*, 141, 501-513. doi:<https://doi.org/10.1016/j.marpolbul.2019.02.015>
- Imhof, H. K., Laforsch, C., Wiesheu, A. C., Schmid, J., Anger, P. M., Niessner, R., & Ivleva, N. P. (2016). Pigments and plastic in limnetic ecosystems: A qualitative and quantitative study on microparticles of different size classes. *Water Research*, 98, 64-74. doi:<http://dx.doi.org/10.1016/j.watres.2016.03.015>
- Imhof, H. K., Schmid, J., Niessner, R., Ivleva, N. P., & Laforsch, C. (2012). A novel, highly efficient method for the separation and quantification of plastic particles in sediments of aquatic environments. *Limnology and Oceanography: Methods*, 10, 524-537. doi:<https://doi.org/10.4319/lom.2012.10.524>
- IMO. (2004). Resolution MEPC 118(52), Amendments to the Annex of the protocol of 1978 relating to the International Convention for the Prevention of Pollution from Ships, 1973 (Revised Annex II of MARPOL 73/78). Retrieved from <http://www.imo.org/en/KnowledgeCentre/IndexofIMOResolutions/Marine-Environment-Protection-Committee-%28MEPC%29/Documents/MEPC.118%2852%29.pdf>
- IMO. (2019). MARPOL amendments - Cargo residues and tank washings of persistent floating noxious liquid substances. *Marine Environment Protection Committee (MEPC)*, 74th session, 13-17 May 2019 Retrieved from <http://www.imo.org/en/MediaCentre/MeetingSummaries/MEPC/Pages/MEPC-74th-session.aspx>
- Ioakeimidis, C., Fotopoulou, K. N., Karapanagioti, H. K., Geraga, M., Zeri, C., Papathanassiou, E., Galgani, F., & Papatheodorou, G. (2016). The degradation potential of PET bottles in the marine environment: An ATR-FTIR based approach. *Scientific Reports*, 6, 23501. doi:<https://doi.org/10.1038/srep23501>
- Ivleva, N. P., Wiesheu, A. C., & Niessner, R. (2016). Microplastic in Aquatic Ecosystems. *Angewandte Chemie (International Edition)*, 56(7), 1720-1739. doi:<https://doi.org/10.1002/anie.201606957>
- Jambeck, J. R., Geyer, R., Wilcox, C., Siegler, T. R., Perryman, M., Andrady, A., Narayan, R., & Law, K. L. (2015). Plastic waste inputs from land into the ocean. *Science*, 347(6223), 768-771. doi:<https://doi.org/10.1126/science.1260352>
- Jensen, H. K. B., & Cramer, J. (2017). *MAREANOs pilotprosjekt på mikroplast- resultater og forslag til videre arbeid* (NGU, 2017.043.). Retrieved from https://www.ngu.no/upload/Publikasjoner/Rapporter/2019/2019_027.pdf
- Jiang, Y., Zhao, Y., Wang, X., Yang, F., Chen, M., & Wang, J. (2020). Characterization of microplastics in the surface seawater of the South Yellow Sea as affected by season.

References

- Science of the Total Environment*, 724, 138375.
doi:<https://doi.org/10.1016/j.scitotenv.2020.138375>
- JPI-Oceans. (2020, 05/06/2020). Six new JPI Oceans microplastics research projects launched and off to a good start. Retrieved from <https://www.jpi-oceans.eu/news-events/news/six-new-jpi-oceans-microplastics-research-projects-launched-and-good-start>
- Julienne, F., Delorme, N., & Lagarde, F. (2019). From macroplastics to microplastics: Role of water in the fragmentation of polyethylene. *Chemosphere*, 236, 124409. doi:<https://doi.org/10.1016/j.chemosphere.2019.124409>
- Kane, I. A., Clare, M. A., Miramontes, E., Wogelius, R., Rothwell, J. J., Garreau, P., & Pohl, F. (2020). Seafloor microplastic hotspots controlled by deep-sea circulation. *Science*, 30, eaba5899. doi:<https://doi.org/10.1126/science.aba5899>
- Kanhai, L. D. K., Gårdfeldt, K., Lyashevskaya, O., Hassellöv, M., Thompson, R. C., & O'Connor, I. (2018). Microplastics in sub-surface waters of the Arctic Central Basin. *Marine Pollution Bulletin*, 130, 8-18. doi:<https://doi.org/10.1016/j.marpolbul.2018.03.011>
- Kanhai, L. D. K., Officer, R., Lyashevskaya, O., Thompson, R. C., & O'Connor, I. (2017). Microplastic abundance, distribution and composition along a latitudinal gradient in the Atlantic Ocean. *Marine Pollution Bulletin*, 115(1-2), 307-314. doi:<http://dx.doi.org/10.1016/j.marpolbul.2016.12.025>
- Karami, A., Golieskardi, A., Choo, C. K., Romano, N., Ho, Y. B., & Salamatnia, B. (2017). A high-performance protocol for extraction of microplastics in fish. *Science of the Total Environment*, 578, 485-494. doi:<http://dx.doi.org/10.1016/j.scitotenv.2016.10.213>
- Karlsson, T. M., Hassellöv, M., & Jakubowicz, I. (2018). Influence of thermooxidative degradation on the in situ fate of polyethylene in temperate coastal waters. *Marine Pollution Bulletin*, 135, 187-194. doi:<https://doi.org/10.1016/j.marpolbul.2018.07.015>
- Karlsson, T. M., Vethaak, A. D., Almroth, B. C., Ariese, F., van Velzen, M., Hassellöv, M., & Leslie, H. A. (2017). Screening for microplastics in sediment, water, marine invertebrates and fish: Method development and microplastic accumulation. *Marine Pollution Bulletin*, 122(1), 403-408. doi:<http://dx.doi.org/10.1016/j.marpolbul.2017.06.081>
- Katija, K., Choy, C. A., Sherlock, R. E., Sherman, A. D., & Robison, B. H. (2017). From the surface to the seafloor: How giant larvaceans transport microplastics into the deep sea. *Science Advances*, 3(8), e1700715. doi:<http://doi.org/10.1126/sciadv.1700715>
- Kedzierski, M., Falcou-Préfol, M., Kerros, M. E., Henry, M., Pedrotti, M. L., & Bruzard, S. (2019). A machine learning algorithm for high throughput identification of FTIR spectra: Application on microplastics collected in the Mediterranean Sea. *Chemosphere*, 234, 242-251. doi:<https://doi.org/10.1016/j.chemosphere.2019.05.113>
- Kedzierski, M., Le Tilly, V., Bourseau, P., Bellegou, H., César, G., Sire, O., & Bruzard, S. (2016). Microplastics elutriation from sandy sediments: A granulometric approach. *Marine Pollution Bulletin*, 107(1), 315-323. doi:<http://dx.doi.org/10.1016/j.marpolbul.2016.03.041>
- Kedzierski, M., Le Tilly, V., César, G., Sire, O., & Bruzard, S. (2017). Efficient microplastics extraction from sand. A cost effective methodology based on sodium iodide recycling. *Marine Pollution Bulletin*, 115(1), 120-129. doi:<http://dx.doi.org/10.1016/j.marpolbul.2016.12.002>
- Kienhuis, P. G. M., Fitz, N., Tolosa, I., Blaga, C., & Peschier, L. (2018). Chapter 8 - Paraffin Wax Spill Identification by GC-FID and GC-MS. In S. A. Stout & Z. Wang (Eds.), *Oil Spill Environmental Forensics Case Studies* (pp. 157-186): Butterworth-Heinemann.
- Kirstein, I. V., Kirmizi, S., Wichels, A., Garin-Fernandez, A., Erler, R., Löder, M., & Gerdt, G. (2016). Dangerous hitchhikers? Evidence for potentially pathogenic *Vibrio* spp. on microplastic particles. *Marine Environmental Research*, 120, 1-8. doi:<http://dx.doi.org/10.1016/j.marenvres.2016.07.004>
- Klein, S., Worch, E., & Knepper, T. P. (2015). Occurrence and Spatial Distribution of Microplastics in River Shore Sediments of the Rhine-Main Area in Germany.

References

- Environmental Science & Technology*, 49(10), 6070-6076. doi:<http://dx.doi.org/10.1021/acs.est.5b00492>
- Koelmans, A. A., Kooi, M., Law, K. L., & van Sebillie, E. (2017). All is not lost: deriving a top-down mass budget of plastic at sea. *Environmental Research Letters*, 12(11), 114028. doi:<https://doi.org/10.1088/1748-9326/aa9500>
- Koelmans, A. A., Mohamed Nor, N. H., Hermesen, E., Kooi, M., Mintenig, S. M., & De France, J. (2019). Microplastics in freshwaters and drinking water: Critical review and assessment of data quality. *Water Research*, 155, 410-422. doi:<https://doi.org/10.1016/j.watres.2019.02.054>
- Kole, P. J., Löhr, A. J., Van Belleghem, F. G. A. J., & Ragas, A. M. J. (2017). Wear and Tear of Tyres: A Stealthy Source of Microplastics in the Environment. *International Journal of Environmental Research and Public Health*, 14(10), 1265. doi:<https://doi.org/10.3390/ijerph14101265>
- Kooi, M., Reisser, J., Slat, B., Ferrari, F. F., Schmid, M. S., Cunsolo, S., Brambini, R., Noble, K., Sirks, L.-A., Linders, T. E. W., Schoeneich-Argent, R. I., & Koelmans, A. A. (2016). The effect of particle properties on the depth profile of buoyant plastics in the ocean. *Scientific Reports*, 6, 33882. doi:<http://dx.doi.org/10.1038/srep33882>
- Kowalski, N., Reichardt, A. M., & Waniek, J. J. (2016). Sinking rates of microplastics and potential implications of their alteration by physical, biological, and chemical factors. *Marine Pollution Bulletin*, 109(1), 310-319. doi:<http://dx.doi.org/10.1016/j.marpolbul.2016.05.064>
- Krehula, L. K., Katančić, Z., Siročić, A. P., & Hrnjak-Murgić, Z. (2014). Weathering of High-Density Polyethylene-Wood Plastic Composites. *Journal of Wood Chemistry and Technology*, 34(1), 39-54. doi:<https://doi.org/10.1080/02773813.2013.827209>
- Kroon, F., Motti, C., Talbot, S., Sobral, P., & Puotinen, M. (2018). A workflow for improving estimates of microplastic contamination in marine waters: A case study from North-Western Australia. *Environmental Pollution*, 238, 26-38. doi:<https://doi.org/10.1016/j.envpol.2018.03.010>
- Kukulka, T., Proskurowski, G., Morét-Ferguson, S., Meyer, D. W., & Law, K. L. (2012). The effect of wind mixing on the vertical distribution of buoyant plastic debris. *Geophysical Research Letters*, 39(7), 1-6. doi:<http://dx.doi.org/10.1029/2012GL051116>
- Kvalø, S. E., Haave, M., Torvanger, R., Alme, Ø., & Johannessen, P. (2014). *Resipientovervåking av fjordsystemene rundt Bergen 2011-2015* (SAM e-Rapport 27-2014). Retrieved from <https://norceresearch.brage.unit.no/norceresearch-xmlui/handle/11250/2629300>
- Kvalø, S. E., Torvanger, R., Hadler-Jacobsen, S., Alme, Ø., Bye-Ingebrigtsen, E., & Johannessen, P. (2016). *Resipientovervåking av fjordsystemene rundt Bergen 2011-2015, Årsrapport 2015* (SAM e-Rapport 3-2016). Retrieved from <https://norceresearch.brage.unit.no/norceresearch-xmlui/handle/11250/2627674>
- Kvalø, S. E., Torvanger, R., Haave, M., Hadler-Jacobsen, S., Lode, T., Johannessen, P., & Alme, Ø. (2015). *Resipientovervåking av fjordsystemene rundt Bergen 2011-2015-Årsrapport 2014* (SAM e-Rapport 4-2015). Retrieved from <https://norceresearch.brage.unit.no/norceresearch-xmlui/handle/11250/2627814>
- Käppler, A., Fischer, D., Oberbeckmann, S., Schernewski, G., Labrenz, M., Eichhorn, K.-J., & Voit, B. (2016). Analysis of environmental microplastics by vibrational microspectroscopy: FTIR, Raman or both? *Analytical and Bioanalytical Chemistry*, 408(29), 8377-8391. doi:<http://dx.doi.org/10.1007/s00216-016-9956-3>
- Käppler, A., Windrich, F., Löder, M. J., Malanin, M., Fischer, D., Labrenz, M., Eichhorn, K.-J., & Voit, B. (2015). Identification of microplastics by FTIR and Raman microscopy: a novel silicon filter substrate opens the important spectral range below 1300 cm⁻¹ for FTIR transmission measurements. *Analytical and Bioanalytical Chemistry*, 407(22), 6791-6801. doi:<http://dx.doi.org/10.1007/s00216-015-8850-8>

References

- Kögel, T., Bjørøy, Ø., Toto, B., Bienfait, A. M., & Sanden, M. (2020). Micro- and nanoplastic toxicity on aquatic life: Determining factors. *Science of the Total Environment*, 709, 136050. doi:<https://doi.org/10.1016/j.scitotenv.2019.136050>
- Lachowicz, T., Zieba-Palus, J., & Kościelniak, P. (2012). Analysis of rubber samples by PY-GC/MS for forensic purposes. *Problems of Forensic Science*, 91, 195-207.
- Lambert, S., & Wagner, M. (2016). Formation of microscopic particles during the degradation of different polymers. *Chemosphere*, 161, 510-517. doi:<http://dx.doi.org/10.1016/j.chemosphere.2016.07.042>
- Lattin, G. L., Moore, C. J., Zellers, A. F., Moore, S. L., & Weisberg, S. B. (2004). A comparison of neustonic plastic and zooplankton at different depths near the southern California shore. *Marine Pollution Bulletin*, 49(4), 291-294. doi:<http://dx.doi.org/10.1016/j.marpolbul.2004.01.020>
- Lavers, J. L., Oppel, S., & Bond, A. L. (2016). Factors influencing the detection of beach plastic debris. *Marine Environmental Research*, 119, 245-251. doi:<http://dx.doi.org/10.1016/j.marenvres.2016.06.009>
- Law, K. L., Morét-Ferguson, S. E., Goodwin, D. S., Zettler, E. R., DeForce, E., Kukulka, T., & Proskurowski, G. (2014). Distribution of Surface Plastic Debris in the Eastern Pacific Ocean from an 11-Year Data Set. *Environmental Science & Technology*, 48(9), 4732-4738. doi:<http://dx.doi.org/10.1021/es4053076>
- Lebreton, L. C. M., Slat, B., Ferrari, F., Sainte-Rose, B., Aitken, J., Marthouse, R., Hajbane, S., Cunsolo, S., Schwarz, A., Levivier, A., Noble, K., Debeljak, P., Maral, H., Schoeneich-Argent, R., Brambini, R., & Reisser, J. (2018). Evidence that the Great Pacific Garbage Patch is rapidly accumulating plastic. *Scientific Reports*, 8(1), 4666. doi:<https://doi.org/10.1038/s41598-018-22939-w>
- Lebreton, L. C. M., van der Zwet, J., Damsteeg, J.-W., Slat, B., Andrady, A., & Reisser, J. (2017). River plastic emissions to the world's oceans. *Nature Communications*, 8, 15611. doi:<http://dx.doi.org/10.1038/ncomms15611>
- Legendre, P., & Gallagher, E. D. (2001). Ecologically meaningful transformations for ordination of species data. *Oecologia*, 129(2), 271-280. doi:<https://doi.org/10.1007/s004420100716>
- Lehtiniemi, M., Hartikainen, S., Näkki, P., Engström-Öst, J., Koistinen, A., & Setälä, O. (2018). Size matters more than shape: Ingestion of primary and secondary microplastics by small predators. *Food Webs*, 17, e00097. doi:<https://doi.org/10.1016/j.fooweb.2018.e00097>
- Lenz, R., Enders, K., Stedmon, C. A., Mackenzie, D. M. A., & Nielsen, T. G. (2015). A critical assessment of visual identification of marine microplastic using Raman spectroscopy for analysis improvement. *Marine Pollution Bulletin*, 100(1), 82-91. doi:<http://dx.doi.org/10.1016/j.marpolbul.2015.09.026>
- Leslie, H. A., Brandsma, S. H., van Velzen, M. J. M., & Vethaak, A. D. (2017). Microplastics en route: Field measurements in the Dutch river delta and Amsterdam canals, wastewater treatment plants, North Sea sediments and biota. *Environment International*, 101, 133-142. doi:<http://dx.doi.org/10.1016/j.envint.2017.01.018>
- Leslie, H. A., van der Meulen, M. D., Kleissen, F. M., & Vethaak, A. D. (2011). Microplastic Litter in the Dutch Marine Environment. *Deltares, Netherlands*, 104.
- Li, P., Li, Q., Hao, Z., Yu, S., & Liu, J. (2020). Analytical methods and environmental processes of nanoplastics. *Journal of Environmental Sciences*, 94, 88-99. doi:<https://doi.org/10.1016/j.jes.2020.03.057>
- Li, Q., Wu, J., Zhao, X., Gu, X., & Ji, R. (2019). Separation and identification of microplastics from soil and sewage sludge. *Environmental Pollution*, 254, 113076. doi:<https://doi.org/10.1016/j.envpol.2019.113076>
- Li, W. C. (2018). Chapter 5 - The Occurrence, Fate, and Effects of Microplastics in the Marine Environment. In E. Y. Zeng (Ed.), *Microplastic Contamination in Aquatic Environments* (pp. 133-173): Elsevier.

References

- Lindeque, P. K., Cole, M., Coppock, R. L., Lewis, C. N., Miller, R. Z., Watts, A. J. R., Wilson-McNeal, A., Wright, S. L., & Galloway, T. S. (2020). Are we underestimating microplastic abundance in the marine environment? A comparison of microplastic capture with nets of different mesh-size. *Environmental Pollution*, 265, 114721. doi:<https://doi.org/10.1016/j.envpol.2020.114721>
- Lithner, D., Larsson, Å., & Dave, G. (2011). Environmental and health hazard ranking and assessment of plastic polymers based on chemical composition. *Science of the Total Environment*, 409(18), 3309-3324. doi:<http://dx.doi.org/10.1016/j.scitotenv.2011.04.038>
- Liu, F., Olesen, K. B., Borregaard, A. R., & Vollertsen, J. (2019a). Microplastics in urban and highway stormwater retention ponds. *Science of the Total Environment*, 671, 992-1000. doi:<https://doi.org/10.1016/j.scitotenv.2019.03.416>
- Liu, F., Vianello, A., & Vollertsen, J. (2019b). Retention of microplastics in sediments of urban and highway stormwater retention ponds. *Environmental Pollution*, 255, 113335. doi:<https://doi.org/10.1016/j.envpol.2019.113335>
- Liu, K., Wang, X., Fang, T., Xu, P., Zhu, L., & Li, D. (2019a). Source and potential risk assessment of suspended atmospheric microplastics in Shanghai. *Science of the Total Environment*, 675, 462-471. doi:<https://doi.org/10.1016/j.scitotenv.2019.04.110>
- Liu, K., Zhang, F., Song, Z., Zong, C., Wei, N., & Li, D. (2019b). A novel method enabling the accurate quantification of microplastics in the water column of deep ocean. *Marine Pollution Bulletin*, 146, 462-465. doi:<https://doi.org/10.1016/j.marpolbul.2019.07.008>
- Lobelle, D., & Cunliffe, M. (2011). Early microbial biofilm formation on marine plastic debris. *Marine Pollution Bulletin*, 62(1), 197-200. doi:<http://dx.doi.org/10.1016/j.marpolbul.2010.10.013>
- Long, M., Moriceau, B., Gallinari, M., Lambert, C., Huvet, A., Raffray, J., & Soudant, P. (2015). Interactions between microplastics and phytoplankton aggregates: Impact on their respective fates. *Marine Chemistry*, 175, 39-46. doi:<http://dx.doi.org/10.1016/j.marchem.2015.04.003>
- Long, M., Paul-Pont, I., Hégaret, H., Moriceau, B., Lambert, C., Huvet, A., & Soudant, P. (2017). Interactions between polystyrene microplastics and marine phytoplankton lead to species-specific hetero-aggregation. *Environmental Pollution*, 228, 454-463. doi:<https://doi.org/10.1016/j.envpol.2017.05.047>
- Lorenz, C., Roscher, L., Meyer, M. S., Hildebrandt, L., Prume, J., Löder, M. G. J., Primpke, S., & Gerdt, G. (2019). Spatial distribution of microplastics in sediments and surface waters of the southern North Sea. *Environmental Pollution*, 252, 1719-1729. doi:<https://doi.org/10.1016/j.envpol.2019.06.093>
- Lusher, A. L. (2015). Microplastics in the Marine Environment: Distribution, Interactions and Effects. In M. Bergmann, L. Gutow, & M. Klages (Eds.), *Marine Anthropogenic Litter* (pp. 245-307). Cham: Springer International Publishing.
- Lusher, A. L., Burke, A., O'Connor, I., & Officer, R. (2014). Microplastic pollution in the Northeast Atlantic Ocean: Validated and opportunistic sampling. *Marine Pollution Bulletin*, 88(1-2), 325-333. doi:<http://dx.doi.org/10.1016/j.marpolbul.2014.08.023>
- Lusher, A. L., Hernandez-Milian, G., O'Brien, J., Berrow, S., O'Connor, I., & Officer, R. (2015a). Microplastic and macroplastic ingestion by a deep diving, oceanic cetacean: The True's beaked whale *Mesoplodon mirus*. *Environmental Pollution*, 199, 185-191. doi:<http://dx.doi.org/10.1016/j.envpol.2015.01.023>
- Lusher, A. L., McHugh, M., & Thompson, R. C. (2013). Occurrence of microplastics in the gastrointestinal tract of pelagic and demersal fish from the English Channel. *Marine Pollution Bulletin*, 67(1-2), 94-99. doi:<http://dx.doi.org/10.1016/j.marpolbul.2012.11.028>
- Lusher, A. L., Tirelli, V., O'Connor, I., & Officer, R. (2015b). Microplastics in Arctic polar waters: the first reported values of particles in surface and sub-surface samples. *Scientific Reports*, 5, 14947. doi:<http://dx.doi.org/10.1038/srep14947>

References

- Lv, Y., Huang, Y., Kong, M., Yang, Q., & Li, G. (2017). Multivariate correlation analysis of outdoor weathering behavior of polypropylene under diverse climate scenarios. *Polymer Testing*, 64, 65-76. doi:<https://doi.org/10.1016/j.polymertesting.2017.09.040>
- Lv, Y., Huang, Y., Yang, J., Kong, M., Yang, H., Zhao, J., & Li, G. (2015). Outdoor and accelerated laboratory weathering of polypropylene: A comparison and correlation study. *Polymer Degradation and Stability*, 112, 145-159. doi:<https://doi.org/10.1016/j.polymdegradstab.2014.12.023>
- Löder, M. G. J., & Gerdt, G. (2015). Methodology Used For The Detection And Identification Of Microplastics—A Critical Appraisal. In M. Bergmann, L. Gutow, & M. Klages (Eds.), *Marine Anthropogenic Litter* (pp. 201-227): Springer International Publishing.
- Löder, M. G. J., Imhof, H. K., Ladehoff, M., Löschel, L. A., Lorenz, C., Mintenig, S., Piehl, S., Primpke, S., Schrank, I., Laforsch, C., & Gerdt, G. (2017). Enzymatic Purification of Microplastics in Environmental Samples. *Environmental Science & Technology*, 51(24), 14283-14292. doi:<http://dx.doi.org/10.1021/acs.est.7b03055>
- Löder, M. G. J., Kuczera, M., Mintenig, S., Lorenz, C., & Gerdt, G. (2015). Focal plane array detector-based micro-Fourier-transform infrared imaging for the analysis of microplastics in environmental samples. *Environmental Chemistry* 12(5), 563-581. doi:<http://dx.doi.org/10.1071/EN14205>
- Maes, T., Jessop, R., Wellner, N., Haupt, K., & Mayes, A. G. (2017a). A rapid-screening approach to detect and quantify microplastics based on fluorescent tagging with Nile Red. *Scientific Reports*, 7, 44501. doi:<https://doi.org/10.1038/srep44501>
- Maes, T., Van der Meulen, M. D., Devriese, L. I., Leslie, H. A., Huvet, A., Frère, L., Robbens, J., & Vethaak, A. D. (2017b). Microplastics Baseline Surveys at the Water Surface and in Sediments of the North-East Atlantic. *Frontiers in Marine Science* 4(135). doi:<https://doi.org/10.3389/fmars.2017.00135>
- Magnusson, K. (2014). *Mikroskräp i avloppsvatten från tre norska avloppsreningsverk* (C 71). Retrieved from <https://www.ivl.se/download/18.343dc99d14e8bb0f58b771e/1445517851411/C71.pdf>
- Maia, M., Barros, A. I. R. N. A., & Nunes, F. M. (2013). A novel, direct, reagent-free method for the detection of beeswax adulteration by single-reflection attenuated total reflectance mid-infrared spectroscopy. *Talanta*, 107, 74-80. doi:<https://doi.org/10.1016/j.talanta.2012.09.052>
- Mani, T., Blarer, P., Storck, F. R., Pittroff, M., Wernicke, T., & Burkhardt-Holm, P. (2019a). Repeated detection of polystyrene microbeads in the lower Rhine River. *Environmental Pollution*, 245, 634-641. doi:<https://doi.org/10.1016/j.envpol.2018.11.036>
- Mani, T., Frehland, S., Kalberer, A., & Burkhardt-Holm, P. (2019b). Using castor oil to separate microplastics from four different environmental matrices. *Analytical Methods*. doi:<http://dx.doi.org/10.1039/C8AY02559B>
- Mani, T., Hauk, A., Walter, U., & Burkhardt-Holm, P. (2015). Microplastics profile along the Rhine River. *Scientific Reports*, 5, 17988. doi:<http://dx.doi.org/10.1038/srep17988>
- Mani, T., Primpke, S., Lorenz, C., Gerdt, G., & Burkhardt-Holm, P. (2019c). Microplastic pollution in benthic midstream sediments of the Rhine river. *Environmental Science & Technology*, 53(10), 6053-6062. doi:<https://doi.org/10.1021/acs.est.9b01363>
- Mark, J. E. (2009). *Polymer Data Handbook* (2nd ed. ed.): Oxford University Press.
- Martin, J., Lusher, A., Thompson, R. C., & Morley, A. (2017). The Deposition and Accumulation of Microplastics in Marine Sediments and Bottom Water from the Irish Continental Shelf. *Scientific Reports*, 7(1), 10772. doi:<https://doi.org/10.1038/s41598-017-11079-2>
- Mason, S. A., Garneau, D., Sutton, R., Chu, Y., Ehmann, K., Barnes, J., Fink, P., Papazissimos, D., & Rogers, D. L. (2016). Microplastic pollution is widely detected in US municipal wastewater treatment plant effluent. *Environmental Pollution*, 218, 1045-1054. doi:<http://dx.doi.org/10.1016/j.envpol.2016.08.056>
- Masura, J., Baker, J., Foster, G., & Arthur, C. (2015). *Laboratory methods for the analysis of microplastics in the marine environment: recommendations for quantifying synthetic particles in waters and sediments*. Retrieved from

References

- <https://marinedebris.noaa.gov/technical-memorandum/laboratory-methods-analysis-microplastics-marine-environment>
- Materić, D., Kasper-Giebl, A., Kau, D., Anten, M., Greilinger, M., Ludewig, E., van Seville, E., Röckmann, T., & Holzinger, R. (2020). Micro- and Nanoplastics in Alpine Snow: A New Method for Chemical Identification and (Semi)Quantification in the Nanogram Range. *Environmental Science & Technology*, 54(4), 2353-2359. doi:<https://doi.org/10.1021/acs.est.9b07540>
- Matsuguma, Y., Takada, H., Kumata, H., Kanke, H., Sakurai, S., Suzuki, T., Itoh, M., Okazaki, Y., Boonyatumanond, R., Zakaria, M. P., Weerts, S., & Newman, B. (2017). Microplastics in Sediment Cores from Asia and Africa as Indicators of Temporal Trends in Plastic Pollution. *Archives of Environmental Contamination and Toxicology*, 73(2), 230-239. doi:<https://doi.org/10.1007/s00244-017-0414-9>
- Maximenko, N., Hafner, J., & Niler, P. (2012). Pathways of marine debris derived from trajectories of Lagrangian drifters. *Marine Pollution Bulletin*, 65(1–3), 51-62. doi:<http://dx.doi.org/10.1016/j.marpolbul.2011.04.016>
- McCormick, A., Hoellein, T. J., Mason, S. A., Schluep, J., & Kelly, J. J. (2014). Microplastic is an Abundant and Distinct Microbial Habitat in an Urban River. *Environmental Science & Technology*, 48(20), 11863-11871. doi:<http://dx.doi.org/10.1021/es503610r>
- MEPEX. (2014). *Sources of microplastic- pollution to the marine environment* (M-321-2015). Retrieved from <https://www.miljodirektoratet.no/globalassets/publikasjoner/M321/M321.pdf>
- MEPEX. (2016). *Primary microplastic-pollution: Measures and reduction potentials in Norway* (M-545-2016). Retrieved from <https://www.miljodirektoratet.no/globalassets/publikasjoner/M545/M545.pdf>
- Meyns, M., Primpke, S., & Gerdt, G. (2019). Library based identification and characterisation of polymers with nano-FTIR and IR-sSNOM imaging. *Analytical Methods*, 11(40), 5195-5202. doi:<http://dx.doi.org/10.1039/C9AY01193E>
- Mintenig, S. M., Bäuerlein, P. S., Koelmans, A. A., Dekker, S. C., & van Wezel, A. P. (2018). Closing the gap between small and smaller: towards a framework to analyse nano- and microplastics in aqueous environmental samples. *Environmental Science: Nano*, 5(7), 1640-1649. doi:<http://dx.doi.org/10.1039/C8EN00186C>
- Mintenig, S. M., Int-Veen, I., Löder, M. G. J., Primpke, S., & Gerdt, G. (2017). Identification of microplastic in effluents of waste water treatment plants using focal plane array-based micro-Fourier-transform infrared imaging. *Water Research*, 108, 365-372. doi:<http://dx.doi.org/10.1016/j.watres.2016.11.015>
- Mintenig, S. M., Kooi, M., Erich, M. W., Primpke, S., Redondo- Hasselerharm, P. E., Dekker, S. C., Koelmans, A. A., & van Wezel, A. P. (2020). A systems approach to understand microplastic occurrence and variability in Dutch riverine surface waters. *Water Research*, 176, 115723. doi:<https://doi.org/10.1016/j.watres.2020.115723>
- Mintenig, S. M., Löder, M. G. J., Primpke, S., & Gerdt, G. (2019). Low numbers of microplastics detected in drinking water from ground water sources. *Science of the Total Environment*, 648, 631-635. doi:<https://doi.org/10.1016/j.scitotenv.2018.08.178>
- Moore, C. J., Moore, S. L., Leecaster, M. K., & Weisberg, S. B. (2001). A Comparison of Plastic and Plankton in the North Pacific Central Gyre. *Marine Pollution Bulletin*, 42(12), 1297-1300. doi:[http://dx.doi.org/10.1016/S0025-326X\(01\)00114-X](http://dx.doi.org/10.1016/S0025-326X(01)00114-X)
- Morét-Ferguson, S., Law, K. L., Proskurowski, G., Murphy, E. K., Peacock, E. E., & Reddy, C. M. (2010). The size, mass, and composition of plastic debris in the western North Atlantic Ocean. *Marine Pollution Bulletin*, 60(10), 1873-1878. doi:<http://dx.doi.org/10.1016/j.marpolbul.2010.07.020>
- Morris, A. W., & Hamilton, E. I. (1974). Polystyrene spherules in the Bristol Channel. *Marine Pollution Bulletin*, 5(2), 26-27. doi:[http://dx.doi.org/10.1016/0025-326X\(74\)90311-7](http://dx.doi.org/10.1016/0025-326X(74)90311-7)
- MSFD GES TSG Marine Litter. (2011). *Marine Litter: Technical Recommendations for the Implementation of MSFD Requirements* (Vol. EUR 25009EN). Luxembourg: Publications Office of the European Union. doi:<https://doi.org/10.2788/92438>

References

- Möhlenkamp, P., Purser, A., & Thomsen, L. (2018). Plastic microbeads from cosmetic products: an experimental study of their hydrodynamic behaviour, vertical transport and resuspension in phytoplankton and sediment aggregates. *Elementa Science of the Anthropocene*, 6(1), 61. doi:<http://doi.org/10.1525/elementa.317>
- Neumann, D., Callies, U., & Matthies, M. (2014). Marine litter ensemble transport simulations in the southern North Sea. *Marine Pollution Bulletin*, 86(1–2), 219–228. doi:<http://dx.doi.org/10.1016/j.marpolbul.2014.07.016>
- Ng, K. L., & Obbard, J. P. (2006). Prevalence of microplastics in Singapore's coastal marine environment. *Marine Pollution Bulletin*, 52(7), 761–767. doi:<https://doi.org/10.1016/j.marpolbul.2005.11.017>
- Norén, F. (2007). *Small Plastic Particles In Coastal Swedish Waters*. Retrieved from <http://www.n-research.se/pdf/Small%20plastic%20particles%20in%20Swedish%20West%20Coast%20Waters.pdf>
- NorthSEE. (2016). Current shipping routes and maritime traffic. Retrieved from <https://northsearegion.eu/northsee/s-hipping/current-shipping-routes-and-martime-traffic-2016/>
- Nuelle, M.-T., Dekiff, J. H., Remy, D., & Fries, E. (2014). A new analytical approach for monitoring microplastics in marine sediments. *Environmental Pollution*, 184(0), 161–169. doi:<http://dx.doi.org/10.1016/j.envpol.2013.07.027>
- O'Brine, T., & Thompson, R. C. (2010). Degradation of plastic carrier bags in the marine environment. *Marine Pollution Bulletin*, 60(12), 2279–2283. doi:<http://dx.doi.org/10.1016/j.marpolbul.2010.08.005>
- Obbard, R. W., Sadri, S., Wong, Y. Q., Khitun, A. A., Baker, I., & Thompson, R. C. (2014). Global warming releases microplastic legacy frozen in Arctic Sea ice. *Earth's Future*, 2(6), 315–320. doi:<http://dx.doi.org/10.1002/2014EF000240>
- Olesen, K. B., Stephansen, D. A., van Alst, N., & Vollertsen, J. (2019). Microplastics in a Stormwater Pond. *Water*, 11(7), 1466. doi:<https://doi.org/10.3390/w11071466>
- OSPAR. (1992). *Convention for the protection of the marine environment of the North-East Atlantic*. Retrieved from https://www.ospar.org/site/assets/files/1290/ospar_convention_e_updated_text_in_2007_no_revs.pdf
- OSPAR. (2000). *Overview of geography, hydrography and climate of the North Sea (Chapter II of the Quality Status Report)*. Retrieved from <http://www.ospar.org/eng/doc/pdfs/r2c2.pdf>
- OSPAR. (2010). *Quality Status Report 2010*. Retrieved from https://qsr2010.ospar.org/en/media/chapter_pdf/QSR_complete_EN.pdf
- Osswald, T. A., Baur, E., Brinkmann, S., Oberbach, K., & Schmachtenberg, E. (2006). Material Property Tables. In *International Plastics Handbook* (pp. 717–902): Carl Hanser Verlag GmbH & Co. KG.
- Otto, L., Zimmerman, J. T. F., Furnes, G. K., Mork, M., Saetre, R., & Becker, G. (1990). Review of the physical oceanography of the North Sea. *Netherlands Journal of Sea Research*, 26(2), 161–238. doi:[http://dx.doi.org/10.1016/0077-7579\(90\)90091-T](http://dx.doi.org/10.1016/0077-7579(90)90091-T)
- Pagter, E., Frias, J., & Nash, R. (2018). Microplastics in Galway Bay: A comparison of sampling and separation methods. *Marine Pollution Bulletin*, 135, 932–940. doi:<https://doi.org/10.1016/j.marpolbul.2018.08.013>
- Paul-Pont, I., Tallec, K., Gonzalez-Fernandez, C., Lambert, C., Vincent, D., Mazurais, D., Zambonino-Infante, J.-L., Brotons, G., Lagarde, F., Fabioux, C., Soudant, P., & Huvet, A. (2018). Constraints and Priorities for Conducting Experimental Exposures of Marine Organisms to Microplastics. *Frontiers in Marine Science* 5(252). doi:<https://doi.org/10.3389/fmars.2018.00252>
- Peeken, I., Primpke, S., Beyer, B., Gütermann, J., Katlein, C., Krumpfen, T., Bergmann, M., Hehemann, L., & Gerdt, G. (2018). Arctic sea ice is an important temporal sink and

References

- means of transport for microplastic. *Nature Communications*, 9(1), 1505. doi:<https://doi.org/10.1038/s41467-018-03825-5>
- Peters, E. N. (2015). Thermoplastics, Thermosets, and Elastomers—Descriptions and Properties. In M. Kutz (Ed.), *Mechanical Engineers' Handbook* (4th ed., pp. 1-48): John Wiley & Sons, Inc.
- Phuong, N. N., Poirier, L., Lagarde, F., Kamari, A., & Zalouk-Vergnoux, A. (2018). Microplastic abundance and characteristics in French Atlantic coastal sediments using a new extraction method. *Environmental Pollution*, 243, 228-237. doi:<https://doi.org/10.1016/j.envpol.2018.08.032>
- Piarulli, S., Scapinello, S., Comandini, P., Magnusson, K., Granberg, M., Wong, J. X. W., Sciutto, G., Prati, S., Mazzeo, R., Booth, A. M., & Airoidi, L. (2019). Microplastic in wild populations of the omnivorous crab *Carcinus aestuarii*: A review and a regional-scale test of extraction methods, including microfibrils. *Environmental Pollution*, 251, 117-127. doi:<https://doi.org/10.1016/j.envpol.2019.04.092>
- PlasticsEurope. (2012). *Plastics - the Facts 2012: An analysis of European latest plastics production, demand and waste data*. Retrieved from Brussels: <https://www.plasticseurope.org/en/resources/publications/109-plastics-facts-2012>
- PlasticsEurope. (2015). *Plastics - the Facts 2015: An analysis of European plastics production, demand and waste data*. Retrieved from Brussels: <https://www.plasticseurope.org/en/resources/publications/93-plastics-facts-2015>
- PlasticsEurope. (2018). *Plastics - the Facts 2018: An analysis of European plastics production, demand and waste data*. Retrieved from Brussels: <https://www.plasticseurope.org/en/resources/publications/619-plastics-facts-2018>
- PlasticsEurope. (2019). *Plastics - the Facts 2019: An analysis of European plastics production, demand and waste data*. Retrieved from Brussels: <https://www.plasticseurope.org/en/resources/publications/1804-plastics-facts-2019>
- Pohl, F., Eggenhuisen, J. T., Kane, I. A., & Clare, M. A. (2020). Transport and Burial of Microplastics in Deep-Marine Sediments by Turbidity Currents. *Environmental Science & Technology*. doi:<https://doi.org/10.1021/acs.est.9b07527>
- Porter, A., Lyons, B. P., Galloway, T. S., & Lewis, C. (2018). Role of Marine Snows in Microplastic Fate and Bioavailability. *Environmental Science & Technology*, 52(12), 7111-7119. doi:<https://doi.org/10.1021/acs.est.8b01000>
- Potthoff, A., Oelschlägel, K., Schmitt-Jansen, M., Rummel, C. D., & Kühnel, D. (2017). From the sea to the laboratory: Characterization of microplastic as prerequisite for the assessment of ecotoxicological impact. *Integrated Environmental Assessment and Management*, 13(3), 500-504. doi:<https://doi.org/10.1002/ieam.1902>
- Primpke, S., Christiansen, S. H., Cowger, W., De Frond, H., Deshpande, A., Fischer, M., Holland, E., Meyns, M., O'Donnell, B. A., Ossmann, B., Pittroff, M., Sarau, G., Scholz-Böttcher, B. M., & Wiggan, K. (2020a). EXPRESS: Critical Assessment of Analytical Methods for the Harmonized and Cost Efficient Analysis of Microplastics. *Applied Spectroscopy*, 0(ja), 0003702820921465. doi:<https://doi.org/10.1177/0003702820921465>
- Primpke, S., Cross, R. K., Mintenig, S. M., Simon, M., Vianello, A., Gerdts, G., & Vollertsen, J. (2020b). EXPRESS: Toward the Systematic Identification of Microplastics in the Environment: Evaluation of a New Independent Software Tool (siMPle) for Spectroscopic Analysis. *Applied Spectroscopy*, 0(ja), 0003702820917760. doi:<https://doi.org/10.1177/0003702820917760>
- Primpke, S., Dias, P. A., & Gerdts, G. (2019). Automated Identification and Quantification of Microfibrils and Microplastics. *Analytical Methods*, 11, 2138-2147. doi:<http://dx.doi.org/10.1039/C9AY00126C>
- Primpke, S., Imhof, H., Piehl, S., Lorenz, C., Löder, M., Laforsch, C., & Gerdts, G. (2017a). Mikroplastik in der Umwelt. *Chemie in unserer Zeit*, 51(6), 402-412. doi:<http://dx.doi.org/10.1002/ciuz.201700821>

References

- Primpke, S., Lorenz, C., Rascher-Friesenhausen, R., & Gerdt, G. (2017b). An automated approach for microplastics analysis using focal plane array (FPA) FTIR microscopy and image analysis. *Analytical Methods*, 9(9), 1499-1511. doi:<http://dx.doi.org/10.1039/C6AY02476A>
- Primpke, S., Wirth, M., Lorenz, C., & Gerdt, G. (2018). Reference database design for the automated analysis of microplastic samples based on Fourier transform infrared (FTIR) spectroscopy. *Analytical and Bioanalytical Chemistry*, 410(21), 5131-5141. doi:<https://doi.org/10.1007/s00216-018-1156-x>
- Puig, P., Palanques, A., & Martín, J. (2014). Contemporary Sediment-Transport Processes in Submarine Canyons. *Annual Review of Marine Science*, 6(1), 53-77. doi:<https://doi.org/10.1146/annurev-marine-010213-135037>
- Rajakumar, K., Sarasvathy, V., Thamarai Chelvan, A., Chitra, R., & Vijayakumar, C. T. (2009). Natural Weathering Studies of Polypropylene. *Journal of Polymers and the Environment*, 17(3), 191. doi:<https://doi.org/10.1007/s10924-009-0138-7>
- Rani, M., Shim, W., Han, G., Jang, M., Al-Odaini, N., Song, Y., & Hong, S. (2015). Qualitative Analysis of Additives in Plastic Marine Debris and Its New Products. *Archives of Environmental Contamination and Toxicology*, 69(3), 352-366. doi:<http://dx.doi.org/10.1007/s00244-015-0224-x>
- Rao, C. R. (1995). A review of canonical coordinates and an alternative to correspondence analysis using Hellinger distance. *Qüestió*, 19(1-3), 23-63. Retrieved from <http://hdl.handle.net/2099/4059>
- Reisser, J., Slat, B., Noble, K., du Plessis, K., Epp, M., Proietti, M., de Sonnevile, J., Becker, T., & Pattiaratchi, C. (2015). The vertical distribution of buoyant plastics at sea: an observational study in the North Atlantic Gyre. *Biogeosciences*, 12(4), 1249-1256. doi:<https://doi.org/10.5194/bg-12-1249-2015>
- Renner, G., Schmidt, T. C., & Schram, J. (2017). A New Chemometric Approach for Automatic Identification of Microplastics from Environmental Compartments Based on FT-IR Spectroscopy. *Analytical Chemistry*, 89(22), 12045-12053. doi:<http://dx.doi.org/10.1021/acs.analchem.7b02472>
- Renner, G., Schmidt, T. C., & Schram, J. (2020). Automated rapid & intelligent microplastics mapping by FTIR microscopy: A Python-based workflow. *MethodsX*, 7, 100742. doi:<https://doi.org/10.1016/j.mex.2019.11.015>
- Renzi, M., Blašković, A., Fastelli, P., Marcelli, M., Guerranti, C., Cannas, S., Barone, L., & Massara, F. (2018). Is the microplastic selective according to the habitat? Records in amphioxus sands, Mäerl bed habitats and Cymodocea nodosa habitats. *Marine Pollution Bulletin*, 130, 179-183. doi:<https://doi.org/10.1016/j.marpolbul.2018.03.019>
- Rist, S., Vianello, A., Winding, M. H. S., Nielsen, T. G., Almeda, R., Torres, R. R., & Vollertsen, J. (2020). Quantification of plankton-sized microplastics in a productive coastal Arctic marine ecosystem. *Environmental Pollution*, 266, 115248. doi:<https://doi.org/10.1016/j.envpol.2020.115248>
- Rivers, M. L., Gwinnett, C., & Woodall, L. C. (2019). Quantification is more than counting: Actions required to accurately quantify and report isolated marine microplastics. *Marine Pollution Bulletin*, 139, 100-104. doi:<https://doi.org/10.1016/j.marpolbul.2018.12.024>
- Rochman, C. M., Browne, M. A., Halpern, B. S., Hentschel, B. T., Hoh, E., Karapanagioti, H. K., Rios-Mendoza, L. M., Takada, H., Teh, S., & Thompson, R. C. (2013). Policy: Classify plastic waste as hazardous. *Nature*, 494(7436), 169-171. Retrieved from <http://dx.doi.org/10.1038/494169a>
- Rochman, C. M., Regan, F., & Thompson, R. C. (2017). On the harmonization of methods for measuring the occurrence, fate and effects of microplastics. *Analytical Methods*, 9(9), 1324-1325. doi:<http://dx.doi.org/10.1039/C7AY90014G>
- Rockström, J., Steffen, W., Noone, K., Persson, Å., Chapin, F. S., Lambin, E. F., Lenton, T. M., Scheffer, M., Folke, C., Schellnhuber, H. J., Nykvist, B., de Wit, C. A., Hughes, T., van der Leeuw, S., Rodhe, H., Sorlin, S., Snyder, P. K., Costanza, R., Svedin, U., Falkenmark, M., Karlberg, L., Corell, R. W., Fabry, V. J., Hansen, J., Walker, B.,

References

- Liverman, D., Richardson, K., Crutzen, P., & Foley, J. A. (2009). A safe operating space for humanity. *Nature*, 461(7263), 472-475. Retrieved from <http://dx.doi.org/10.1038/461472a>
- Rodrigues, M. O., Gonçalves, A. M. M., Gonçalves, F. J. M., & Abrantes, N. (2020). Improving cost-efficiency for MPs density separation by zinc chloride reuse. *MethodsX*, 7, 100785. doi:<https://doi.org/10.1016/j.mex.2020.100785>
- Rummel, C. D., Jahnke, A., Gorokhova, E., Kühnel, D., & Schmitt-Jansen, M. (2017). Impacts of Biofilm Formation on the Fate and Potential Effects of Microplastic in the Aquatic Environment. *Environmental Science & Technology Letters*, 4(7), 258-267. doi:<https://doi.org/10.1021/acs.estlett.7b00164>
- Rummel, C. D., Löder, M. G. J., Fricke, N. F., Lang, T., Griebeler, E.-M., Janke, M., & Gerdts, G. (2016). Plastic ingestion by pelagic and demersal fish from the North Sea and Baltic Sea. *Marine Pollution Bulletin*, 102(1), 134-141. doi:<http://dx.doi.org/10.1016/j.marpolbul.2015.11.043>
- Schmidt, C., Krauth, T., & Wagner, S. (2017). Export of Plastic Debris by Rivers into the Sea. *Environmental Science & Technology*, 51(21), 12246-12253. doi:<http://dx.doi.org/10.1021/acs.est.7b02368>
- Sea-Mer Asso. (2017). Industrial Paraffin-Wax Strandings on the Eastern Coast of the Channel. Contexts and Stakes. Retrieved from <http://sea-mer.org/wp-content/uploads/2018/02/Paraffin-wax-strandings-Sea-Mer-Asso.pdf>
- Searle, N. D. (2005). Environmental Effects on Polymeric Materials. In A. Andrady (Ed.), *Plastics and the Environment* (pp. 311-358).
- Shi, Y., Qin, J., Tao, Y., Jie, G., & Wang, J. (2019). Natural weathering severity of typical coastal environment on polystyrene: Experiment and modeling. *Polymer Testing*, 76, 138-145. doi:<https://doi.org/10.1016/j.polymertesting.2019.03.018>
- Shim, W. J., Hong, S. H., & Eo, S. E. (2017). Identification methods in microplastic analysis: a review. *Analytical Methods*, 9(9), 1384-1391. doi:<http://dx.doi.org/10.1039/C6AY02558G>
- Shim, W. J., Song, Y. K., Hong, S. H., & Jang, M. (2016). Identification and quantification of microplastics using Nile Red staining. *Marine Pollution Bulletin*, 113(1), 469-476. doi:<http://dx.doi.org/10.1016/j.marpolbul.2016.10.049>
- Shim, W. J., & Thompson, R. C. (2015). Microplastics in the Ocean. *Archives of Environmental Contamination and Toxicology*, 69(3), 265-268. doi:<http://dx.doi.org/10.1007/s00244-015-0216-x>
- Silva, A. B., Bastos, A. S., Justino, C. I. L., da Costa, J. P., Duarte, A. C., & Rocha-Santos, T. A. P. (2018). Microplastics in the environment: Challenges in analytical chemistry - A review. *Analytica Chimica Acta*, 1017, 1-19. doi:<https://doi.org/10.1016/j.aca.2018.02.043>
- Simon, M., van Alst, N., & Vollertsen, J. (2018). Quantification of microplastic mass and removal rates at wastewater treatment plants applying Focal Plane Array (FPA)-based Fourier Transform Infrared (FT-IR) imaging. *Water Research*, 142, 1-9. doi:<https://doi.org/10.1016/j.watres.2018.05.019>
- Sokal, R. R., & Rohlf, F. J. (1995). *Biometry: The Principles And Practice Of Statistics In Biological Research* (W. H. Freeman Ed. 3rd edition ed.). New York, USA: Freeman, W.H.
- Song, Y. K., Hong, S. H., Jang, M., Han, G. M., Jung, S. W., & Shim, W. J. (2017). Combined Effects of UV Exposure Duration and Mechanical Abrasion on Microplastic Fragmentation by Polymer Type. *Environmental Science & Technology*, 51(8), 4368-4376. doi:<http://dx.doi.org/10.1021/acs.est.6b06155>
- Song, Y. K., Hong, S. H., Jang, M., Han, G. M., Rani, M., Lee, J., & Shim, W. J. (2015). A comparison of microscopic and spectroscopic identification methods for analysis of microplastics in environmental samples. *Marine Pollution Bulletin*, 93(1-2), 202-209. doi:<http://dx.doi.org/10.1016/j.marpolbul.2015.01.015>

References

- Steffen, W., Richardson, K., Rockström, J., Cornell, S. E., Fetzer, I., Bennett, E. M., Biggs, R., Carpenter, S. R., de Vries, W., de Wit, C. A., Folke, C., Gerten, D., Heinke, J., Mace, G. M., Persson, L. M., Ramanathan, V., Reyers, B., & Sörlin, S. (2015). Planetary boundaries: Guiding human development on a changing planet. *Science*, 347(6223). doi:<https://doi.org/10.1126/science.1259855>
- Stolte, A., Forster, S., Gerdts, G., & Schubert, H. (2015). Microplastic concentrations in beach sediments along the German Baltic coast. *Marine Pollution Bulletin*, 99(1–2), 216–229. doi:<http://dx.doi.org/10.1016/j.marpolbul.2015.07.022>
- Suaria, G., Aliani, S., Merlino, S., & Abbate, M. (2018). The Occurrence of Paraffin and Other Petroleum Waxes in the Marine Environment: A Review of the Current Legislative Framework and Shipping Operational Practices. *Frontiers in Marine Science* 5(94). doi:<https://doi.org/10.3389/fmars.2018.00094>
- Suaria, G., Avio, C. G., Mineo, A., Lattin, G. L., Magaldi, M. G., Belmonte, G., Moore, C. J., Regoli, F., & Aliani, S. (2016). The Mediterranean Plastic Soup: synthetic polymers in Mediterranean surface waters. *Scientific Reports*, 6, 37551. doi:<http://dx.doi.org/10.1038/srep37551>
- Svečnjak, L., Baranović, G., Vinceković, M., Prđun, S., Bubalo, D., & Gajger, I. T. (2015). An Approach for Routine Analytical Detection of Beeswax Adulteration Using FTIR-ATR Spectroscopy. *Journal of Apicultural Science*, 59(2), 37. doi:<https://doi.org/10.1515/jas-2015-0018>
- Sündermann, J., & Pohlmann, T. (2011). A brief analysis of North Sea physics. *Oceanologia*, 53(3), 663–689. doi:<https://doi.org/10.5697/oc.53-3.663>
- Tagg, A. S., Harrison, J. P., Ju-Nam, Y., Sapp, M., Bradley, E. L., Sinclair, C. J., & Ojeda, J. J. (2017). Fenton's reagent for the rapid and efficient isolation of microplastics from wastewater. *Chemical Communications* 1–4. doi:<http://dx.doi.org/10.1039/C6CC08798A>
- Tagg, A. S., Oberbeckmann, S., Fischer, D., Kreikemeyer, B., & Labrenz, M. (2019). Paint particles are a distinct and variable substrate for marine bacteria. *Marine Pollution Bulletin*, 146, 117–124. doi:<https://doi.org/10.1016/j.marpolbul.2019.06.013>
- Tagg, A. S., Sapp, M., Harrison, J. P., & Ojeda, J. J. (2015). Identification and Quantification of Microplastics in Wastewater Using Focal Plane Array-Based Reflectance Micro-FT-IR Imaging. *Analytical Chemistry*, 87(12), 6032–6040. doi:<http://dx.doi.org/10.1021/acs.analchem.5b00495>
- Tekman, M. B., Wekerle, C., Lorenz, C., Primpke, S., Hasemann, C., Gerdts, G., & Bergmann, M. (2020). Tying up loose ends of microplastic pollution in the Arctic: Distribution from the sea surface, through the water column to deep-sea sediments at the HAUSGARTEN observatory. *Environmental Science & Technology*, 54(7), 4079–4090. doi:<https://doi.org/10.1021/acs.est.9b06981>
- Ter Halle, A., Jeanneau, L., Martignac, M., Jardé, E., Pedrono, B., Brach, L., & Gigault, J. (2017a). Nanoplastic in the North Atlantic Subtropical Gyre. *Environmental Science & Technology*, 51(23), 13689–13697. doi:<https://doi.org/10.1021/acs.est.7b03667>
- Ter Halle, A., Ladirat, L., Gendre, X., Goudouneche, D., Pusineri, C., Routaboul, C., Tenailleau, C., Duployer, B., & Perez, E. (2016). Understanding the Fragmentation Pattern of Marine Plastic Debris. *Environmental Science & Technology*, 50(11), 5668–5675. doi:<http://dx.doi.org/10.1021/acs.est.6b00594>
- Ter Halle, A., Ladirat, L., Martignac, M., Mingotaud, A. F., Boyron, O., & Perez, E. (2017b). To what extent are microplastics from the open ocean weathered? *Environmental Pollution*, 227, 167–174. doi:<https://doi.org/10.1016/j.envpol.2017.04.051>
- Thiel, M., Hinojosa, I. A., Joschko, T., & Gutow, L. (2011). Spatio-temporal distribution of floating objects in the German Bight (North Sea). *Journal of Sea Research*, 65(3), 368–379. doi:<http://dx.doi.org/10.1016/j.seares.2011.03.002>
- Thompson, R. C., Olsen, Y., Mitchell, R. P., Davis, A., Rowland, S. J., John, A. W. G., McGonigle, D., & Russell, A. E. (2004). Lost at Sea: Where Is All the Plastic? *Science*, 304(5672), 838. doi:<https://doi.org/10.1126/science.1094559>

References

- Tokiwa, Y., Calabia, B. P., Ugwu, C. U., & Aiba, S. (2009). Biodegradability of Plastics. *International Journal of Molecular Sciences*, 10(9), 3722-3742. doi:<https://doi.org/10.3390/ijms10093722>
- Transportation Research Board National Research Council. (2003). *Oil in the Sea III: Inputs, Fates, and Effects*. Washington, DC: The National Academies Press. doi:<https://doi.org/10.17226/10388>
- Turner, A. (2010). Marine pollution from antifouling paint particles. *Marine Pollution Bulletin*, 60(2), 159-171. doi:<https://doi.org/10.1016/j.marpolbul.2009.12.004>
- UEG. (2014). *Pollution of the North and Baltic Seas with Paraffin*. Retrieved from <http://www.bfr.bund.de/cm/349/pollution-of-the-north-and-baltic-seas-with-paraffin.pdf>
- Unice, K. M., Kreider, M. L., & Panko, J. M. (2013). Comparison of Tire and Road Wear Particle Concentrations in Sediment for Watersheds in France, Japan, and the United States by Quantitative Pyrolysis GC/MS Analysis. *Environmental Science & Technology*, 47(15), 8138-8147. doi:<https://doi.org/10.1021/es400871j>
- Van Cauwenberghe, L., Vanreusel, A., Mees, J., & Janssen, C. R. (2013). Microplastic pollution in deep-sea sediments. *Environmental Pollution*, 182(0), 495-499. doi:<http://dx.doi.org/10.1016/j.envpol.2013.08.013>
- van Franeker, J. A., Blaize, C., Danielsen, J., Fairclough, K., Gollan, J., Guse, N., Hansen, P.-L., Heubeck, M., Jensen, J.-K., Le Guillou, G., Olsen, B., Olsen, K.-O., Pedersen, J., Stienen, E. W. M., & Turner, D. M. (2011). Monitoring plastic ingestion by the northern fulmar *Fulmarus glacialis* in the North Sea. *Environmental Pollution*, 159(10), 2609-2615. doi:<http://dx.doi.org/10.1016/j.envpol.2011.06.008>
- van Seville, E., England, M. H., & Froyland, G. (2012). Origin, dynamics and evolution of ocean garbage patches from observed surface drifters. *Environmental Research Letters*, 7(4), 044040. Retrieved from <http://stacks.iop.org/1748-9326/7/i=4/a=044040>
- van Seville, E., Wilcox, C., Lebreton, L., Maximenko, N., Hardesty, B. D., van Franeker, J. A., Eriksen, M., Siegel, D., Galgani, F., & Law, K. L. (2015). A global inventory of small floating plastic debris. *Environmental Research Letters*, 10(12), 11. Retrieved from <http://stacks.iop.org/1748-9326/10/i=12/a=124006>
- Vianello, A., Boldrin, A., Guerriero, P., Moschino, V., Rella, R., Sturaro, A., & Da Ros, L. (2013). Microplastic particles in sediments of Lagoon of Venice, Italy: First observations on occurrence, spatial patterns and identification. *Estuarine, Coastal and Shelf Science*, 130(0), 54-61. doi:<http://dx.doi.org/10.1016/j.ecss.2013.03.022>
- Vianello, A., Da Ros, L., Boldrin, A., Marceta, T., & Moschino, V. (2018). First evaluation of floating microplastics in the Northwestern Adriatic Sea. *Environmental Science and Pollution Research* 25(28), 28546-28561. doi:<https://doi.org/10.1007/s11356-018-2812-6>
- Vianello, A., Jensen, R. L., Liu, L., & Vollertsen, J. (2019). Simulating human exposure to indoor airborne microplastics using a Breathing Thermal Manikin. *Scientific Reports*, 9(1), 8670. doi:<https://doi.org/10.1038/s41598-019-45054-w>
- Villarrubia-Gómez, P., Cornell, S. E., & Fabres, J. (2018). Marine plastic pollution as a planetary boundary threat – The drifting piece in the sustainability puzzle. *Marine Policy*, 96, 213-220. doi:<https://doi.org/10.1016/j.marpol.2017.11.035>
- Vogelsang, C., Lusher, A., Dadkhah, M. E., Sundvor, I., Umar, M., Rannekleiv, S. B., Eidsvoll, D. P., & Meland, S. (2018). *Microplastics in road dust - characteristics, pathways and measures*. Retrieved from <http://www.miljodirektoratet.no/Documents/publikasjoner/M959/M959.pdf>
- von Friesen, L. W., Granberg, M. E., Hassellöv, M., Gabrielsen, G. W., & Magnusson, K. (2019). An efficient and gentle enzymatic digestion protocol for the extraction of microplastics from bivalve tissue. *Marine Pollution Bulletin*, 142, 129-134. doi:<https://doi.org/10.1016/j.marpolbul.2019.03.016>
- Ward, J. E., & Kach, D. J. (2009). Marine aggregates facilitate ingestion of nanoparticles by suspension-feeding bivalves. *Marine Environmental Research*, 68(3), 137-142. doi:<http://dx.doi.org/10.1016/j.marenvres.2009.05.002>

References

- Weinstein, J. E., Crocker, B. K., & Gray, A. D. (2016). From macroplastic to microplastic: Degradation of high-density polyethylene, polypropylene, and polystyrene in a salt marsh habitat. *Environmental Toxicology and Chemistry*, 35(7), 1632-1640. doi:<https://doi.org/10.1002/etc.3432>
- Wenneker, B., & Oosterbaan, L. (2018). *Paraffin on the Dutch Coast*. Retrieved from <https://www.noordzeeloket.nl/functies-gebruik/zwerfvuil-noordzee/paraffine/@205930/paraffin-dutch-coast/>
- Wessel, P., & Smith, W. H. F. (1996). A global, self-consistent, hierarchical, high-resolution shoreline database. *Journal of Geophysical Research: Solid Earth*, 101(B4), 8741-8743. doi:<https://doi.org/10.1029/96JB00104>
- Wilcox, C., Heathcote, G., Goldberg, J., Gunn, R., Peel, D., & Hardesty, B. D. (2014). Understanding the Sources and Effects of Abandoned, Lost, and Discarded Fishing Gear on Marine Turtles in Northern Australia. *Conservation Biology*, 29(1), 198-206. doi:<http://dx.doi.org/10.1111/cobi.12355>
- Woodall, L. C., Sanchez-Vidal, A., Canals, M., Paterson, G. L. J., Coppock, R., Sleight, V., Calafat, A., Rogers, A. D., Narayanaswamy, B. E., & Thompson, R. C. (2014). The deep sea is a major sink for microplastic debris. *Royal Society Open Science* 1(4). doi:<https://doi.org/10.1098/rsos.140317>
- Wright, S. L., Thompson, R. C., & Galloway, T. S. (2013). The physical impacts of microplastics on marine organisms: A review. *Environmental Pollution*, 178(0), 483-492. doi:<http://dx.doi.org/10.1016/j.envpol.2013.02.031>
- Wright, S. L., Ulke, J., Font, A., Chan, K. L. A., & Kelly, F. J. (2020). Atmospheric microplastic deposition in an urban environment and an evaluation of transport. *Environment International*, 136, 105411. doi:<https://doi.org/10.1016/j.envint.2019.105411>
- Zarfl, C. (2019). Promising techniques and open challenges for microplastic identification and quantification in environmental matrices. *Analytical and Bioanalytical Chemistry*, 411(17), 3743-3756. doi:<https://doi.org/10.1007/s00216-019-01763-9>
- Zettler, E. R., Mincer, T. J., & Amaral-Zettler, L. A. (2013). Life in the "Plastisphere": Microbial Communities on Plastic Marine Debris. *Environmental Science & Technology*, 47(13), 7137-7146. doi:<http://dx.doi.org/10.1021/es401288x>
- Zhu, X. (2015). Optimization of elutriation device for filtration of microplastic particles from sediment. *Marine Pollution Bulletin*, 92(1-2), 69-72. doi:<https://doi.org/10.1016/j.marpolbul.2014.12.054>
- Zobkov, M. B., Esiukova, E. E., Zyubin, A. Y., & Samusev, I. G. (2019). Microplastic content variation in water column: The observations employing a novel sampling tool in stratified Baltic Sea. *Marine Pollution Bulletin*, 138, 193-205. doi:<https://doi.org/10.1016/j.marpolbul.2018.11.047>

References

List of publications

Further scientific publications with contribution during the period of my PhD

- i. Löder, M. G. J., Kuczera, M., Mintenig, S., Lorenz, C., & Gerdts, G. (2015). Focal plane array detector-based micro-Fourier-transform infrared imaging for the analysis of microplastics in environmental samples. *Environmental Chemistry* 12(5), 563-581. doi:<http://dx.doi.org/10.1071/EN14205>
- ii. Bergmann, M., Wirzberger, V., Krumpen, T., Lorenz, C., Primpke, S., Tekman, M. B., & Gerdts, G. (2017). High quantities of microplastic in Arctic deep-sea sediments from the HAUSGARTEN Observatory. *Environmental Science & Technology*, 51(19), 11000-11010. doi:<https://doi.org/10.1021/acs.est.7b03331>
- iii. Löder, M. G. J., Imhof, H. K., Ladehoff, M., Löschel, L. A., Lorenz, C., Mintenig, S., Piehl, S., Primpke, S., Schrank, I., Laforsch, C., & Gerdts, G. (2017). Enzymatic Purification of Microplastics in Environmental Samples. *Environmental Science & Technology*, 51(24), 14283-14292. doi:<http://dx.doi.org/10.1021/acs.est.7b03055>
- iv. Primpke, S., Imhof, H., Piehl, S., Lorenz, C., Löder, M., Laforsch, C., & Gerdts, G. (2017). Mikroplastik in der Umwelt. *Chemie in unserer Zeit*, 51(6), 402-412. doi:<http://dx.doi.org/10.1002/ciuz.201700821>
- v. Primpke, S., Lorenz, C., Rascher-Friesenhausen, R., & Gerdts, G. (2017). An automated approach for microplastics analysis using focal plane array (FPA) FTIR microscopy and image analysis. *Analytical Methods*, 9(9), 1499-1511. doi:<http://dx.doi.org/10.1039/C6AY02476A>
- vi. Cabernard, L., Roscher, L., Lorenz, C., Gerdts, G., & Primpke, S. (2018). Comparison of Raman and Fourier Transform Infrared Spectroscopy for the Quantification of Microplastics in the Aquatic Environment. *Environmental Science & Technology*, 52(22), 13279-13288. doi:<https://doi.org/10.1021/acs.est.8b03438>
- vii. Hamm T., Lorenz C., Piehl S. (2018) Microplastics in Aquatic Systems – Monitoring Methods and Biological Consequences. In: Jungblut S., Liebich V., Bode M. (eds) YOUNARES 8 – Oceans Across Boundaries: Learning from each other. *Springer, Cham*. doi:https://doi.org/10.1007/978-3-319-93284-2_13

List of publications

- viii. Primpke, S., Wirth, M., Lorenz, C., & Gerdts, G. (2018). Reference database design for the automated analysis of microplastic samples based on Fourier transform infrared (FTIR) spectroscopy. *Analytical and Bioanalytical Chemistry*, 410(21), 5131-5141. doi:<https://doi.org/10.1007/s00216-018-1156-x>
- ix. Mani, T., Primpke, S., Lorenz, C., Gerdts, G., & Burkhardt-Holm, P. (2019). Microplastic pollution in benthic midstream sediments of the Rhine river. *Environmental Science & Technology*, 53(10), 6053-6062. doi:<https://doi.org/10.1021/acs.est.9b01363>
- x. Tekman, M. B., Wekerle, C., Lorenz, C., Primpke, S., Hasemann, C., Gerdts, G., & Bergmann, M. (2020). Tying up loose ends of microplastic pollution in the Arctic: Distribution from the sea surface, through the water column to deep-sea sediments at the HAUSGARTEN observatory. *Environmental Science & Technology*, 54(7), 4079-4090. doi:<https://doi.org/10.1021/acs.est.9b06981>

Acknowledgments

First and foremost, I would like to sincerely thank all the members of my PhD committee at Jacobs University: Professor Dr Matthias Ullrich, Professor Dr Laurenz Thomsen and Dr Gunnar Gerdts for agreeing to supervise my PhD and for providing constant support and scientific suggestions whenever needed. Here I would especially thank Dr Gunnar Gerdts for encouraging and supporting me to apply for a PhD scholarship at the DBU in the first place.

My deepest gratitude goes to the DBU for funding my PhD for three years but also providing a platform for exchange with others who were in the same boat. Special thanks to Dr Volker Wachendörfer and Sabine Dannhauer for being understanding that it took me now a bit longer.

I would also like to thank the Alfred Wegener Institute for Polar and Marine Research (AWI) for providing me with financial and moral support through the graduate school POLMAR and for the infrastructure and possibility to conduct my thesis work at the Biologische Anstalt Helgoland (BAH). Thanks also to the whole BAH for welcoming me on the island, especially to Kathrin Böhmer and Renate Beissner. Thanks also to Matthias Wunderlich for building the MP-reactors, which have been an indispensable asset for my studies and various others.

It was a great pleasure to be part of the Microbial Ecology Working group, and I am thankful for Gunnar and Antje, being both equally the head and the heart of it. I am truly grateful for your encouragements, scientific guidance and support. Thank you also for your patience but also for nudging me when I needed a push.

I want to thank Michaela for her valuable advice both on an academic and personal level.

A huge thank you to Sebastian for being there for me this whole journey, always committed and helpful. Thank you for sharing your knowledge on FTIR spectroscopy and your contribution to this thesis. I also enjoyed all the moments we spent trying not to talk about work, so, also thanks for being a good friend.

A very special thank you to my officemates-now-close-friends – Inga, Ale and Sidi – for accompanying me during the whole PhD, showing me how it's done and encouraging me that I can manage it, too. I don't think I could have done it without you, though! Thank you for all the quality time spent together also to the other members of our *Pizza Pizza* group – Birte, Steffen, Ivo and Ced – I cherish these shared moments very much.

A big thank you to all the bachelor and master students I had the pleasure to work with and who greatly supported the work featured in this thesis, namely Linn Speidel, Lisa Roscher, Vanessa Wirzberger, Melanie Meyer, Lars Hildebrandt, Julia Prume and Florentina Münzner.

I enjoyed working with all of you! It is a pleasure to see you continue on your (academic) way, and I am looking forward to our paths crossing again.

I am also grateful for meeting a lot of wonderful and inspiring people on Helgoland: Svenja Mintenig (for mentoring me when I first arrived on the island and being my role model since then), Mine Tekman (for great collaborations but also the wonderful time spent together discussing life, laughing and encouraging each other), and Dr Marte Haave (for accepting to include our collaboration in this thesis).

Thanks also to all the other wonderful people who made my life on the island of Helgoland so memorable: My flatmates for the shared dinners, conversations and fabulous parties, all the fellow PhD candidates for fruitful discussions, feedback and organizing events like the Pint of Science, and the Volleyball group for reminding me there are also other things than work. You all made my time on the island into a great experience, and I was very reluctant to leave you all behind and continue my journey elsewhere. It helped that Inga was there to continue this journey with me. So again thanks for being an amazing friend and now flatmate, too.

It also helped that I have been lucky to work again with a wonderful group of people. I want to thank my new colleagues at Aalborg University very much for welcoming me so heartedly into their team. I want to express my gratitude to Professor Jes Vollersten for getting me on the team although I still had this “baggage” with me, granting me the time to finish it and providing insightful scientific comments. Big thanks to Lucian for always being helpful in your cheerful and easygoing way. Thank you, Fides for your hard work in the lab and also your moral support. Special thanks also to Alvise for shouldering the FanPLESStic project together, the inspiring brainstorming but also for always listening to my struggles and doubts and having the right words to encourage me again.

I want to thank all my new colleagues for supporting me through this first year, all the fruitful scientific discussions but also all the other conversations at the cheerful coffee/lunch breaks.

By now, colleagues also became friends, so thanks to my fellow *Aalborgians*.

Speaking of friends, a lot of patience was needed from my friends back home (be it where I grew up or where I spend my time at university). Thank you, Bianca, Xenia, Marion, Kathrin, Martin, Mona, Chrissi, Carmen, Susi, Steffi, Lisa and Ina for staying with me all this time.

Finally yet importantly, I couldn't have done this without the constant support of my family, especially my parents and my sister. Thank you for always believing in me and for your unconditional love and support. Thank you for always giving me what I needed, be it a friendly ear, a shoulder to lean on, words of encouragement or something to laugh about. There are no words to describe how grateful and proud I am to be your daughter and sister!

This PhD taught me to be patient and resilient, to have faith in my own abilities and constantly aim to surpass myself. But it also taught me that the most important thing are the people you are with, the ones that have your back, that help you back up when you stumble and encourage you to go on.

To all of you wonderful people that accompanied me along this seemingly endless journey:

My deepest and sincerest thank you!